**Prelimenary PDF version - missing animations and movies.**
**Updated version will be published in the proceedings.**


Managed by Fermi Research Alliance, LLC for the U.S. Department of Energy Office of Science

# *Pushing bulk Niobium Limits*

Anna Grassellino

*Deputy Head, Applied Physics and Superconducting Technology Division, Fermilab*

SRF 2019 Tutorials, Dresden, Germany

June 27th, 2019

# Particle Acceleration via SRF Cavities

- **Superconducting radiofrequency (SRF) cavities**
- High quality EM resonators: Typical $Q_0 > 10^{10}$
- Over billions of cycles, large electric field generated
- Made of Niobium, Tc ~9.2K; frequency from 100MHz to several GHz

Input RF power at 1.3 GHz

*Slowed down by factor of approximately $4x10^9$*

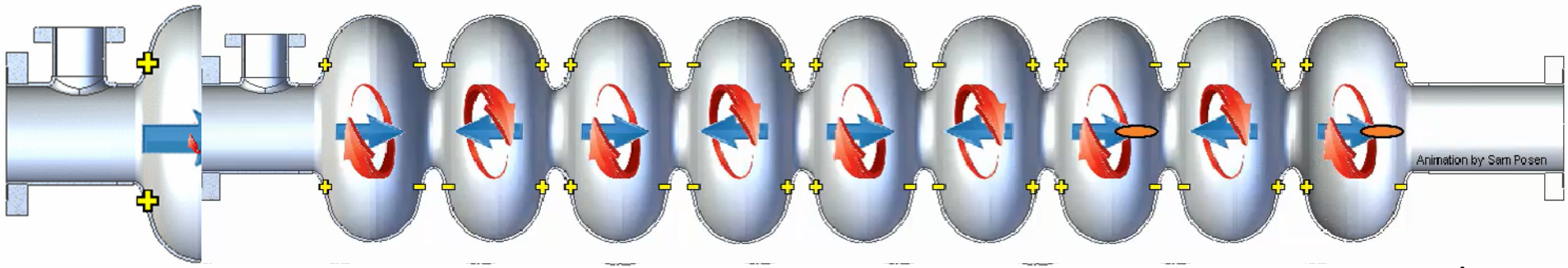


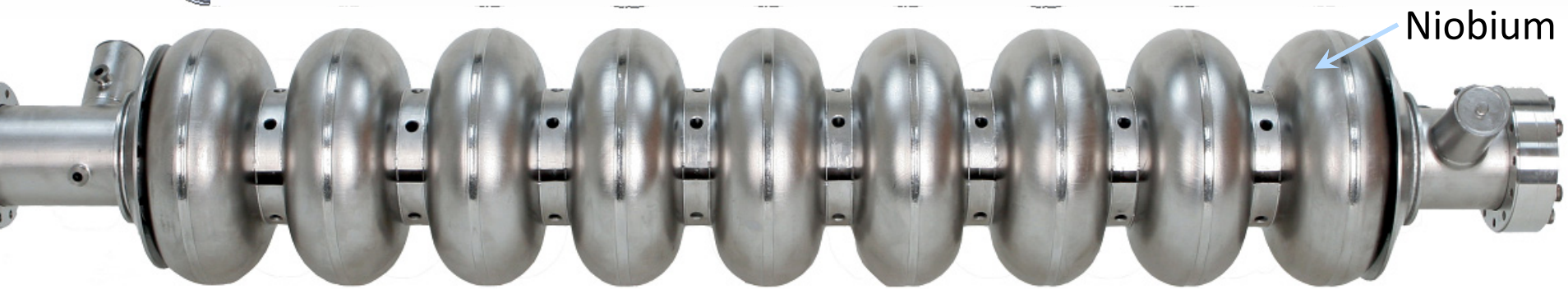


~1 m



*Images from linearcollider.org, WIkipedia*


ACID
DUMP

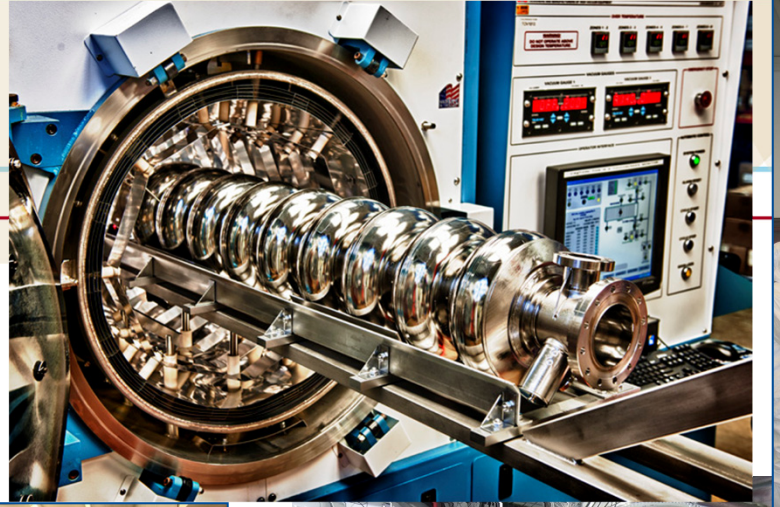

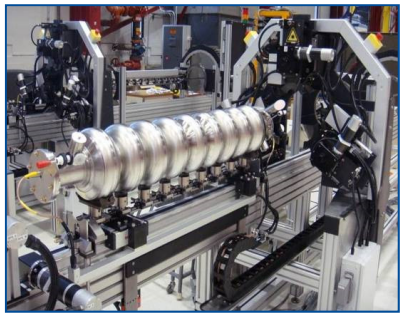

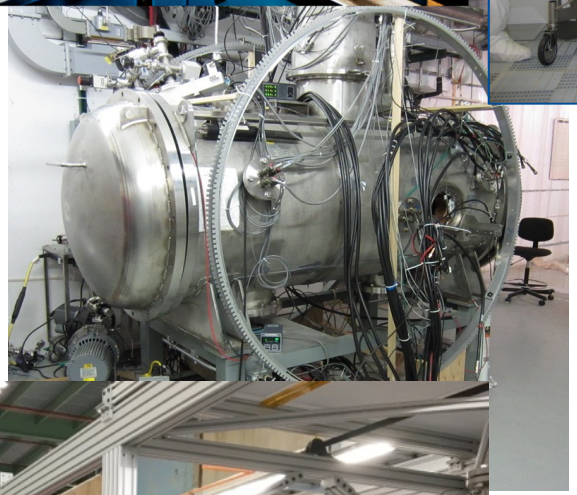

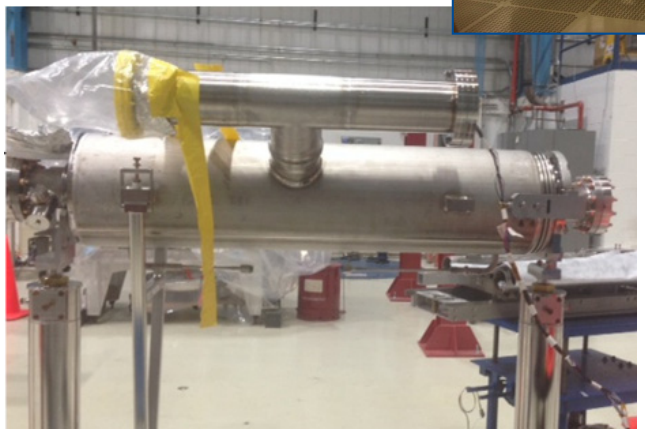




# Large scale specialized infrastructure is required to make/study high Q cavities and assemble/test full accelerating cryomodules

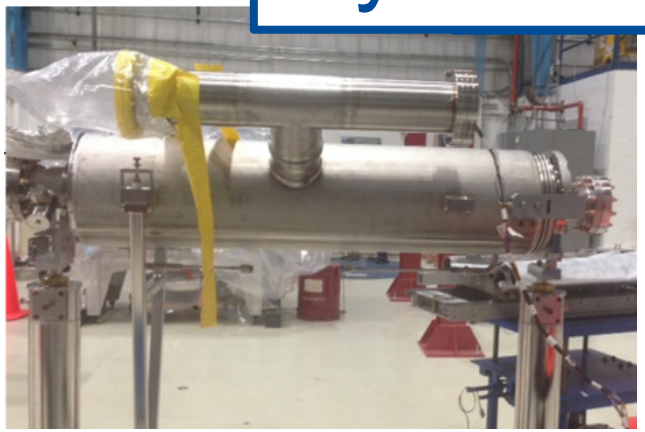

# The punch line

- SRF is a mature technology, currently many machines employing it worldwide and many under construction, very exciting time
  - From colliders to light sources to very sensitive detectors, SRF cavities enable a enormous spectrum of applications, from particle physics to biology, medicine and society
- There has been steady progress in the advancement of this technology, lately with some important breakthroughs that give us confidence that the technology is not at the end of the road
- Progress in SRF technology MUST come from a group effort of : talented engineers and techs at the labs, SRF scientists, superconductivity experts, material scientists at labs and universities

# How to build an SRF accelerator in two minutes: LCLS-II Cryomodule assembly

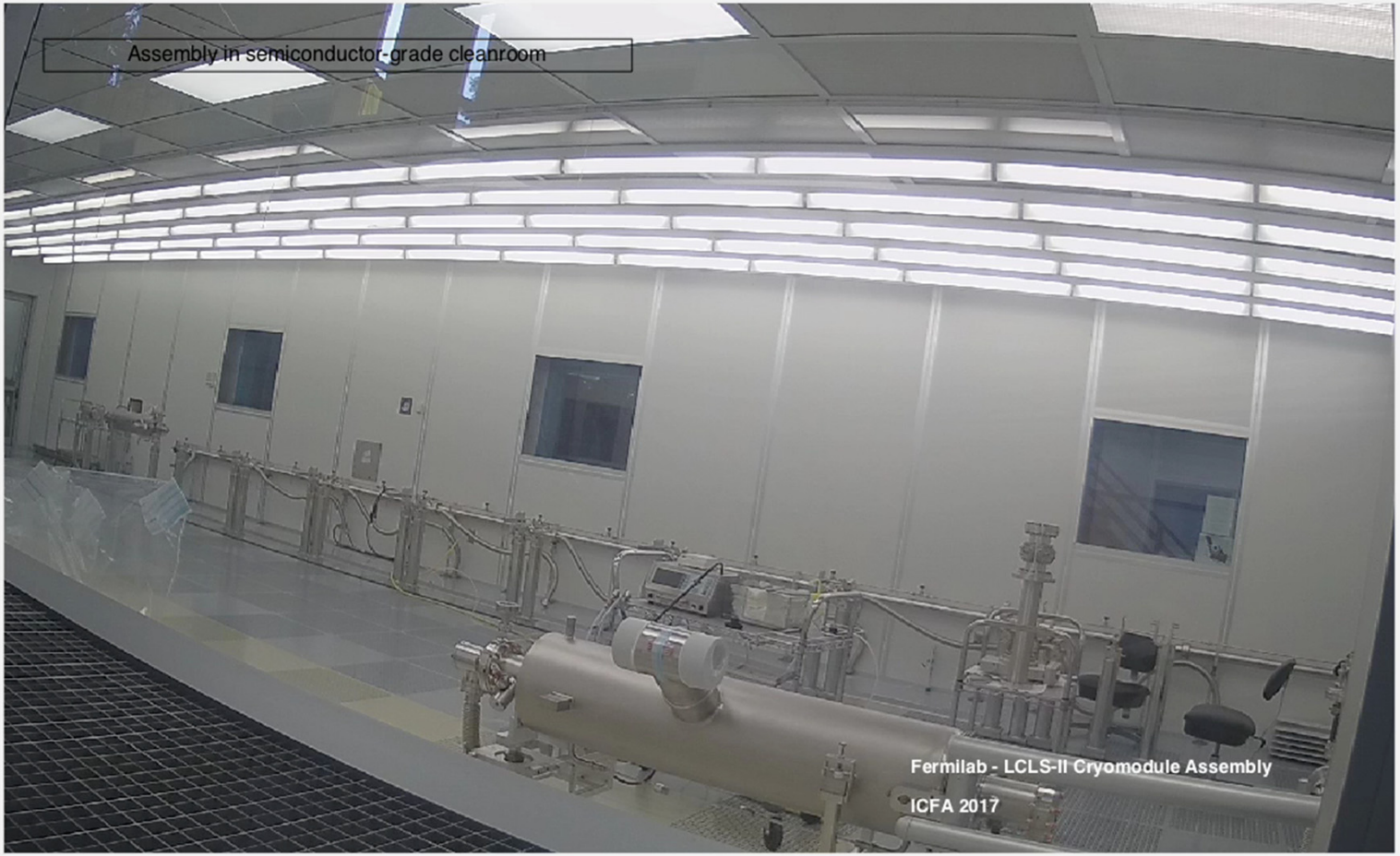

# SRF cavities – extraordinarily high efficiency

- Wall dissipation (proportional to surface resistance $R_s$) is reduced by many orders of magnitude over a normal conducting copper cavity

- Among highest quality factors Q in nature
  - $Q>10^{11}$ nowadays most often achieved, $Q=2x10^{10}$ – routine
  - Extremely sensitive detecting devices – one photon level, mechanical vibrations (sub-nm)
- **Affordable continuous wave and long pulse at high gradients**
  - **Field=acceleration can be ON all the time**

# SRF cavities – extraordinarily high efficiency

- Wall dissipation (proportional to surface resistance $R_s$) is reduced by many orders of magnitude over a normal conducting copper cavity

- Amon
  - Q
  - E
    vi
- **Affor**
  - **Fi**

cal

s

SRF: high current, high energy, high brightness beams

# SRF cavities – extraordinarily high efficiency

- Wall dissipation (proportional to surface resistance $R_s$) is reduced by many orders of magnitude over a normal conducting copper cavity

- Amon
  - Q
  - E
    vi
- **Affor**
  - **Fi**

cal

s

SRF: high current, high energy, high brightness beams

However….not quite zero dissipation in RF →
We battle ~ nanoOhms (or fraction of)

# Factor of merit 1: Gradient -> Length for Linear Accelerator

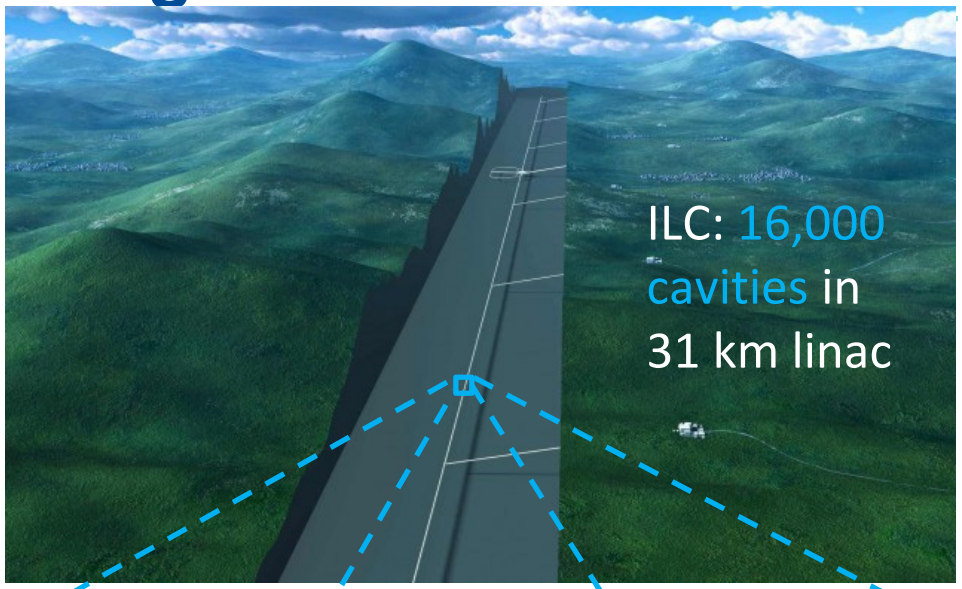



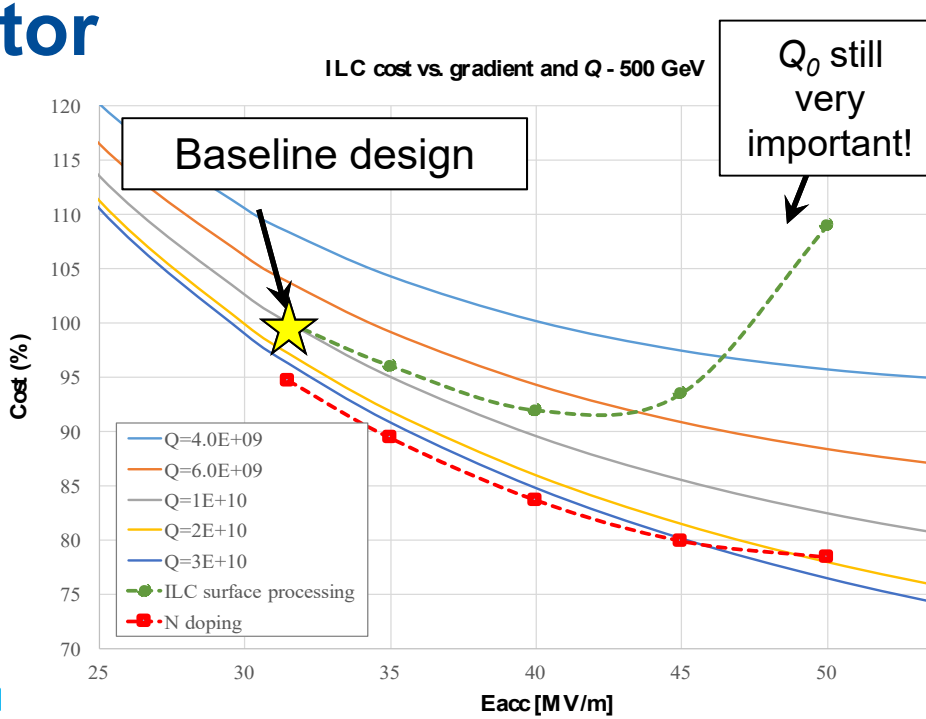





*Image from linearcollider.org. Tunnelflug video by European XFEL. Cost analysis by N. Solyak*

# Factor of merit 2: $Q_0$ -> Cryogenic Infrastructure, Operating Cost

$$P_{diss} \sim E_{acc}/Q_0$$ (for fixed $E_{max}$)



Lower cost

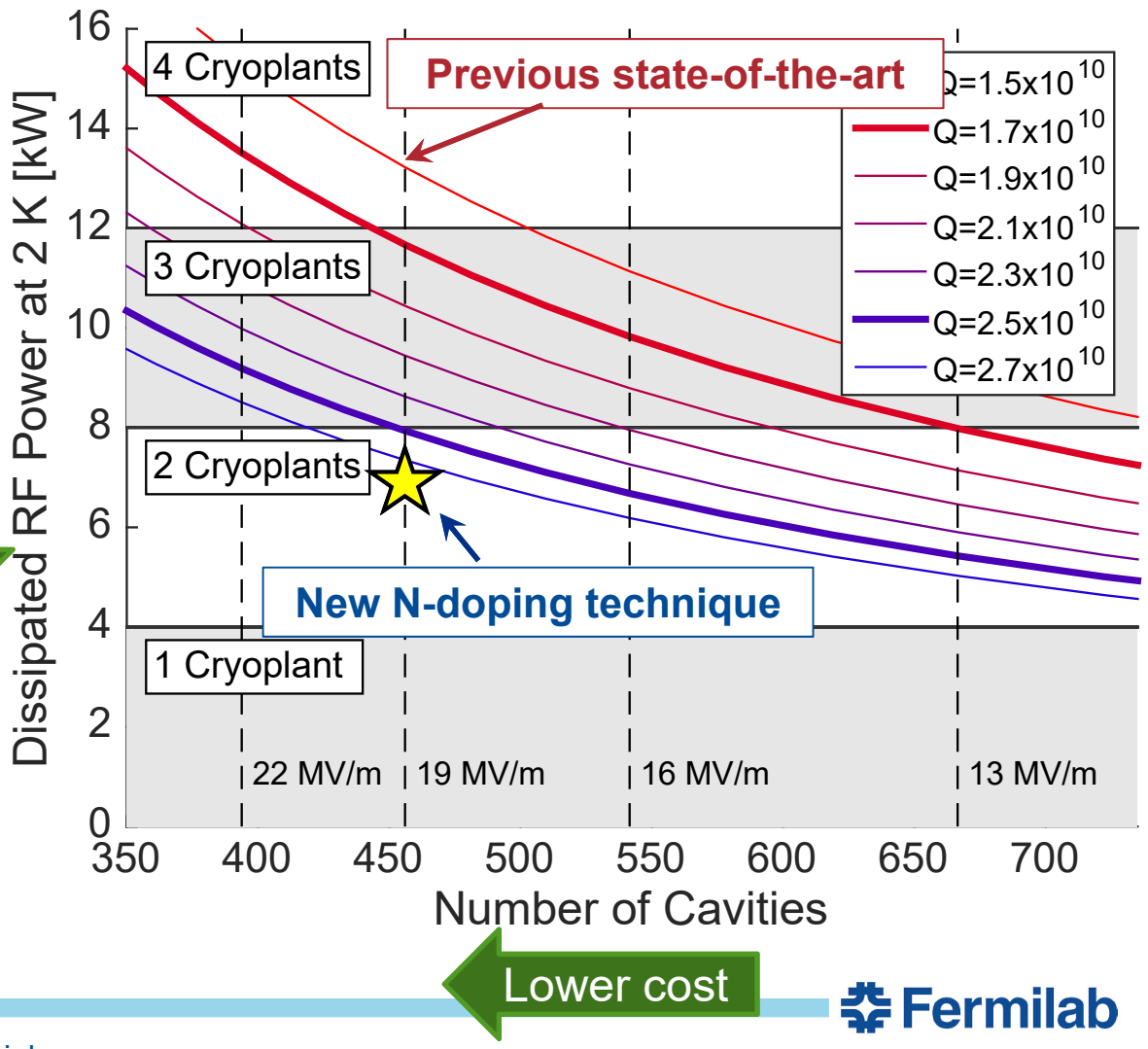


Lower cost

Fermilab

# Performance are determined by nanometer scale structure of inner surface

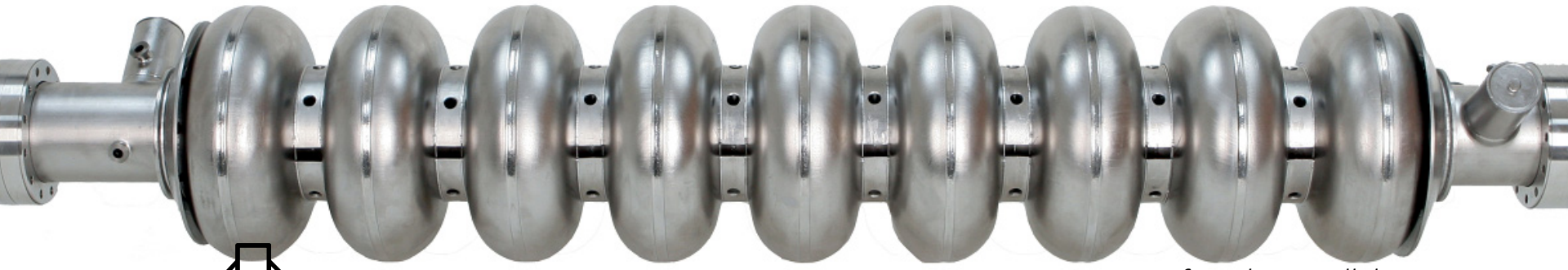

*Image from linearcollider.org*

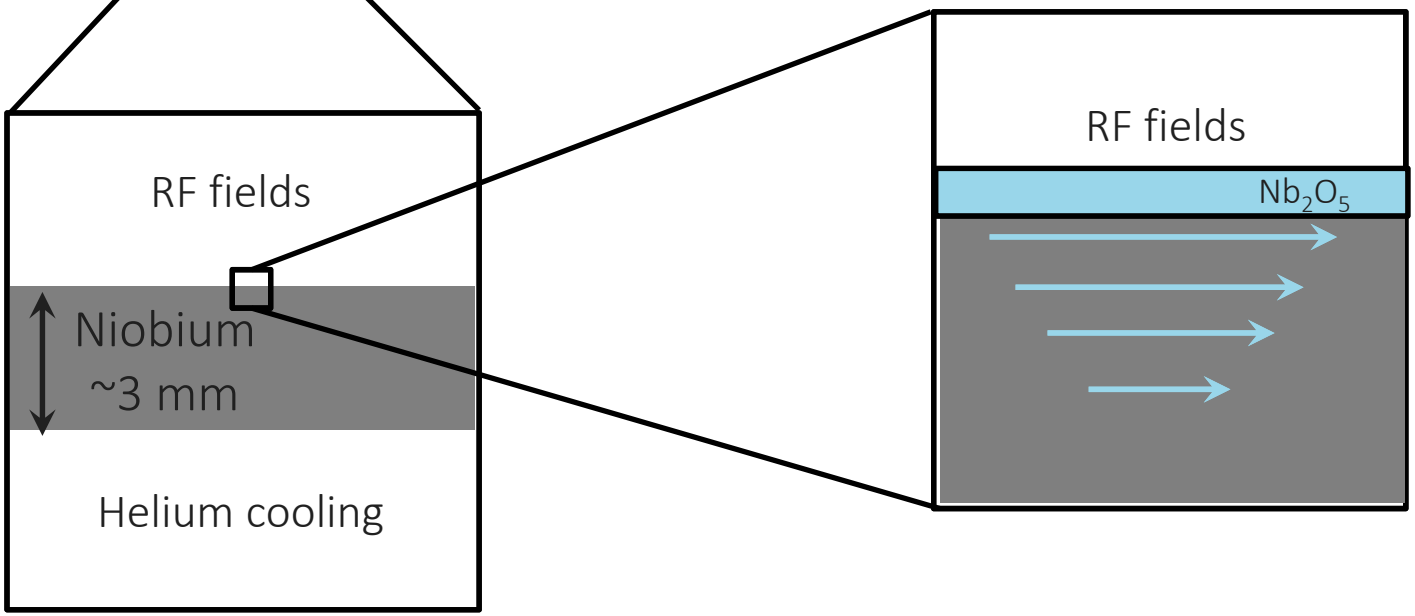


<0.1% of thickness

RF currents <100 nm

# Performance are determined by nanometer scale structure of inner surface

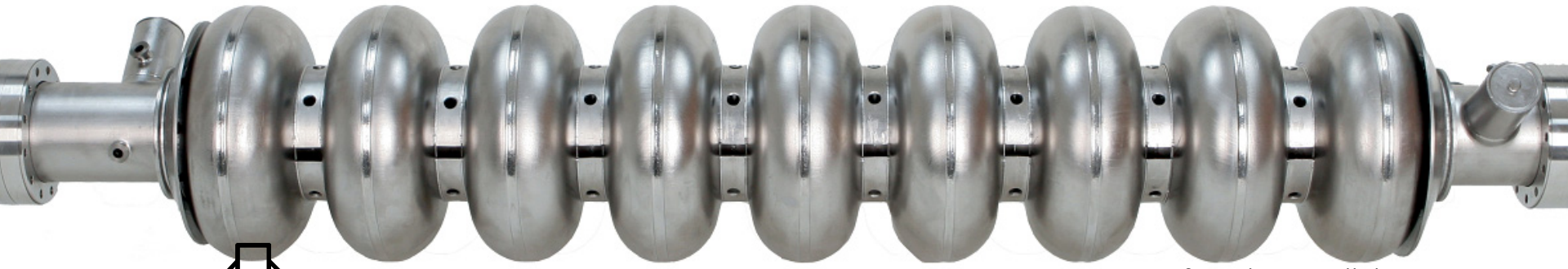

*Image from linearcollider.org*

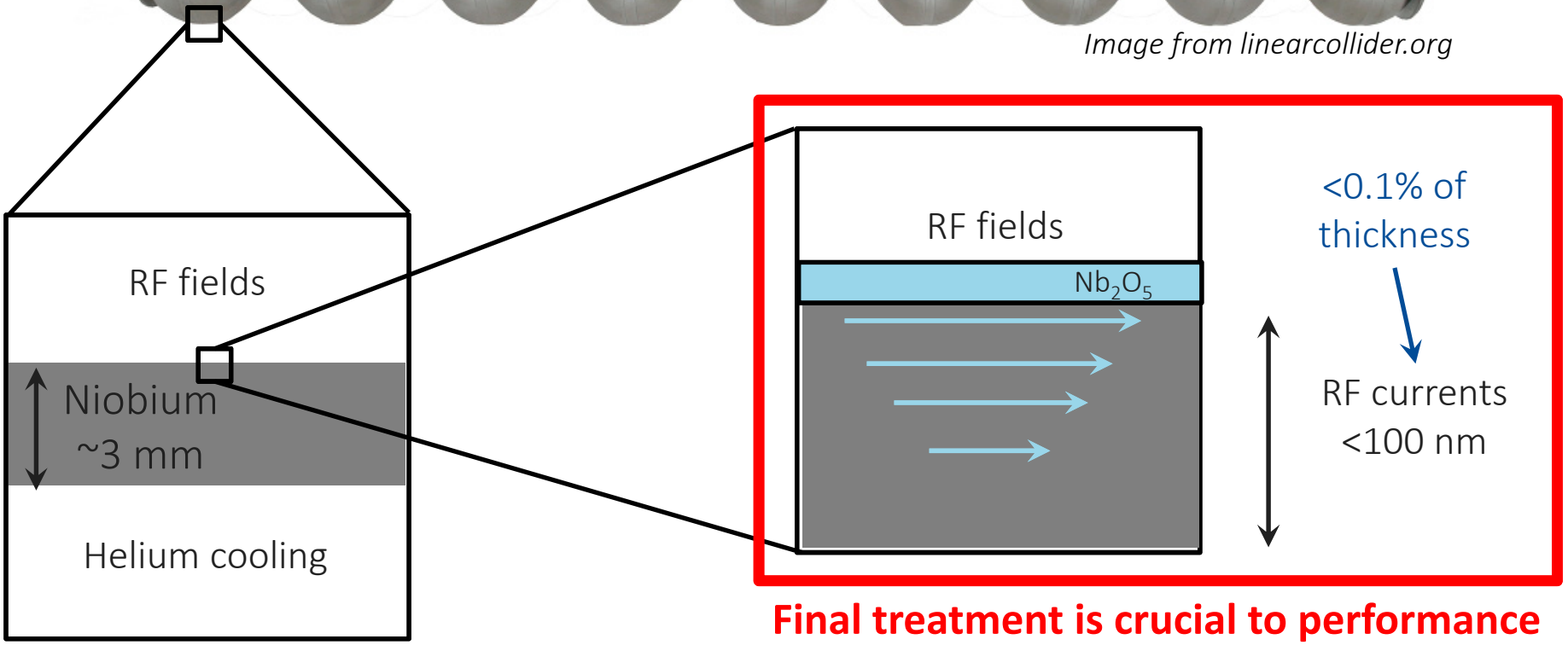


**Final treatment is crucial to performance**

# Beam view, inside the cavity

Extreme attention to surface treatments and surface cleanliness are mandatory

# Key to progress for superconducting RF cavities

- Cavity surface undergoes a series of delicate chemical and heat treatments
- Material science tools are <u>essential</u> to understand the surface nanostructural changes that lead to dramatic changes in performance

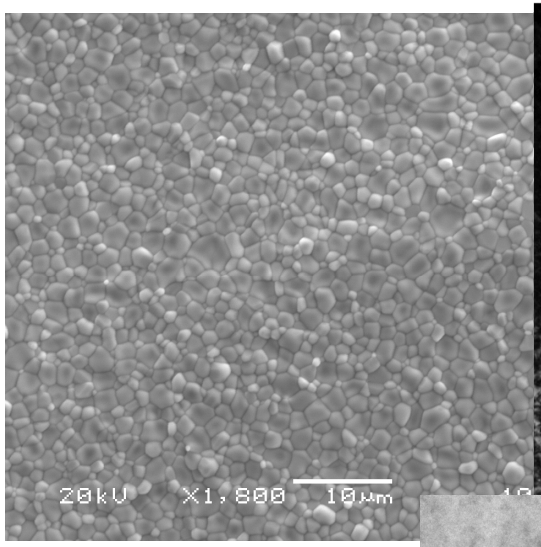


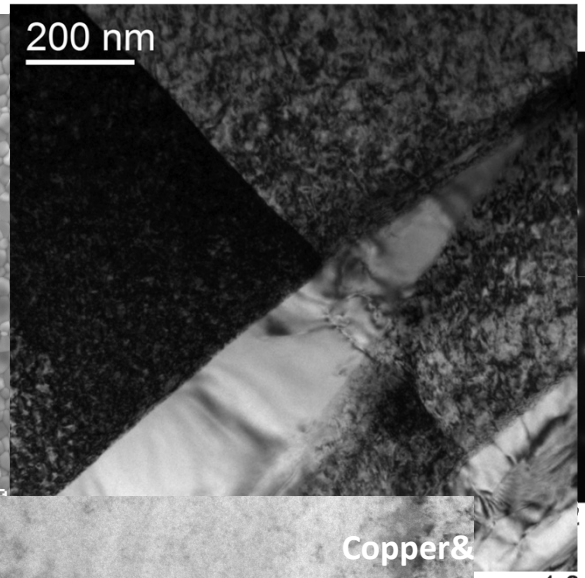


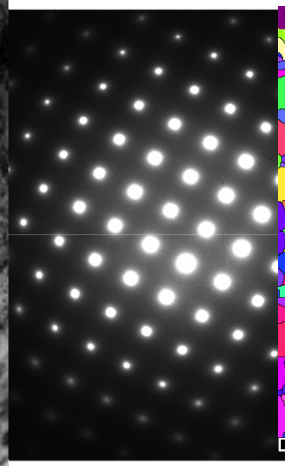

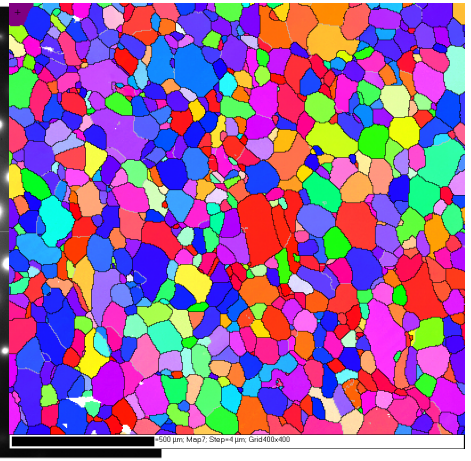

N"#econstruc, on#

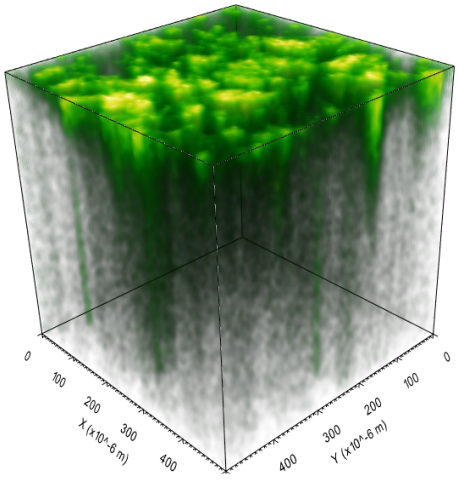

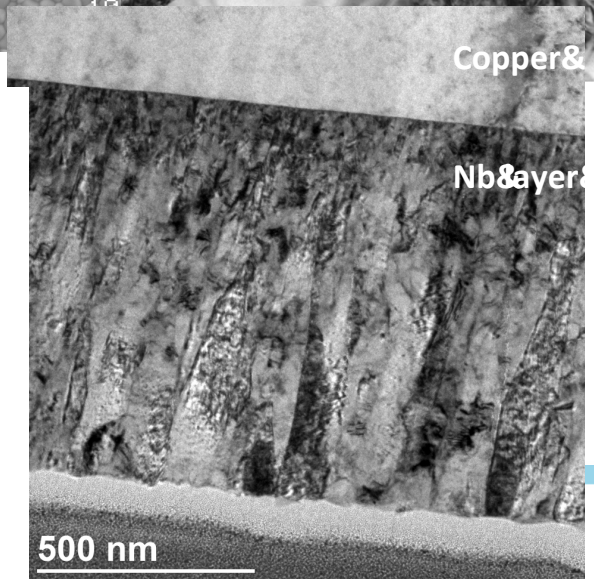


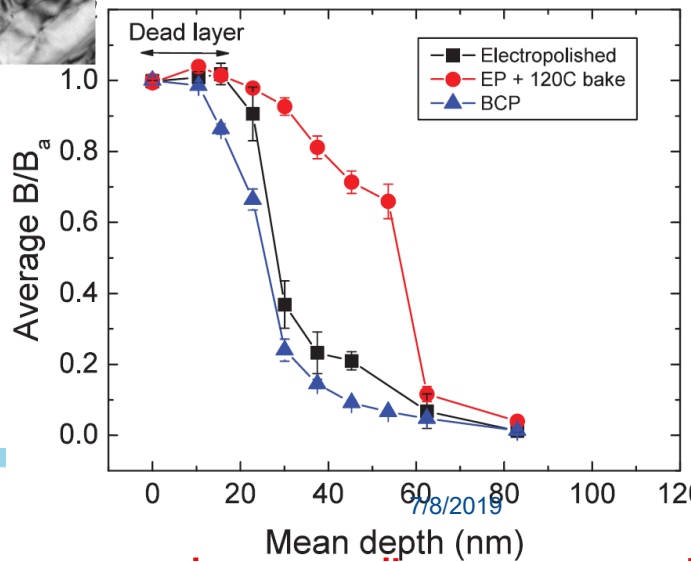

# SRF Performance Evolution

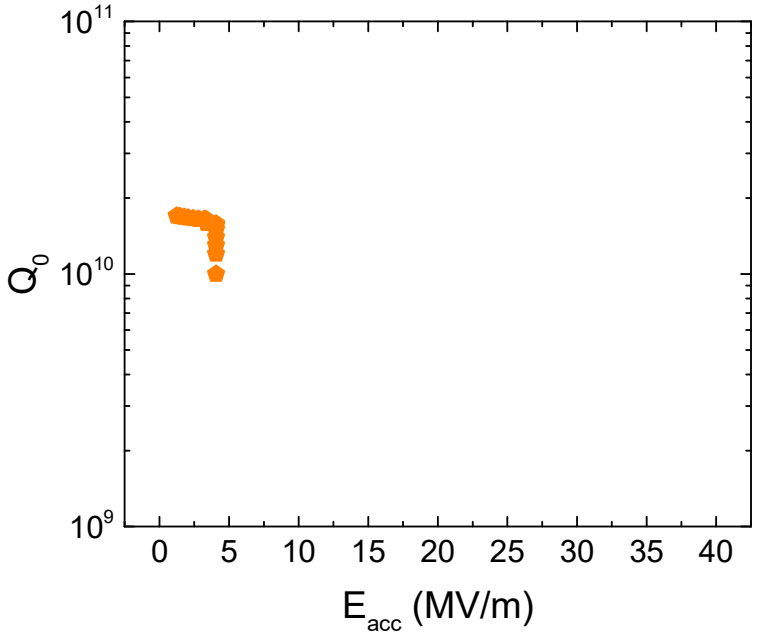


1.3 GHz, 2K

3 – 4 MV/m
Multipacting

# SRF Performance Evolution

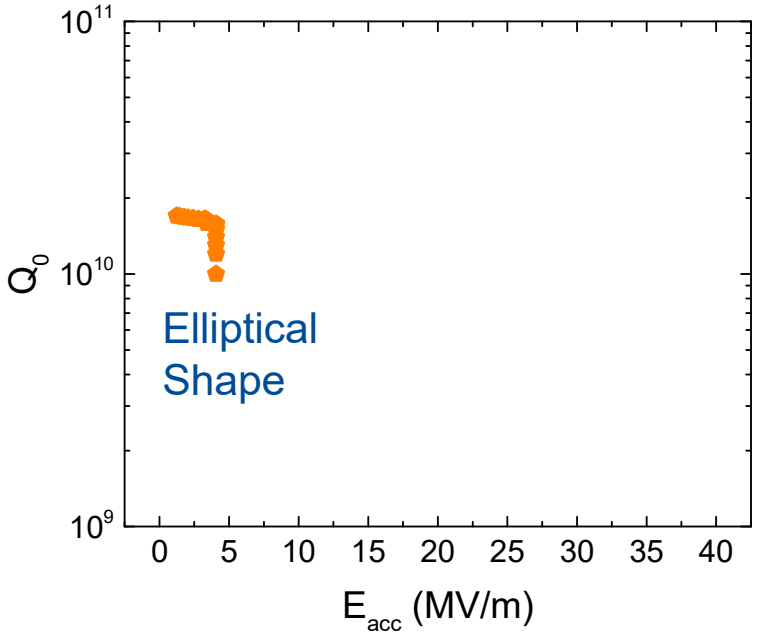


1.3 GHz, 2K

3 – 4 MV/m
Multipacting

# SRF Performance Evolution

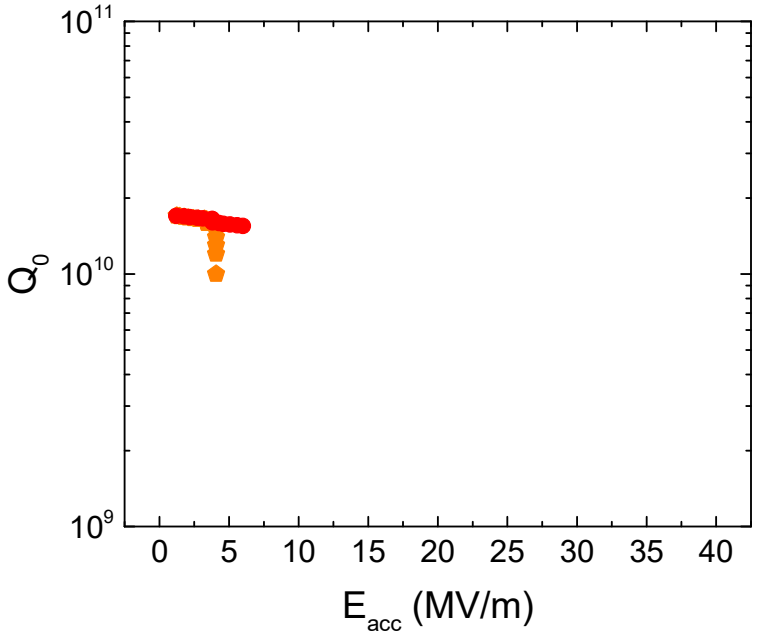


1.3 GHz, 2K

3 – 4 MV/m
Multipacting

5 MV/m
Thermal Breakdown

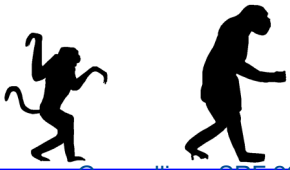

# SRF Performance Evolution

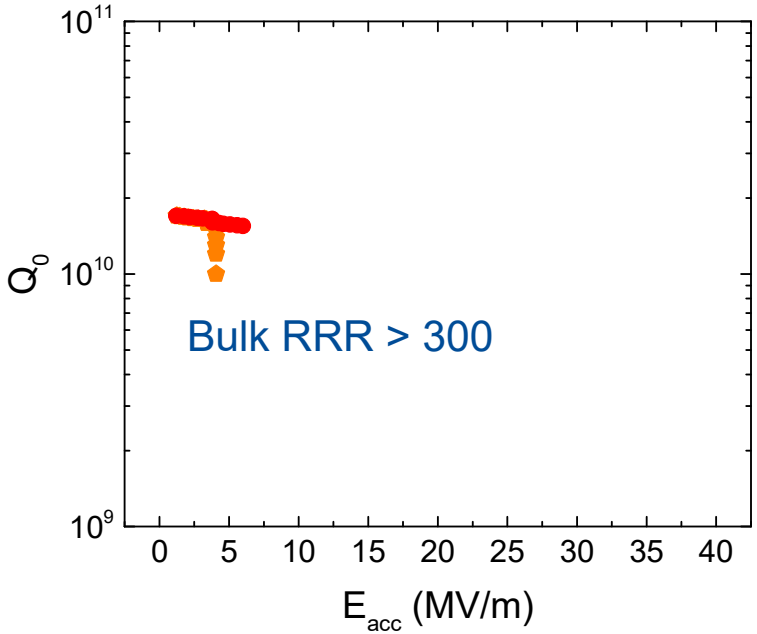


1.3 GHz, 2K

3 – 4 MV/m
Multipacting

5 MV/m
Thermal Breakdown

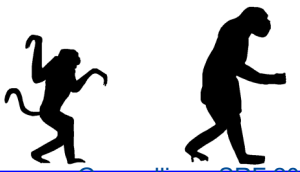

# SRF Performance Evolution

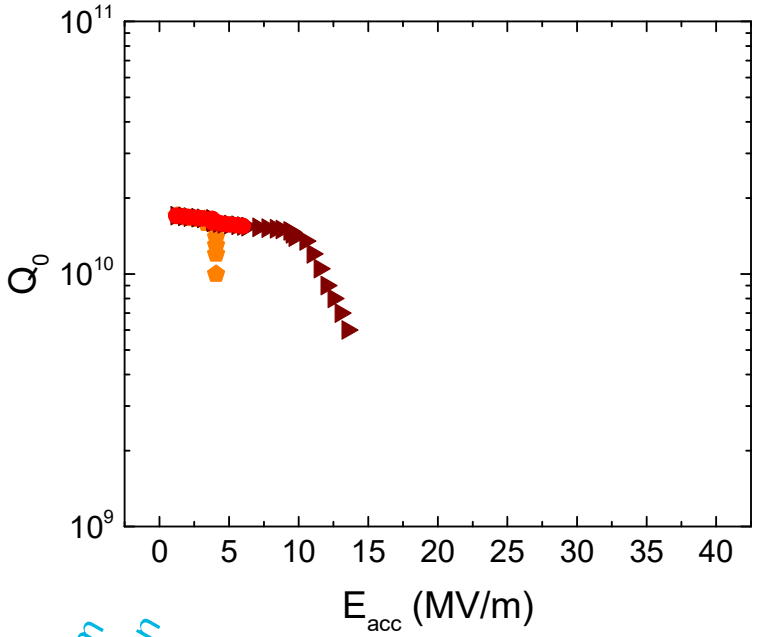


1.3 GHz, 2K

3 – 4 MV/m
Multipacting

5 MV/m
Thermal Breakdown

10 – 15 MV/m
Field Emission

# SRF Performance Evolution

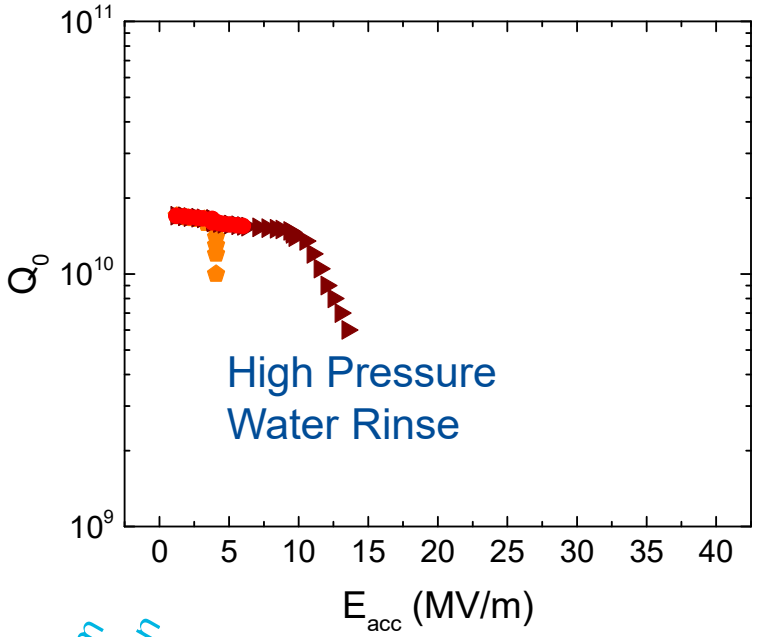


1.3 GHz, 2K

3 – 4 MV/m
Multipacting

5 MV/m
Thermal Breakdown

10 – 15 MV/m
Field Emission

# SRF Performance Evolution

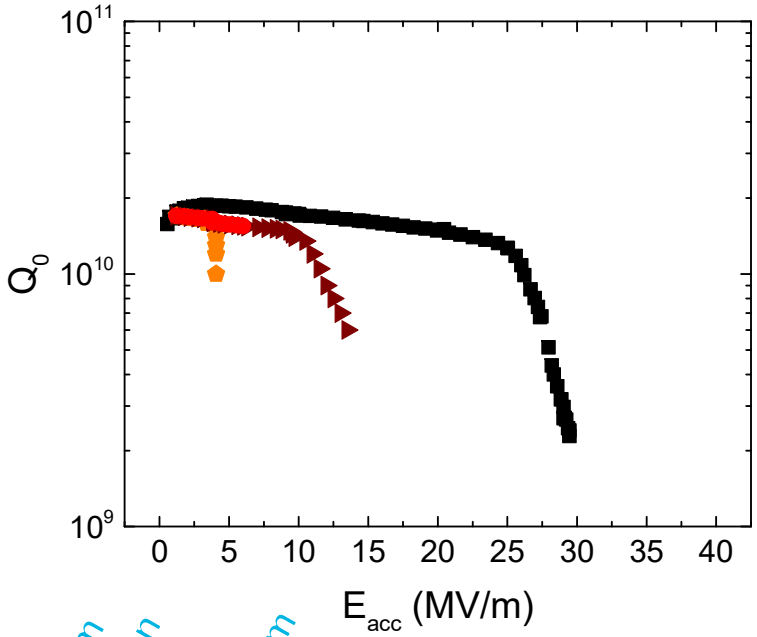


1.3 GHz, 2K

3 – 4 MV/m
Multipacting

5 MV/m
Thermal Breakdown

10 – 15 MV/m
Field Emission

20 - 25 MV/m
High field
Q-SLOPE

# SRF Performance Evolution

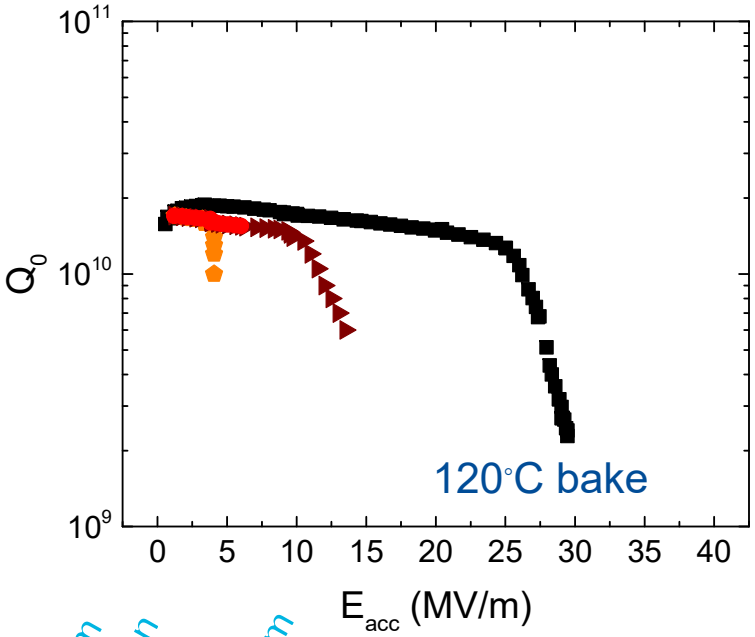


1.3 GHz, 2K

3 – 4 MV/m
Multipacting

5 MV/m
Thermal Breakdown

10 – 15 MV/m
Field Emission

20 - 25 MV/m
High field
Q-SLOPE

# SRF Performance Evolution

1.3 GHz, 2K

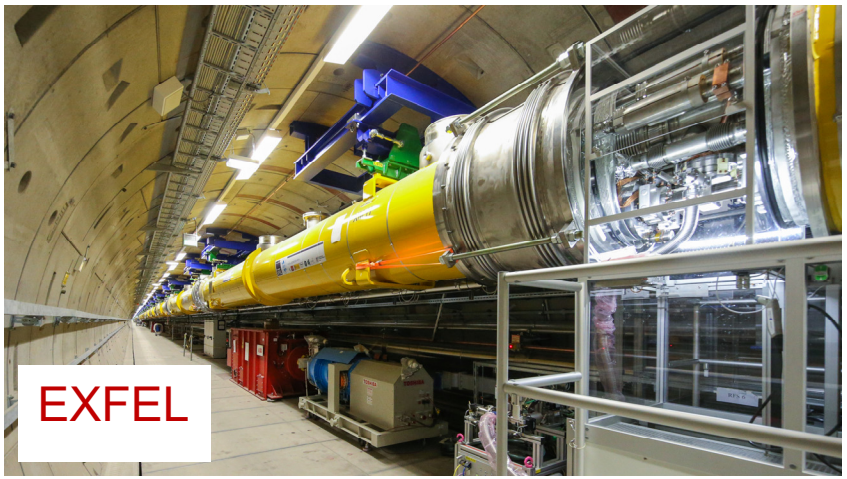


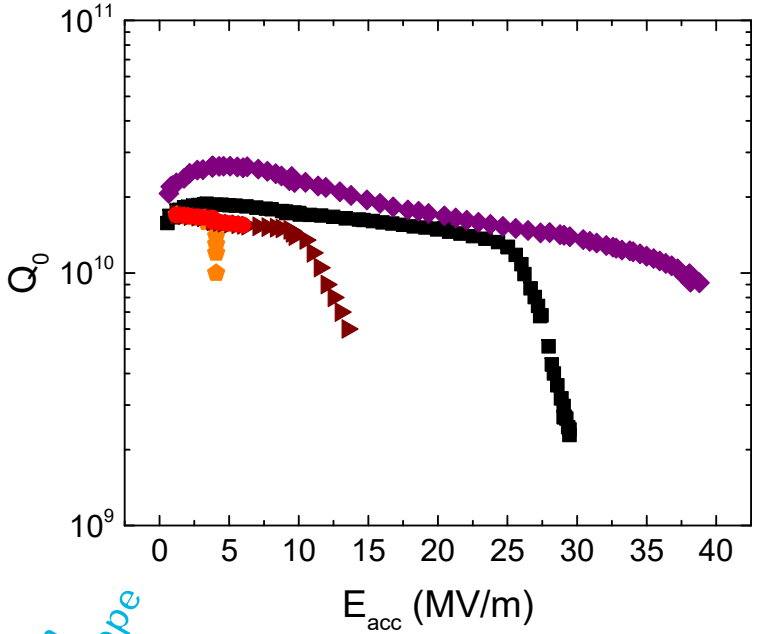


3 – 4 MV/m
Multipacting

5 MV/m
Thermal Breakdown

10 – 15 MV/m
Field Emission

20 - 25 MV/m
High field
Q-SLOPE

35 – 40 MV/m
mid field Q-slope

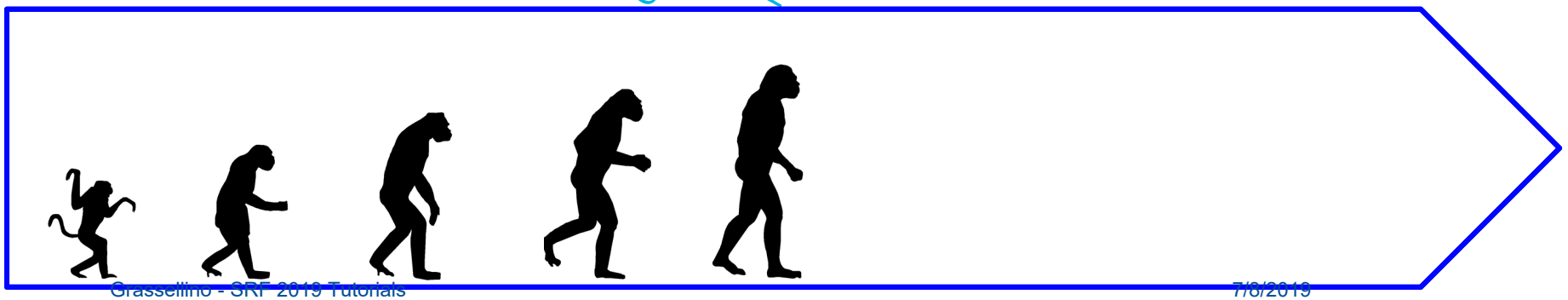

# SRF Performance Evolution

1.3 GHz, 2K

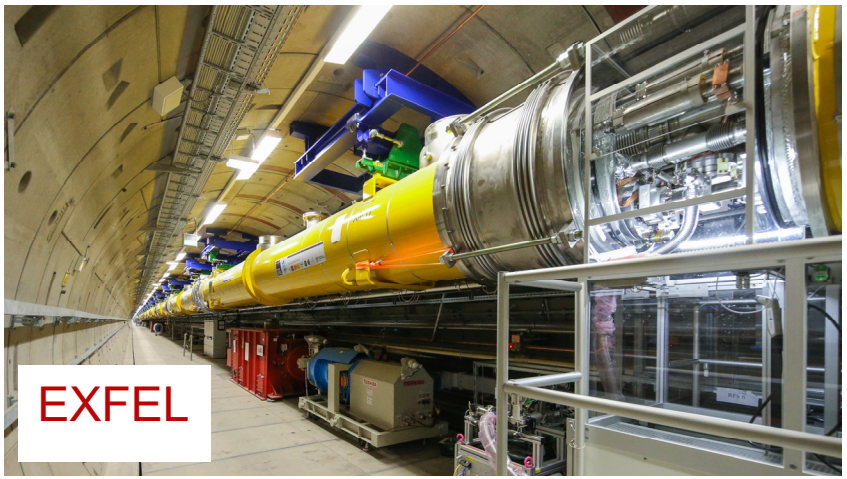


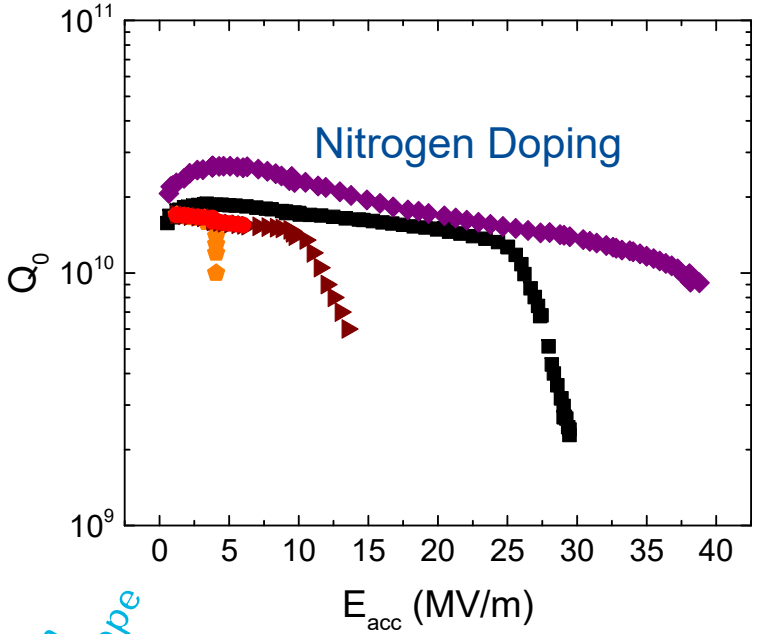


3 – 4 MV/m
Multipacting

5 MV/m
Thermal Breakdown

10 – 15 MV/m
Field Emission

20 - 25 MV/m
High field
Q-SLOPE

35 – 40 MV/m
mid field Q-slope

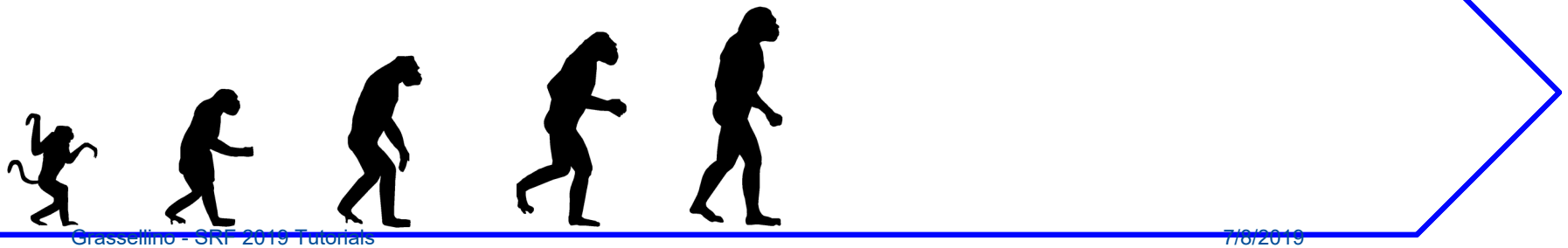

# SRF Performance Evolution – 2013: N doping!


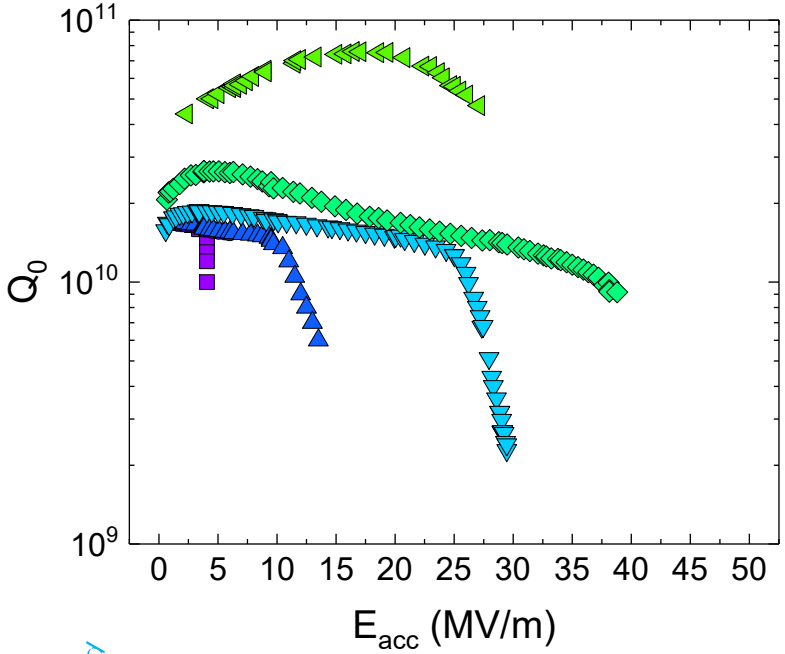


3 – 4 MV/m Multipacting

5 MV/m Thermal Breakdown

10 – 15 MV/m Field Emission

20 - 25 MV/m Q-SLOPE

35 – 40 MV/m

Q > 5e10 At medium field

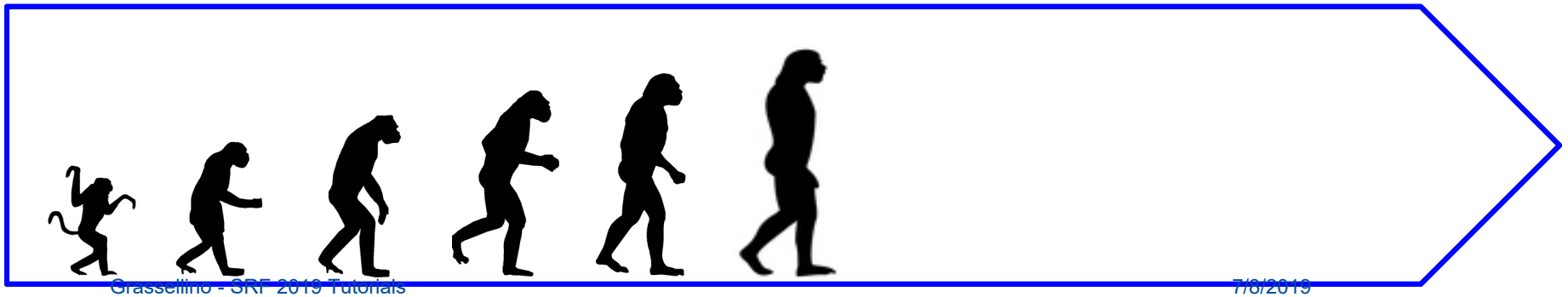

# SRF Performance Evolution – 2014: Magnetic flux trapping with slow cooldown/ efficient expulsion with fast


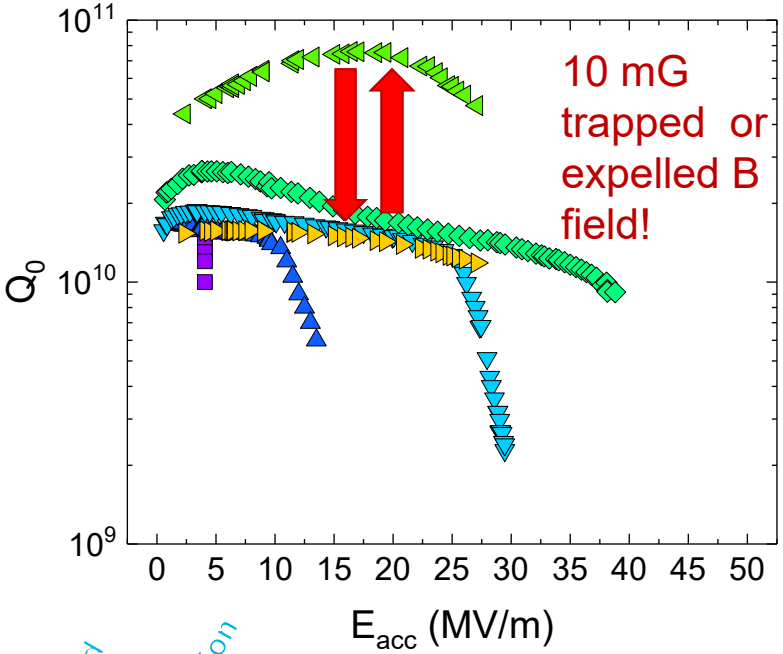


3 – 4 MV/m Multipacting

5 MV/m Thermal Breakdown

10 – 15 MV/m Field Emission

20 - 25 MV/m Q-SLOPE

35 – 40 MV/m

Q > 5e10 At medium field

Flux dissipation Flux expulsion

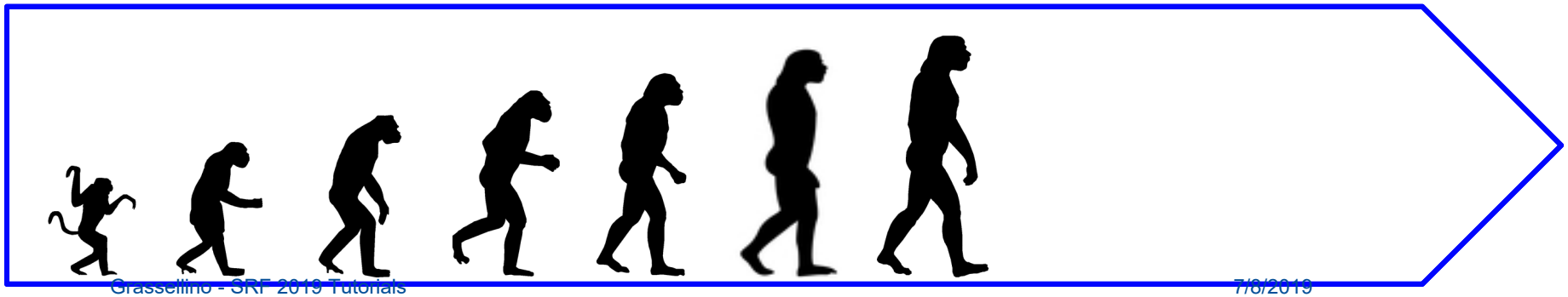

# SRF Performance Evolution – 2017: N infusion

ILC cost reduction??

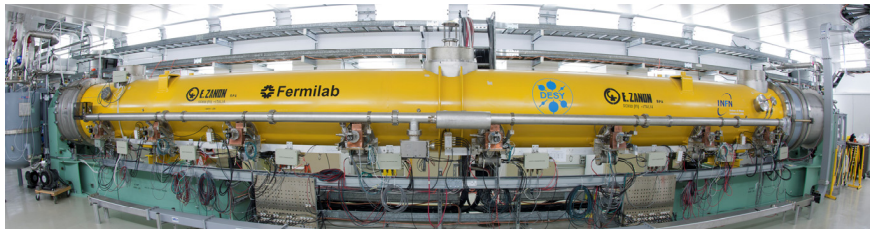


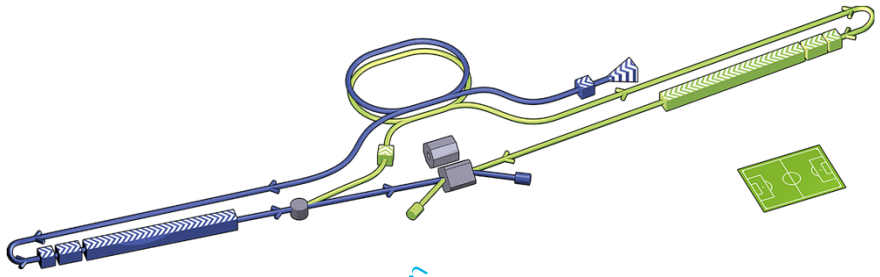

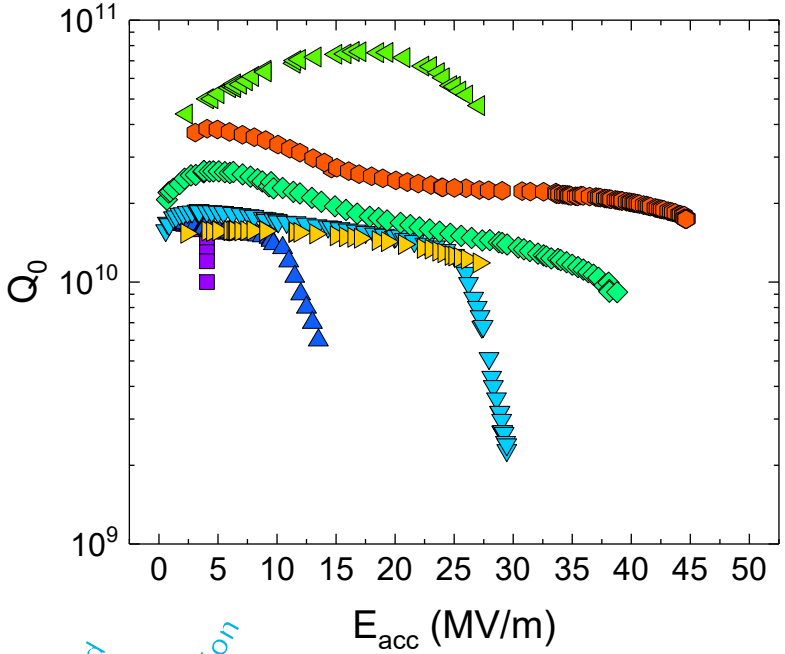


3 – 4 MV/m Multipacting

5 MV/m Thermal Breakdown

10 – 15 MV/m Field Emission

20 - 25 MV/m Q-SLOPE

35 – 40 MV/m

Q > 5e10 At medium field

Flux dissipation Flux expulsion

Q > 2e10 At high field

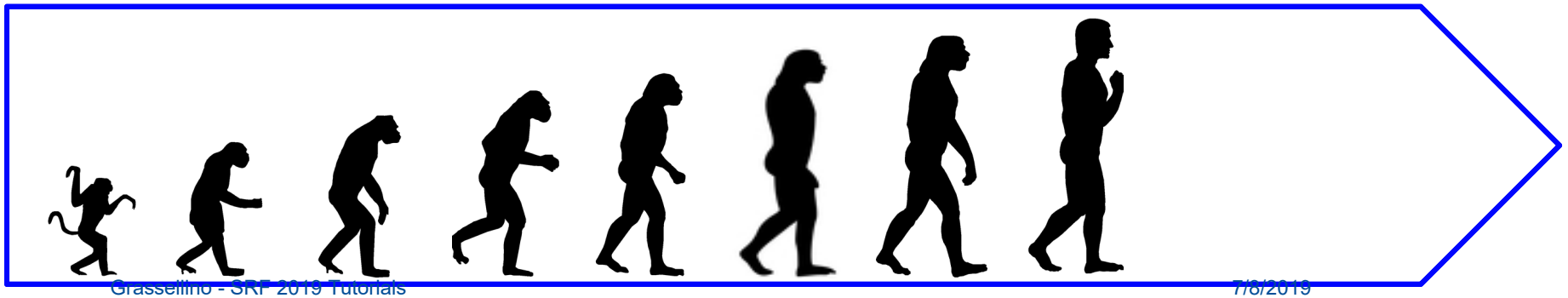

# SRF Performance Evolution – 2018: the 75C bake

ILC cost reduction??

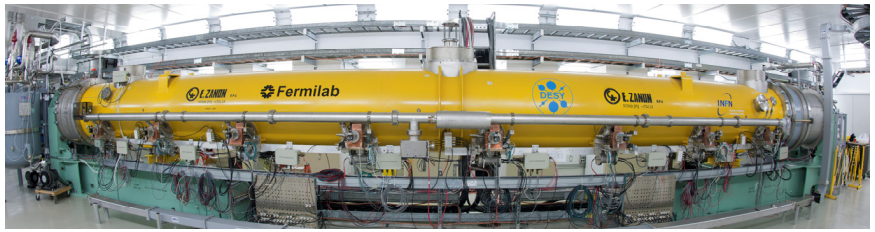


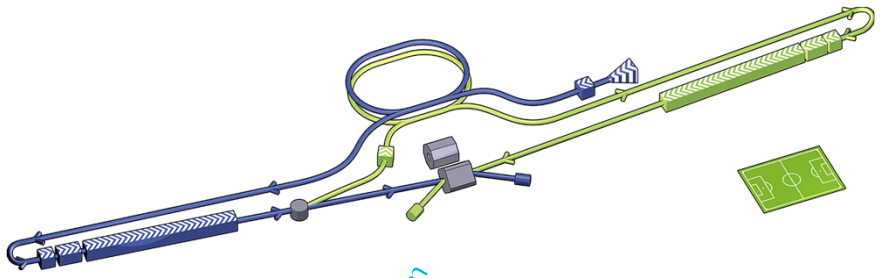

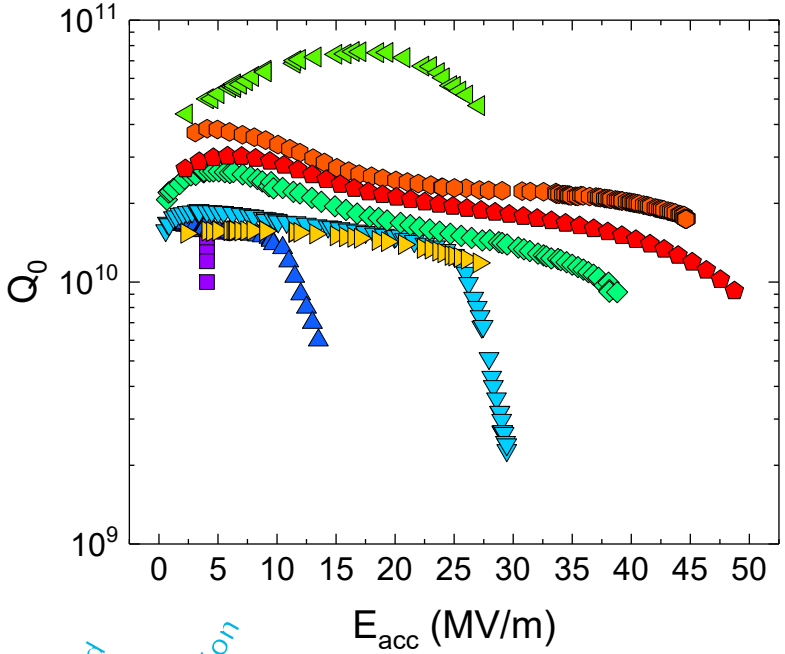


3 – 4 MV/m Multipacting

5 MV/m Thermal Breakdown

10 – 15 MV/m Field Emission

20 - 25 MV/m Q-SLOPE

35 – 40 MV/m

Q > 5e10 At medium field

Flux dissipation Flux expulsion

Q > 2e10 At high field

50 MV/m !!!

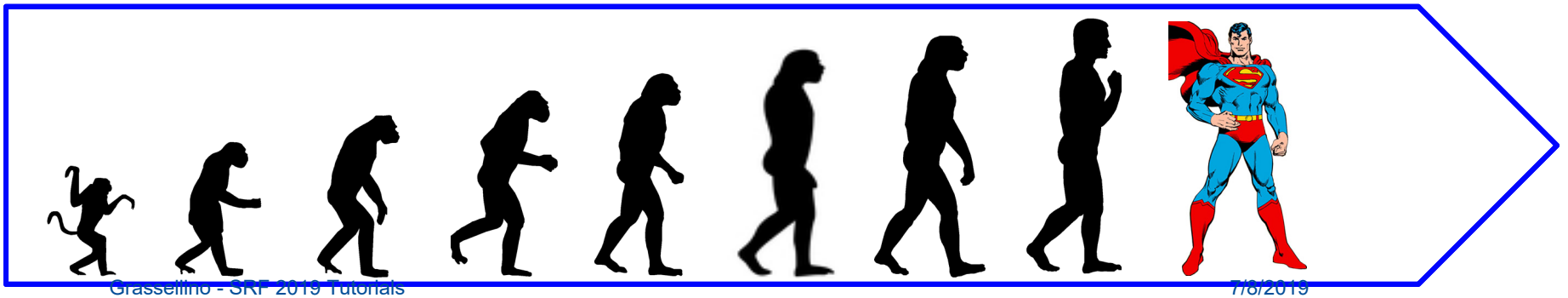

# SRF Performance Evolution

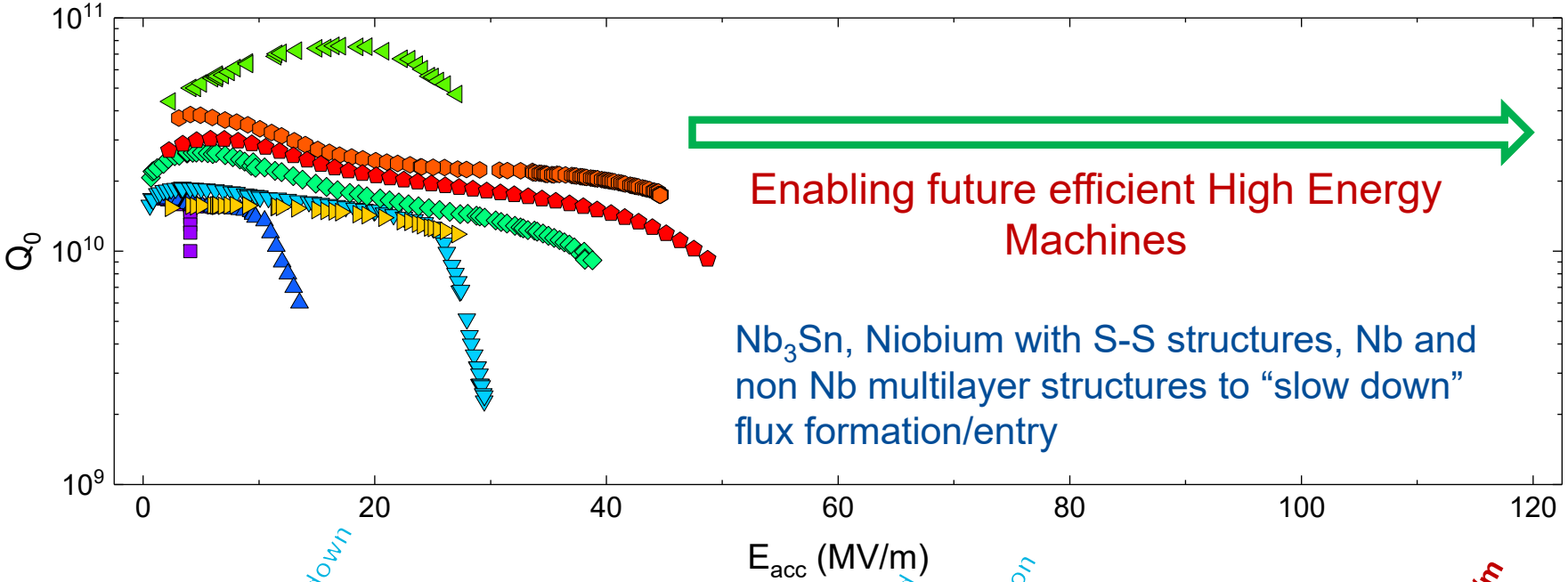


Enabling future efficient High Energy Machines

$Nb_3Sn$, Niobium with S-S structures, Nb and non Nb multilayer structures to "slow down" flux formation/entry

3 – 4 MV/m Multipacting

5 MV/m Thermal Breakdown

10 – 15 MV/m Field Emission

20 - 25 MV/m Q-SLOPE

35 – 40 MV/m

Q > 5e10 At medium field

Flux dissipation Flux expulsion

Q > 2e10 At high field

49 MV/m !!!

$E_{acc}$ > 100 MV/m Q > 5e10

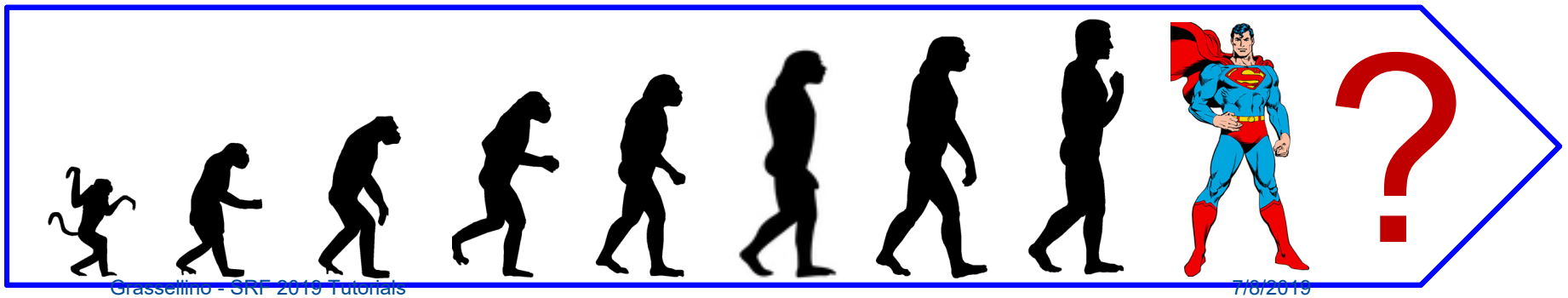

# Motivation State-of-the-Art SRF Technology

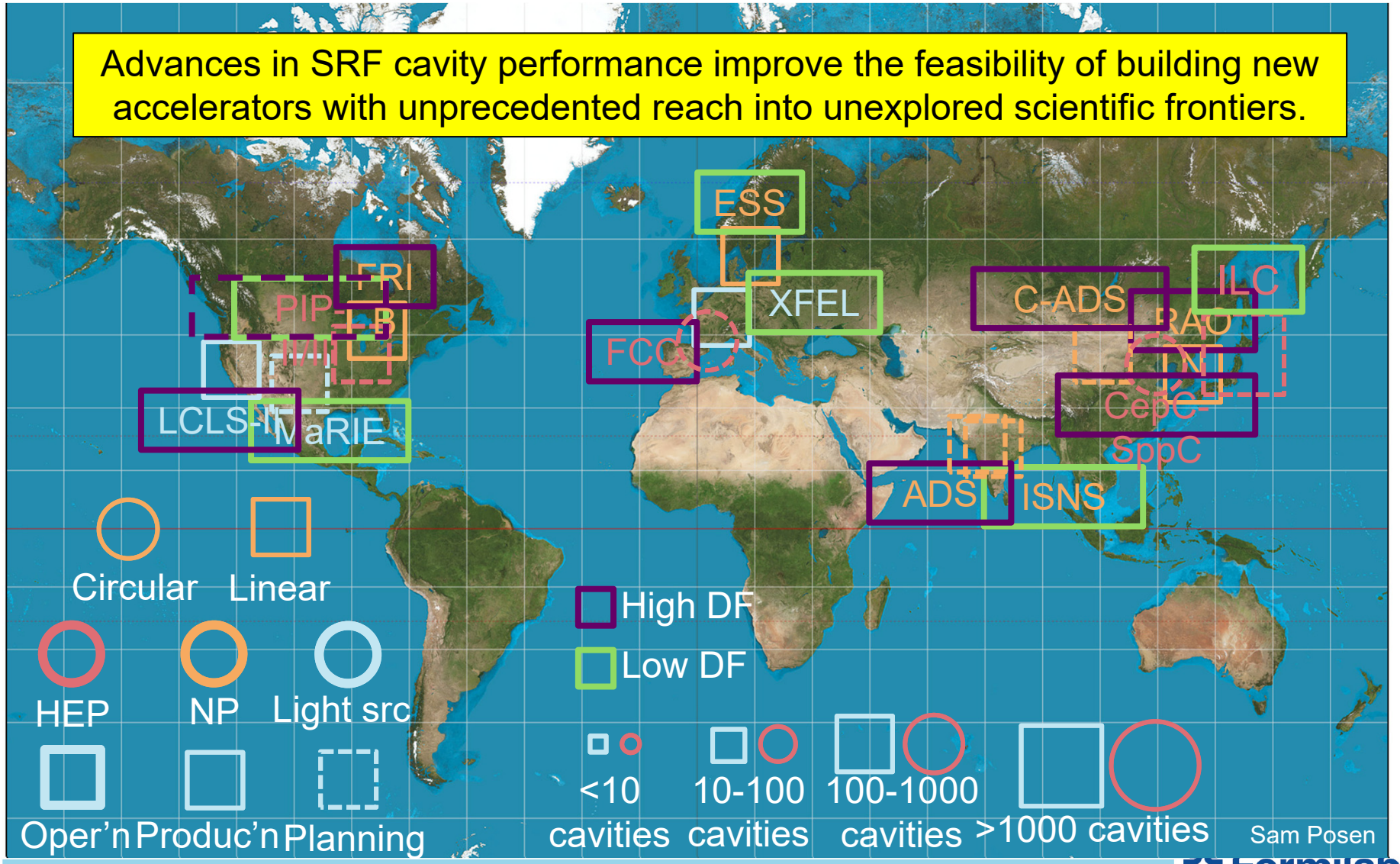


*Map from Wikipedia. Non-exhaustive facility list.*

# Make history!

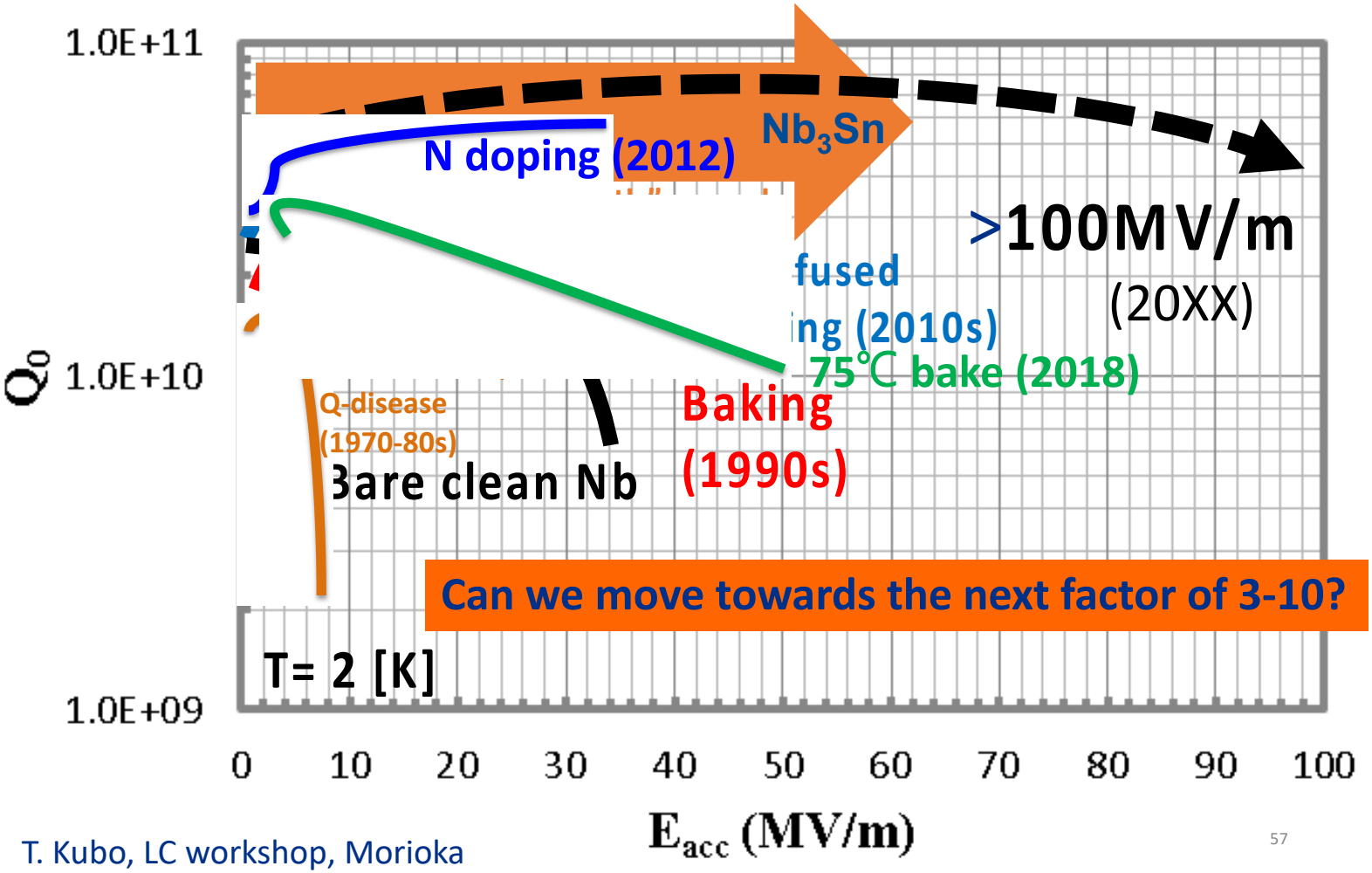


T. Kubo, LC workshop, Morioka

# Intro to SRF

# Superconducting state

- The superconducting state is characterized by the critical temperature $T_c$ and field $H_c$

$$H_c(T) = H_c(0) \cdot \left[1 - \left(\frac{T}{T_c}\right)^2\right]$$

- The external field is expelled from a superconductor if $H_{ext} < H_c$ for Type I superconductors.
- For Type II superconductors the external field can partially penetrate for $H_{ext} > H_{c1}$ and will completely penetrate at $H_{c2}$

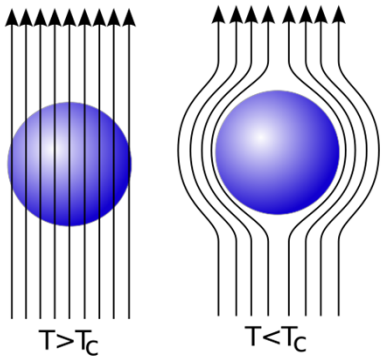


Superconductor in Meissner state = ideal diamagnetic

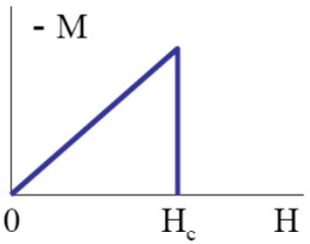


Complete Meissner effect in type-I superconductors

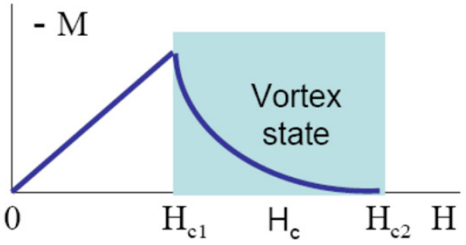


High-field partial Meissner effect in type-II superconductors

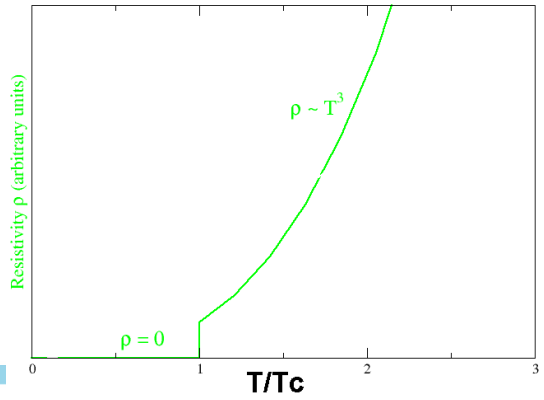


Type-I: Meissner state B = H + M = 0 for $H < H_c$; normal state at $H > H_c$

Type-II: Meissner state B = H + M = 0 for $H < H_{c1}$; partial flux penetration for $H_{c1} < H < H_{c2}$; normal state for $H > H_{c2}$

# Microscopic theory of superconductivity

**Bardeen-Cooper-Schrieffer (BCS) theory (1957).**
**Nobel prize in 1972**

January 7, 2008

## Low-Temperature Superconductivity

December was the 50th anniversary of the theory of superconductivity, the flow of electricity without resistance that can occur in some metals and ceramics.

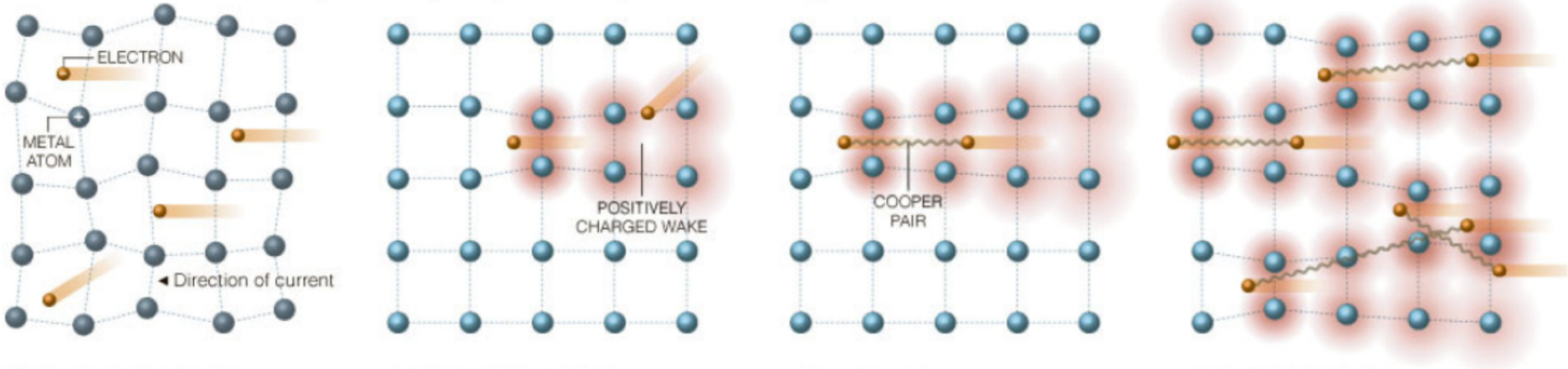


**ELECTRICAL RESISTANCE**
Electrons carrying an electrical current through a metal wire typically encounter resistance, which is caused by collisions and scattering as the particles move through the vibrating lattice of metal atoms.

**CRITICAL TEMPERATURE**
As the metal is cooled to low temperatures, the lattice vibration slows. A moving electron attracts nearby metal atoms, which create a positively charged wake behind the electron. This wake can attract another nearby electron.

**COOPER PAIRS**
The two electrons form a weak bond, called a Cooper pair, which encounters less resistance than two electrons moving separately. When more Cooper pairs form, they behave in the same way.

**SUPERCONDUCTIVITY**
If a pair is scattered by an impurity, it will quickly get back in step with other pairs. This allows the electrons to flow undisturbed through the lattice of metal atoms. With no resistance, the current may persist for years.

*Sources: Oak Ridge National Laboratory; Philip W. Phillips*

JONATHAN CORUM/THE NEW YORK TIMES

# BCS theory

## What is the phase coherence?

Incoherent (normal) crowd:
each electron for itself

Phase-coherent (superconducting) condensate
of electrons

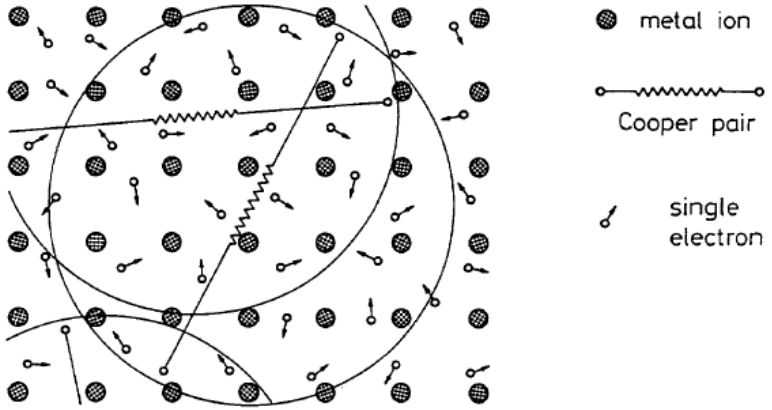


Figure 22: Cooper pairs and single electrons in the crystal lattice of a superconductor. (After Essmann and Träuble [12]).

- **Attraction** between electrons with antiparallel momenta **k** and spins due to exchange of lattice vibration quanta (phonons)
- Instability of the normal Fermi surface due to bound states of electron (Cooper) pairs
- Bose condensation of overlapping Cooper pairs in a coherent superconducting state.
- Scattering on electrons does not cause the electric resistance because it would break the Cooper pair

**The strong overlap of many Cooper pairs results in the macroscopic phase coherence**



Fermilab

# Simplified explanation for zero DC resistivity

- NC
  - Resistance to flow of electric current
  - Free electrons scatter off impurities, lattice vibrations (phonons)
- SC
  - Cooper pairs carry all the current
  - Cooper pairs do not scatter off impurities due to their coherent state
  - Some pairs are broken at **T > 0 K** due to phonon interaction
- But supercurrent component has zero resistance

# Superconductivity: DC case

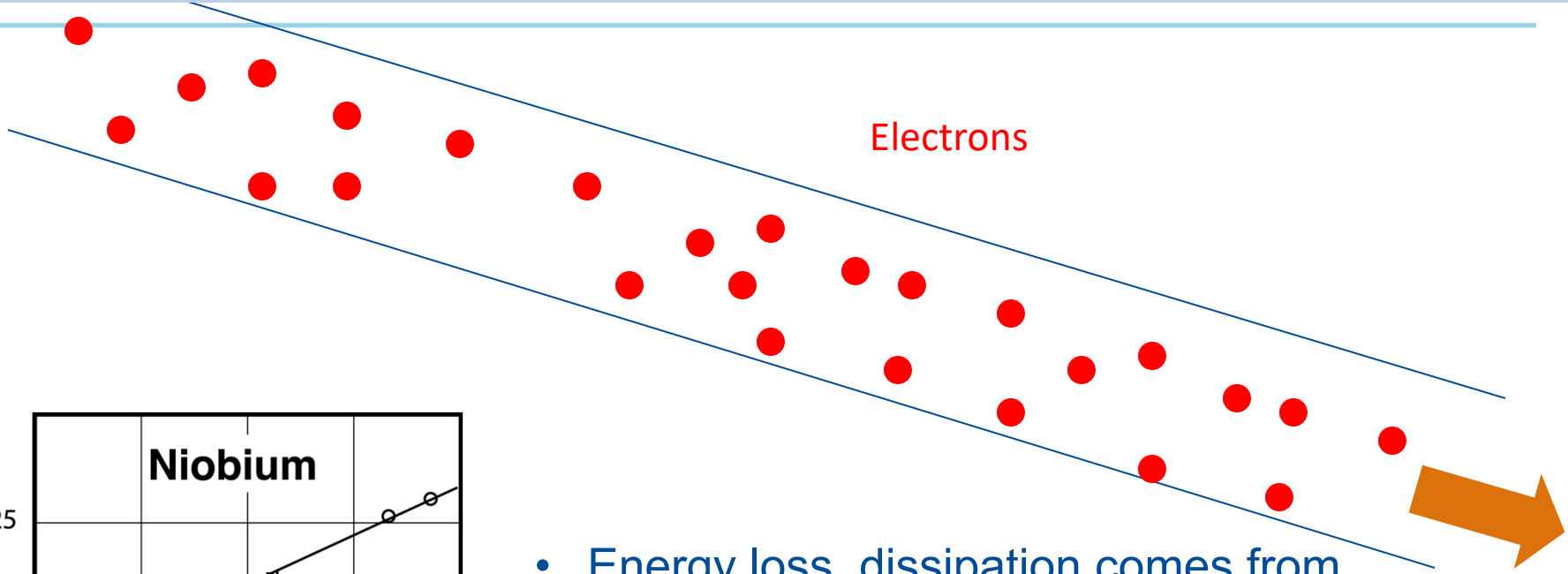


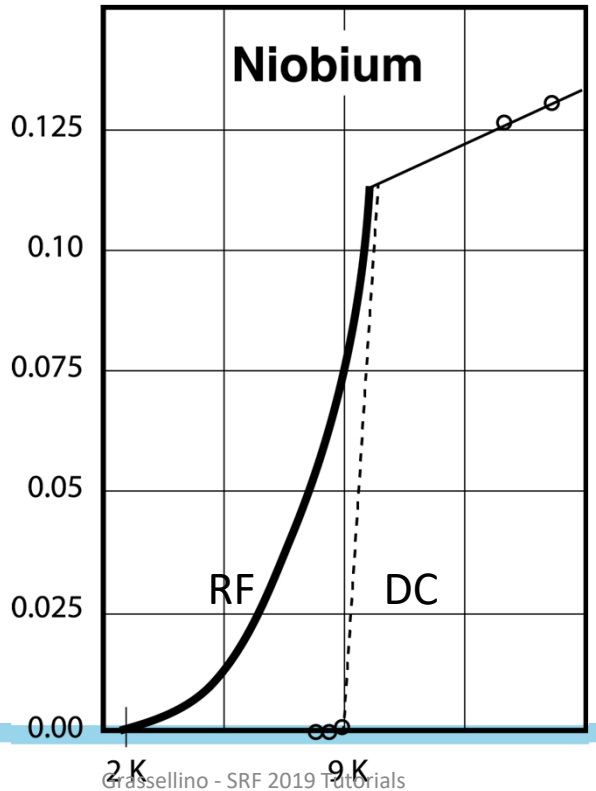


- Energy loss, dissipation comes from scattering of electrons with defects or impurities
- In normal conducting state electrons scatter
- In superconducting state, cooper pairs form and move 'with no friction'

# Superconductivity: DC case

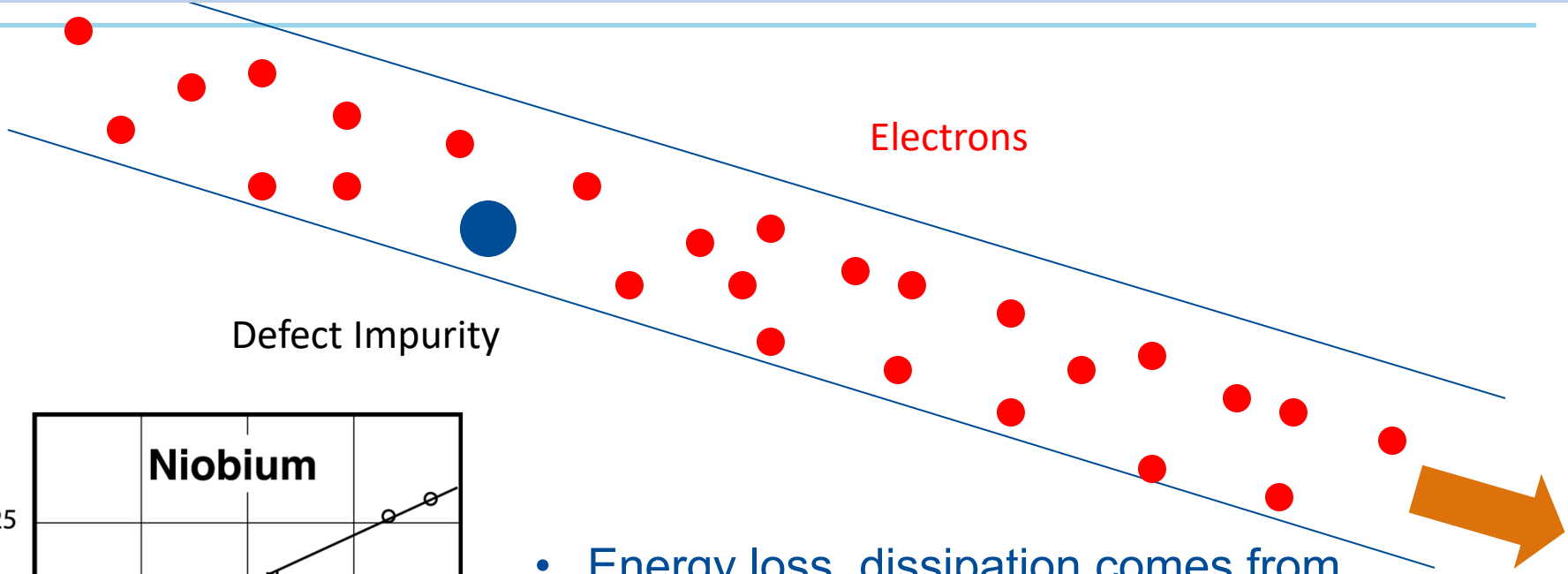


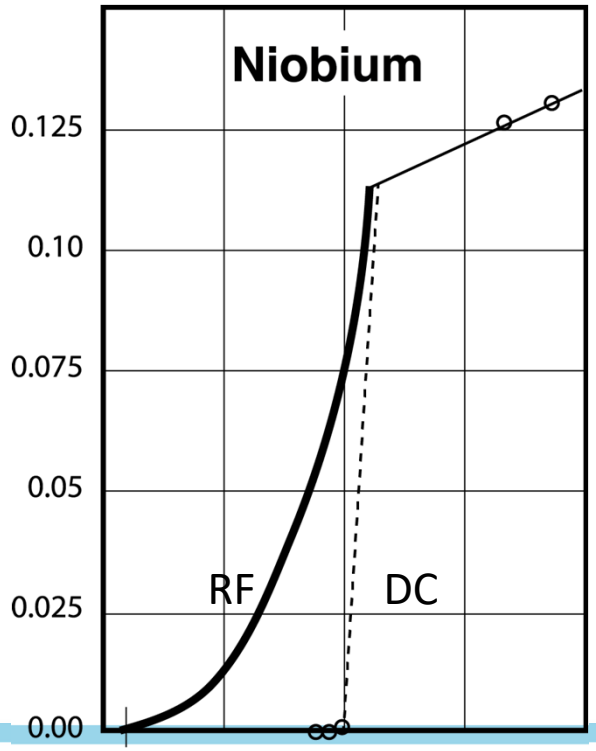


- Energy loss, dissipation comes from scattering of electrons with defects or impurities
- In normal conducting state electrons scatter
- In superconducting state, cooper pairs form and move 'with no friction'

# Superconductivity: DC case

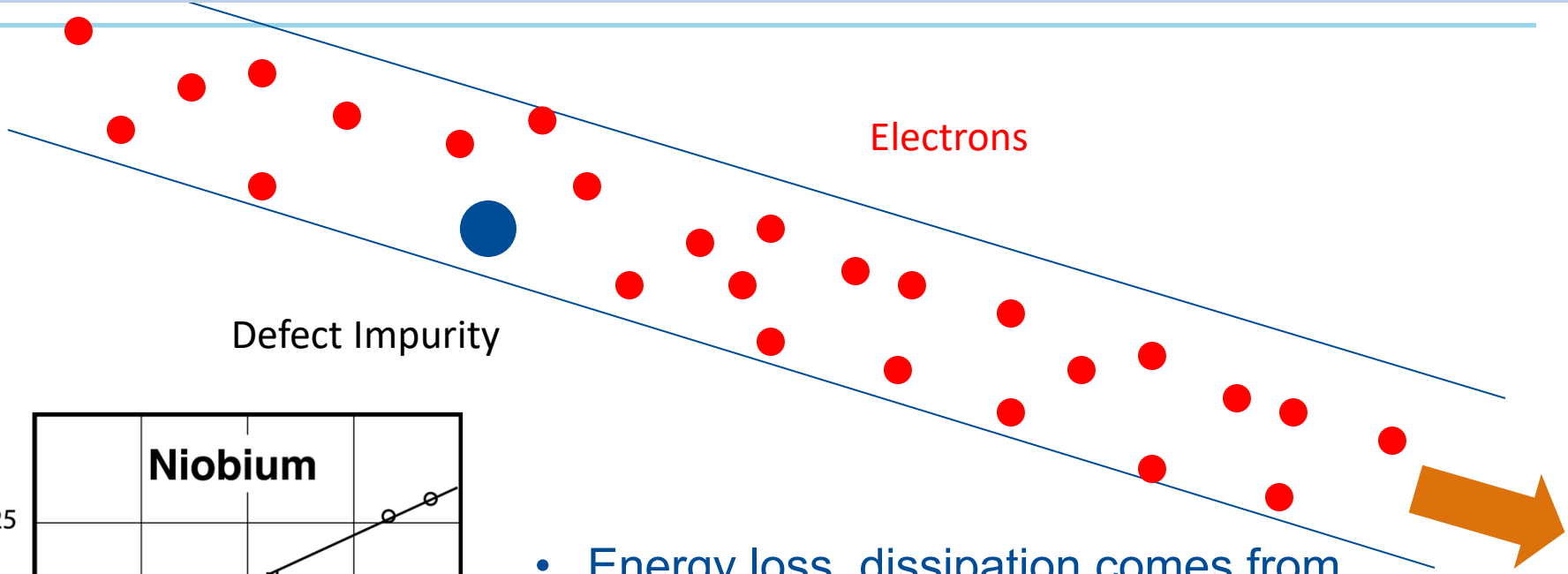


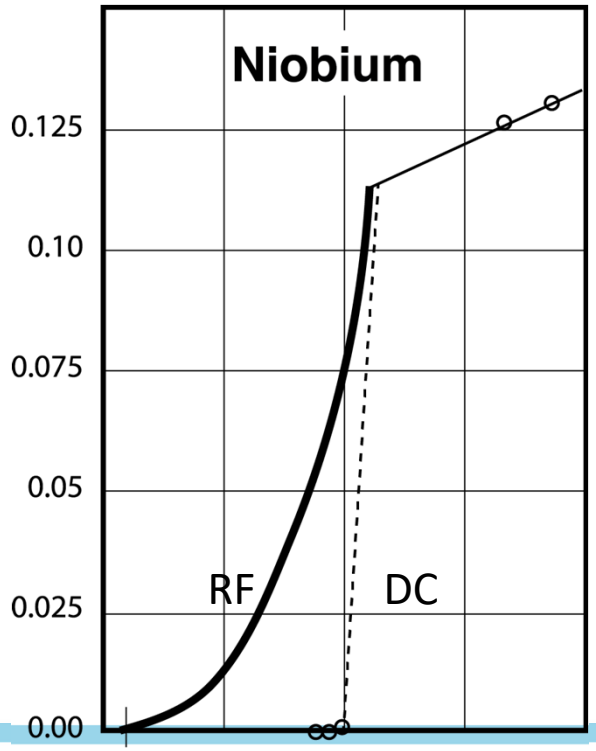


- Energy loss, dissipation comes from scattering of electrons with defects or impurities
- In normal conducting state electrons scatter
- In superconducting state, cooper pairs form and move ‘with no friction’

# Superconductivity: DC case

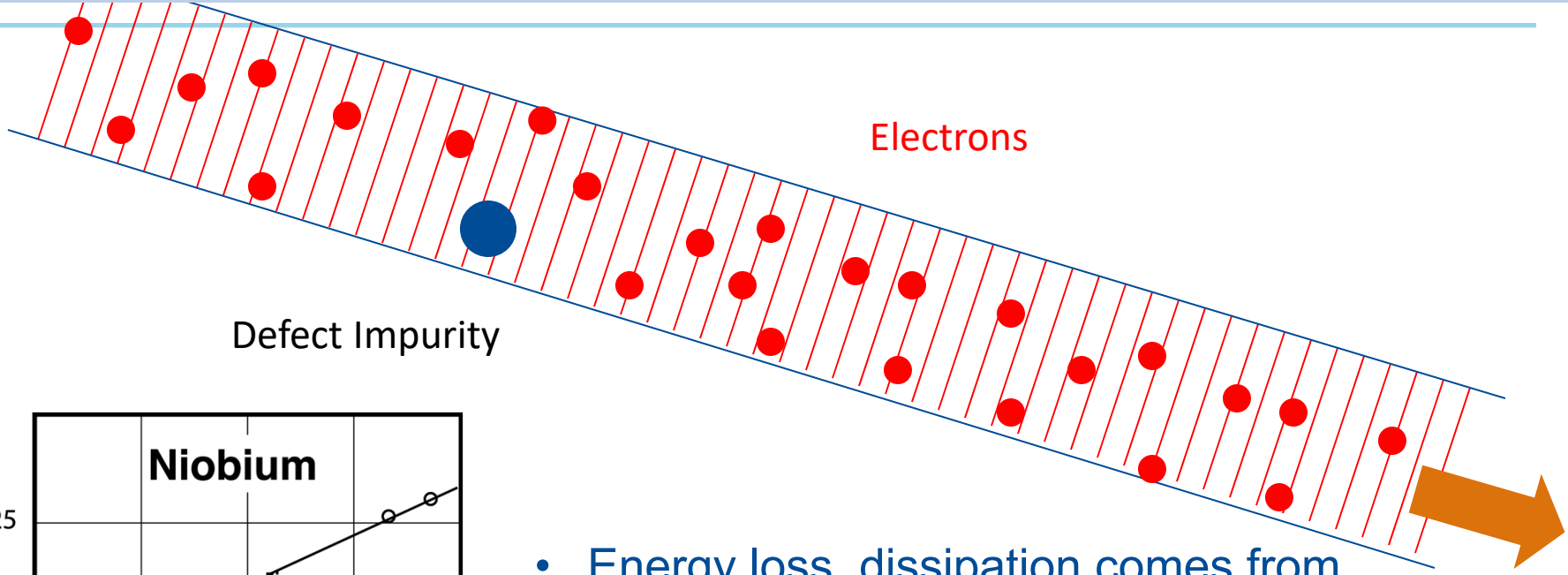


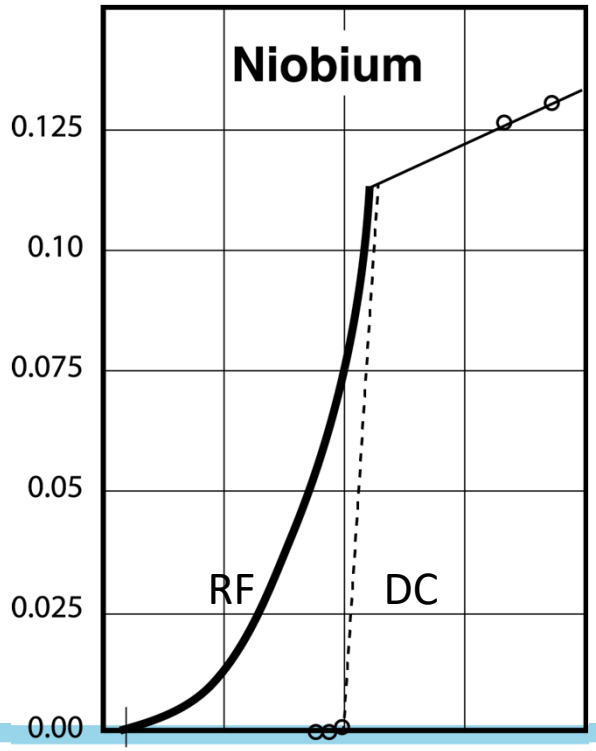


- Energy loss, dissipation comes from scattering of electrons with defects or impurities
- In normal conducting state electrons scatter
- In superconducting state, cooper pairs form and move ‘with no friction’

# Superconductivity: DC case

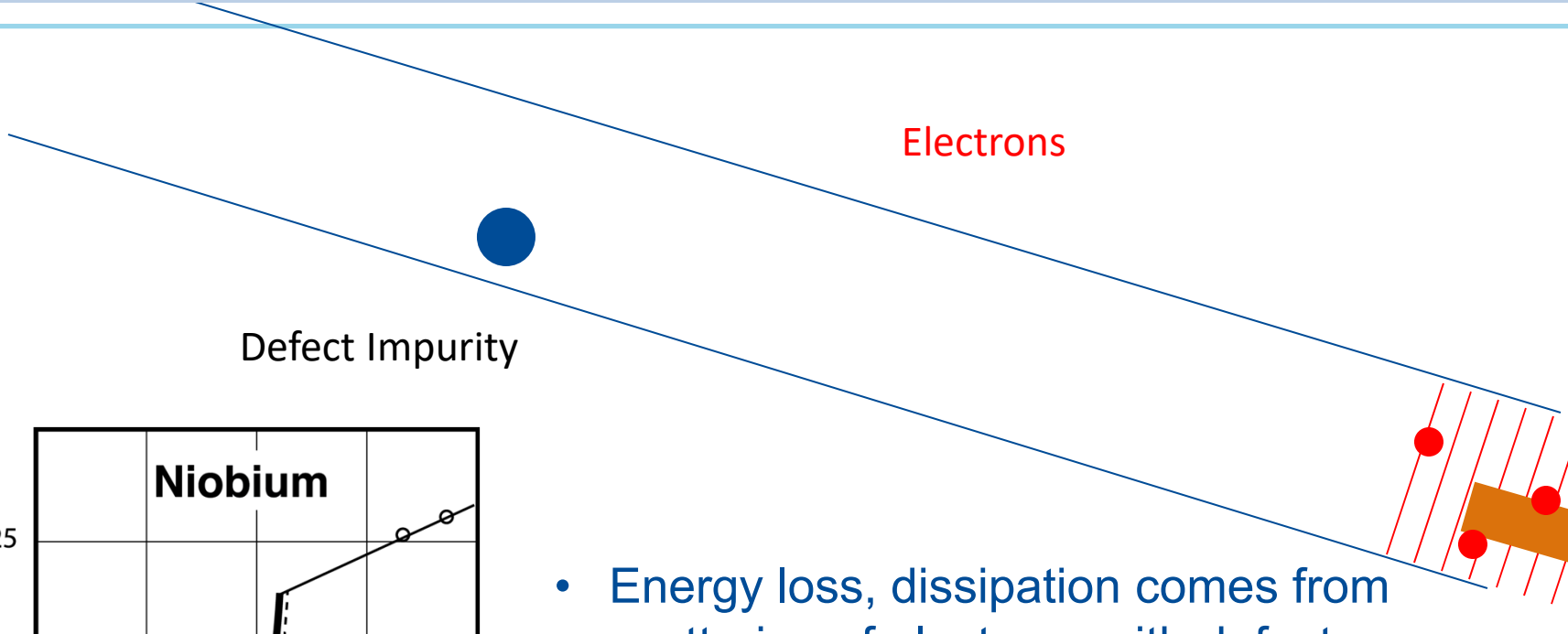


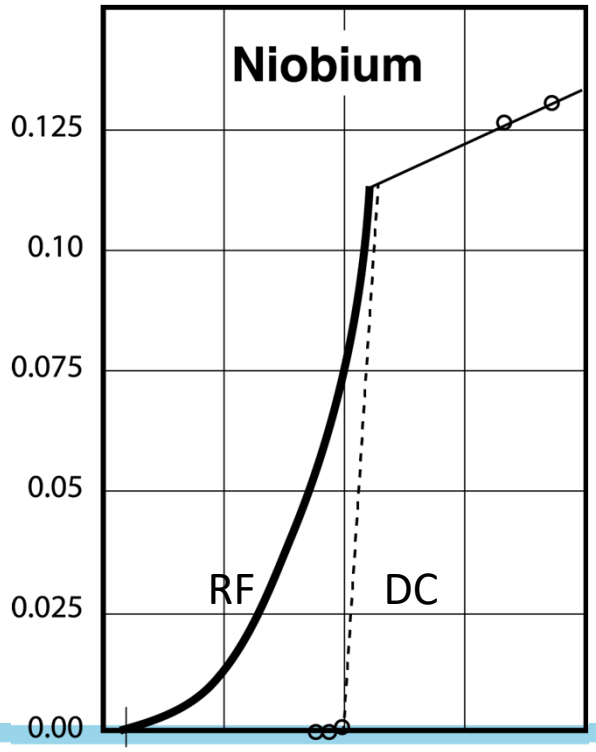


- Energy loss, dissipation comes from scattering of electrons with defects or impurities
- In normal conducting state electrons scatter
- In superconducting state, cooper pairs form and move ‘with no friction’

# Superconductivity RF case- Small Non-Zero Resistance

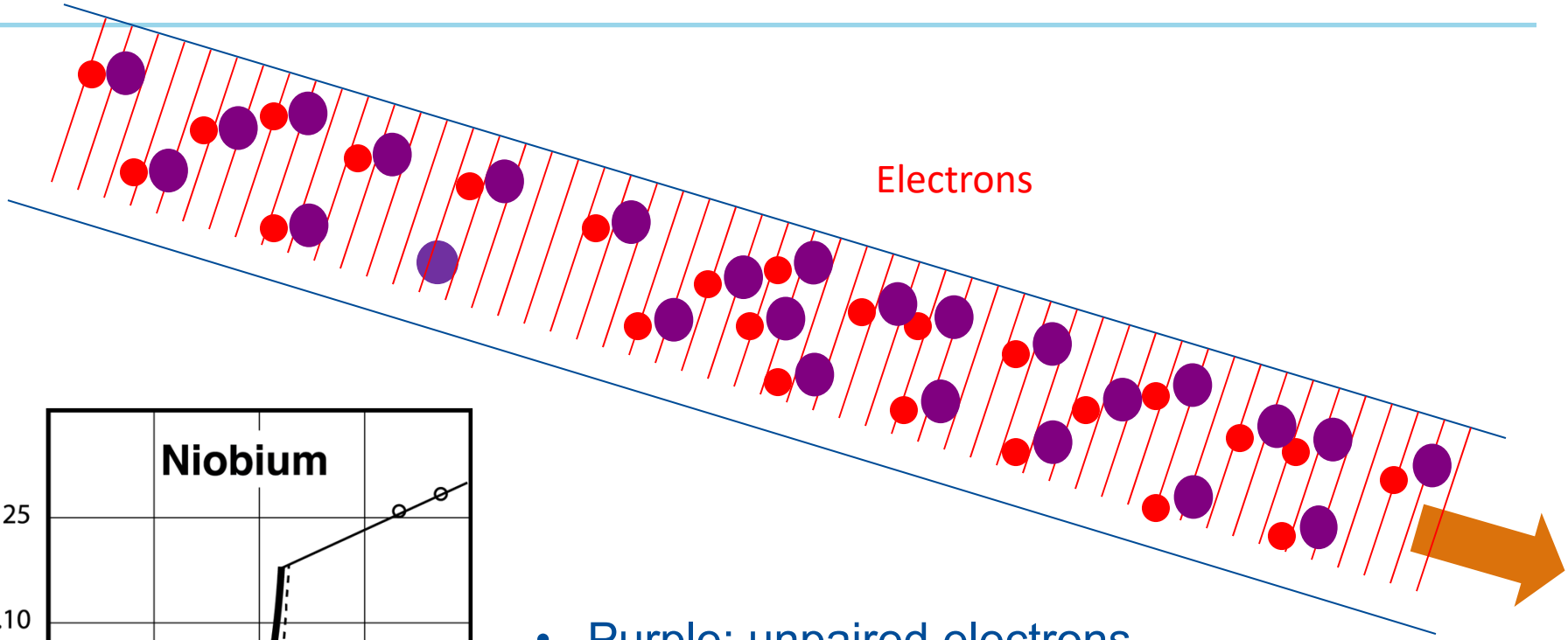


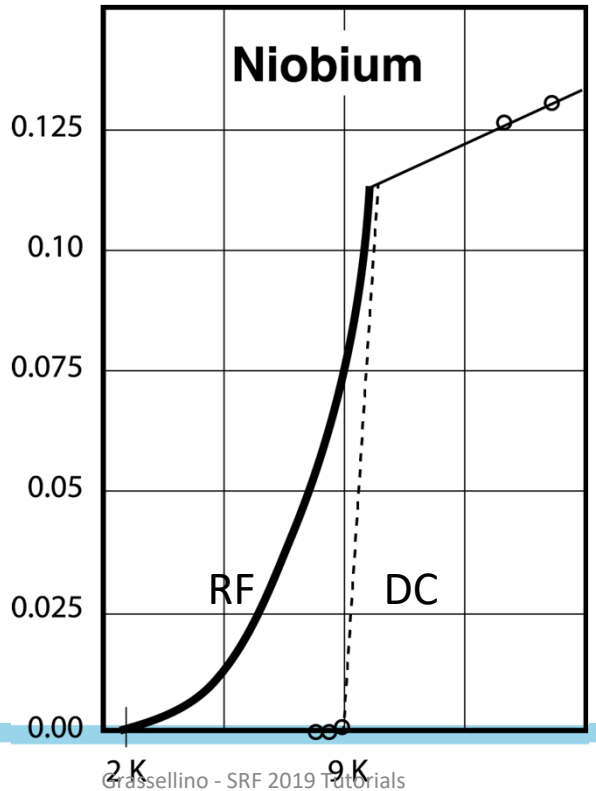


- Purple: unpaired electrons
- Red : Cooper pairs

- Unpaired electrons can scatter and cause RF resistance and loss in efficiency (lower Q)

# Superconductivity RF case- Small Non-Zero Resistance

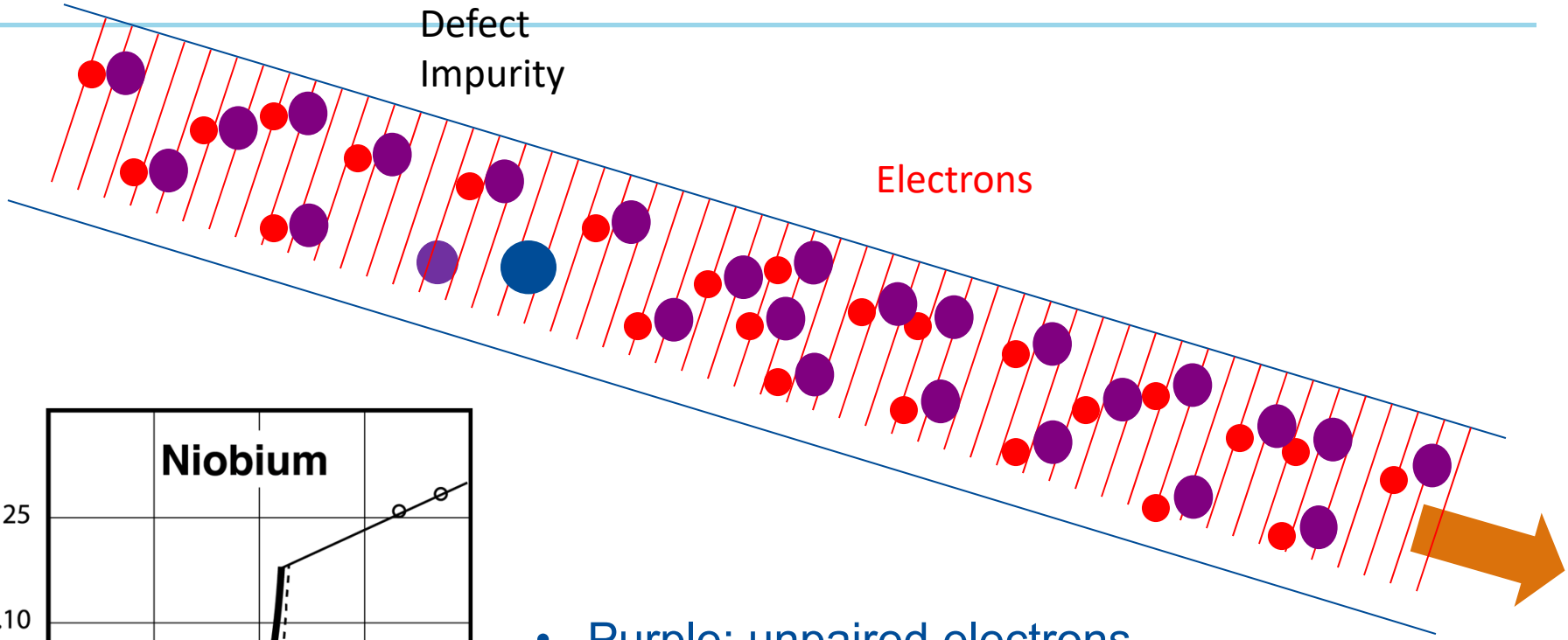


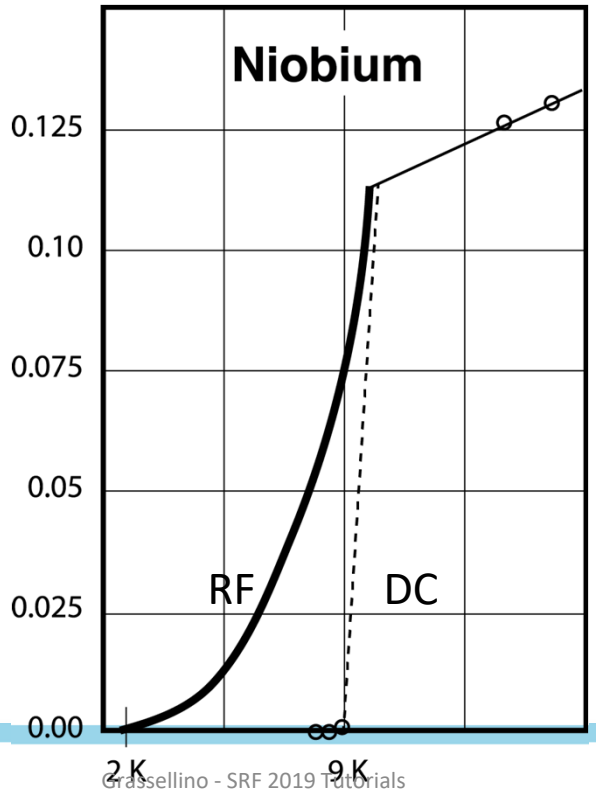


- Purple: unpaired electrons
- Red : Cooper pairs

- Unpaired electrons can scatter and cause RF resistance and loss in efficiency (lower Q)

# Superconductivity RF case- Small Non-Zero Resistance

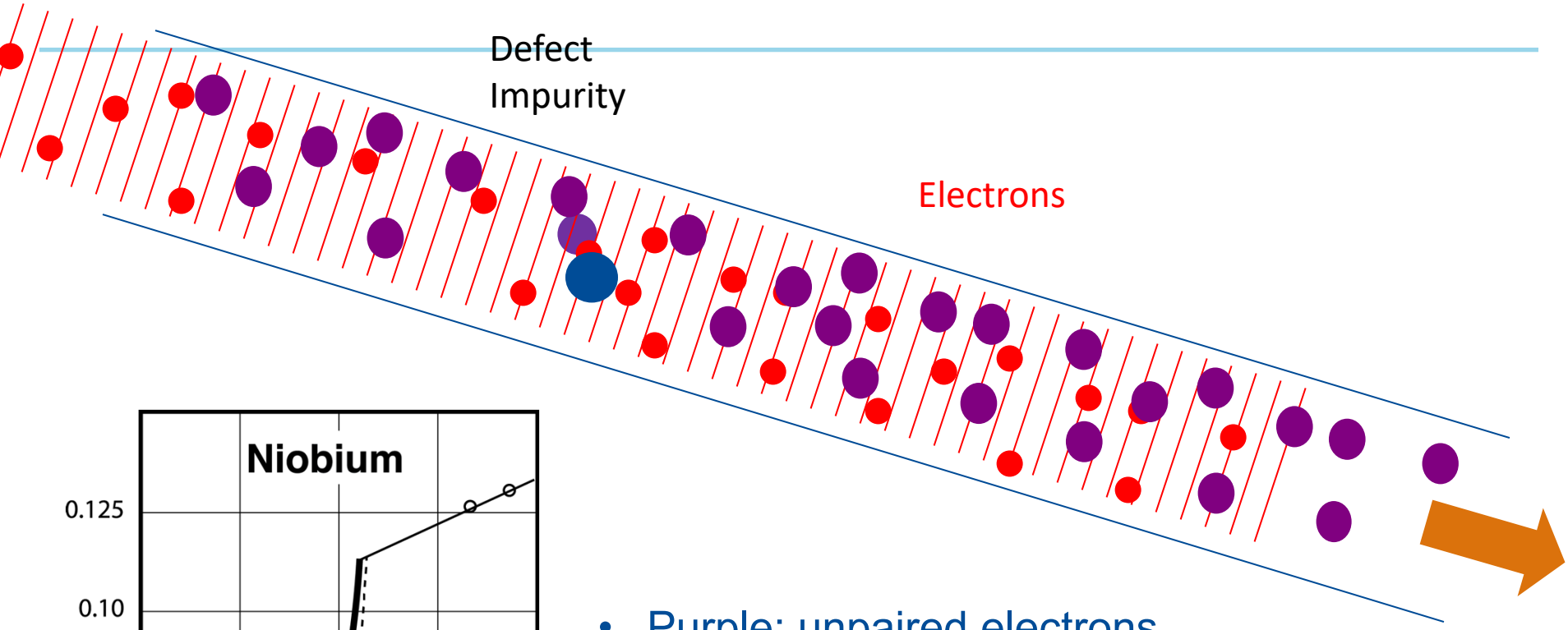


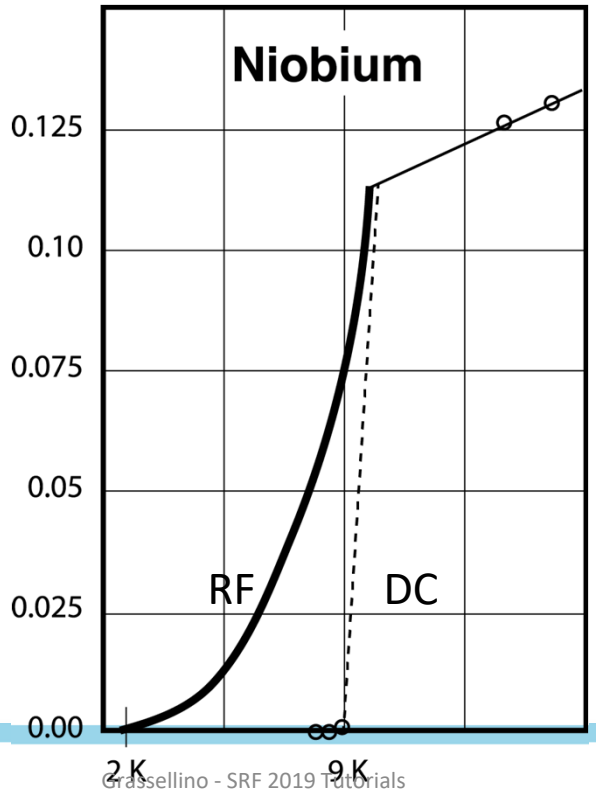


- Purple: unpaired electrons
- Red : Cooper pairs

- Unpaired electrons can scatter and cause RF resistance and loss in efficiency (lower Q)

# Vortex state

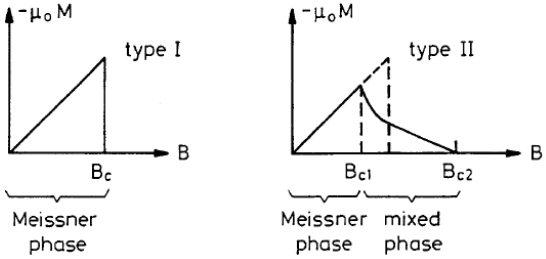


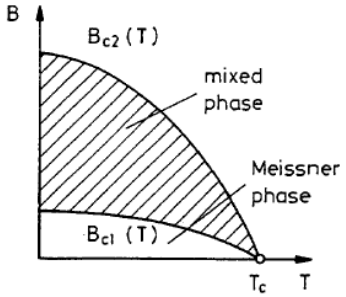


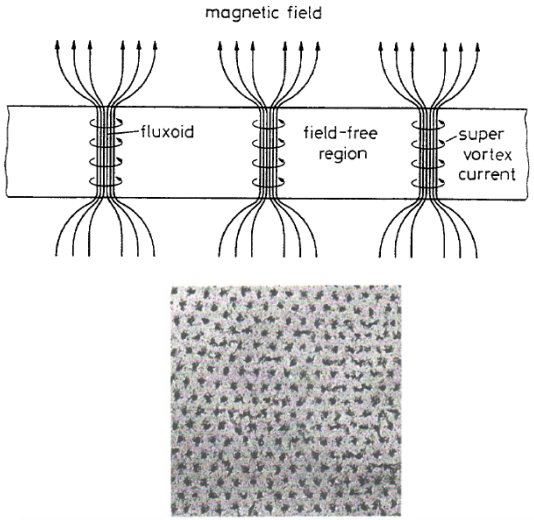




## Single vortex line

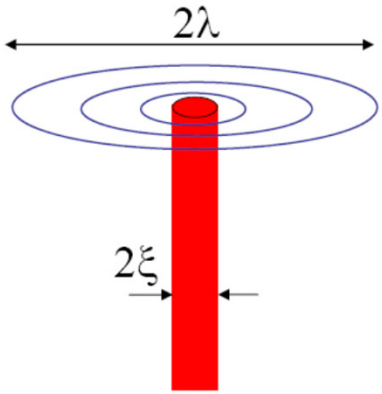


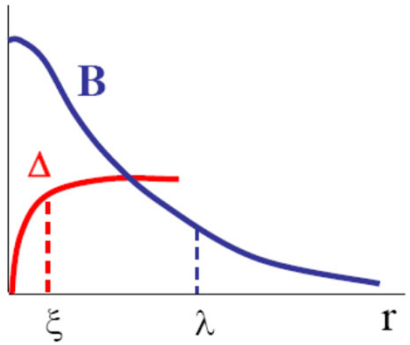


- Small core region $r < \xi$ where $\Delta(r)$ is suppressed
- Region of circulating supercurrents, $r < \lambda$.
- Each vortex carries the flux quantum $\phi_0$

## Important lengths and fields

- Coherence length $\xi$ and magnetic (London) penetration depth $\lambda$

$$B_{c1} = \frac{\phi_0}{2\pi\lambda^2}\left(\ln\frac{\lambda}{\xi} + 0.5\right), \qquad B_c = \frac{\phi_0}{2\sqrt{2}\pi\lambda\xi}, \qquad B_{c2} = \frac{\phi_0}{2\pi\xi^2}$$

Type-II superconductors: $\lambda/\xi > 1/\sqrt{2}$: For clean Nb, $\lambda \approx 40$ nm, $\xi \approx 38$ nm



Fermilab

# Surface resistance

$$R_s(T) = R_{BCS}(T) + R_{residual}$$

Fundamental part described by Bardeen-Cooper-Schrieffer (BCS) theory

Residual resistance due to other contributions

# Surface resistance

$Q \sim 1/R_s$

$$R_s(T) = R_{BCS}(T) + R_{residual}$$

Fundamental part described by Bardeen-Cooper-Schrieffer (BCS) theory

Residual resistance due to other contributions

# Surface resistance of cavities

$$R_s(T) = R_{BCS}(T) + R_{res}$$

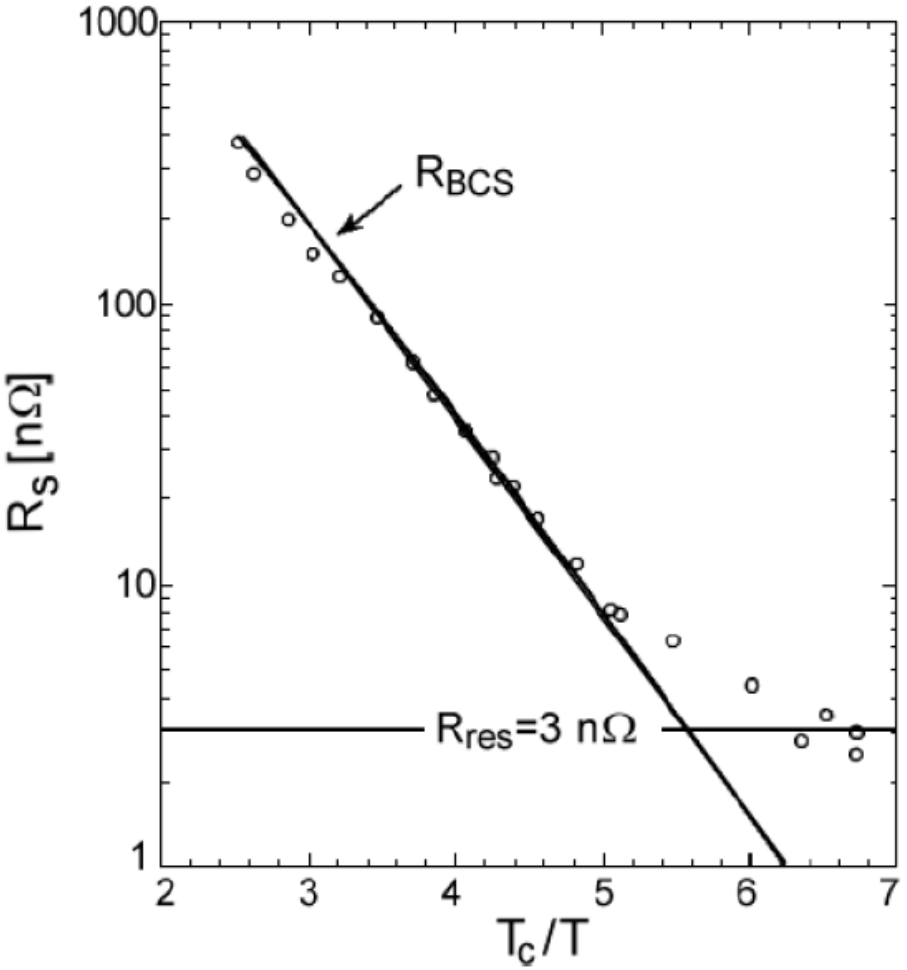


$$\rightarrow \quad R_{BCS}(T) = \frac{A\omega^2}{T} e^{-\frac{\Delta}{k_B T}}$$

The BCS surface resistance is described by Mattis-Bardeen theory and comes from thermally excited quasi-particles

$$\rightarrow \quad R_{res}$$

The residual resistance can come from different extrinsic contributions :

- Impurities/defects in the surface
- Hydrides precipitates
- Trapped flux ($B_{trap}$)
- …

# Q(E) curve

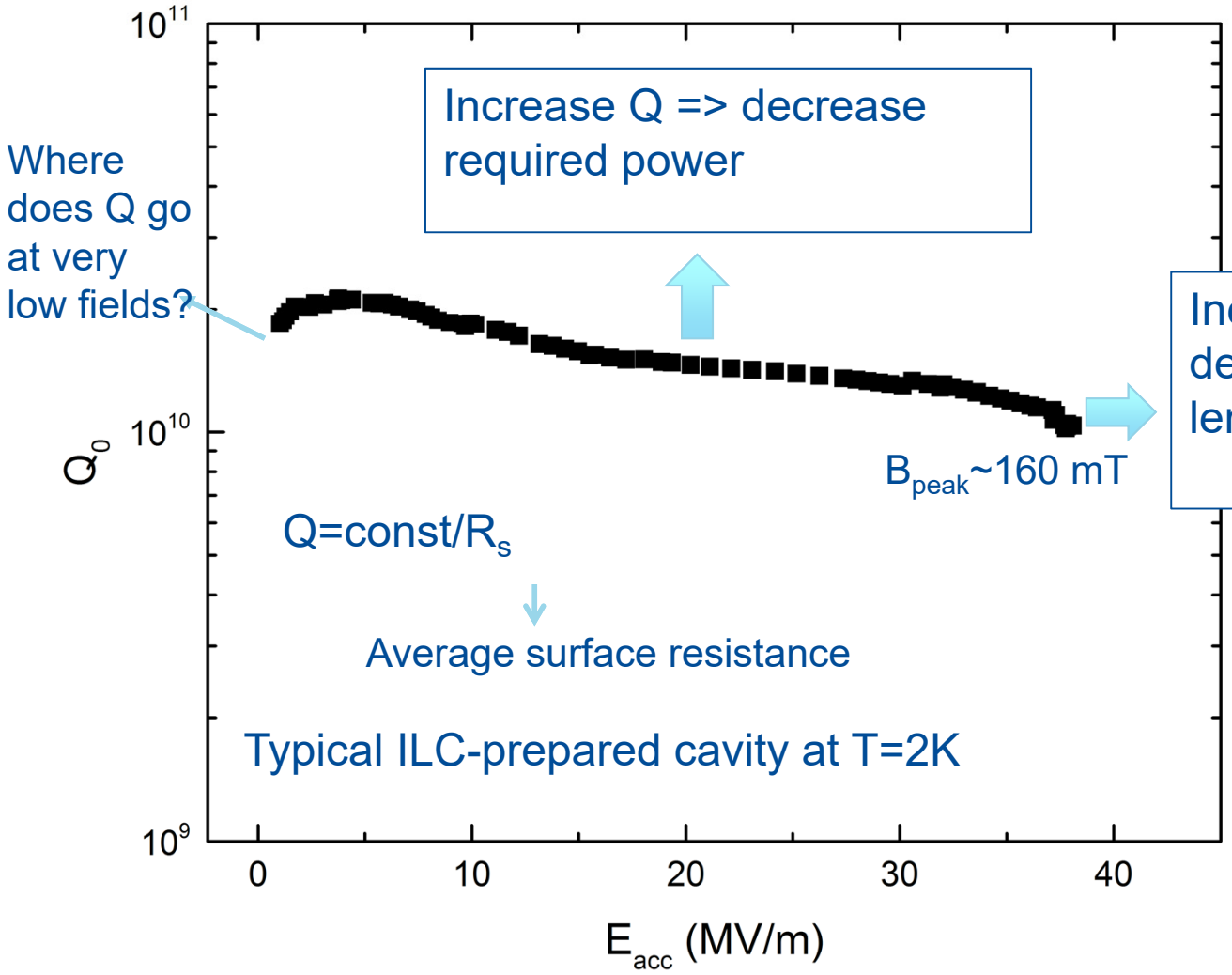


Increase Q => decrease required power

Where does Q go at very low fields?

Increase max $E_{acc}$ => decrease accelerator length

$B_{peak}$~160 mT

Q=const/$R_s$

Average surface resistance

Typical ILC-prepared cavity at T=2K

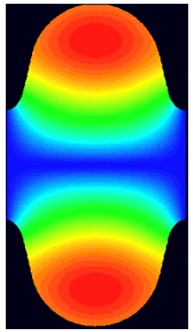

Surface magnetic field B

# Typical Cavity Preparation Steps

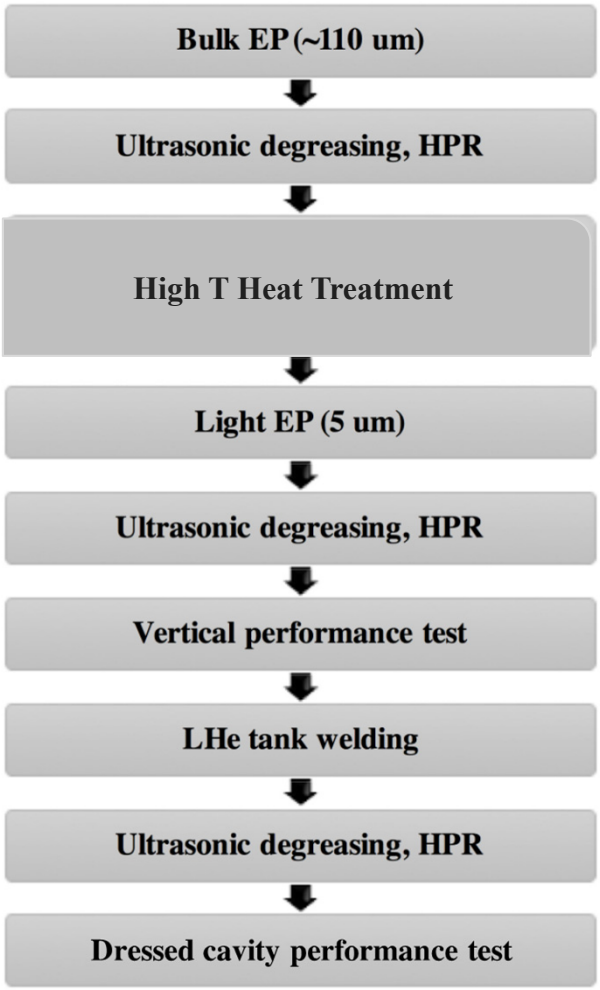

# Q(E) portions – Q slopes

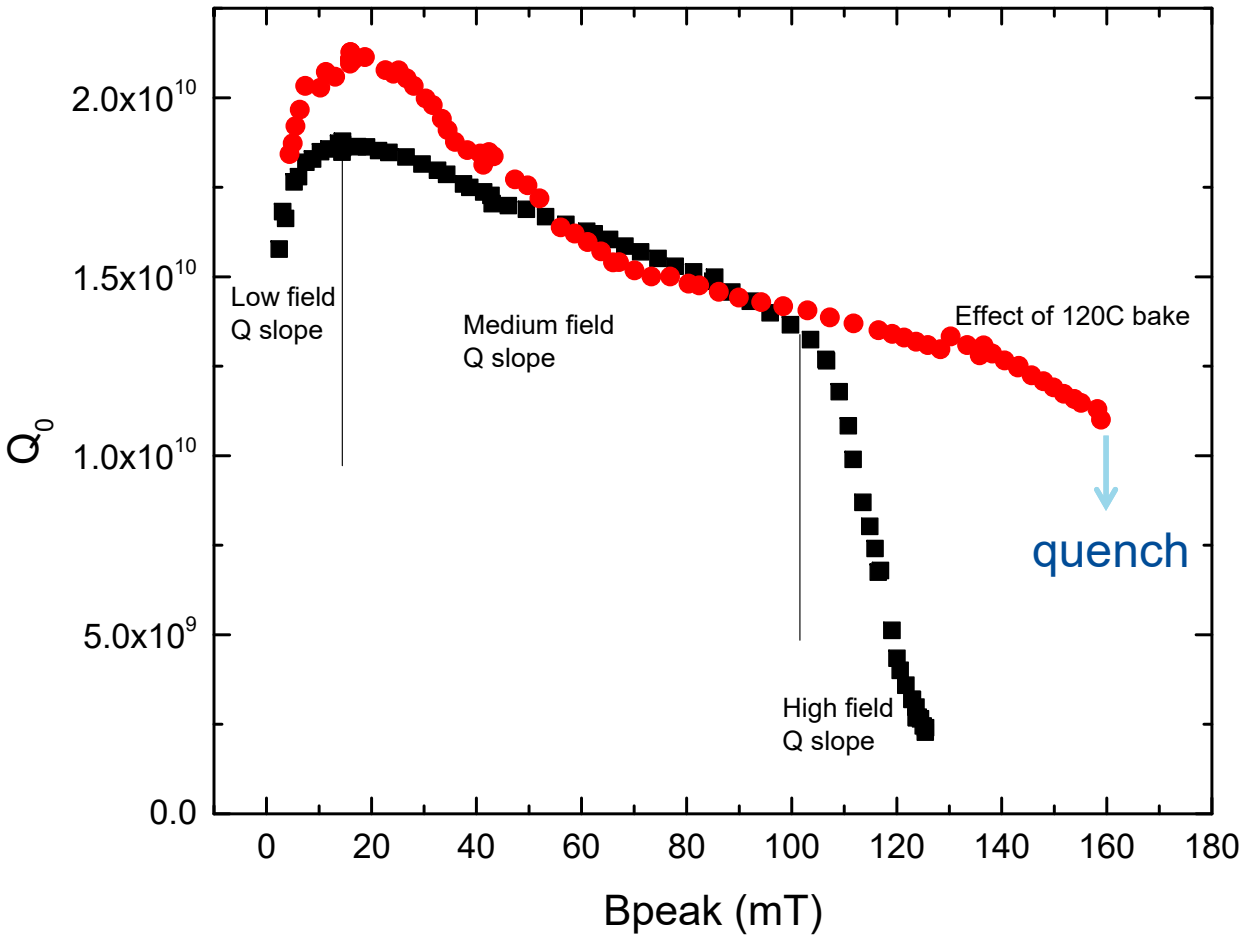

# Tracing to the different surface resiatnce components

- Cavity $Q_0$ is a function of both temperature (T) and surface magnetic field H
  - Q slopes
- Temperature dependence of Rbcs for all treatments is well-understood -> thermally excited quasiparticles give Rbcs ~ 1/T*exp(-Δ/kT) at all RF fields (gap etc may change though)
- Q = G/<Rs>, where <Rs> = Rbcs(T) + Rres
- Crucial question – how does Rs(B) emerge from its components Rbcs(B) and Rres (B)?

# How to decompose the BCS and residual at all fields?

- Obtain as many Q(B,T) measurements as practical at ALL fields (not only at a single low field)
- At each fixed field fit corresponding Q(T) to extract Rres
  - Also gives Rbcs(T) = Rs(T)-Rres
- Or simply measure the lowest T Q(E) curve and take it as residual -> frequently an excellent approximation

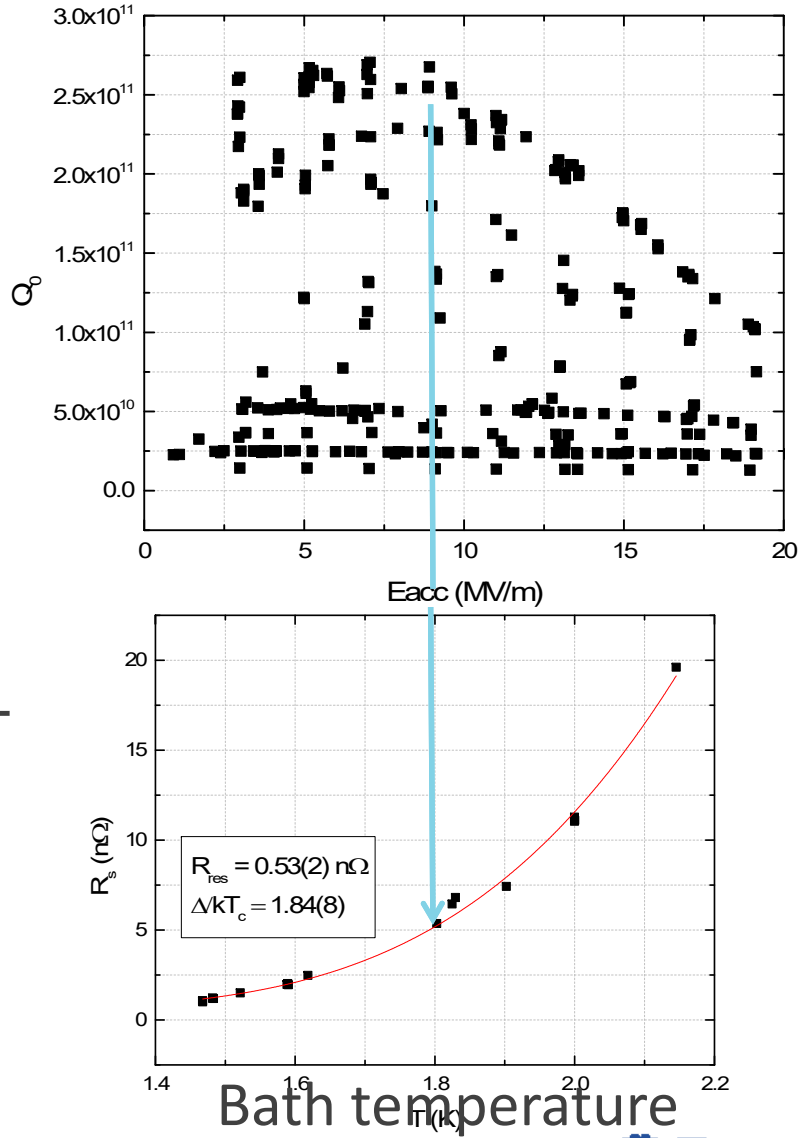


A. Romanenko and A. Grassellino
Appl. Phys. Lett. **102**, 252603 (2013)

# Plethora of insight – standard treatments

A. Romanenko and A. Grassellino, Appl. Phys. Lett. **102**, 252603 (2013)

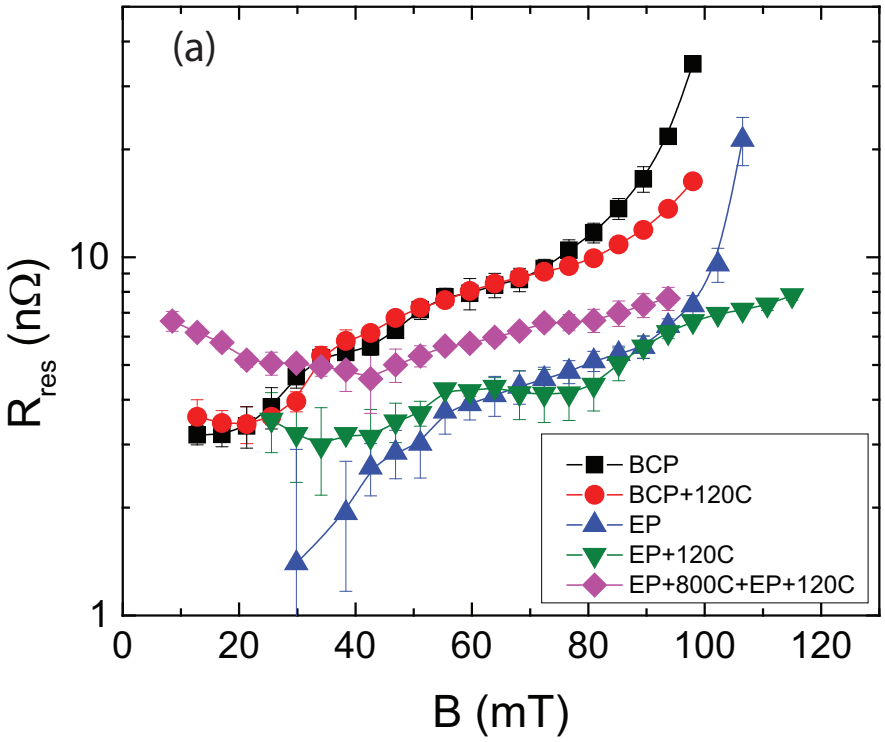


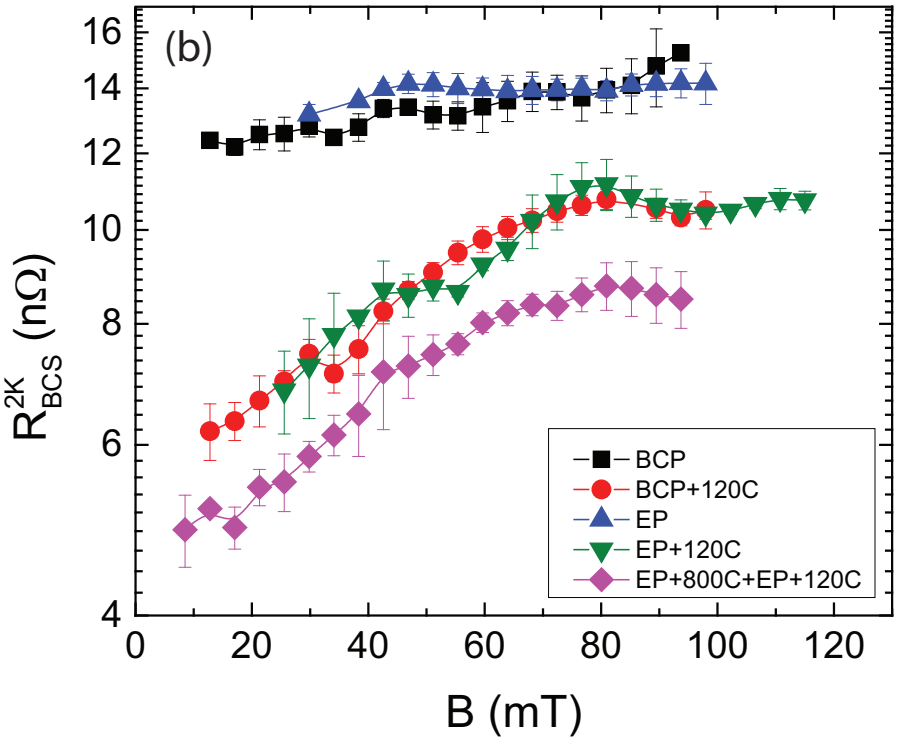


- High field Q slope is due to Rres
- Medium field Q slope is a combination of both Rres and Rbcs
- Low field Q slope is due to Rres
- Rbcs decreases but becomes strongly field dependent after 120C

# Is RF surface temperature increase significant?

- It was suggested that a "thermal feedback" may cause a slope in the Q0(E) curve since Rbcs(T)~1/T*exp(-const/T) – strongly T-dependent
  - Trf increasing at higher fields=> Rbcs(Trf) increases => slope
- Only thermal simulations based on Rs(H) from RF measurements were reported in the literature
  - Kapitza resistance has a big uncertainty

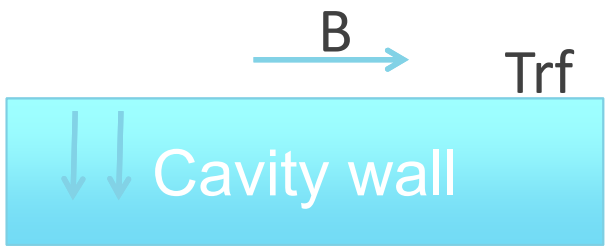


Heat flux= ½ $Rs*H^2$

Helium bath @ Tbath

Trf > Tout > Tbath

$T_{out}$ we can measure by T-mapping independently => only thermal conductivity needed to find Trf

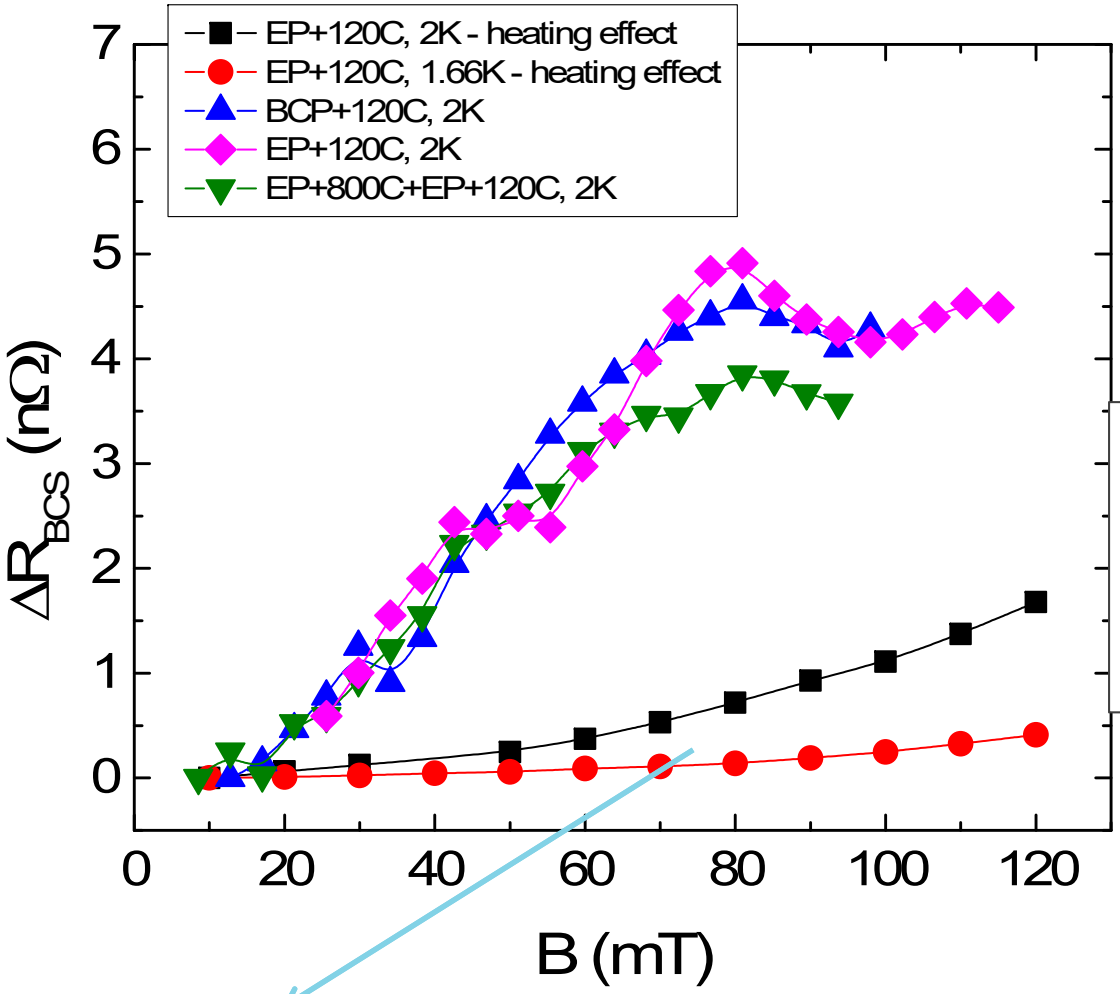


From combined T-map/RF measurements

Heating is negligible, Rbcs increase with field is a genuine effect

- Thermal feedback does not explain the medium field Q slope

# Insights from Rs decomposition into BCS and residual

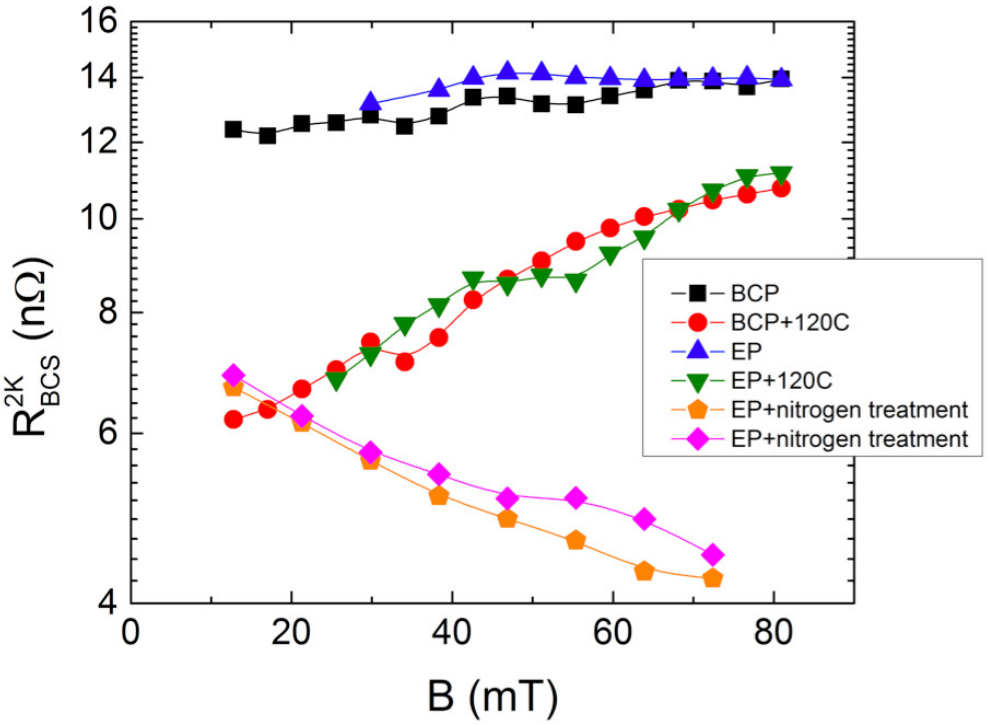


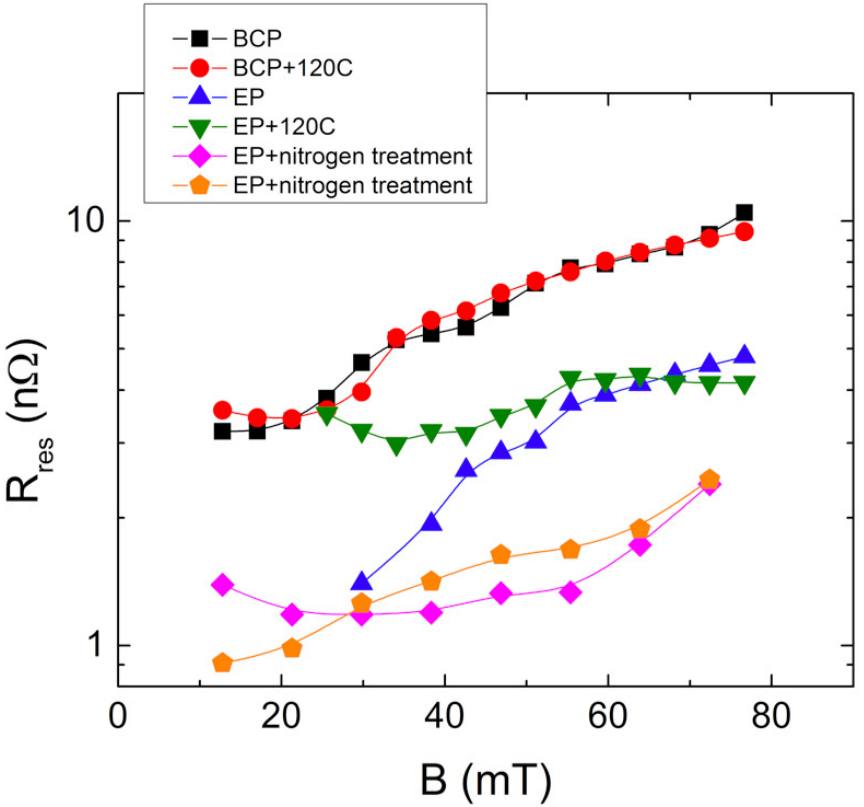


- Specific components driving Q-slopes can be understood
- Quoting Rbcs and Rres always requires to specify at what RF field!

# Insights from Rs decomposition into BCS and residual

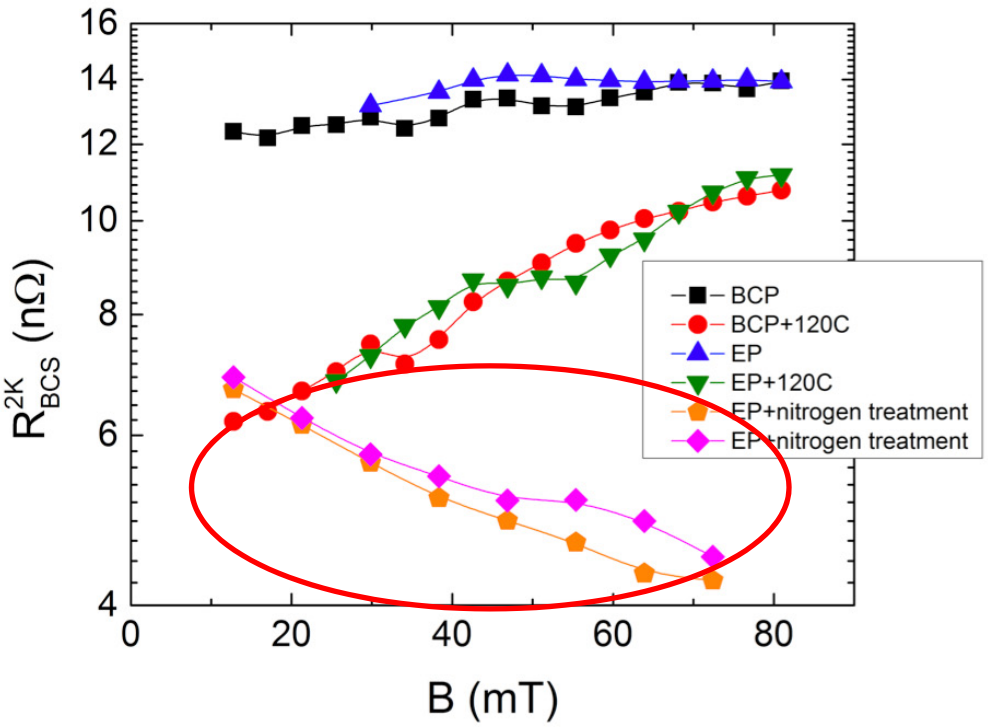


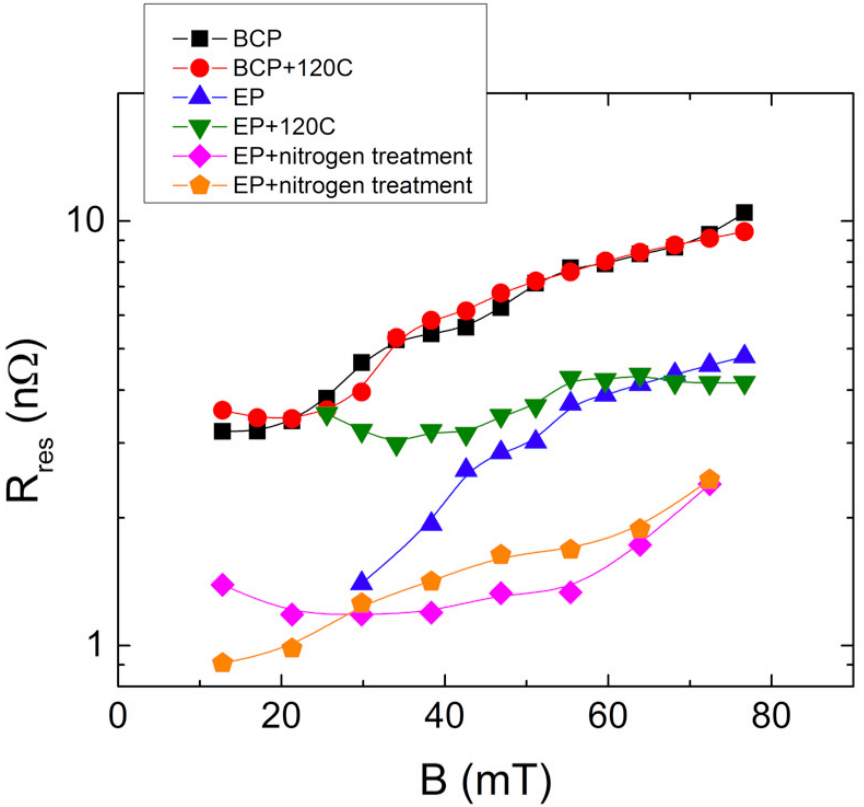


- Specific components driving Q-slopes can be understood
- Quoting Rbcs and Rres always requires to specify at what RF field!

# Cavity performance limitations – progress in understanding

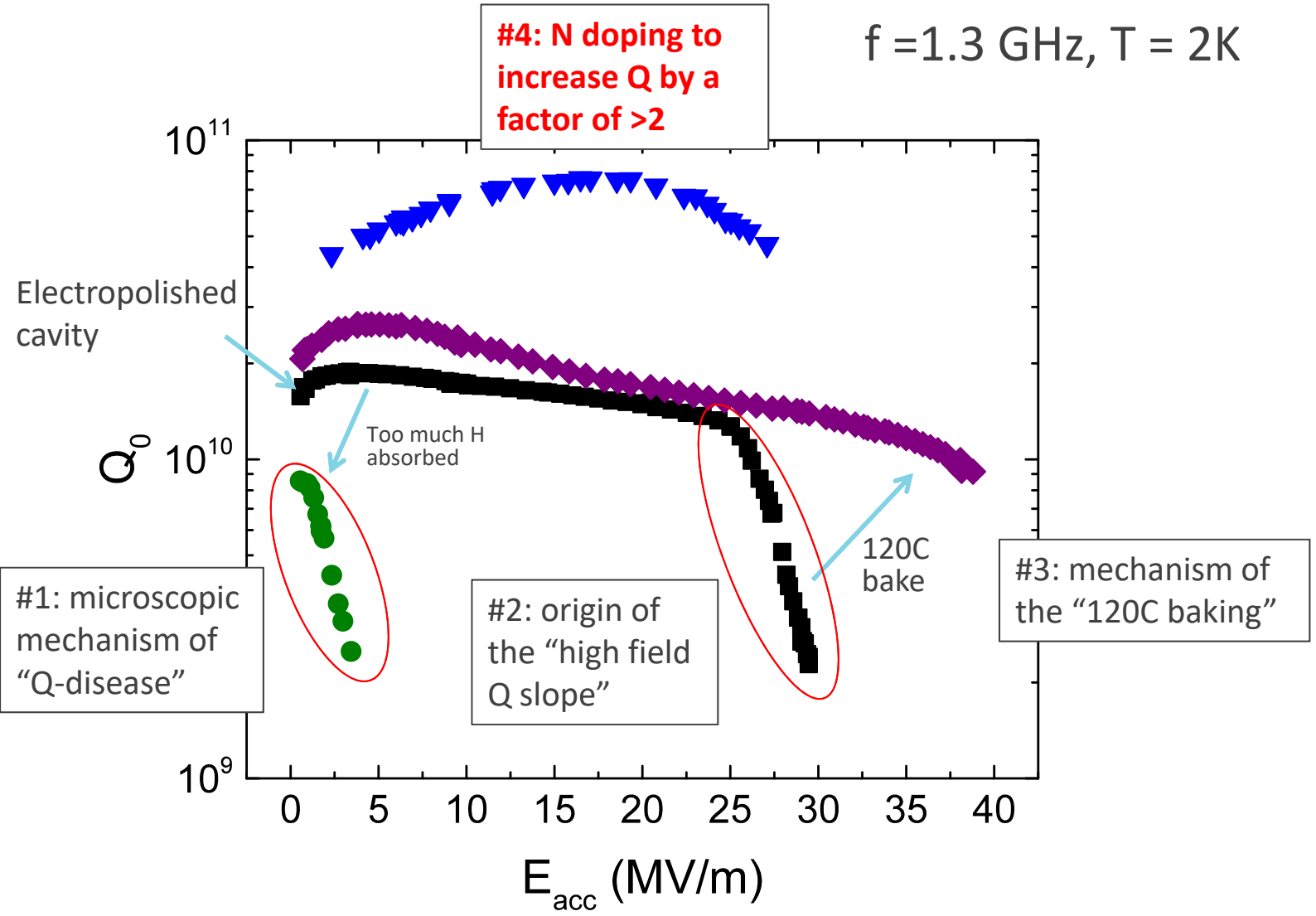

# Topic #1: microscopic details of Q disease

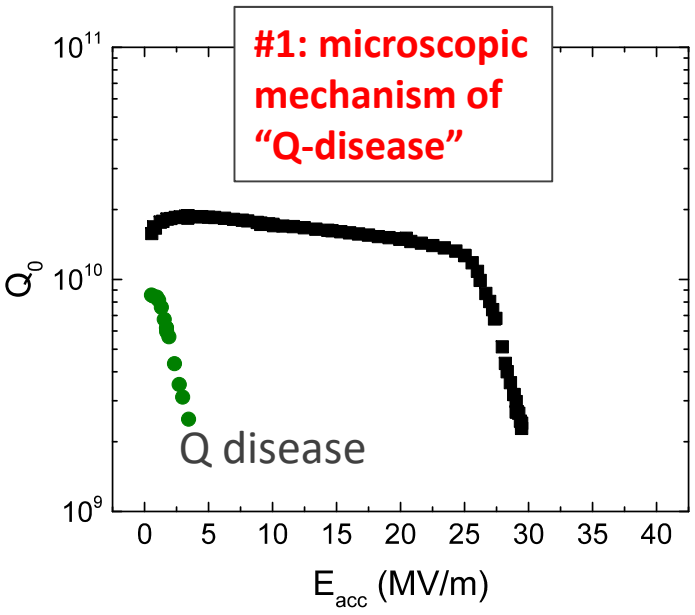


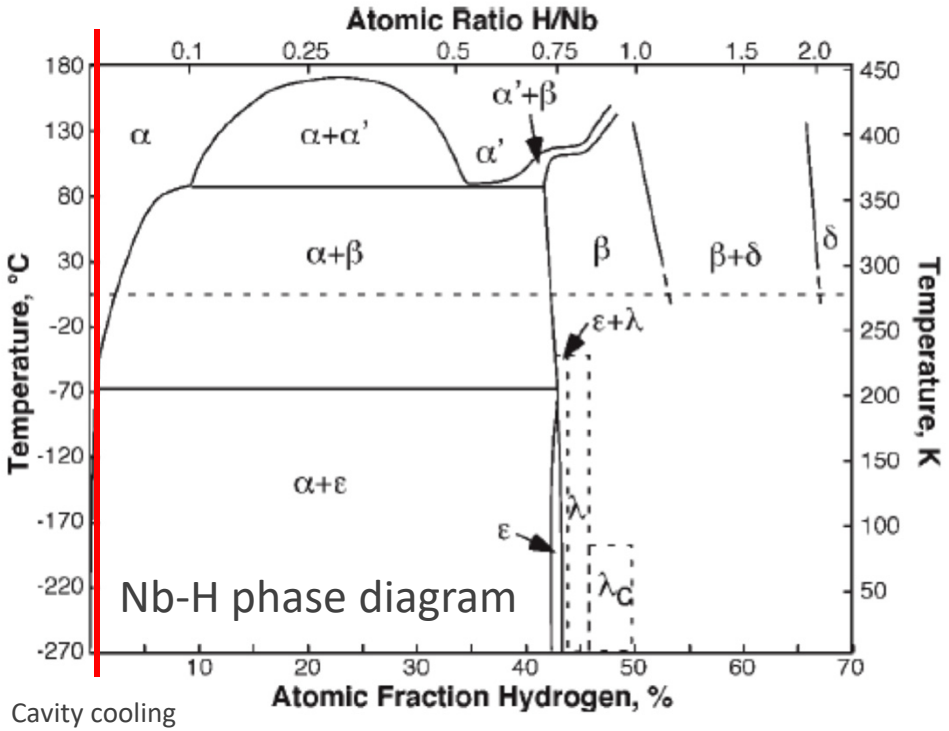


Cavity cooling

- Q-disease was proposed in the past to be caused by excess hydrogen, which forms non-superconducting niobium hydrides upon cooldown
  - Remedy found – 600-800C vacuum anneal to degas hydrogen
  - Microscopic details originally not established

# Microscopic mechanism of Q-disease

- Hydrides observed directly in H-reach niobium samples using the cryostage in the laser confocal scanning microscope

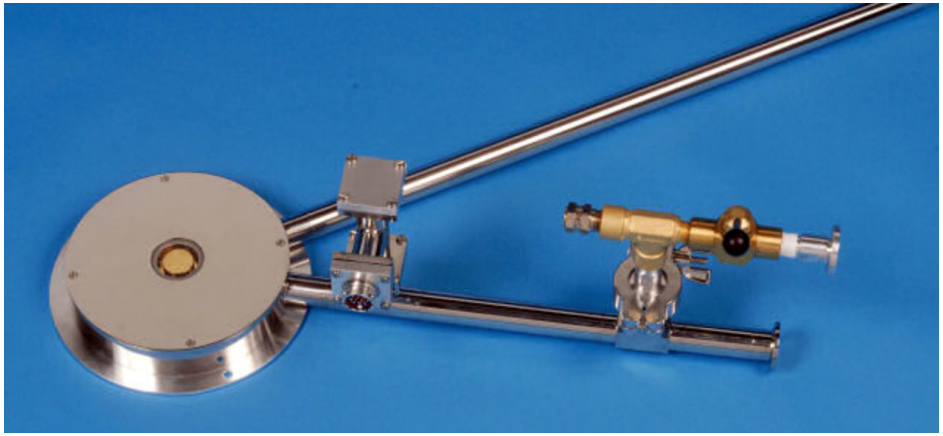




Fermilab

# First cooldown

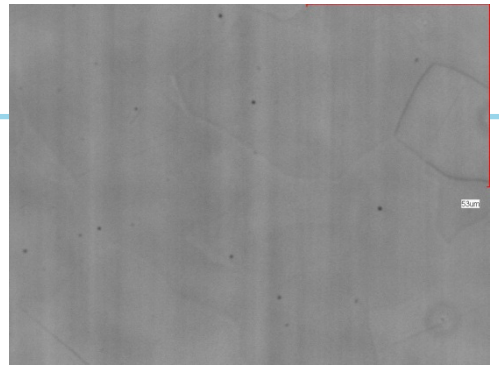


T=300K

First cooldown

50 um

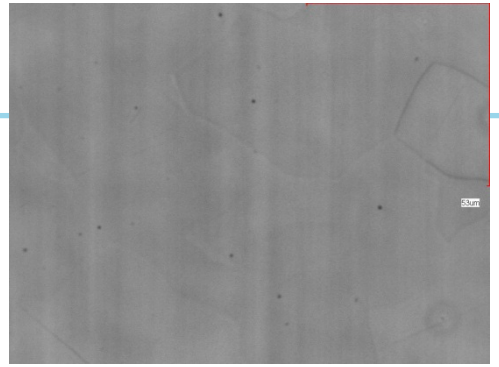

T=300K

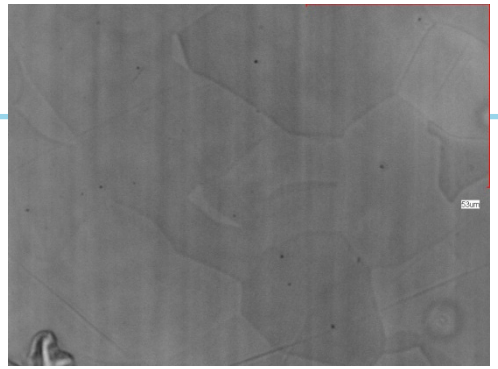

T=160K

First cooldown

50 um

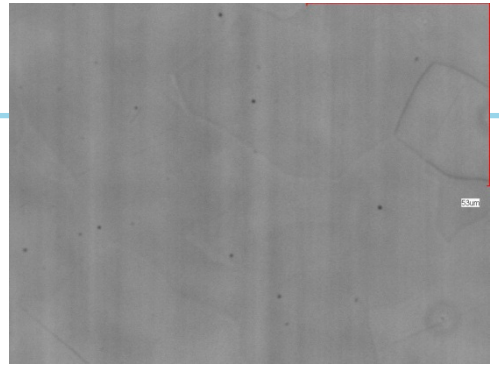

T=300K

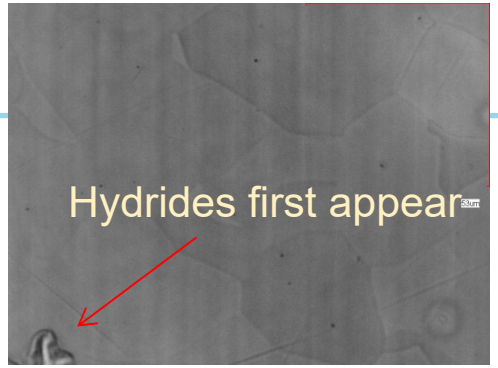


T=160K

First cooldown

50 um

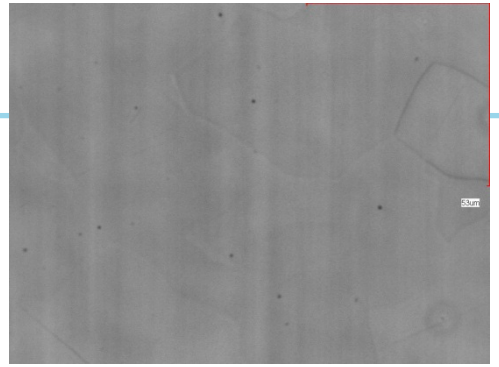

T=300K

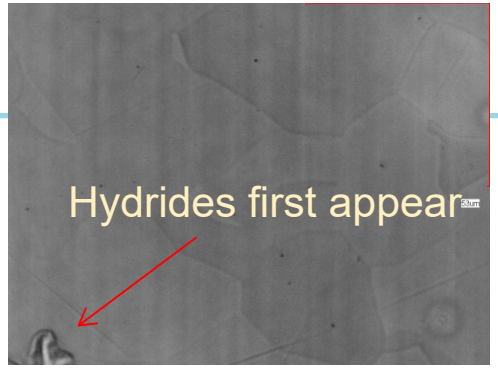


T=160K

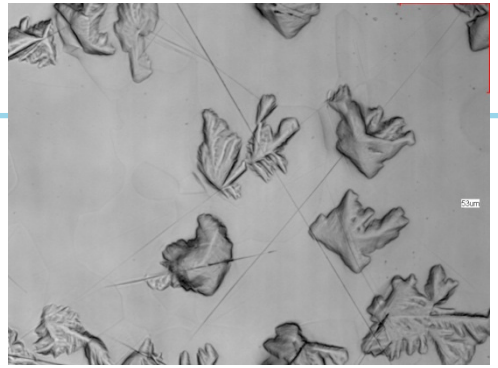

T=140K

First cooldown

50 um

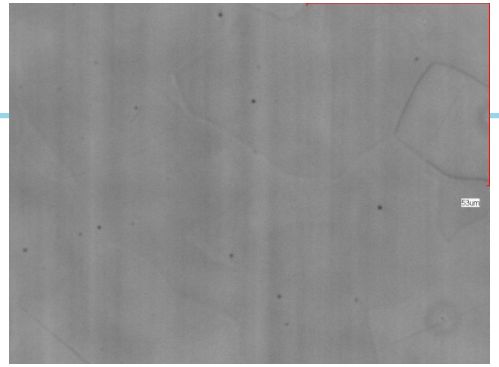

T=300K

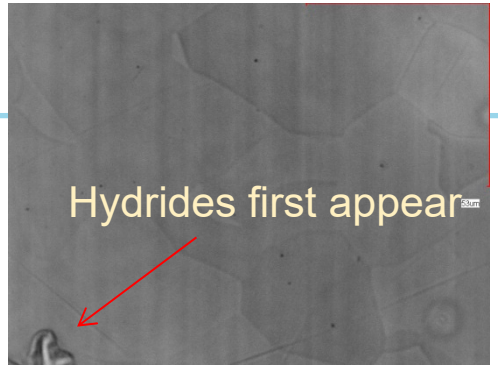


T=160K

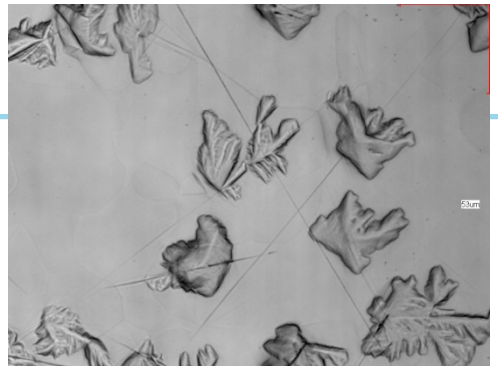

T=140K

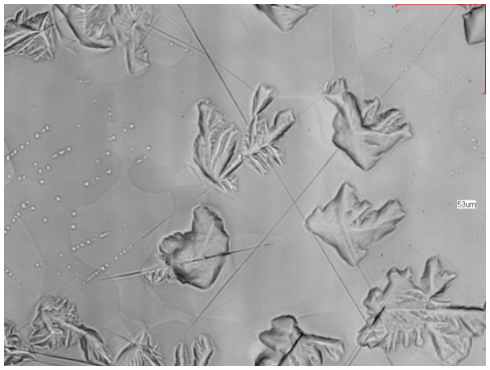

T=100K

First cooldown

50 um

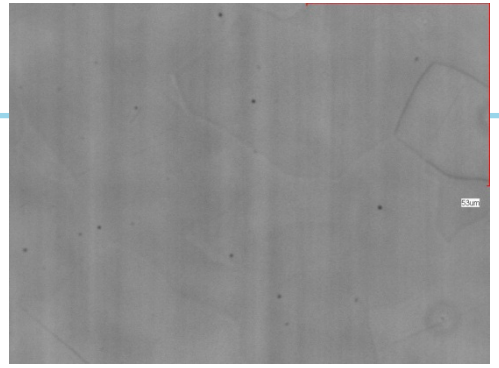

T=300K

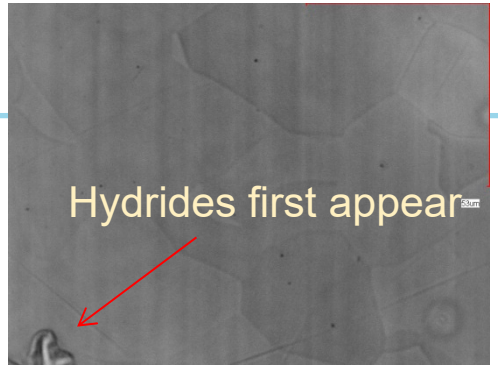


T=160K

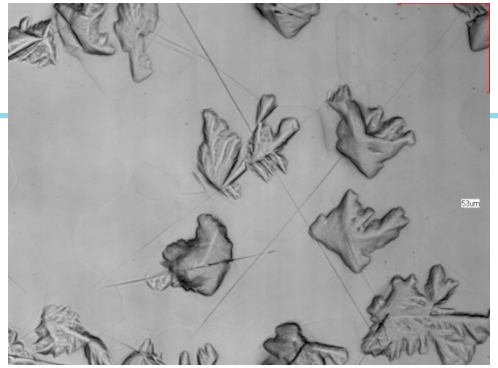

T=140K

Second (smaller) phase of hydride forms

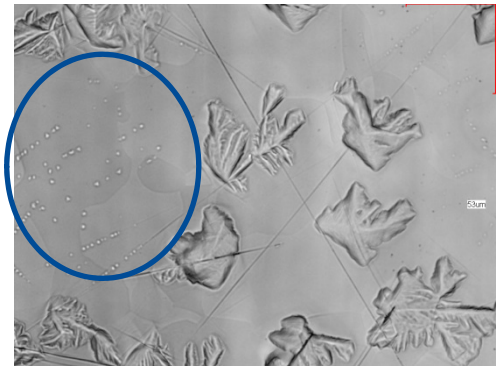

T=100K

First cooldown

50 um

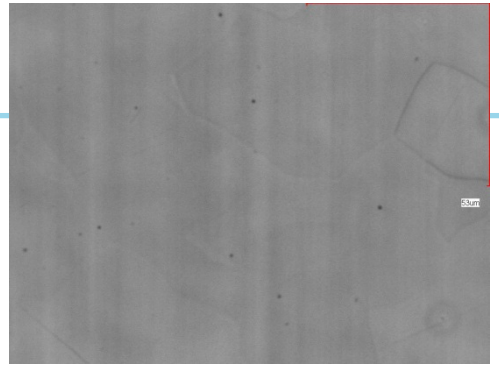

T=300K

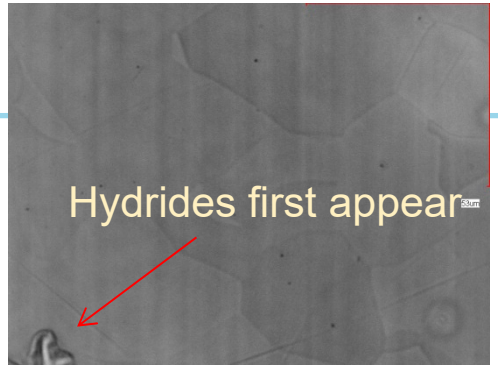


T=160K

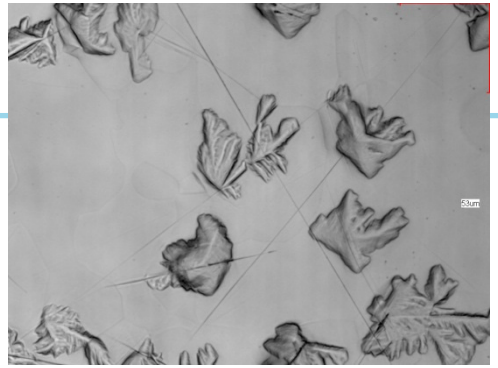

T=140K

Second (smaller) phase of hydride forms

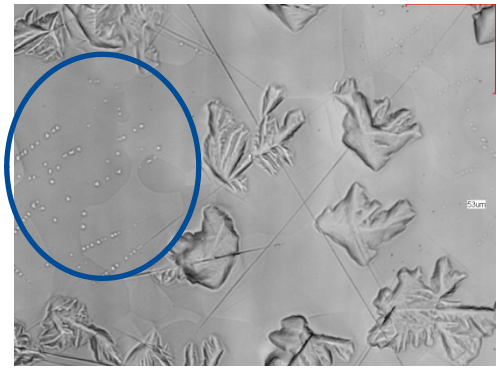

T=100K

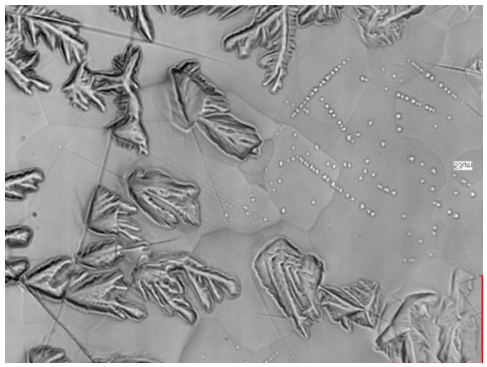

T=6K

First cooldown

50 um

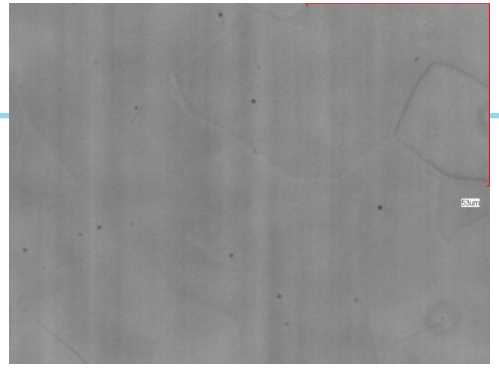

T=300K

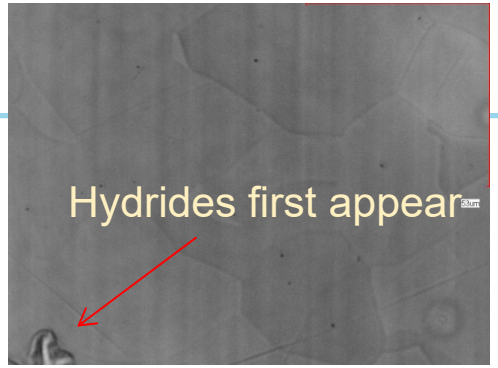


T=160K

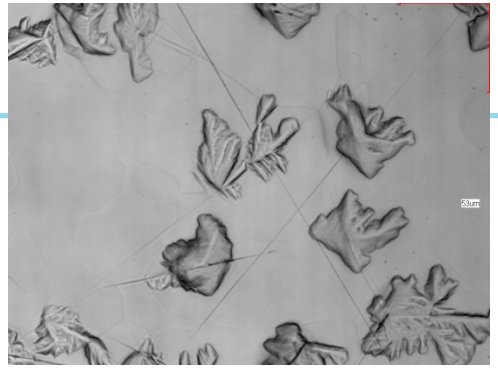

T=140K

Second (smaller) phase of hydride forms

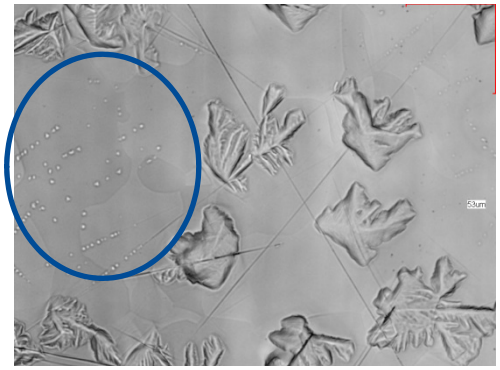

T=100K

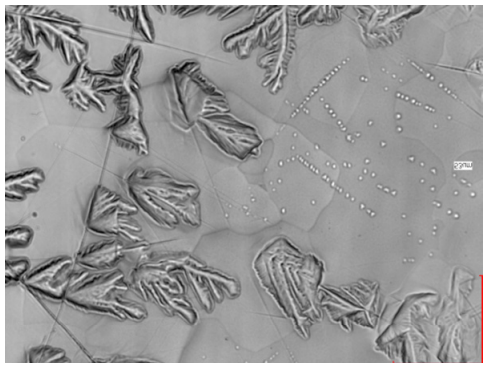

T=6K

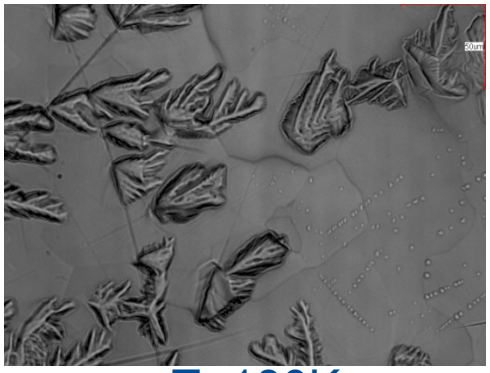

T=180K

First cooldown

50 um

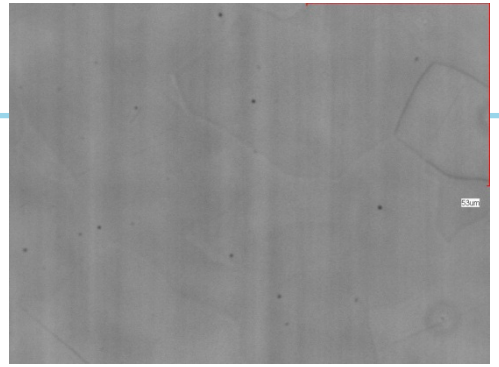

T=300K

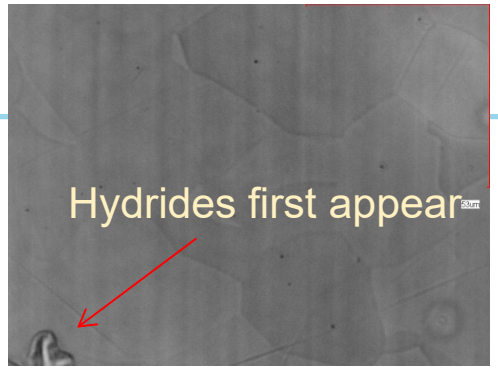


T=160K

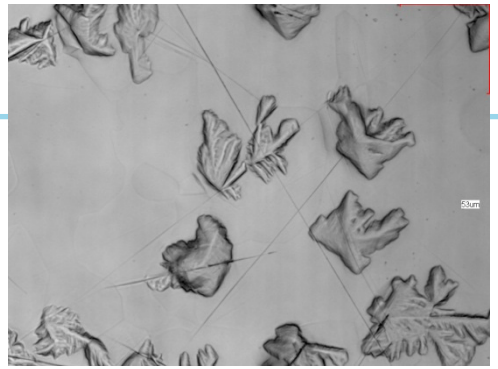

T=140K

Second (smaller) phase of hydride forms

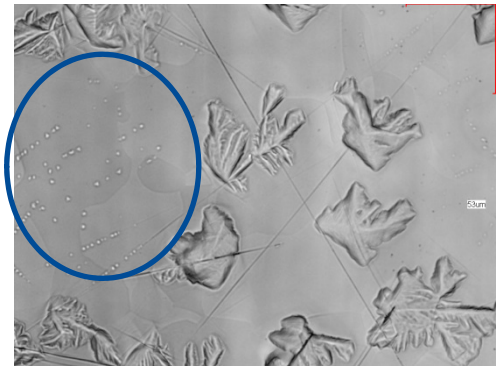

T=100K

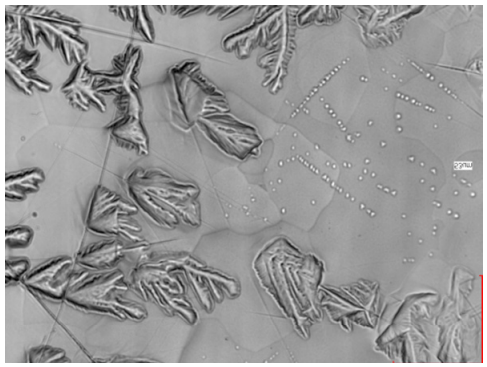

T=6K

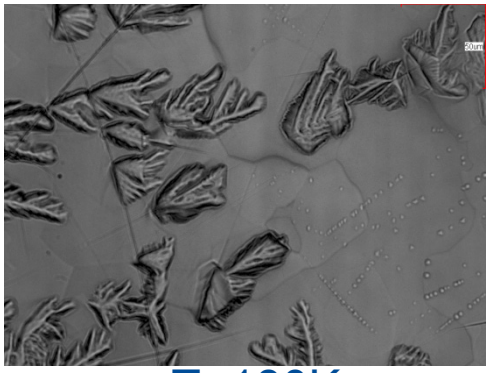

T=180K

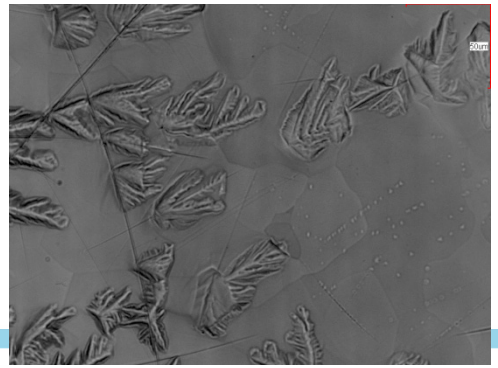

T=210K

First cooldown

50 um

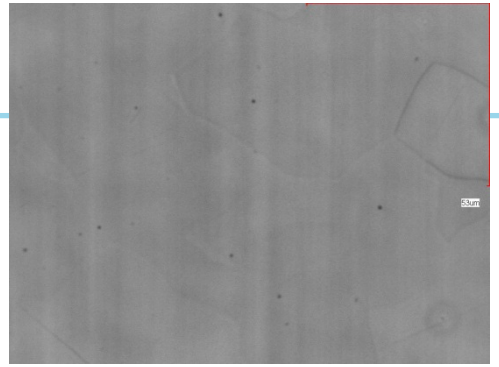

T=300K

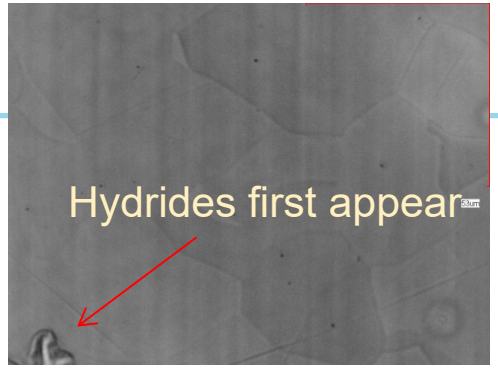


T=160K

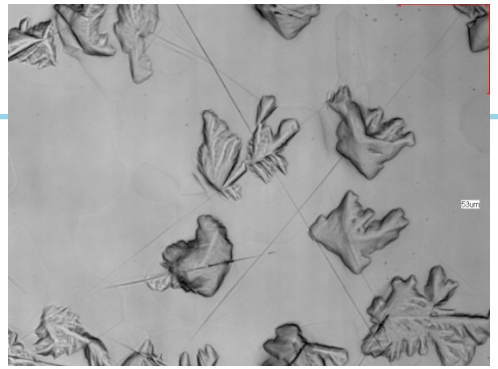

T=140K

Second (smaller) phase of hydride forms

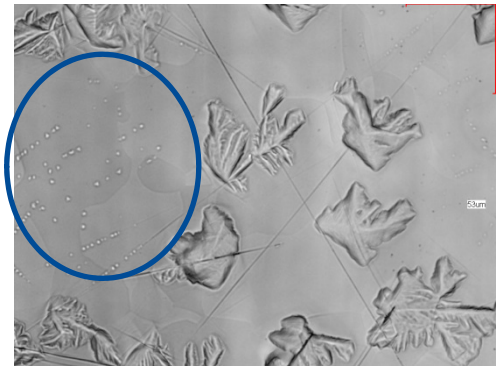

T=100K

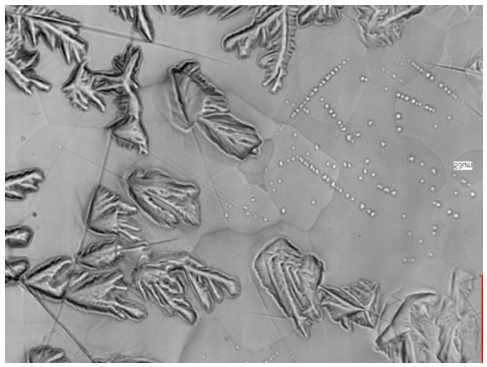

T=6K

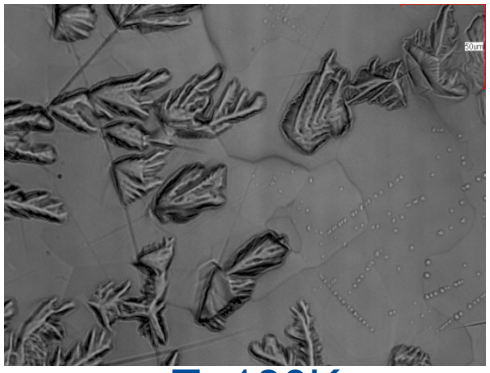

T=180K

Large phase starts to dissolve

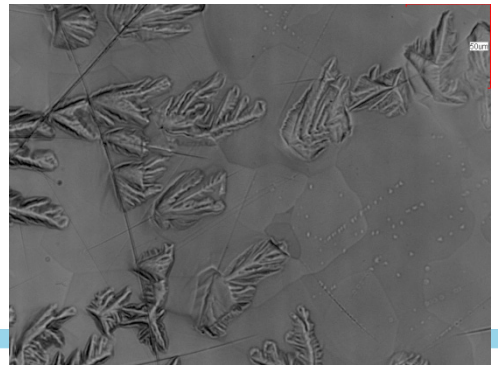

T=210K

First cooldown

50 um

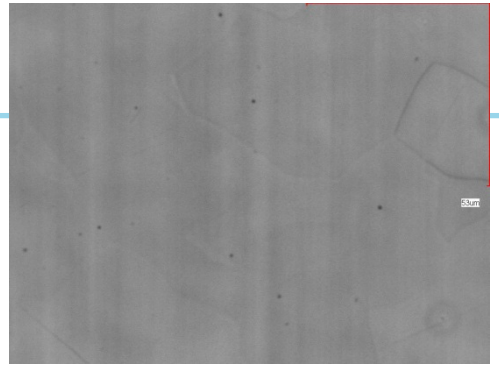

T=300K

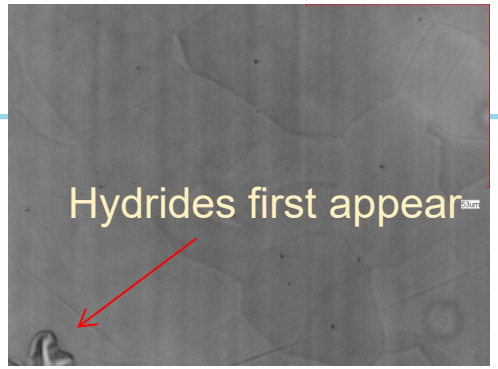


T=160K

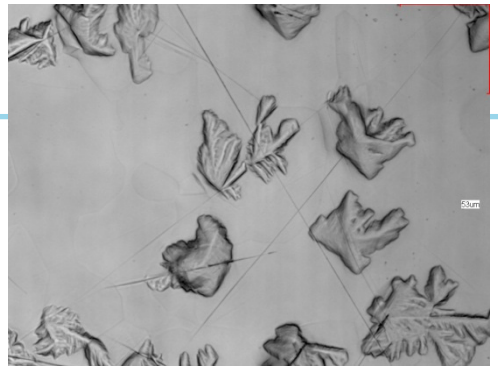

T=140K

Second (smaller) phase of hydride forms

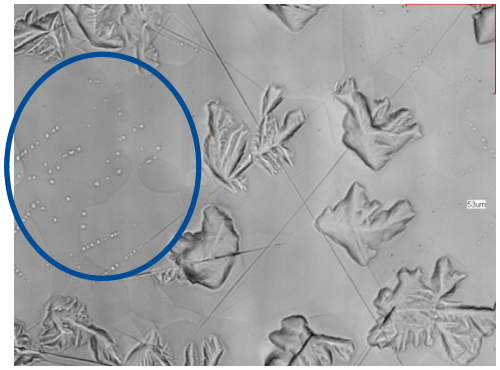

T=100K

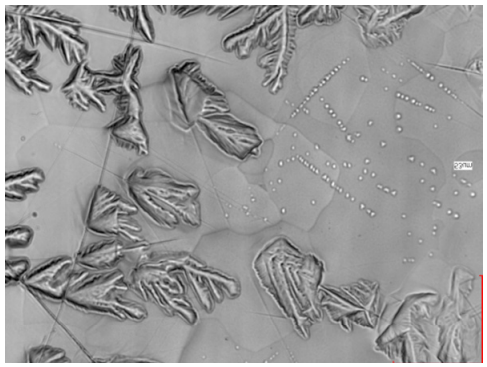

T=6K

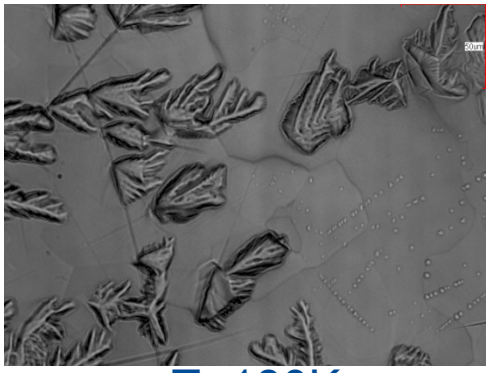

T=180K

Large phase starts to dissolve

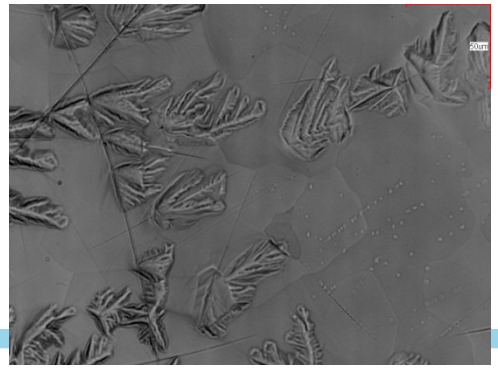

T=210K

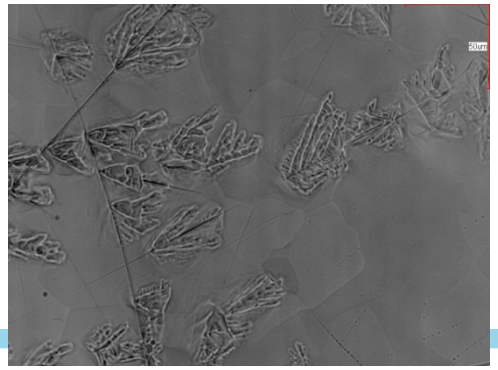

T=260K

First cooldown

50 um

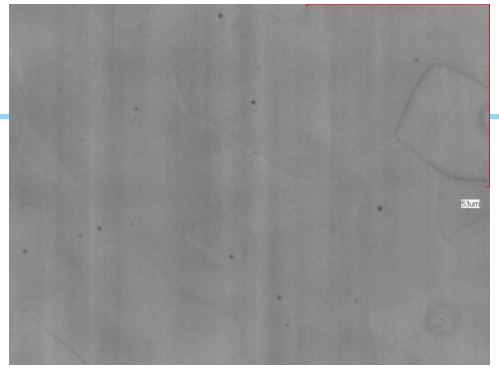

T=300K

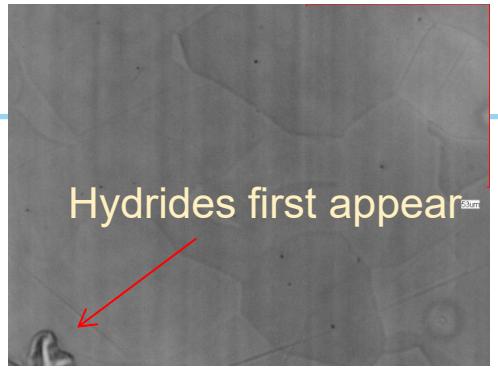


T=160K

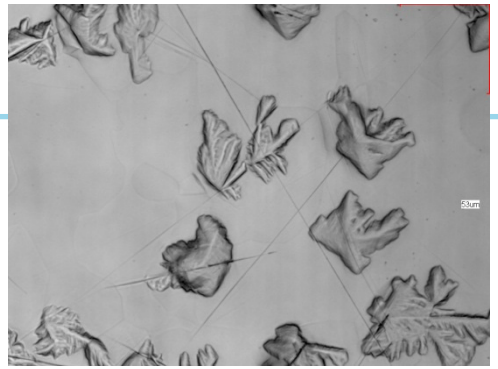

T=140K

Second (smaller) phase of hydride forms

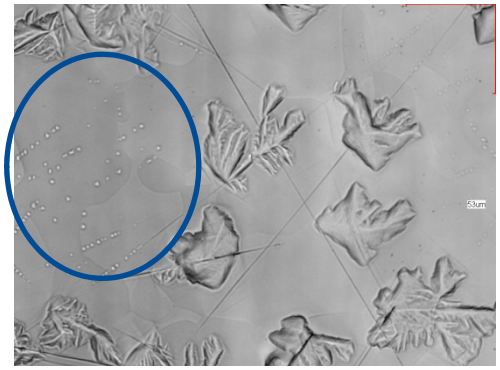

T=100K

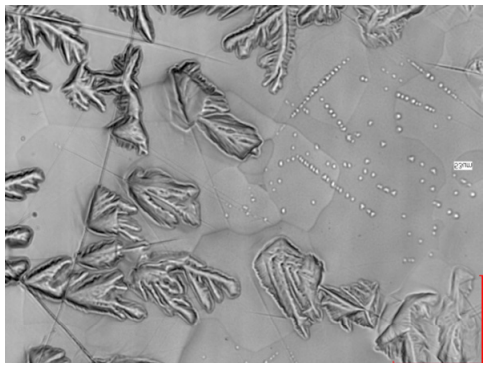

T=6K

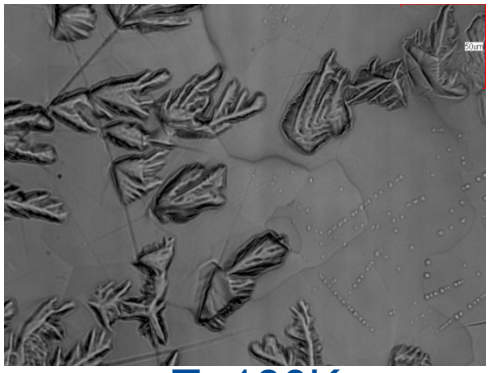

T=180K

Large phase starts to dissolve

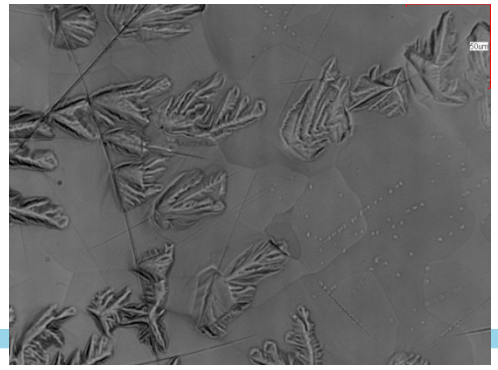

T=210K

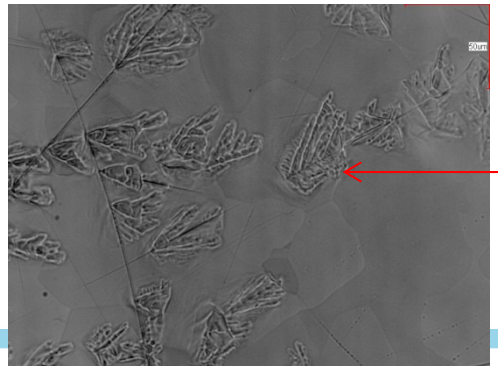

T=260K

Hydrides gone, dislocation skeleton (deformation) remains on the surface

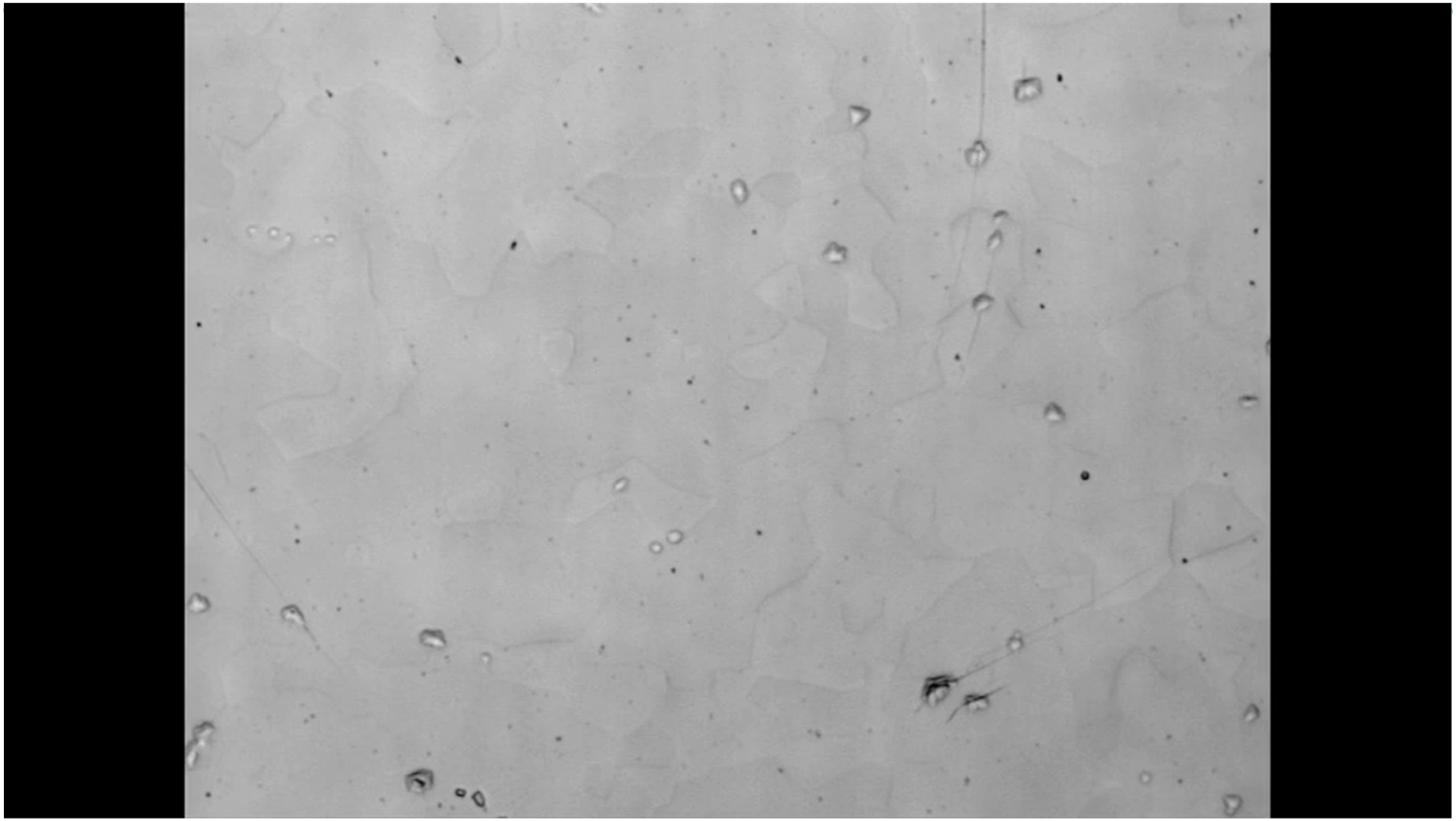

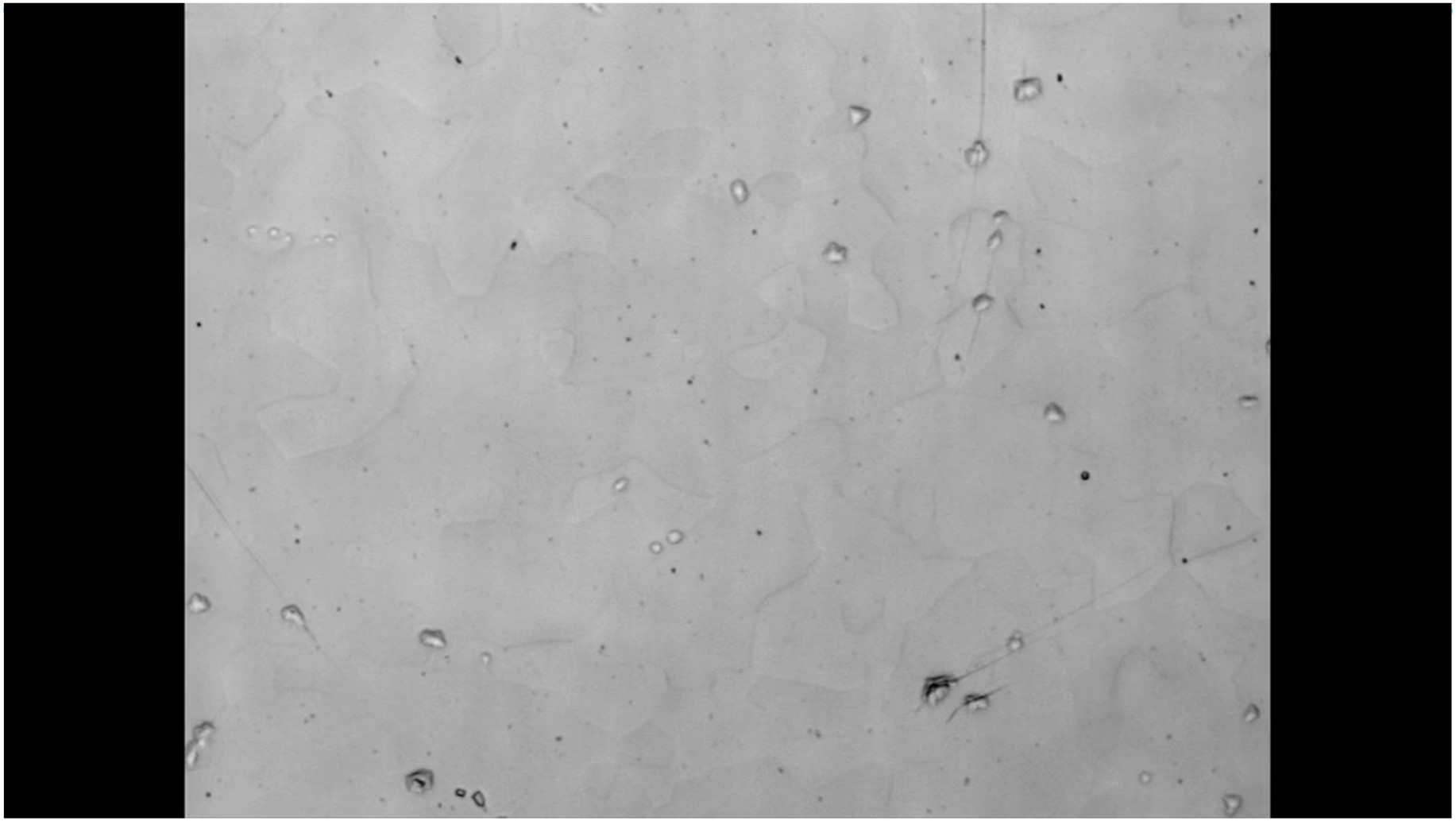

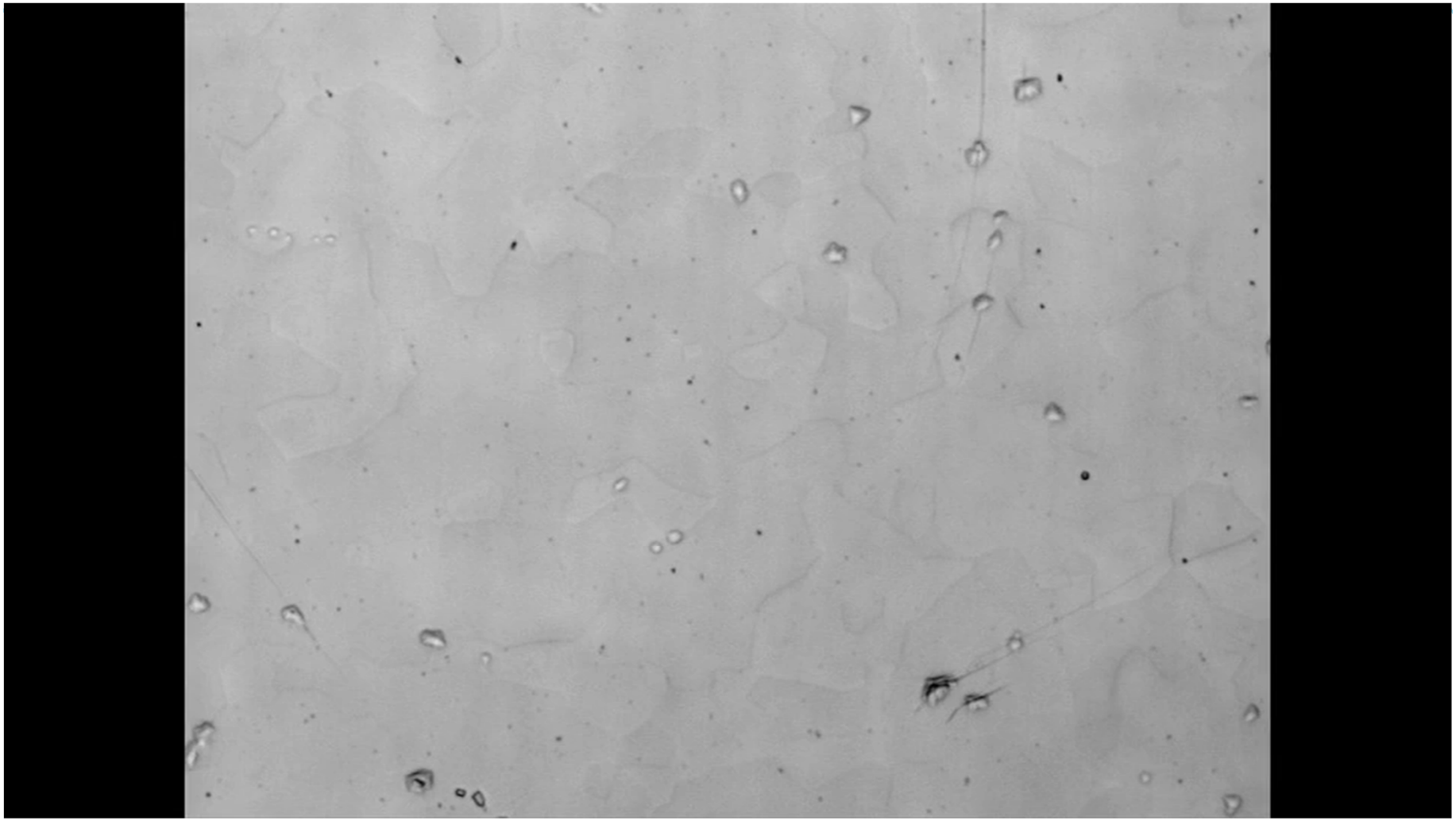

# Near-surface H present even after 600-800C degasing

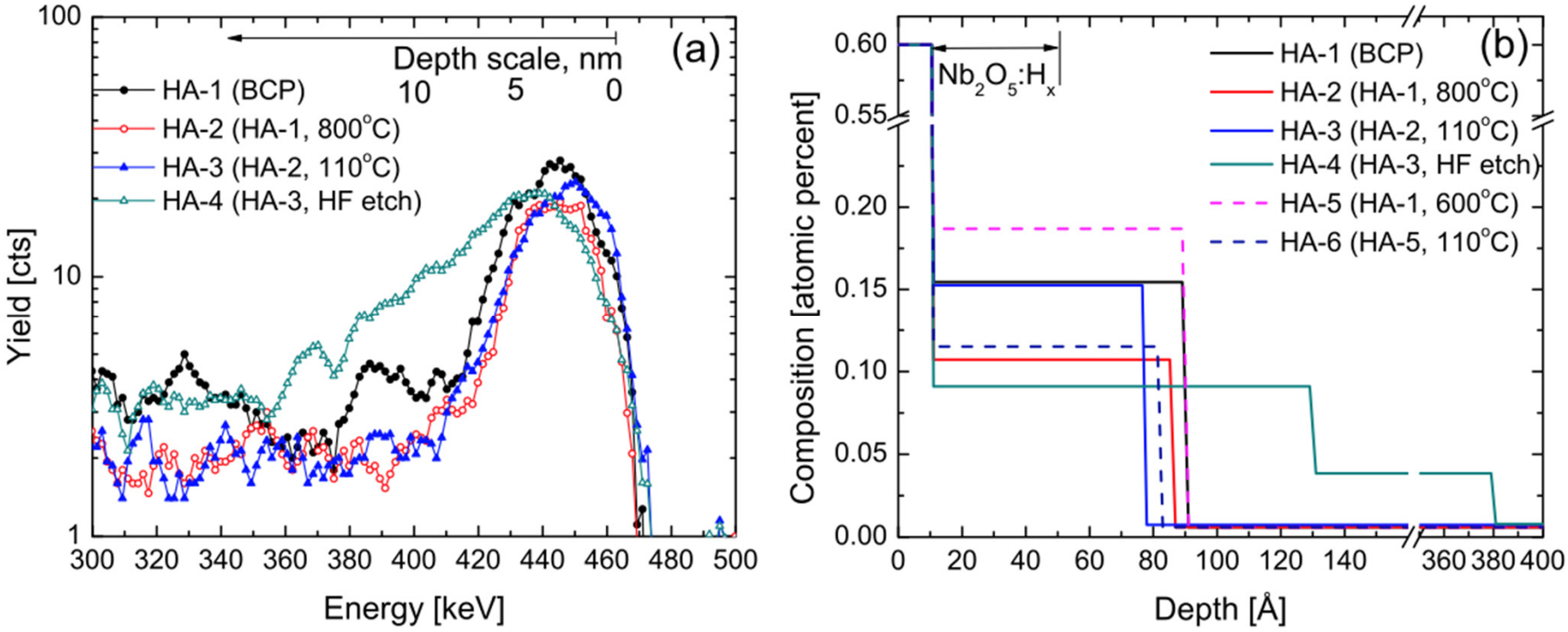


A. Romanenko and L. V. Goncharova, 2011 Supercond. Sci. Tech. **24**, 105017

ERD measurements confirm that Q-disease is eliminated by the 600-800C H degassing (bulk H content drastically reduced), but the near-surface H-rich layer remains

# Topic #2: origin of the “high field Q slope”

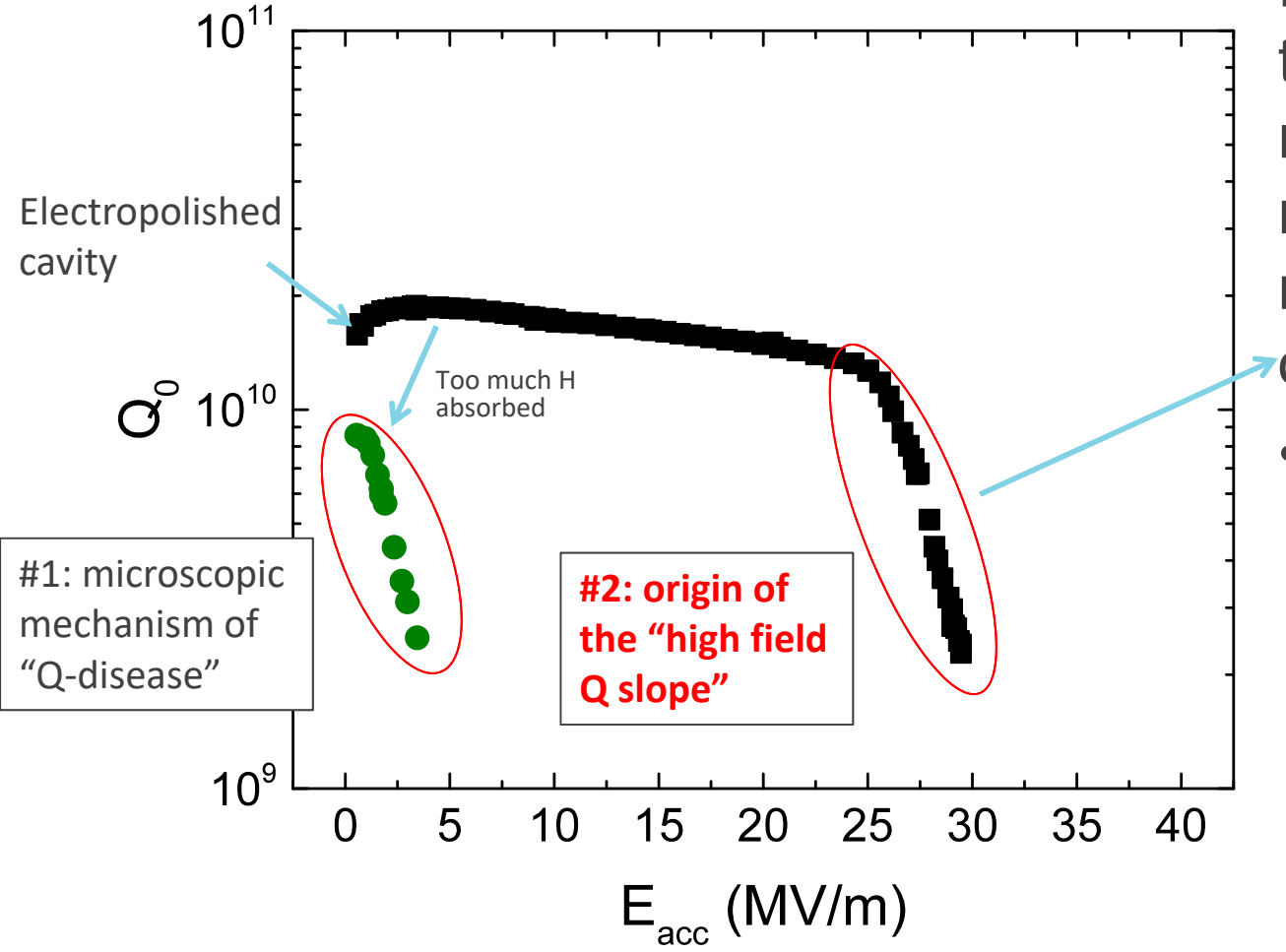


Hypothesis: can it be the Q-disease “in miniature” – same mechanism, but nanohydrides instead of micron-size ones?

- Need free H near surface and enough time to precipitate during cooldown

## Nanohydrides form upon cooldown

# Not 120C baked sample

A. Romanenko, F. Barkov, L. D. Cooley, A. Grassellino, Supercond. Sci. Technol. **26** (2013) 035003 – selected for highlights of 20

# Not 120C baked sample

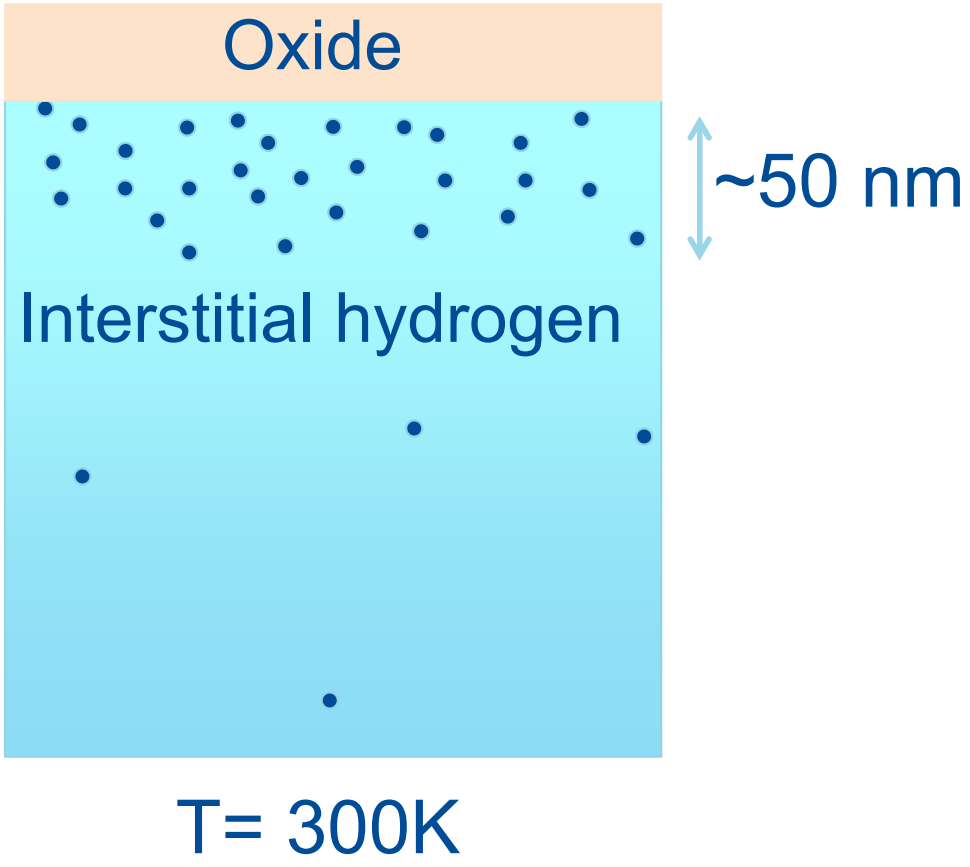


A. Romanenko, F. Barkov, L. D. Cooley, A. Grassellino, Supercond. Sci. Technol. **26** (2013) 035003 – selected for highlights of 20

## Nanohydrides form upon cooldown

# Not 120C baked sample

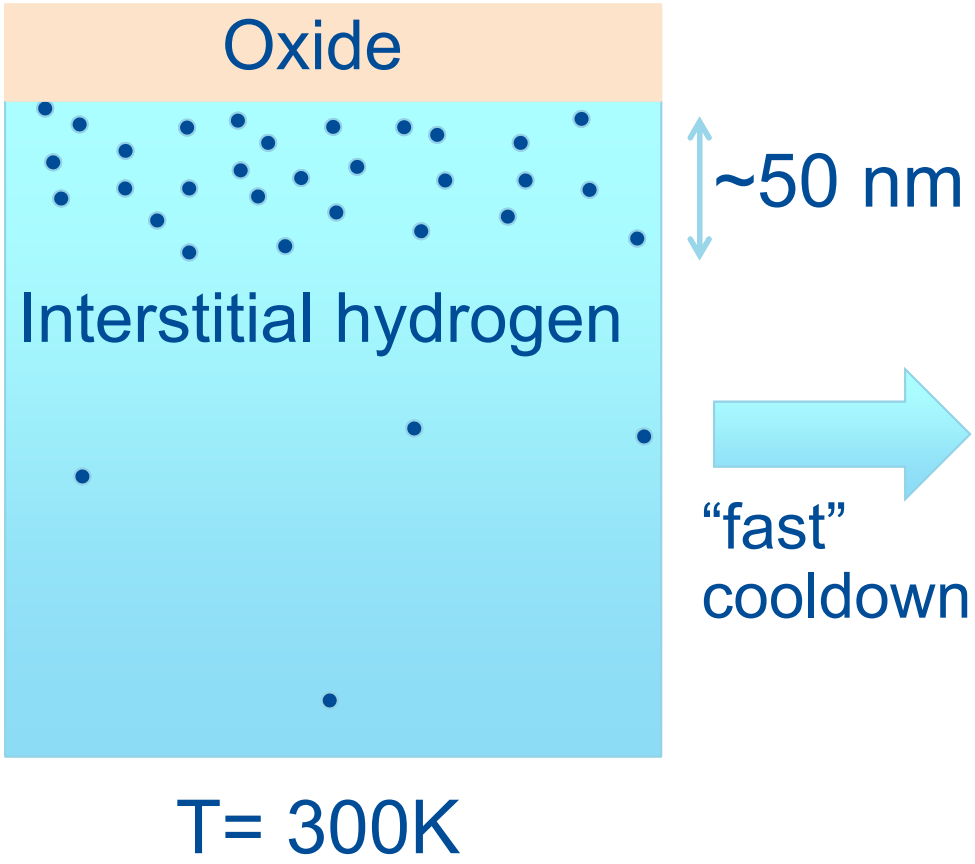


A. Romanenko, F. Barkov, L. D. Cooley, A. Grassellino, Supercond. Sci. Technol. **26** (2013) 035003 – selected for highlights of 20

## Nanohydrides form upon cooldown

# Not 120C baked sample

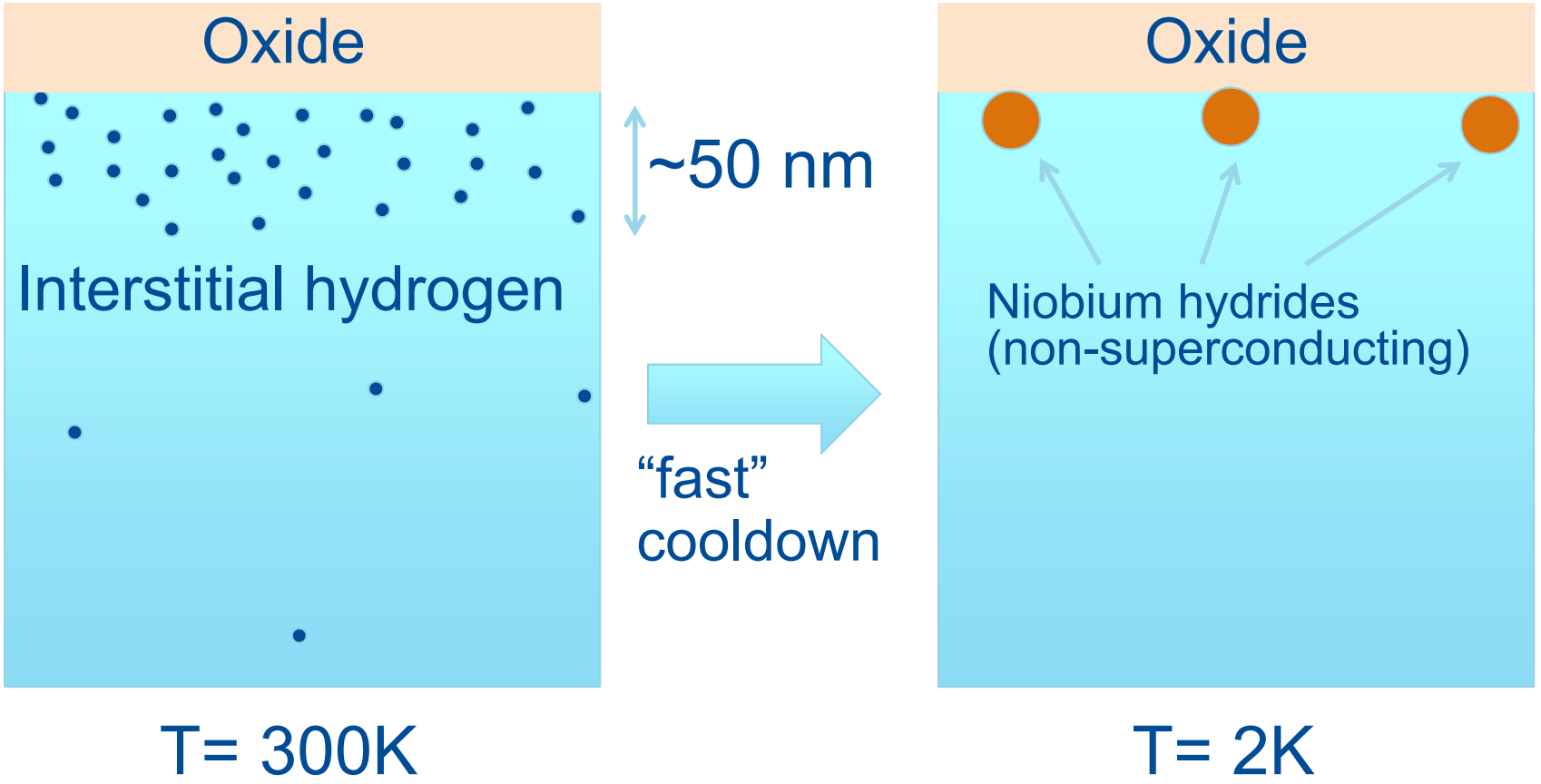


A. Romanenko, F. Barkov, L. D. Cooley, A. Grassellino, Supercond. Sci. Technol. **26** (2013) 035003 – selected for highlights of 20

# Can we find these tiny hydrides?
# Step A: Temperature mapping

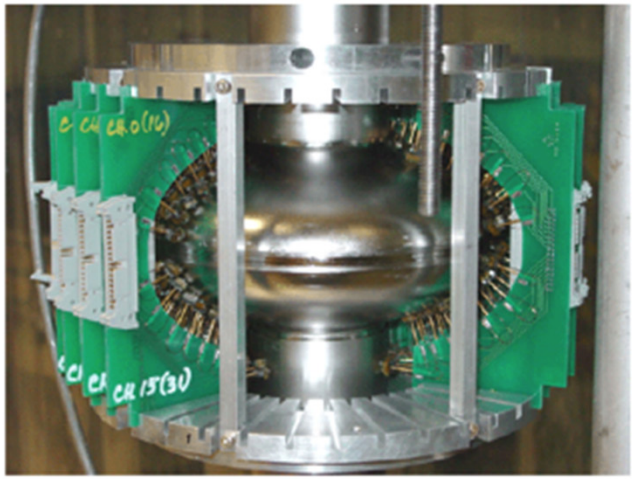

Array of 576 thermometers attached to the outside cavity walls allows mapping wall dissipation

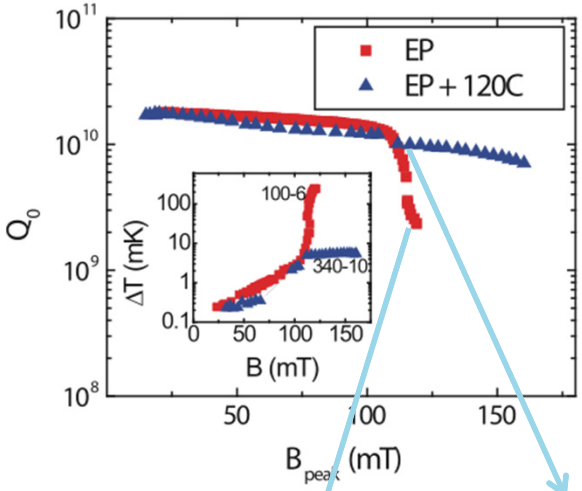


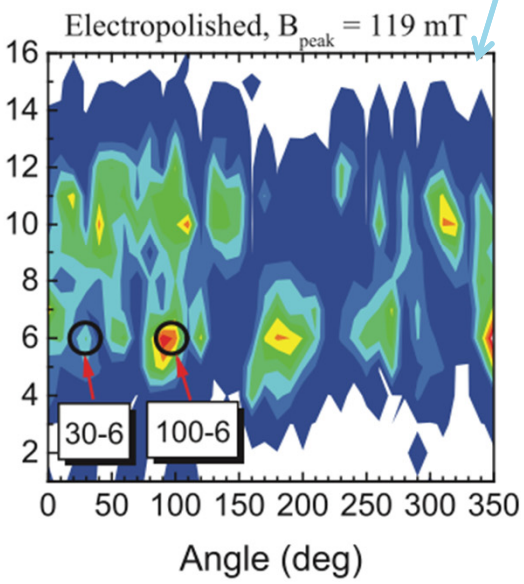


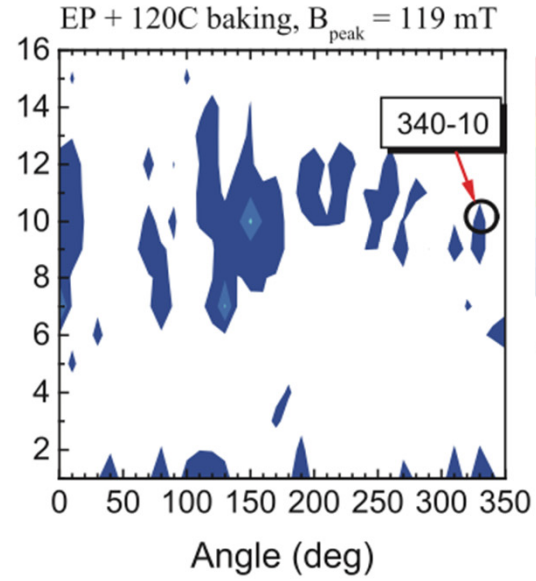


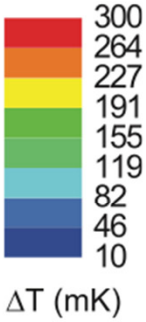

# STEP B: Investigating cutouts

Extract samples from cavity walls locations identified by temperature mapping -> direct correlation of RF losses with material structure


# TEM search for nanohydrides on cutouts

Cold: 120C in situ bake for 48hours

Hot: no such bake

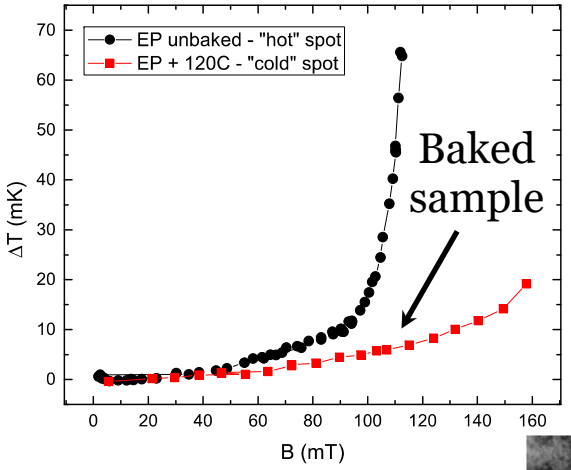


Identify samples based on T-map

Heating: comparison of "cold" and "hot" spots

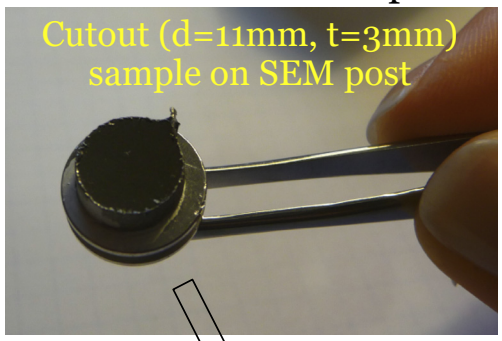


FIB prep sample for TEM

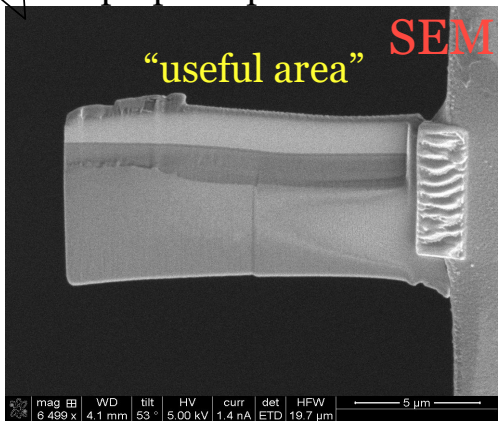


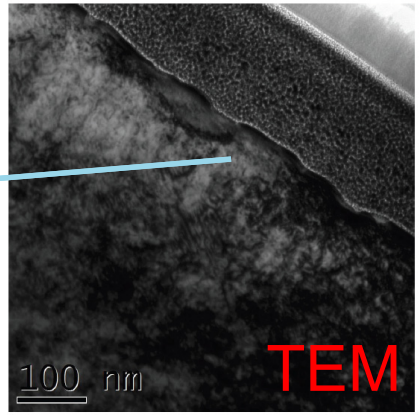


Look at this area with subnanometer resolution in TEM at room AND T<100K temperatures

# FOUND! TEM evidence for nanohydrides

Measurements performed at Univ. of Illinois Urbana-Champai

TEM diffraction on cavity cutouts confirms the existence of nanohydrides

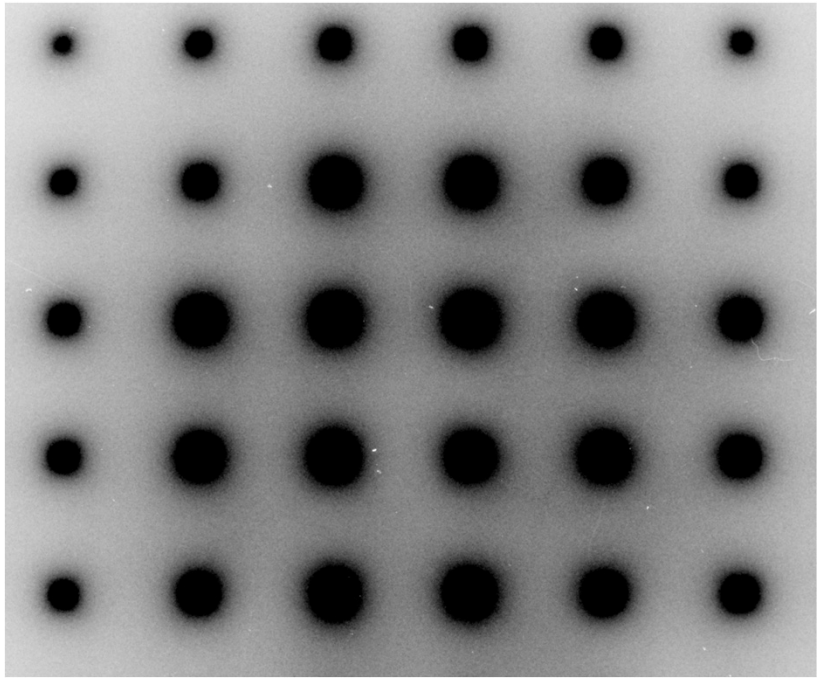

Room T: BCC Nb patterns, NO additional phases

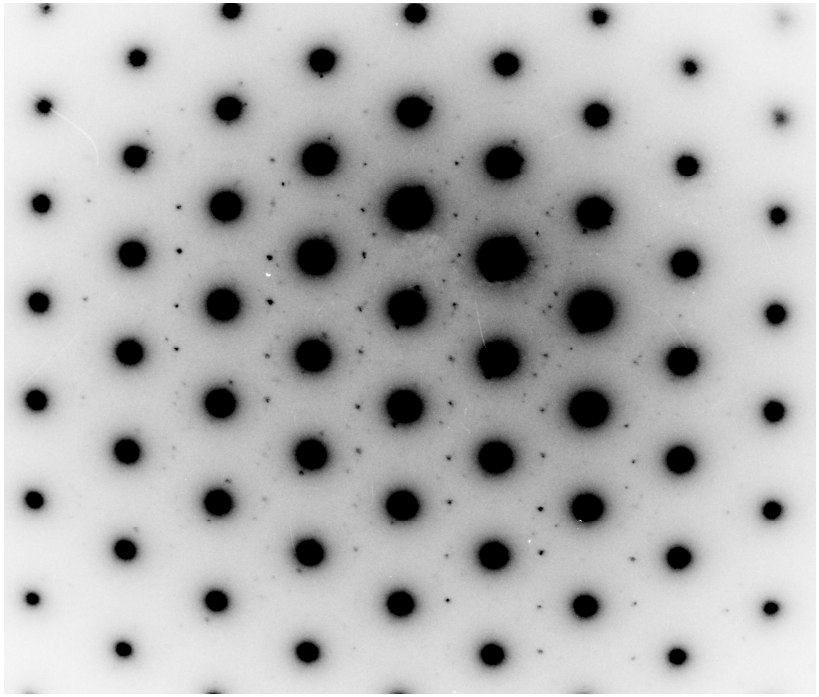

94K: stoichiometric Nb hydride phases!

Y. Trenikhina, A. Romanenko, J. Zasadzinski, Proceedings of SRF'2013, TUP043

# Topic #3: mechanism of the 120C baking

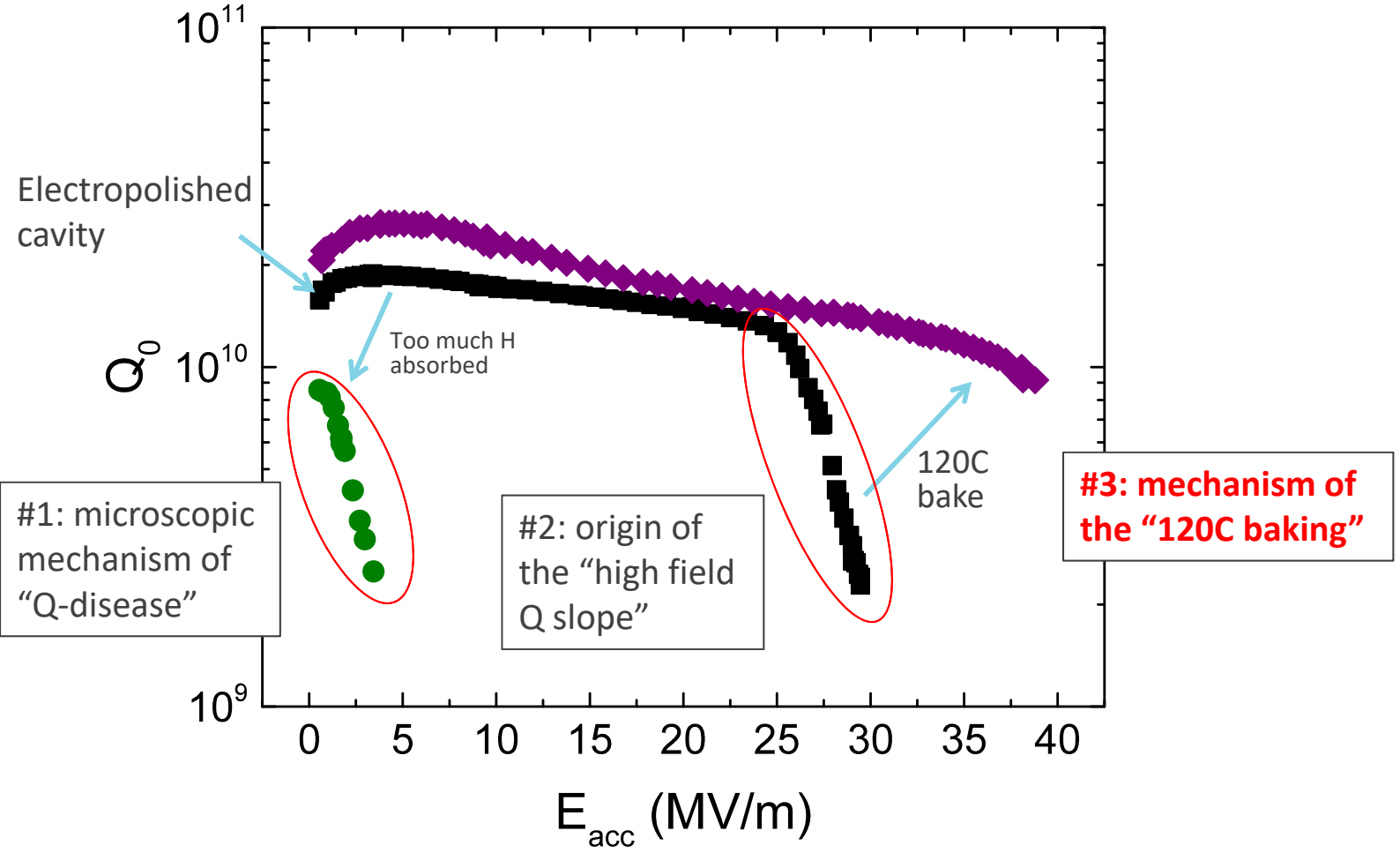

# Muon spin rotation at PSI (Switzerland)

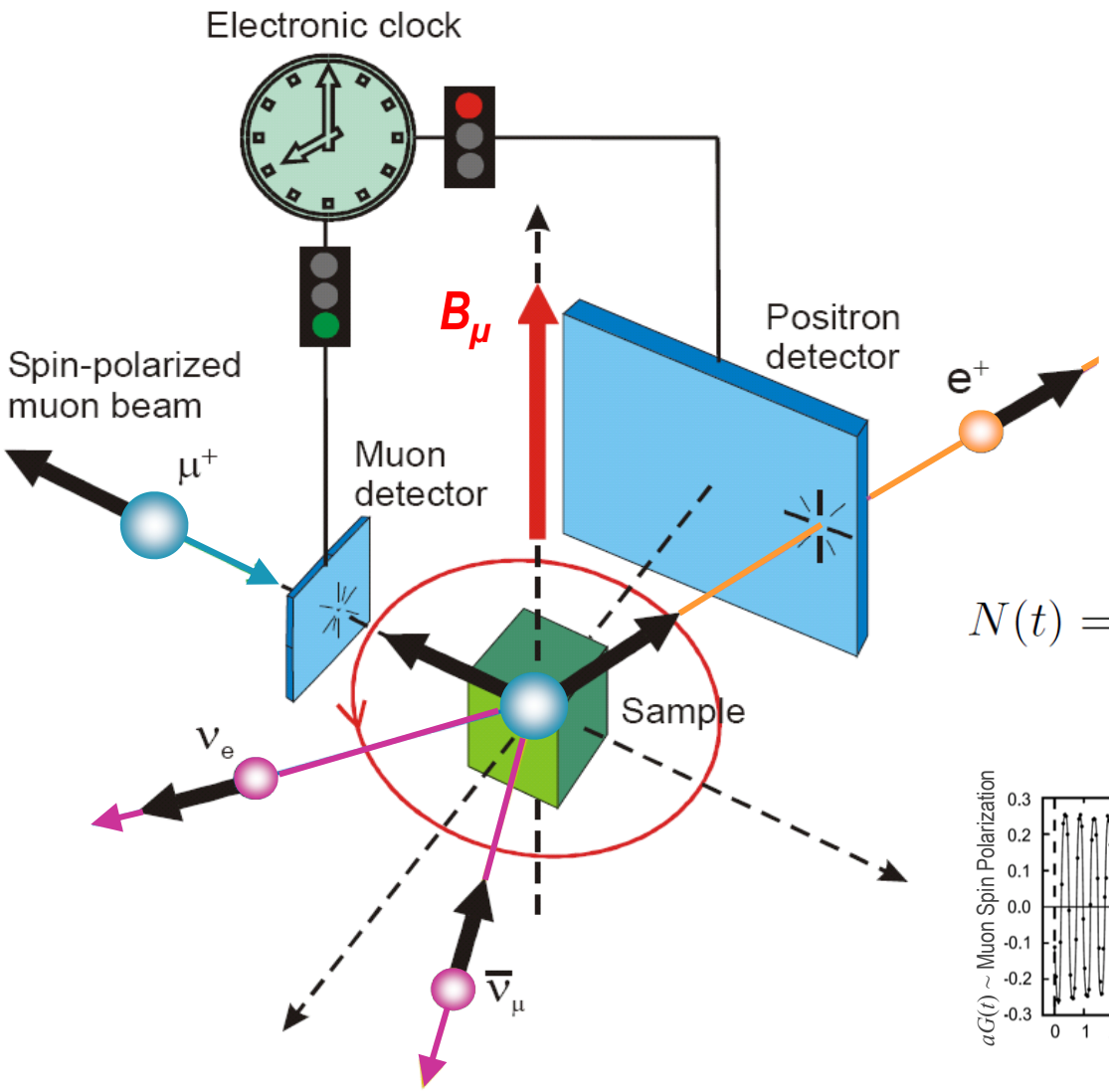


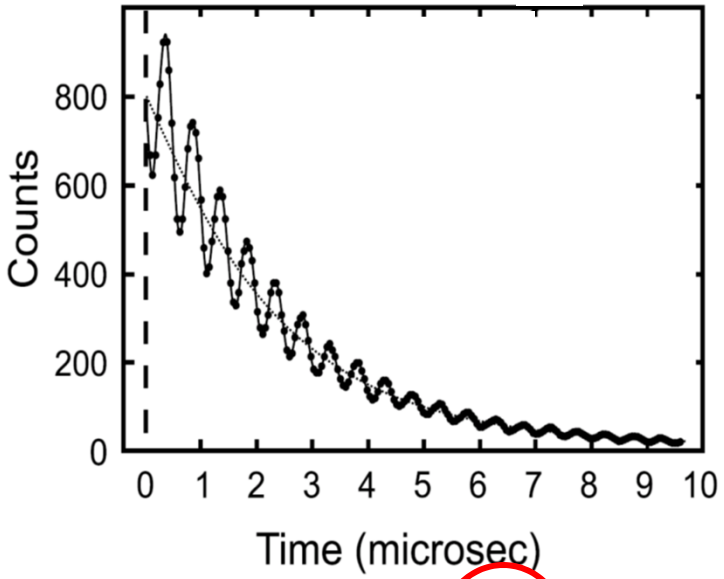


$$N(t) = N_0 \exp(-t/\tau_\mu)\,[1 + a\,G(t)] + \mathrm{Bkg}$$

Contains physics

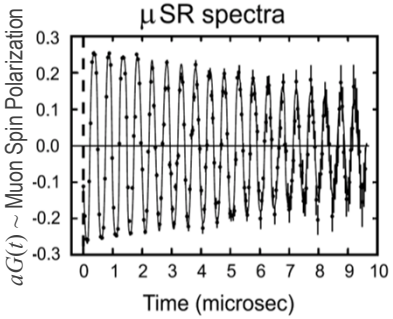


$$\omega_\mu(z) = \gamma_\mu B_{\mathrm{loc}}(z)$$

Frequency – field amplitude
Damping – field non-uniformity

# Muon spin rotation – measure B(z) directly

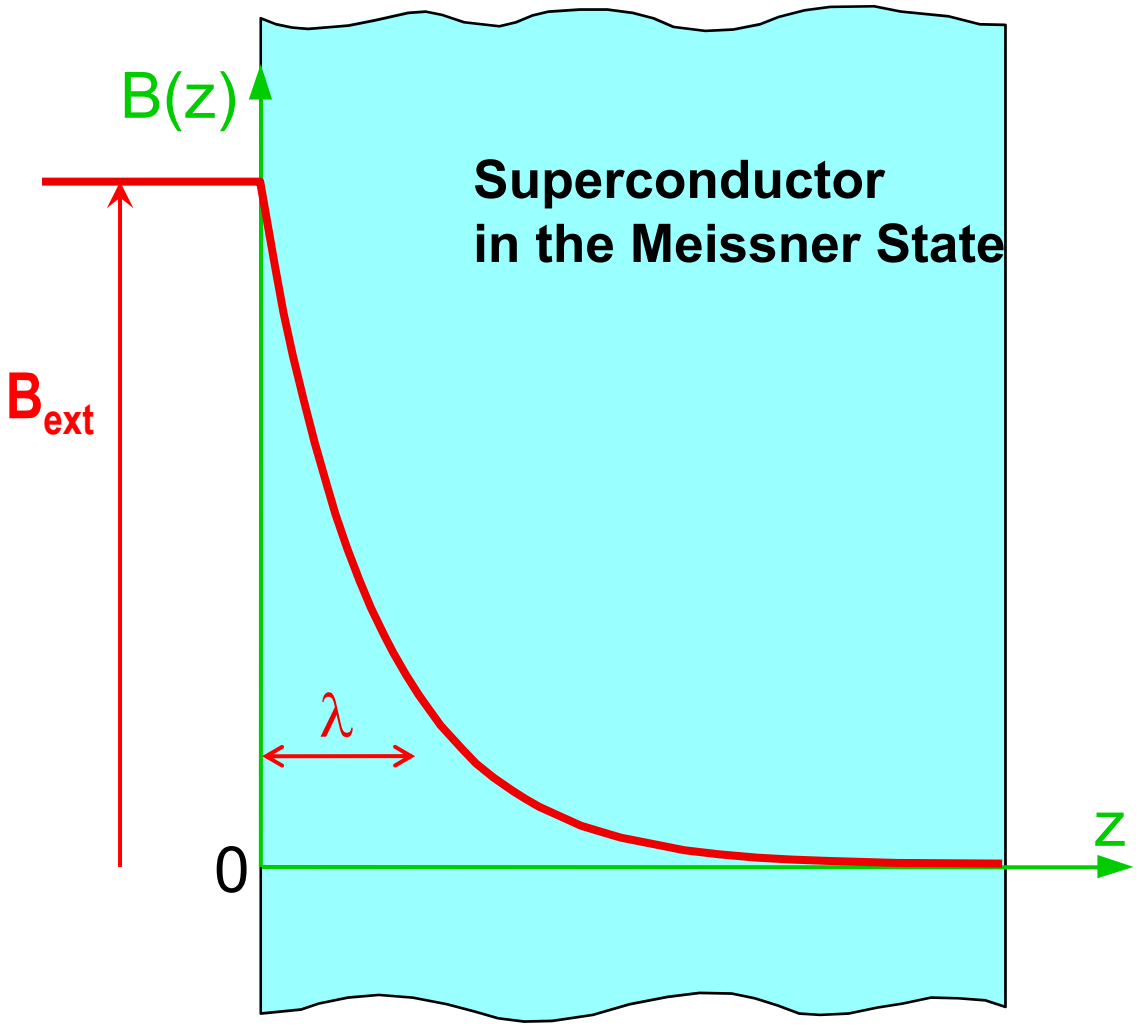


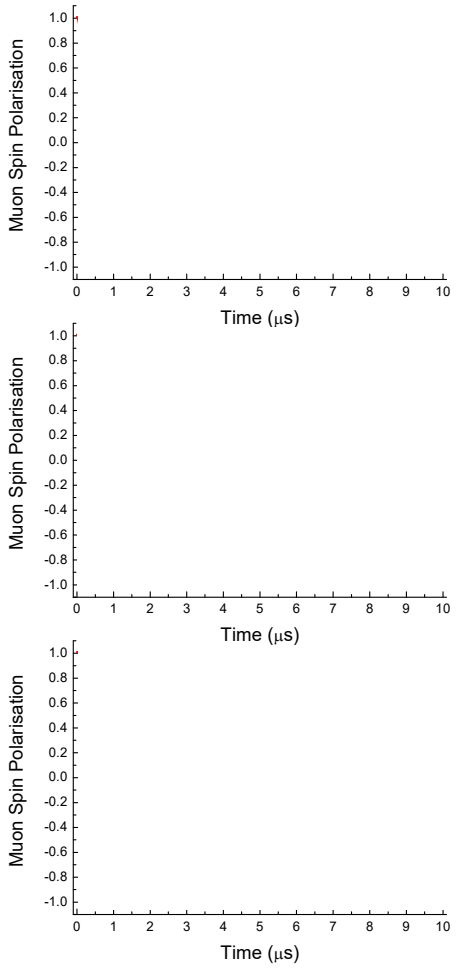


$$\omega_\mu(z) = \gamma_\mu B_{\mathrm{loc}}(z)$$

# Muon spin rotation – measure B(z) directly

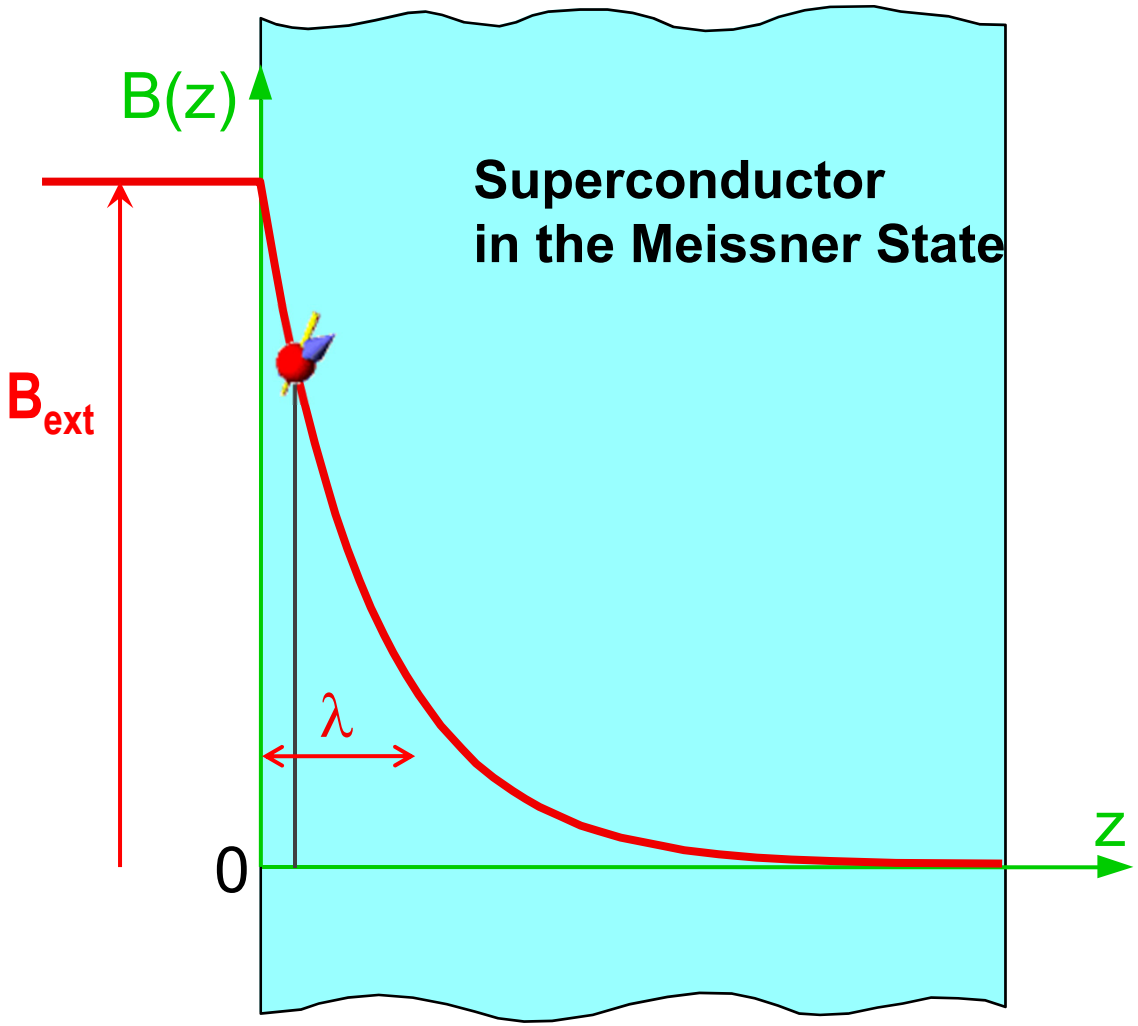


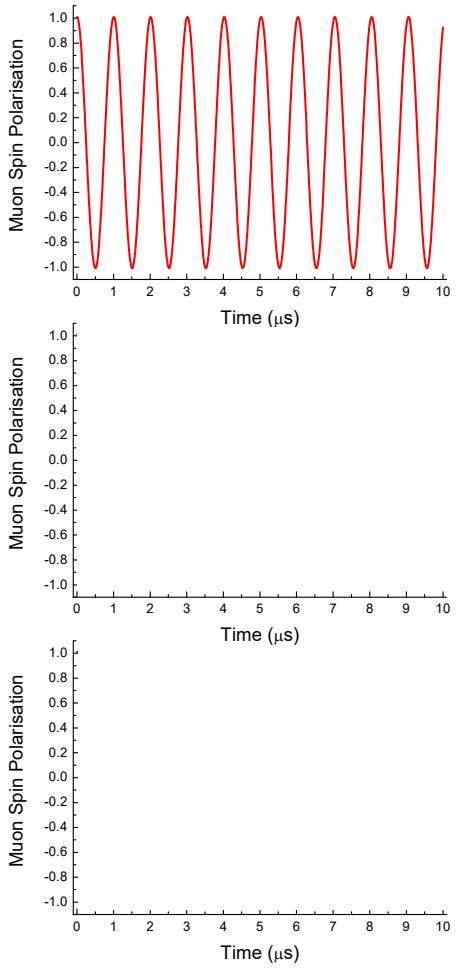


$$\omega_\mu(z) = \gamma_\mu B_{\mathrm{loc}}(z)$$

# Muon spin rotation – measure B(z) directly

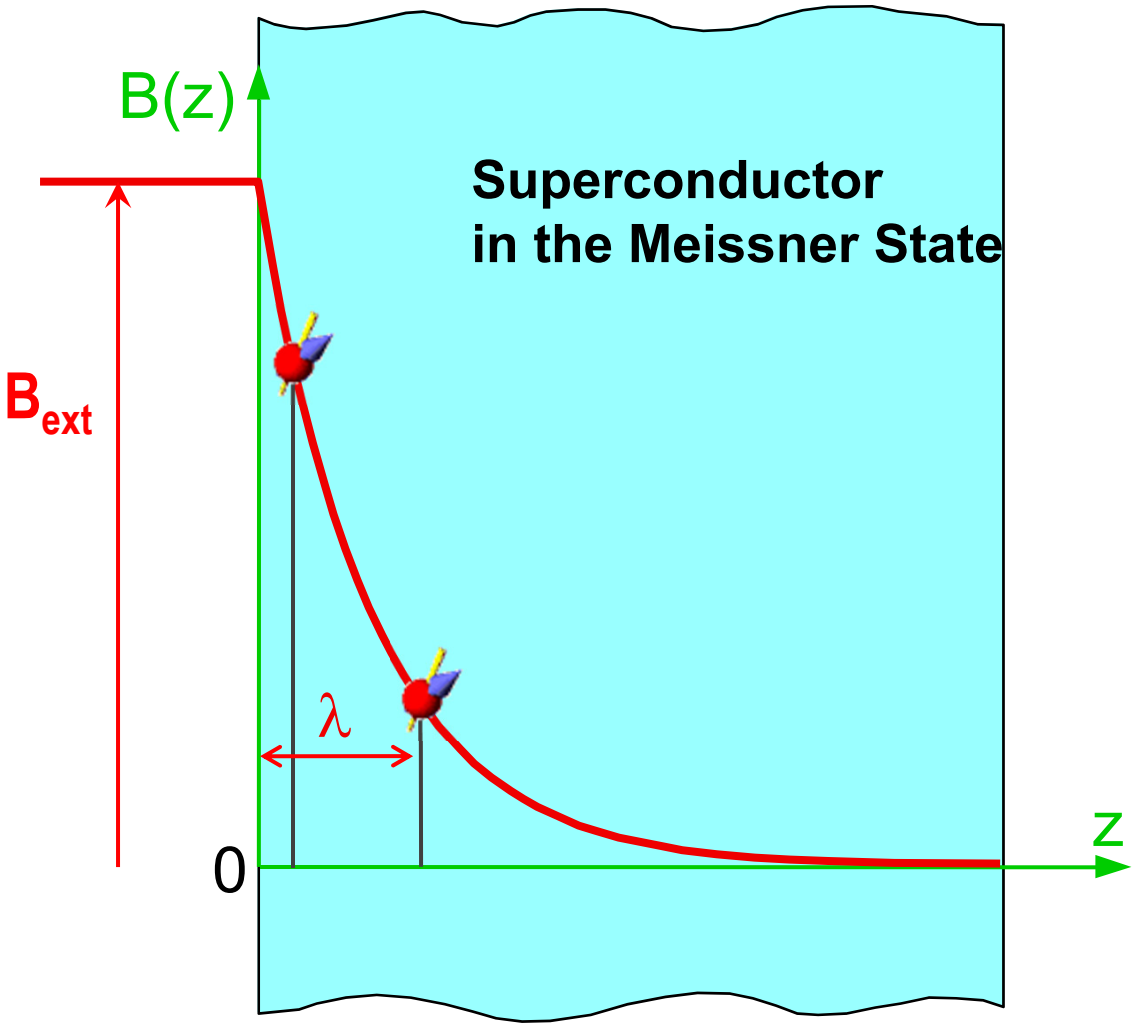


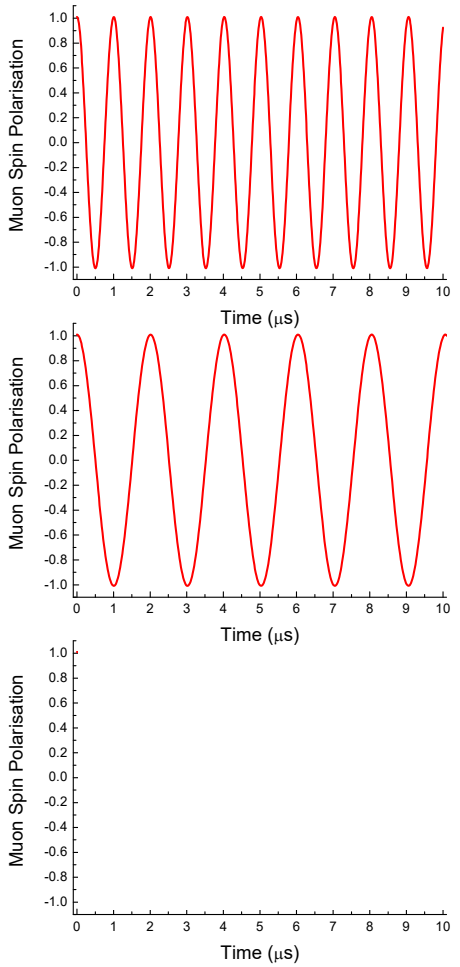


$$\omega_\mu(z) = \gamma_\mu B_{\mathrm{loc}}(z)$$

# Muon spin rotation – measure B(z) directly

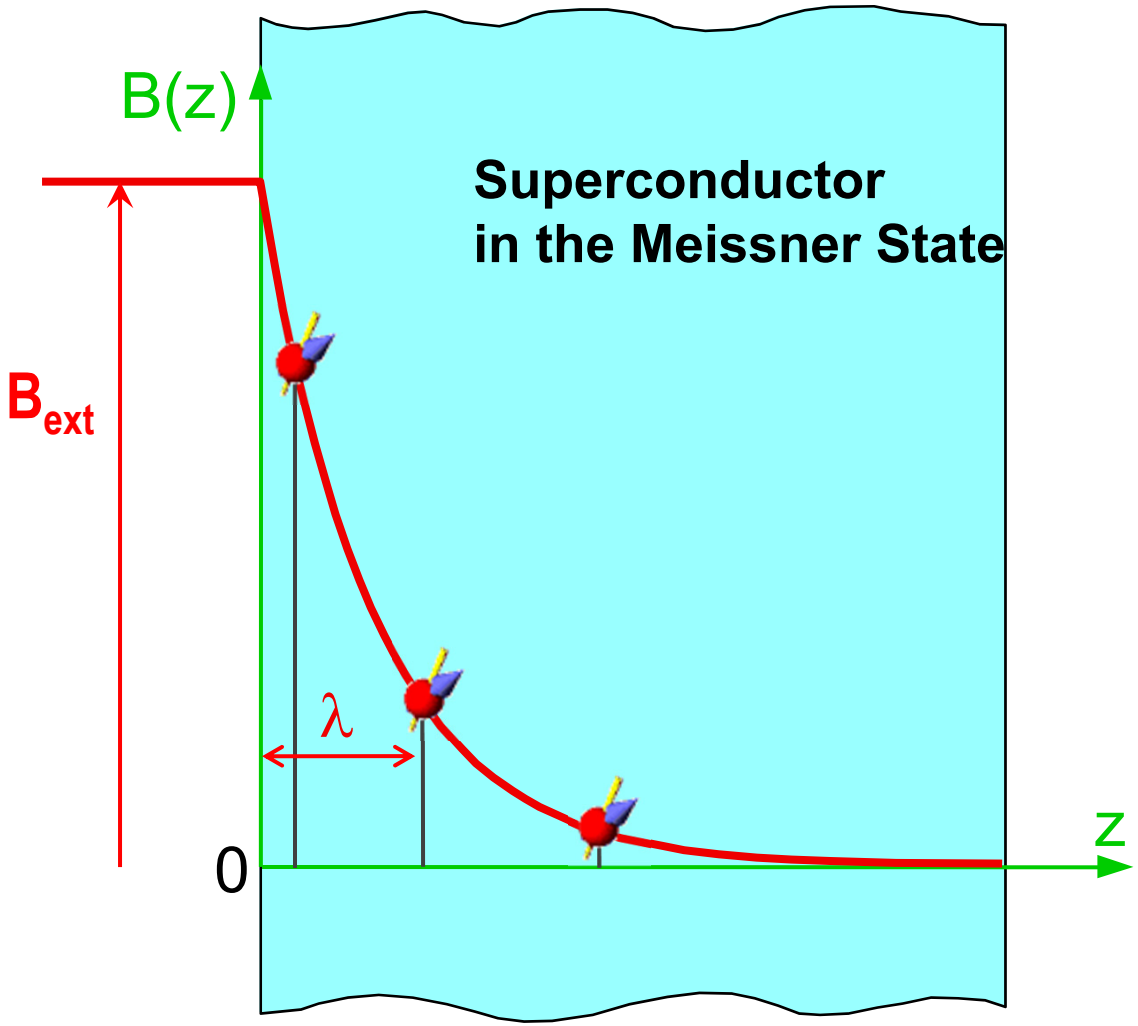


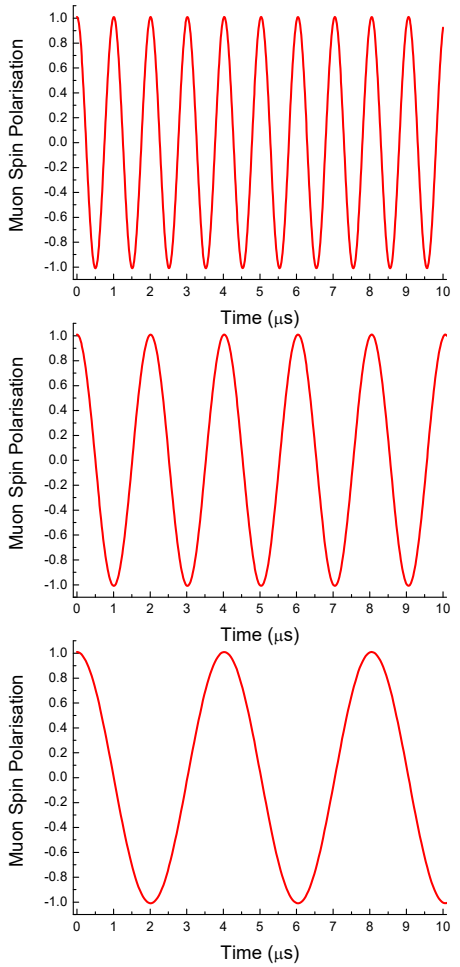


$$\omega_\mu(z) = \gamma_\mu B_{\mathrm{loc}}(z)$$

# 120C bake leads to strong Meissner screening changes

A. Romanenko, A. Grassellino, F. Barkov, A. Suter, Z. Salman, T. Prokscha, Appl. Phys. Lett. **104**, 072601 (2014)

- Heat treatment at 120C leads to the strong increase in the penetration depth
  - Consistent with the depth-dependent mean free path decrease
- Is also the first ever confirmation of non-locality in bulk niobium
  - Textbook example

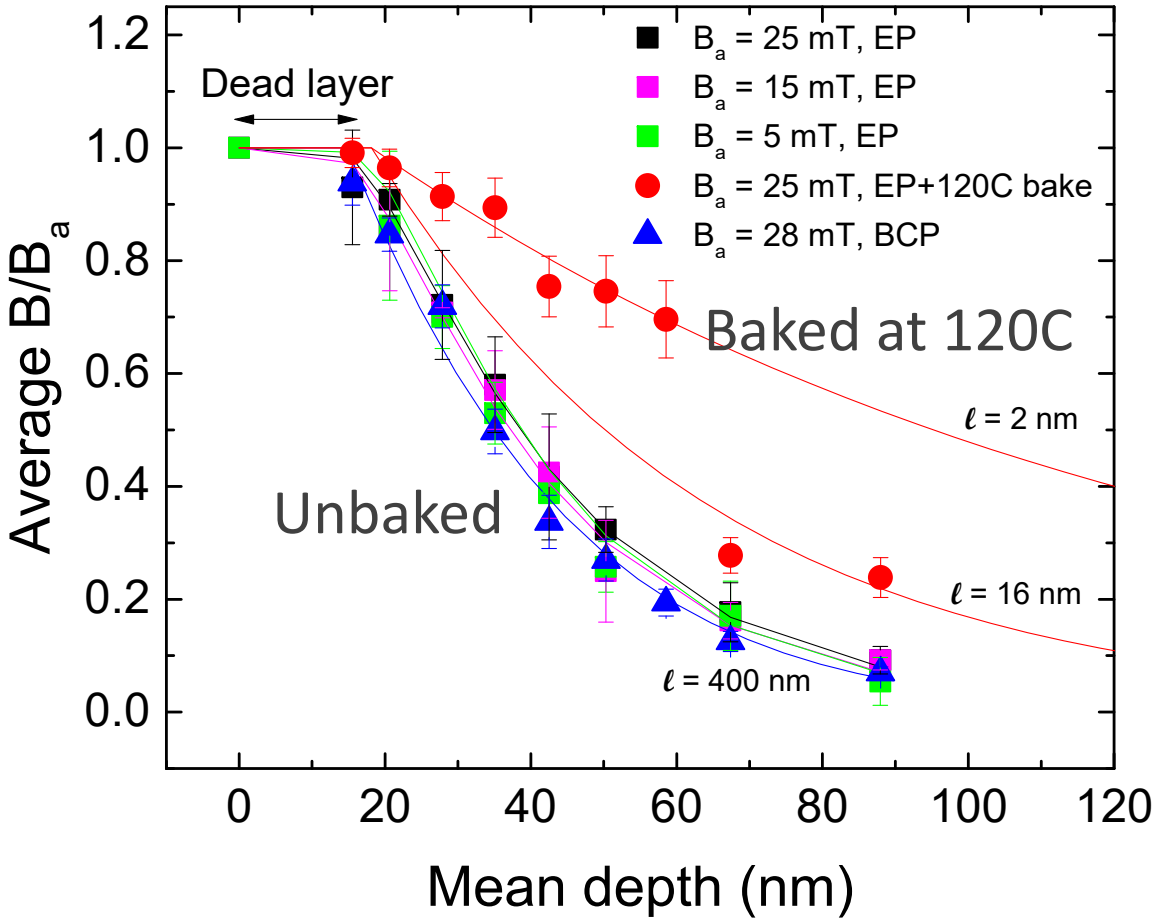

# Positron annihilation Doppler broadening spectroscopy

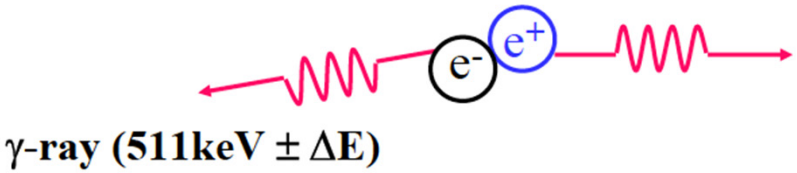


γ-ray (511keV ± ΔE)

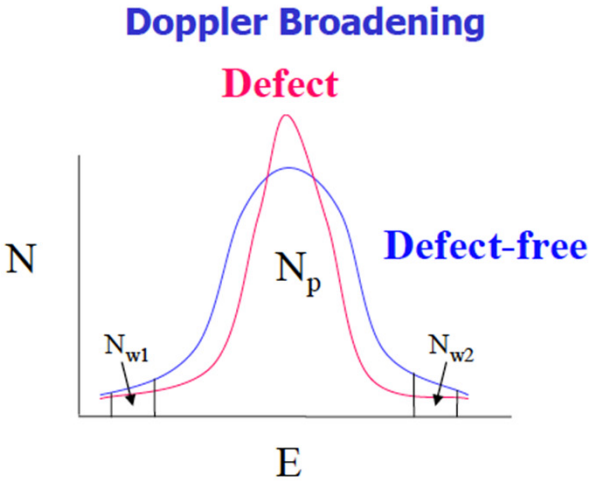


$S = N_p/N_{total}$

$S_{defect} > S_{defect\text{-}free}$

$W = (N_{w1}+N_{w2})/N_{total}$

- S parameter corresponds to positron annihilation with valence electrons, W-> core electrons
- S is sensitive to open-volume defects, W-to chemical surrounding at the annihilation site
- Increase in S parameter indicates presence of vacancy defects

# Positron annihilation studies on cavity cutouts

Collaboration with Bath University (UK) and Western University (Canada)

A. Romanenko, C. J. Edwardson, P. G. Coleman, P. J. Simpson, Appl. Phys. Lett. **102**, 232601 (2013)

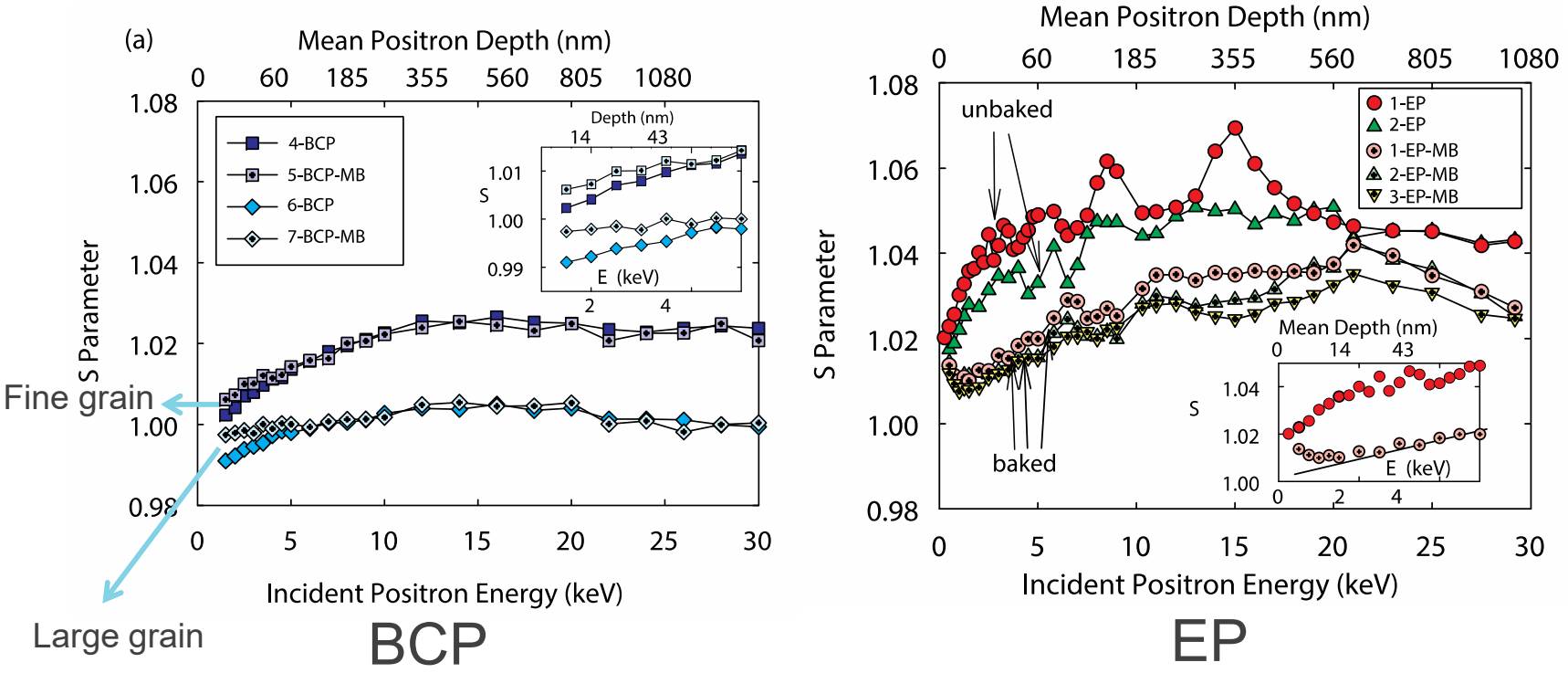


- Positron annihilation spectroscopy: 120C baking results in “doping” of the first ~50 nm from the surface with vacancies
  - So-called superabundant vacancy formation mechanism manifested in niobium [Y. Fukai and N. Okuma, Phys. Rev. Lett. **73**, 1640 (1994)]

# Effect of 120C baking

# Effect of 120C baking

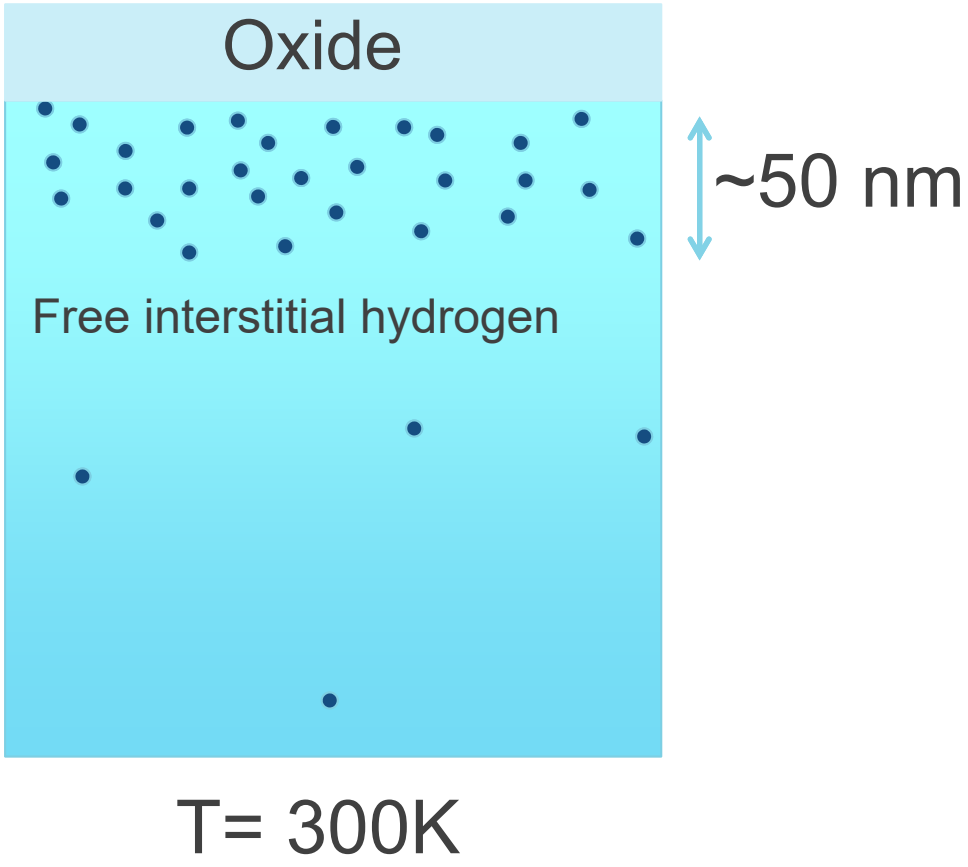

# Effect of 120C baking

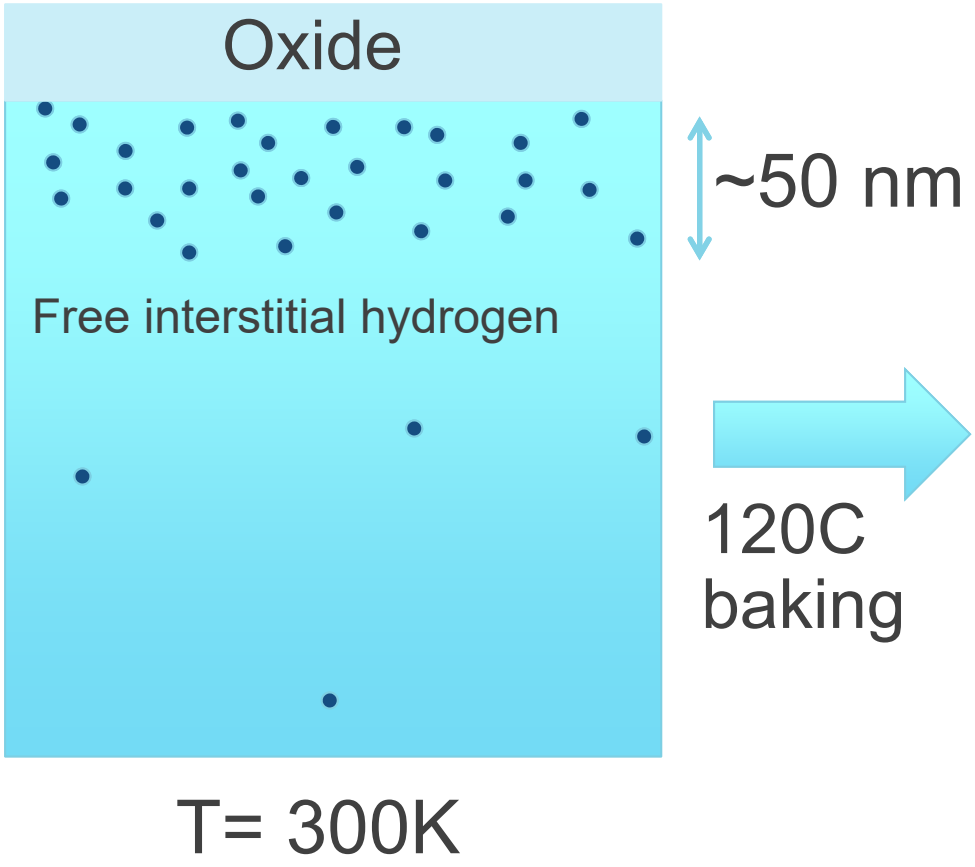

# Effect of 120C baking

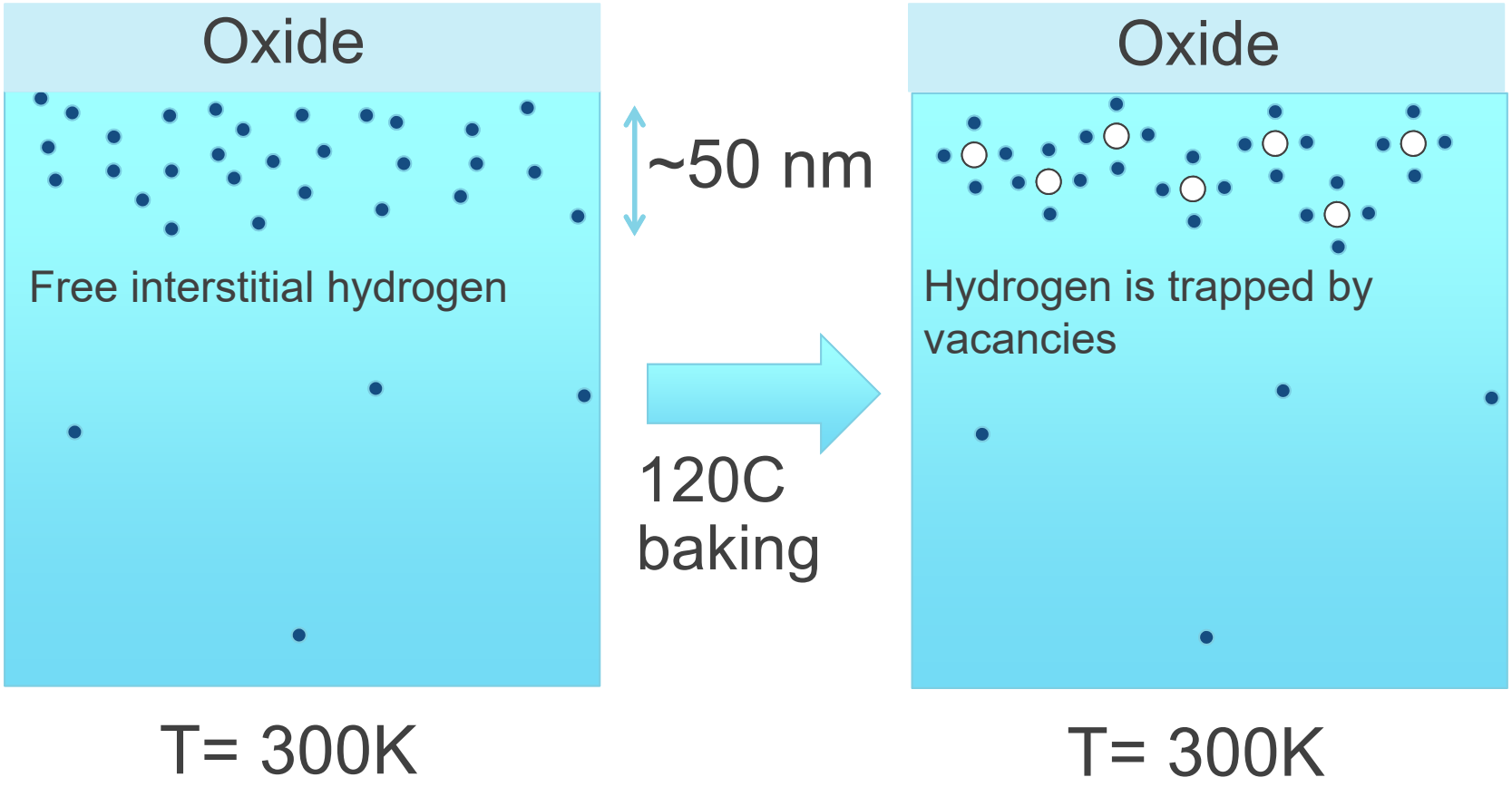

# Effect of 120C baking

Cooling down of 120C baked niobium

# Effect of 120C baking

Cooling down of 120C baked niobium

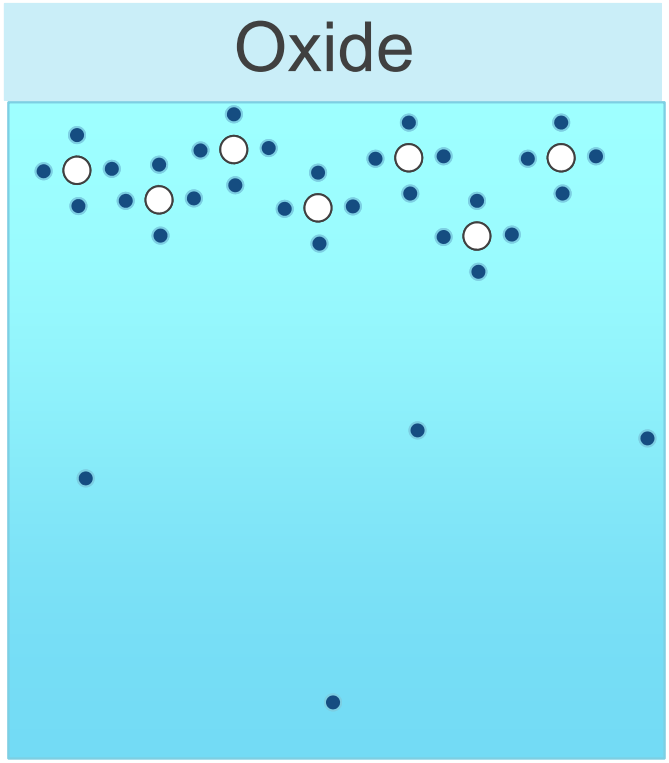


T= 300K

# Effect of 120C baking

## Cooling down of 120C baked niobium

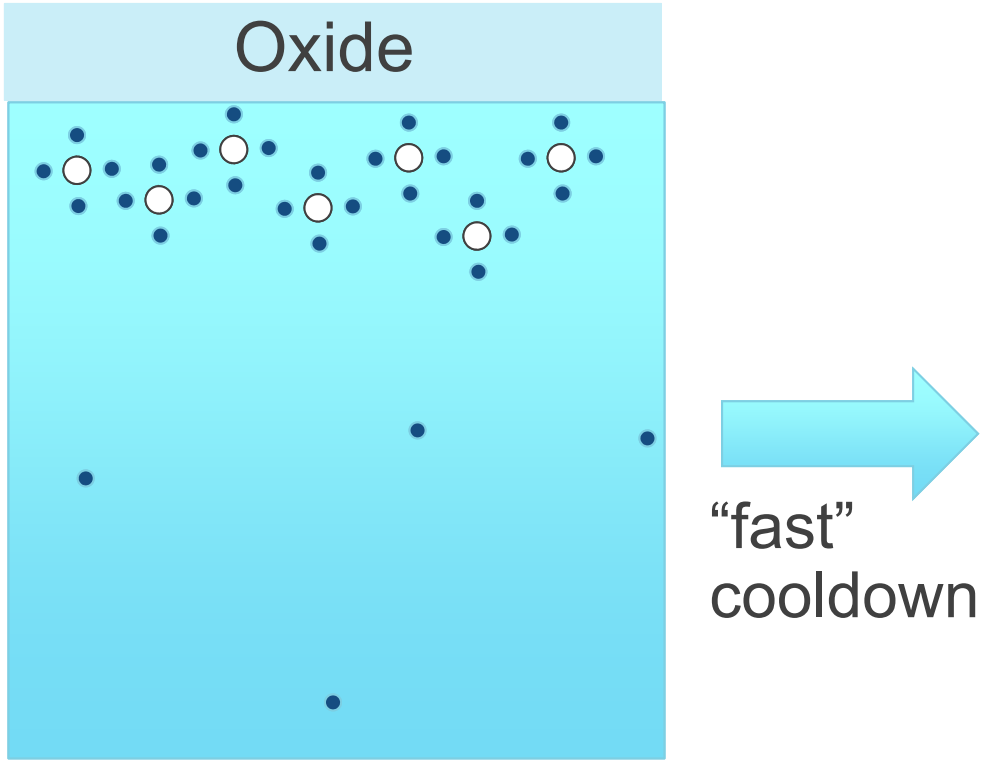


“fast” cooldown

T= 300K

# Effect of 120C baking

## Cooling down of 120C baked niobium

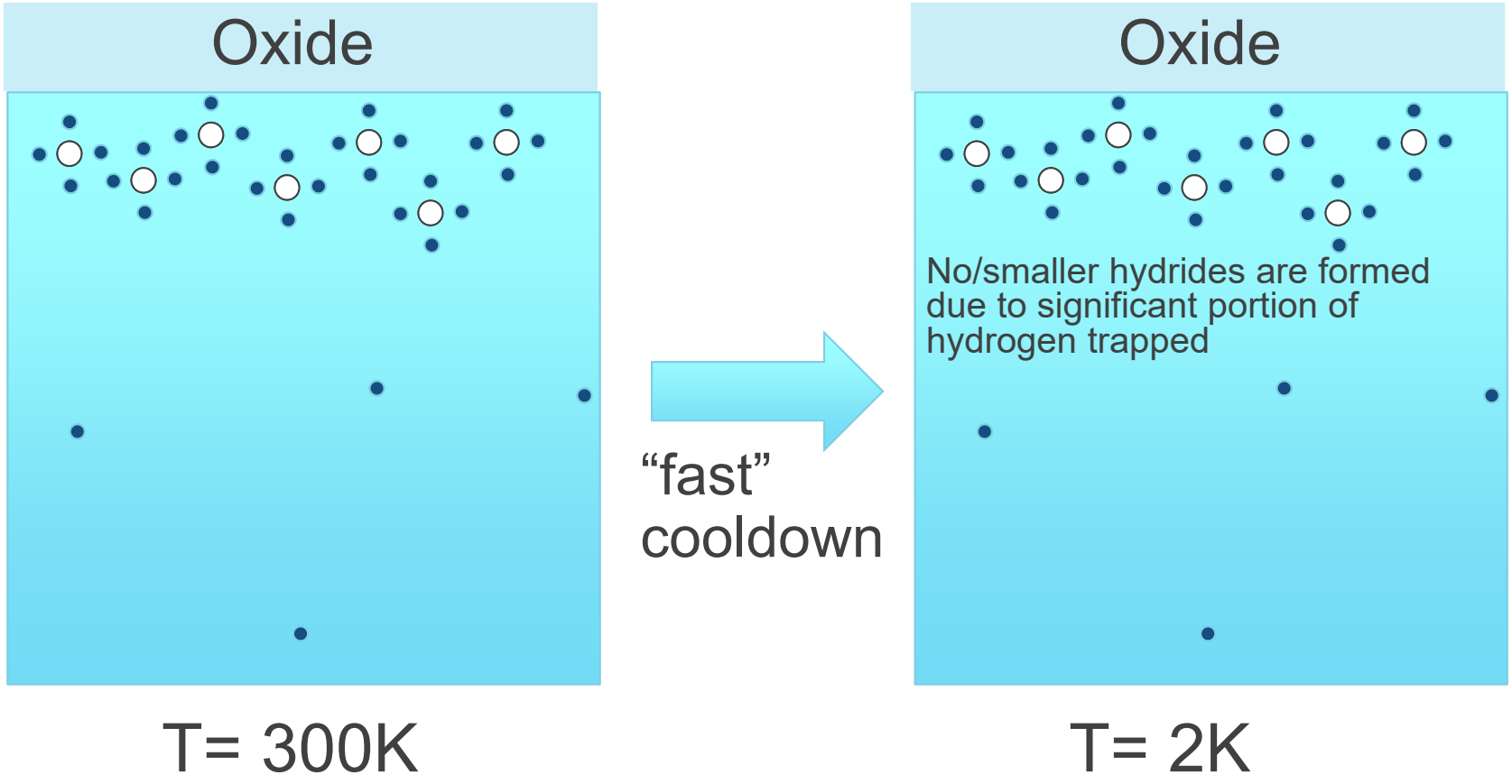

# TEM -> further evidence for 120C baking effect

Measurements performed at Univ. of Illinois Urbana-Champaign

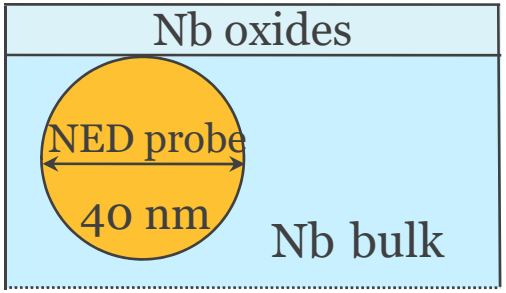


Room T: BCC Nb patterns, NO additional phases

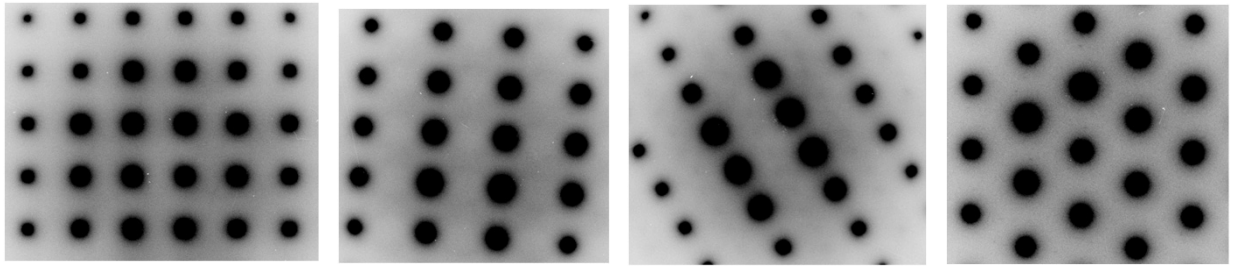

94K: stoichiometric Nb hydride phases

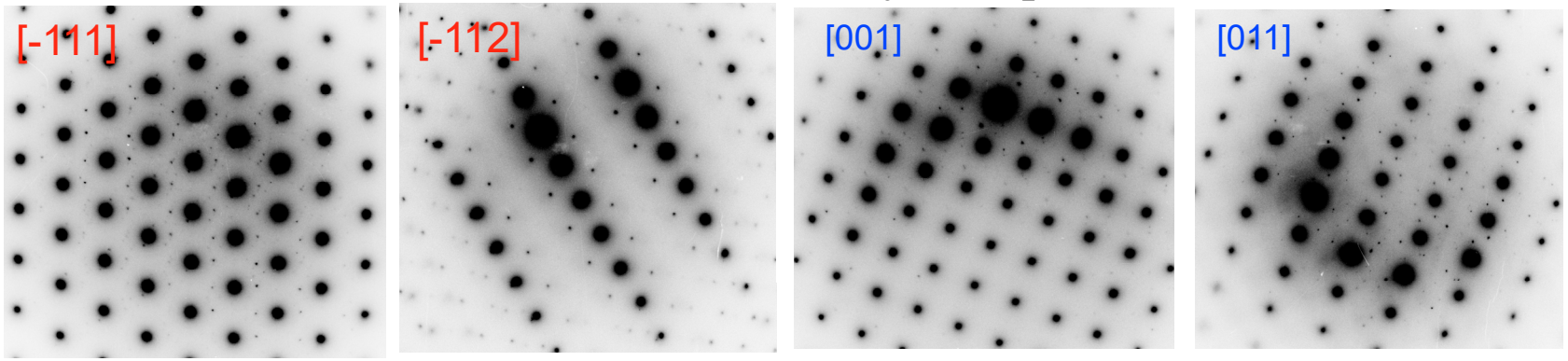


Hot spot: 44-68% of probed spots

Baked spot: 26-29% of probed spots

120C baking leads to the decrease in size/density of the nanohydrides

# High T N doping removes the HFQS

- 20-100 ppm of $N_2$ push the onset of HFQS > 30 MV/m
- First data point that unequivocally tells us that low level of interstitial nitrogen helps removing the HFQS

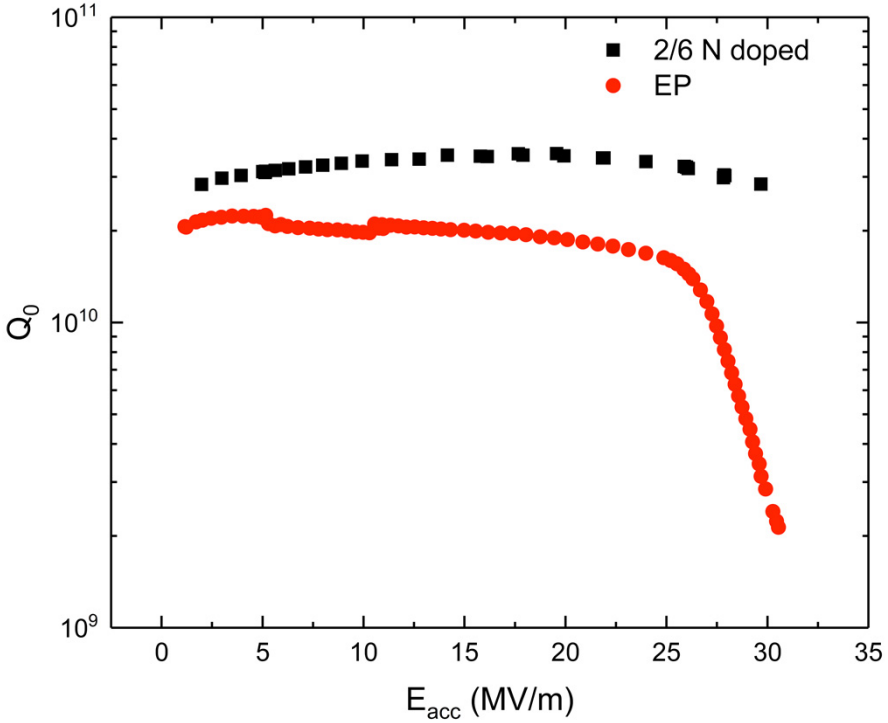


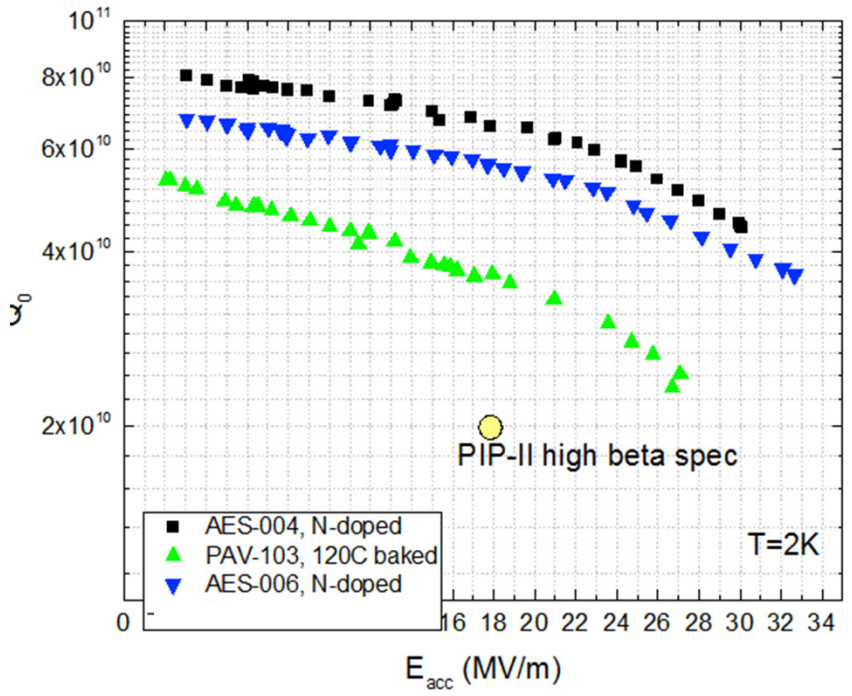

# 120C 48 hrs with no oxide – N infusion versus no N infusion

- Repeated same procedure with and without nitrogen in furnace at 120C
- Holding at 120C in furnace for 48 hours post 800C without the nitrogen does not completely remove the high field Q-slope
- It pushes the onset of HFQS to higher fields ~ 30 MV/m
- **Nitrogen is needed to remove HFQS completely** and achieve highest fields

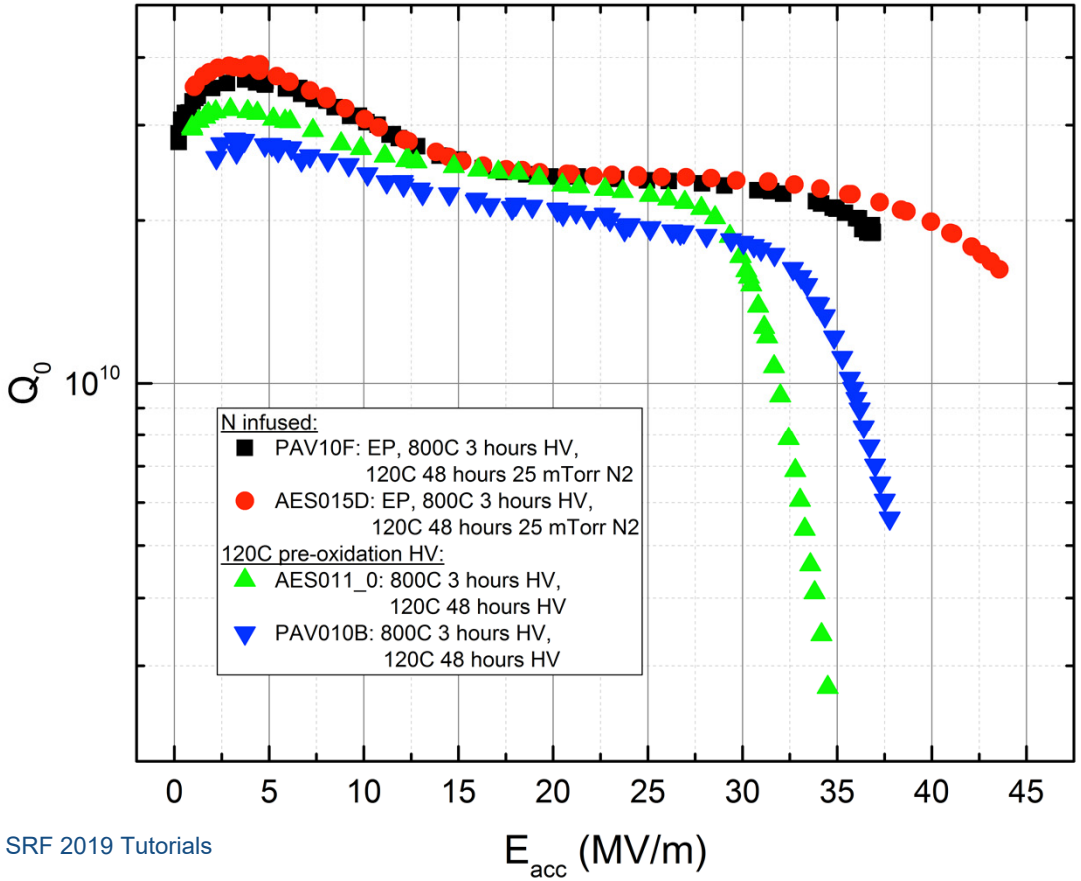


A Grassellino *et al* 2017 *Supercond. Sci. Technol.* **30** 094004

# Low energy muSR measurements are in agreement

A. Romanenko et al, Appl. Phys. Lett. **104**, 072601 (2014)

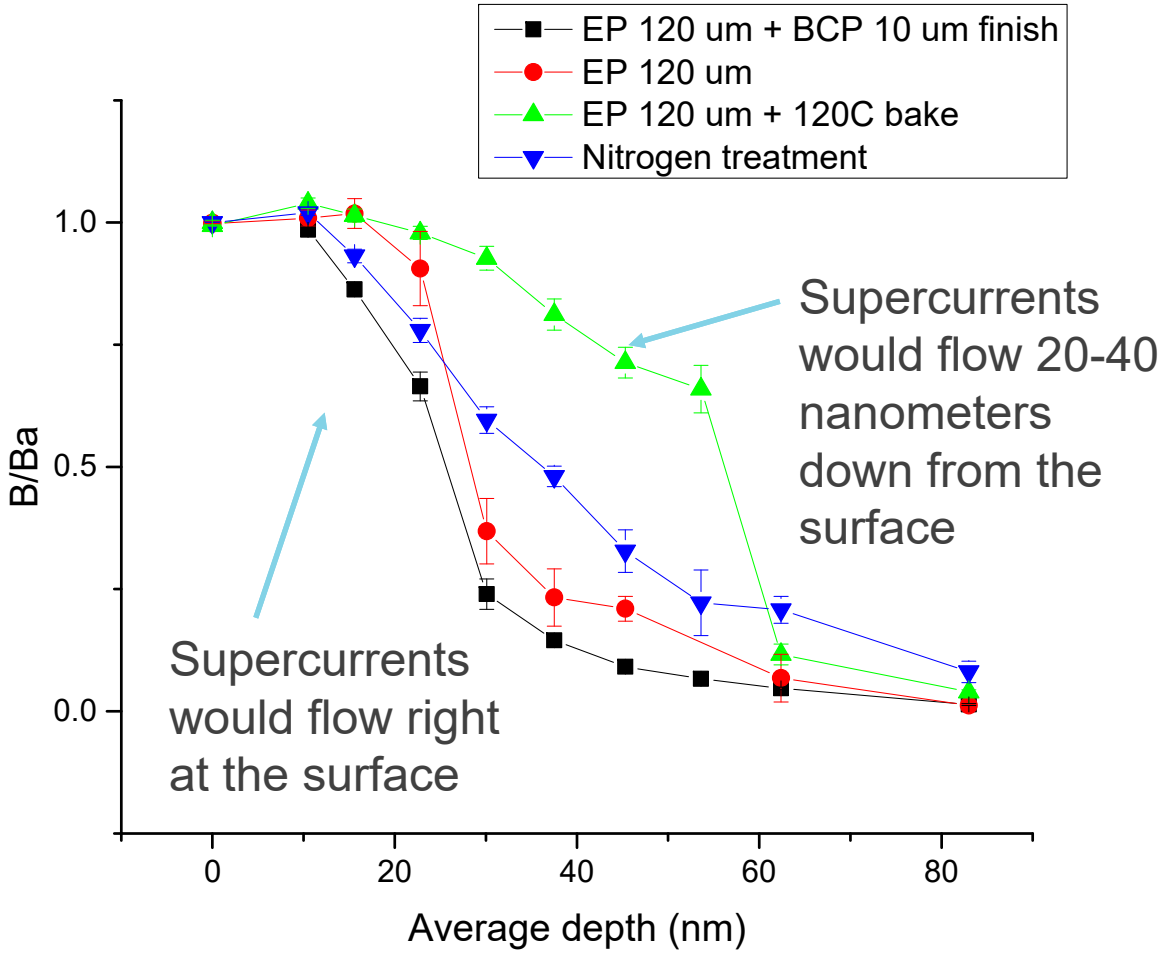


This model would explain why “bad is good”…and for the first time offers a potential explanation of why 120C bake helps roughness

# Frequency dependence of HFQS onset

- No clear dependence found (maybe 650 slightly higher, opposite to what previously reported by G. Ciovati)

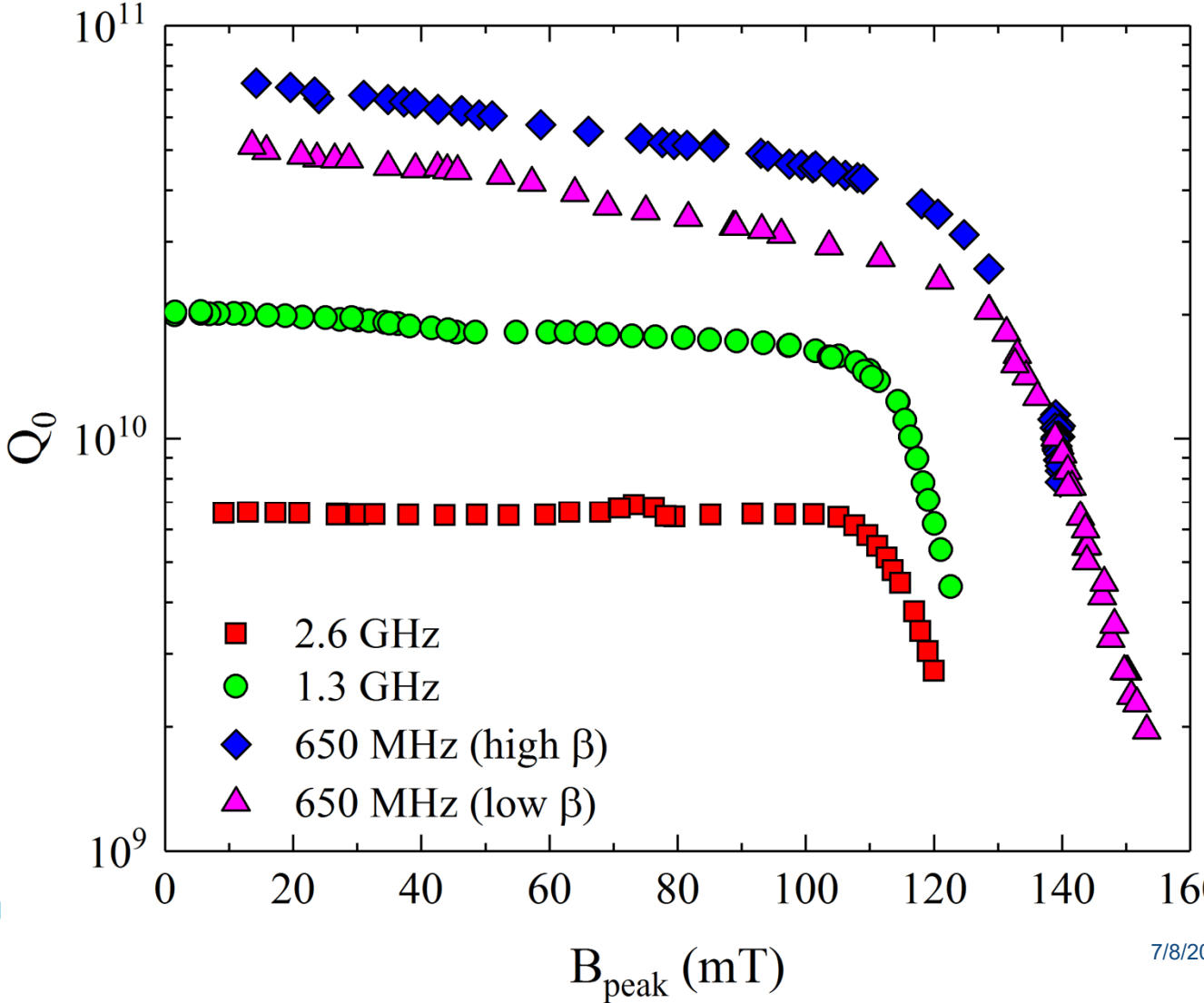

# Summarizing models vs experimental data, where we stand

| | Slope before baking (EP>BCP FG, FG EP=LG BCP) | Slope improvement after 120C baking | Slope cured by interstitial nitrogen, but not fully by 120C alone | Frequency Dependence | Anodization | HF rinse studies post bake | Rs decomposition (HFQS in residual) | Tmap HFQS pattern | HFQS reappear after 800C | SIMS, XPS and other surface characterization data |
|---|---|---|---|---|---|---|---|---|---|---|
| Magnetic Field Enhancement | Y | N | N | Y | ? | N | Y | Y | N | Y |
| Surface Nano-roughness + dead layer | Y | Y | Y | Y | ? | Y | Y | Y | Y | Y |
| Proximity Breakdown of Hydrides | Y | Y | ? | Y | Y | Y | Y | Y | Y | Y |
| Magnetic Flux depinning | N | Y | ? | N | Y | Y | Y | Y | Y | Y |
| Interface Tunnel Exchange | N | Y | ? | N | N | N | Y | N | | N |
| Magnetic Field Dependence of Gap | N | N | ? | Y | Y | ? | N | Y | Y | ? |
| Thermal Feedback | N | N | N | N | Y | N | N | Y | N | Y |
| Oxygen pollution and | Y | Y | ? | Y | ? | Y | Y | Y | N | N |

# The Q Frontier

# Recent breakthrough for Q: N doping of Nb cavities

800C UHV, 3 hours

800C $N_2$ p = 25 mTorr 2 minutes

800C UHV, 6 minutes

UHV cooling

5 um EP

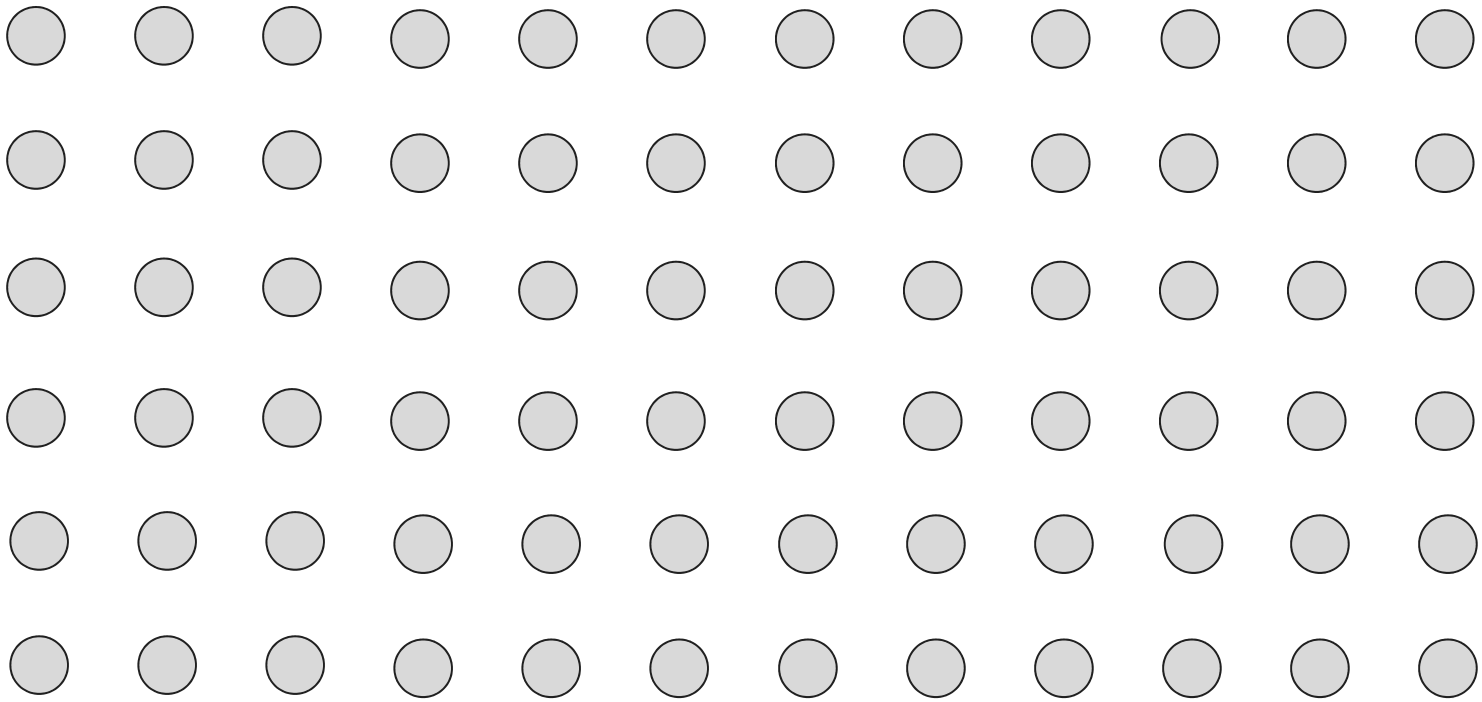

*Slides adapted from M. Martinello*

# Recent breakthrough for Q: N doping of Nb cavities

800C UHV, 3 hours → 800C $N_2$ p = 25 mTorr 2 minutes | 800C UHV, 6 minutes | UHV cooling | 5 um EP

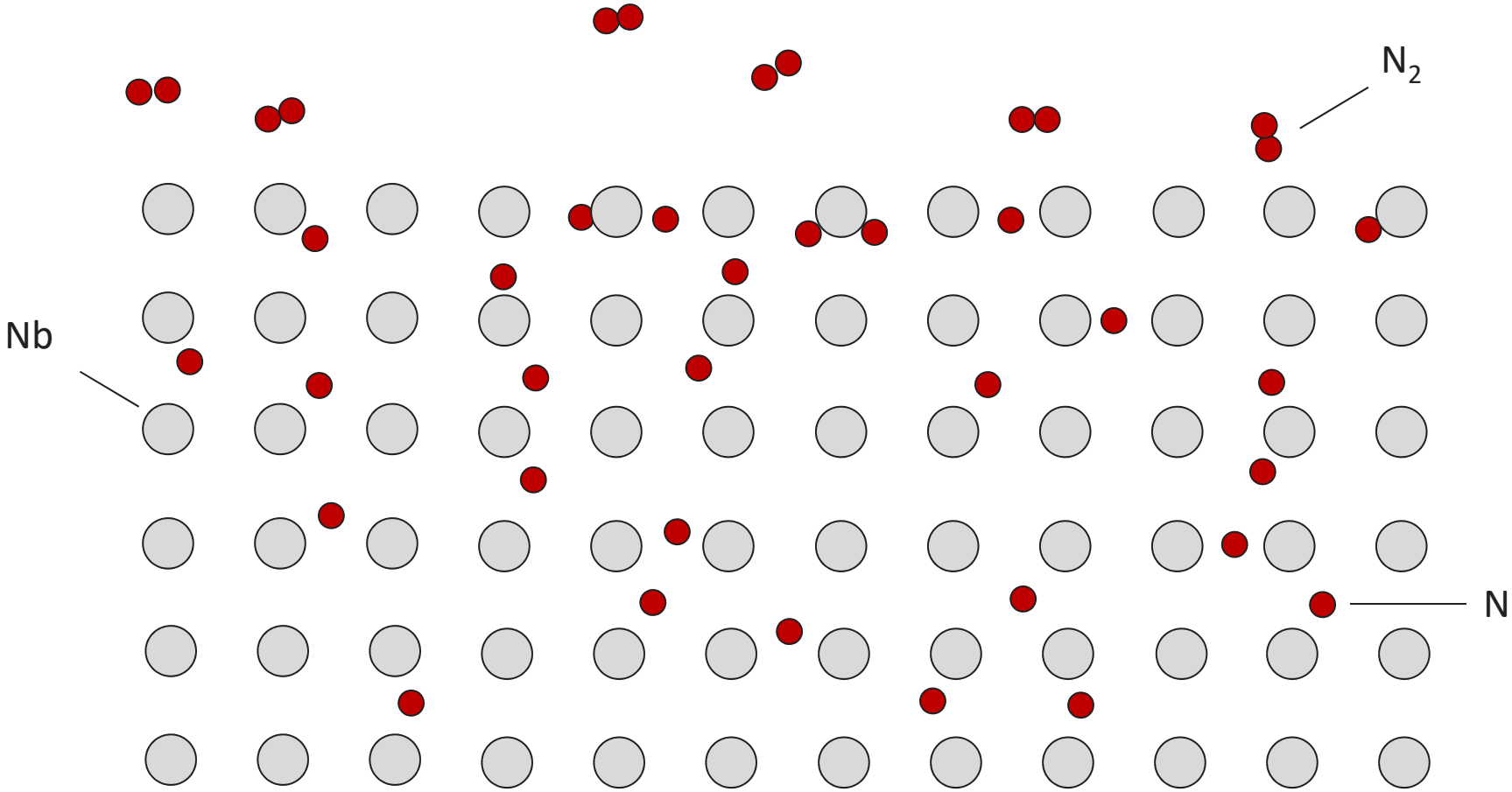


*Slides adapted from M. Martinello*



Fermilab

# Recent breakthrough for Q: N doping of Nb cavities

800C UHV, 3 hours → 800C $N_2$ p = 25 mTorr 2 minutes → 800C UHV, 6 minutes → UHV cooling → 5 um EP

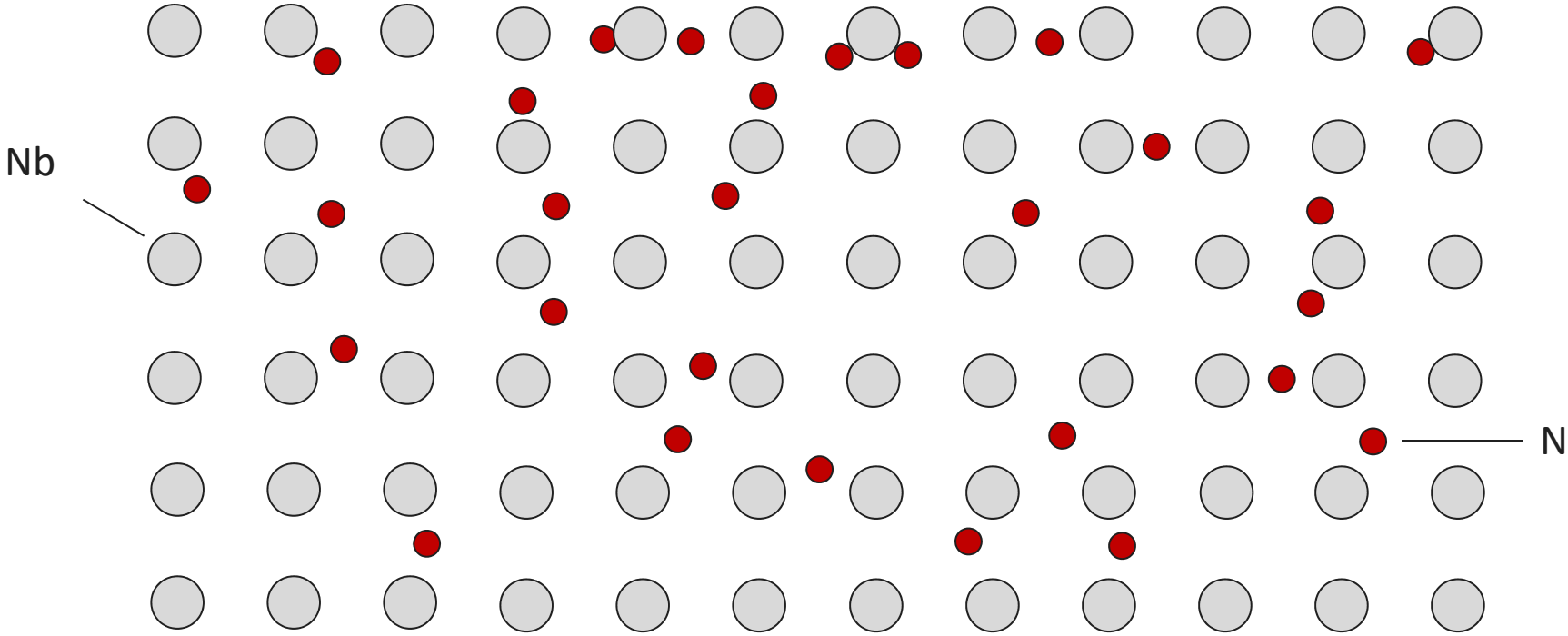


*Slides adapted from M. Martinello*



Fermilab

# Recent breakthrough for Q: N doping of Nb cavities

800C UHV, 3 hours → 800C $N_2$ p = 25 mTorr 2 minutes → 800C UHV, 6 minutes → UHV cooling

5 um EP

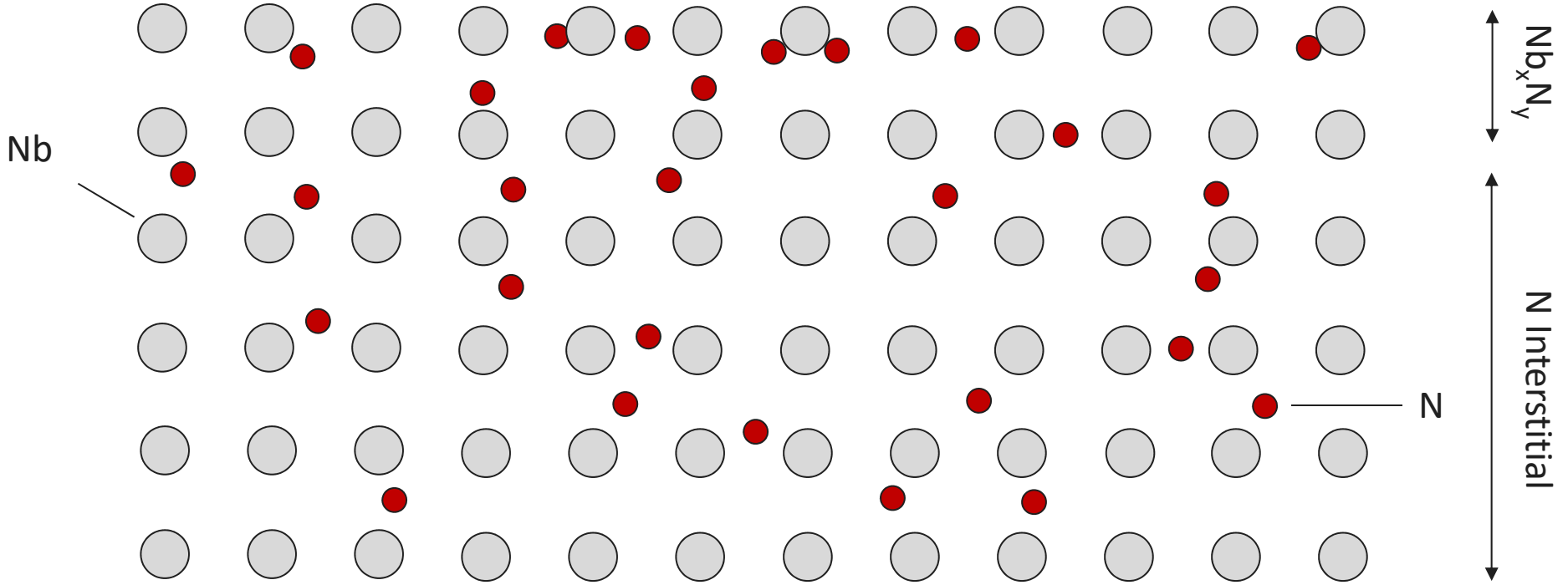


*Slides adapted from M. Martinello*



Fermilab

# Recent breakthrough for Q: N doping of Nb cavities

800C UHV, 3 hours → 800C $N_2$ p = 25 mTorr 2 minutes → 800C UHV, 6 minutes → UHV cooling

5 um EP

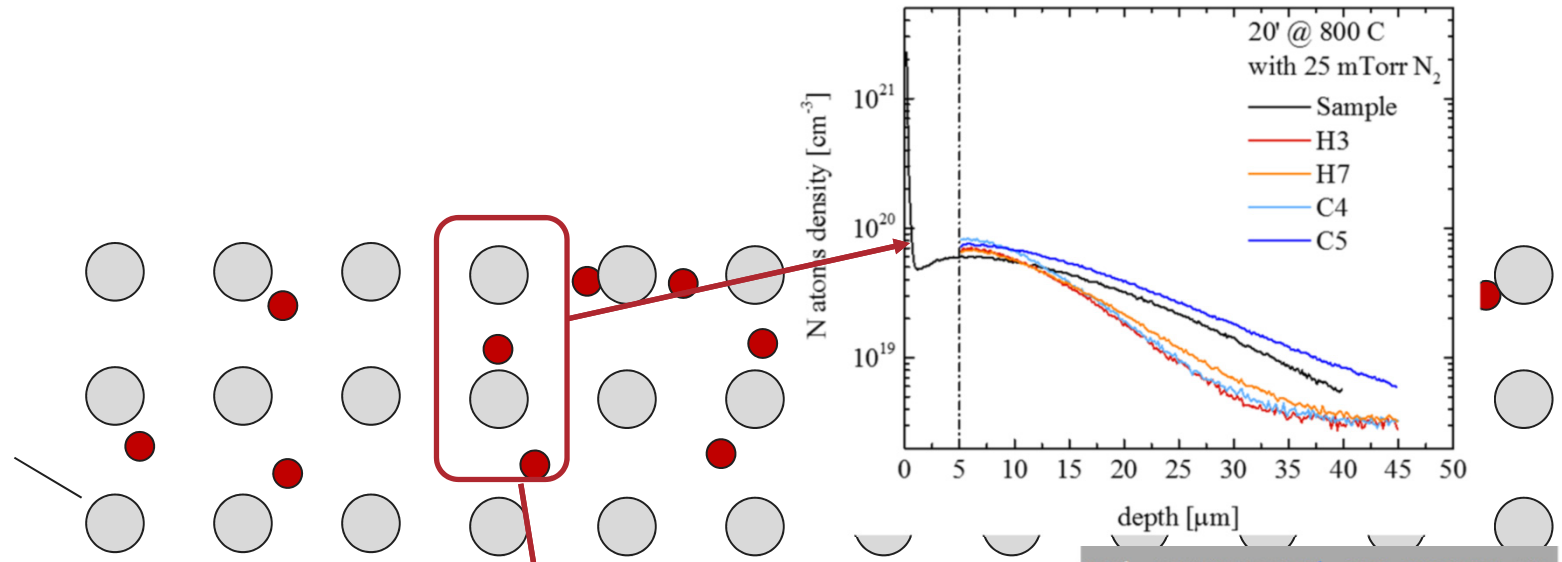


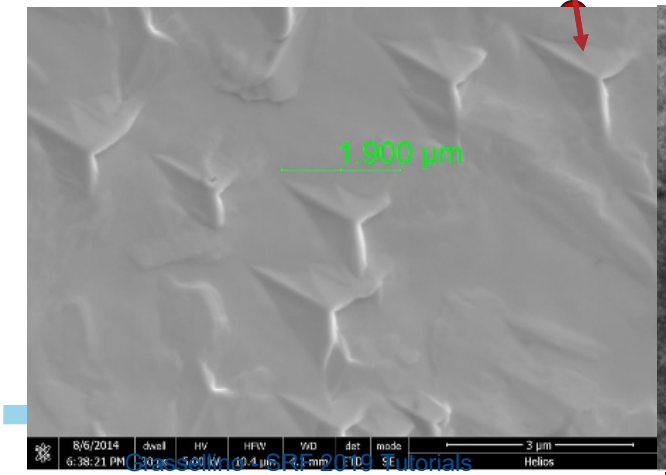


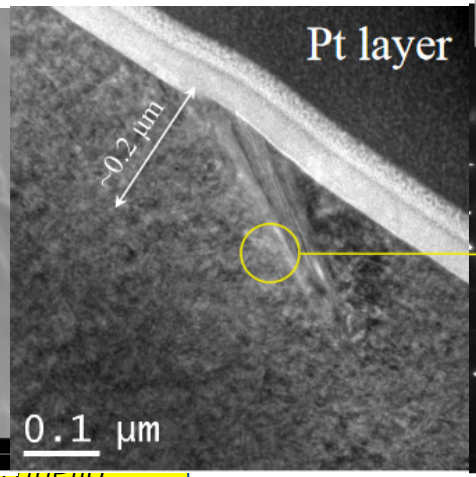


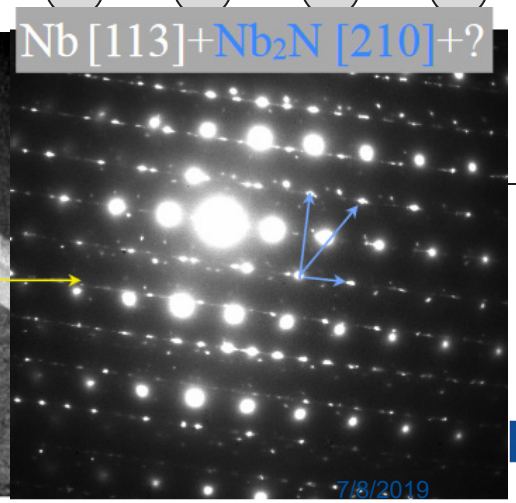


$Nb_xN_y$

N

N Interstitial

# Recent breakthrough for Q: N doping of Nb cavities

800C UHV, 3 hours → 800C $N_2$ p = 25 mTorr 2 minutes → 800C UHV, 6 minutes → UHV cooling

5 um EP

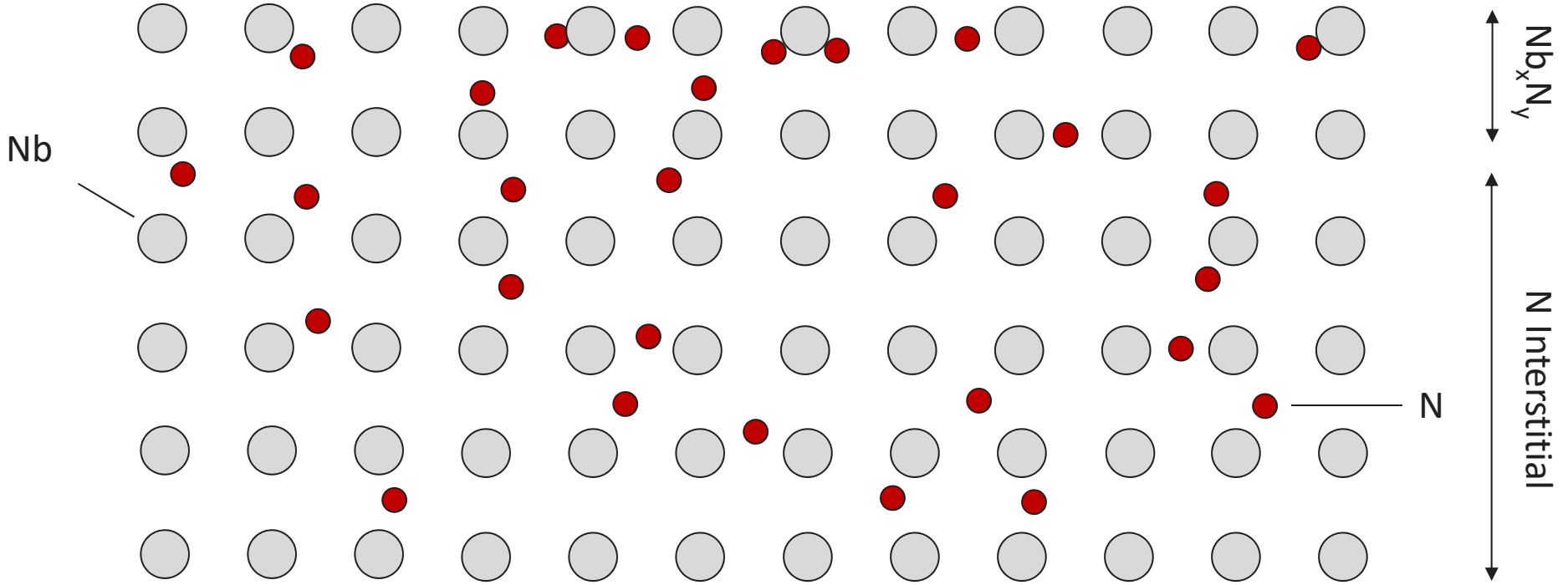


*Slides adapted from M. Martinello*



Fermilab

# Recent breakthrough for Q: N doping of Nb cavities

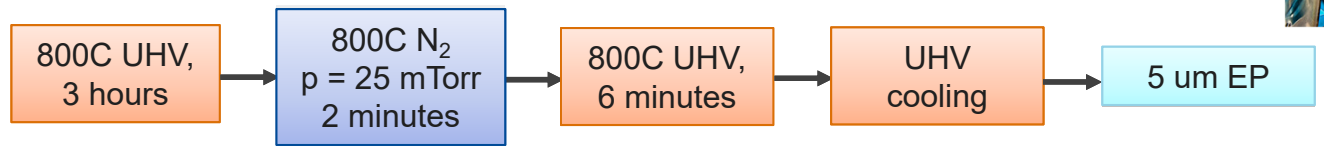


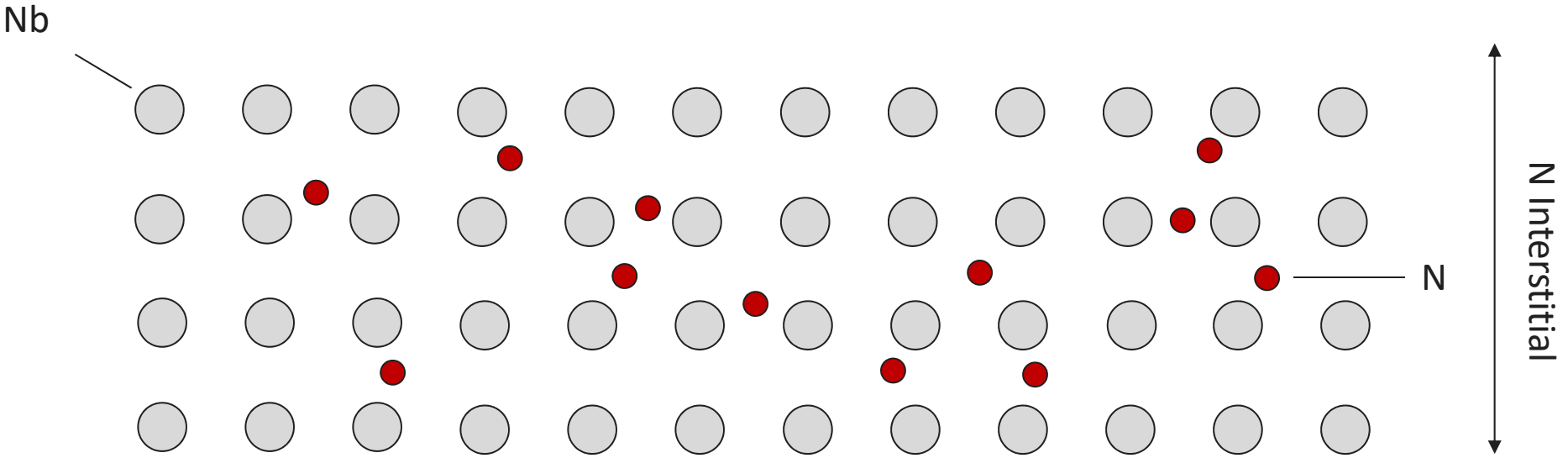


*Slides adapted from M. Martinello*

# Recent breakthrough for Q: N doping of Nb cavities

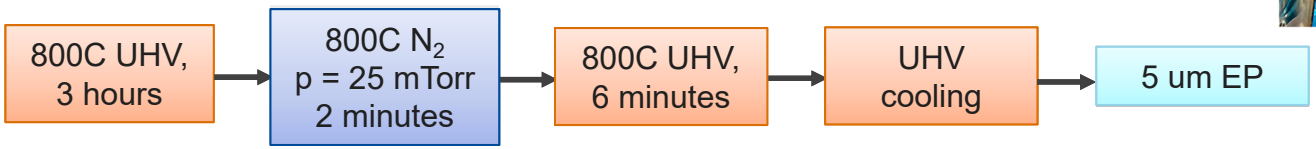


## Final RF Surface

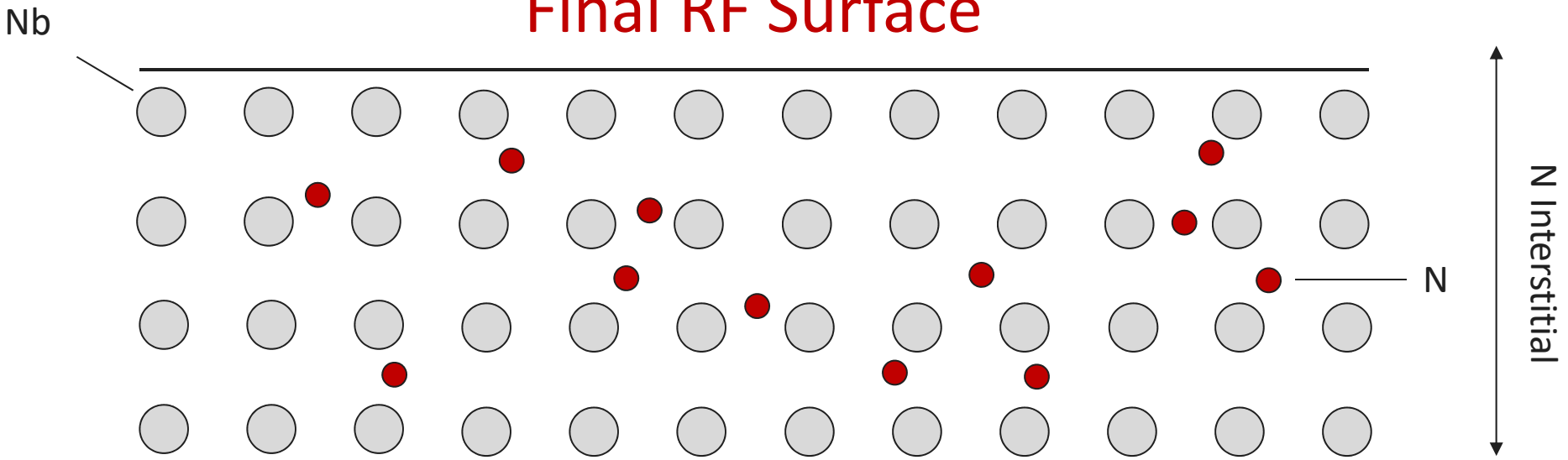


*Slides adapted from M. Martinello*

# Recent breakthrough for Q: N doping of Nb cavities

800C UHV, 3 hours → 800C $N_2$ p = 25 mTorr 2 minutes → 800C UHV, 6 minutes → UHV cooling → 5 um EP

Y. Trenikhina et Al, Proc. of SRF 2015

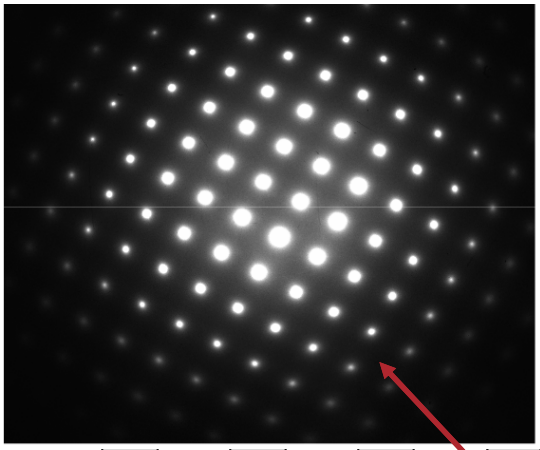

Nb

Final RF

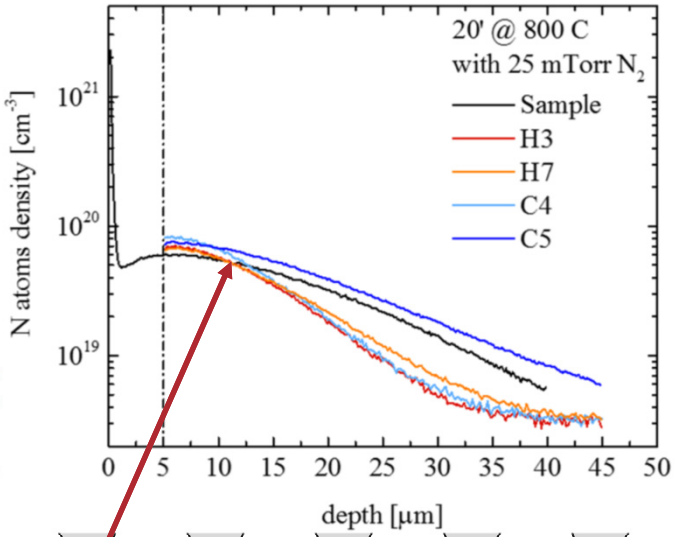


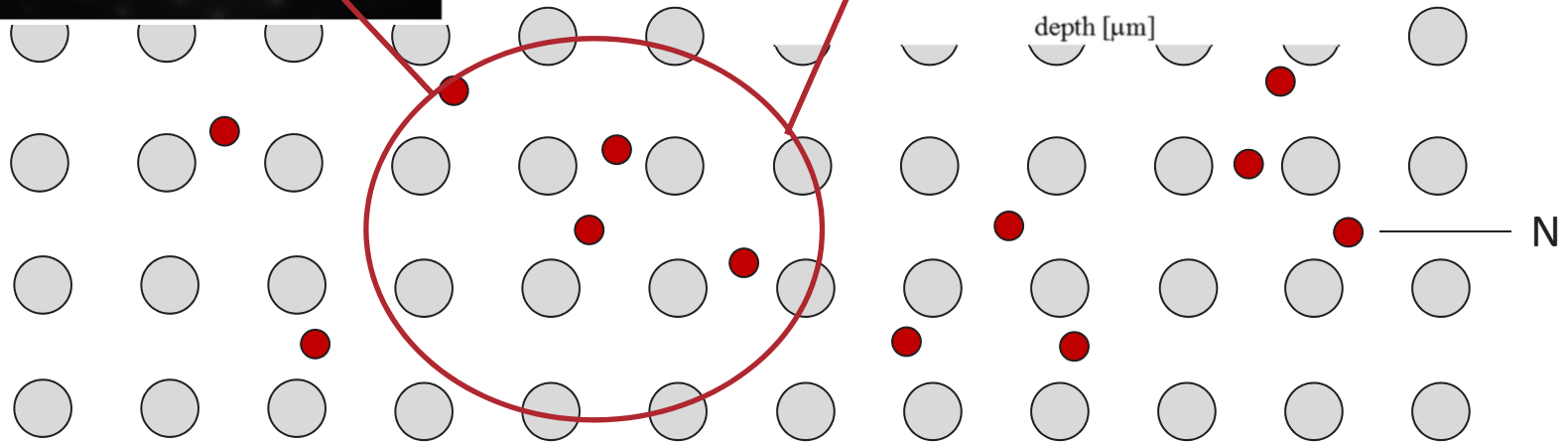




*Slides adapted from M. Martinello*

Fermilab

# Material level understanding

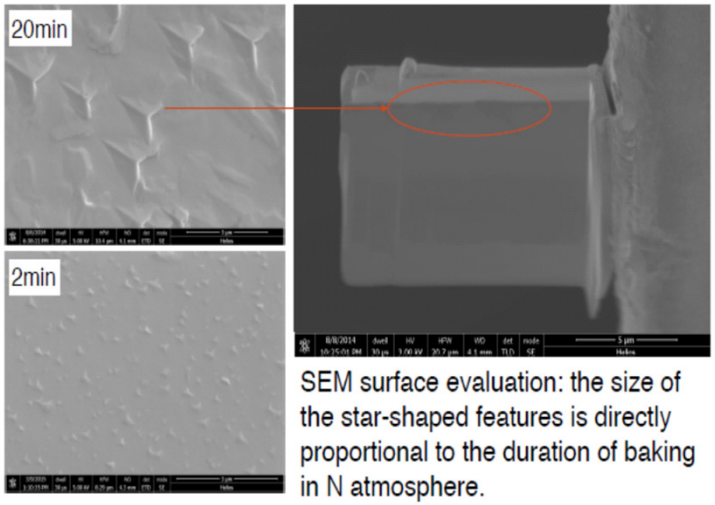


SEM surface evaluation: the size of the star-shaped features is directly proportional to the duration of baking in N atmosphere.

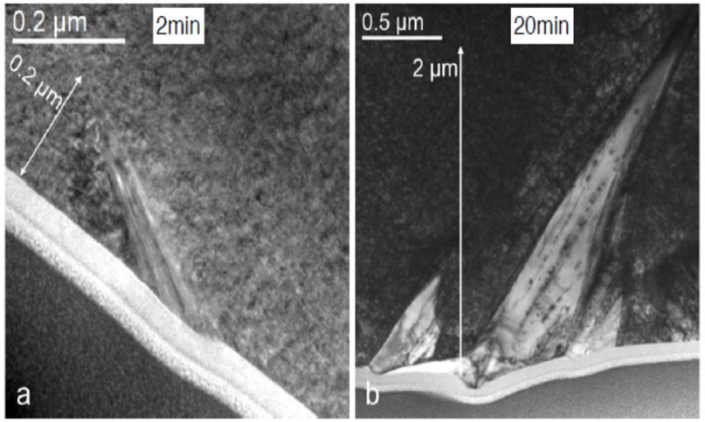


TEM near-surface evaluation: the depth which is affected by Nb nitrides is directly proportional to the duration of baking in N atmosphere.

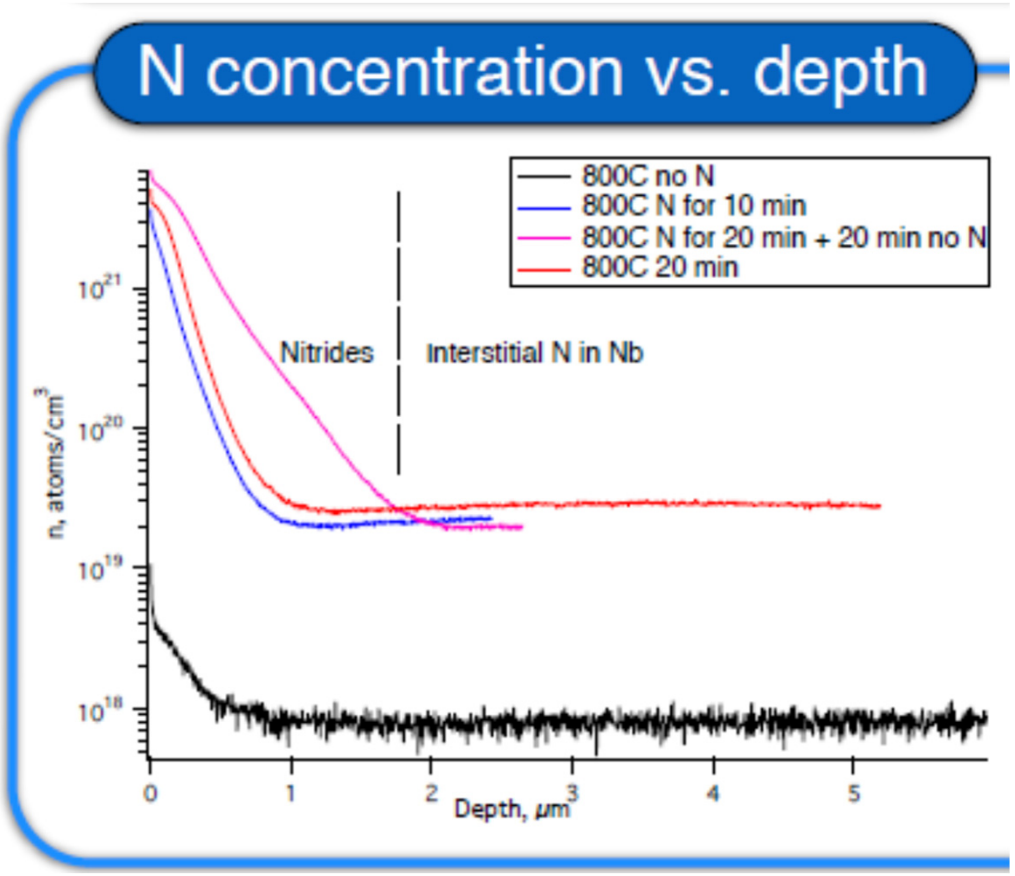

# Effect on Surface Resistance: the curious anti-Q slope effect

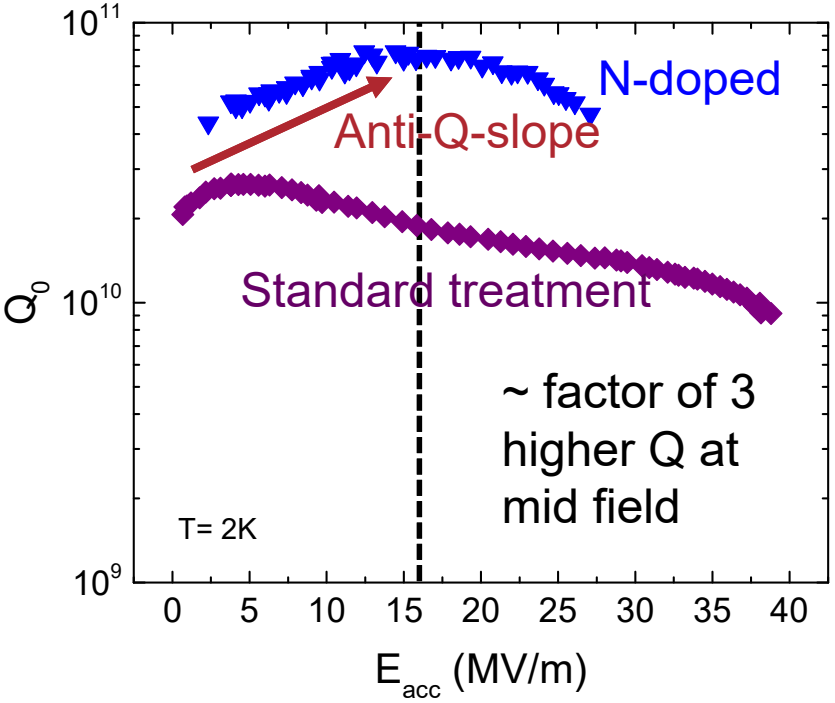


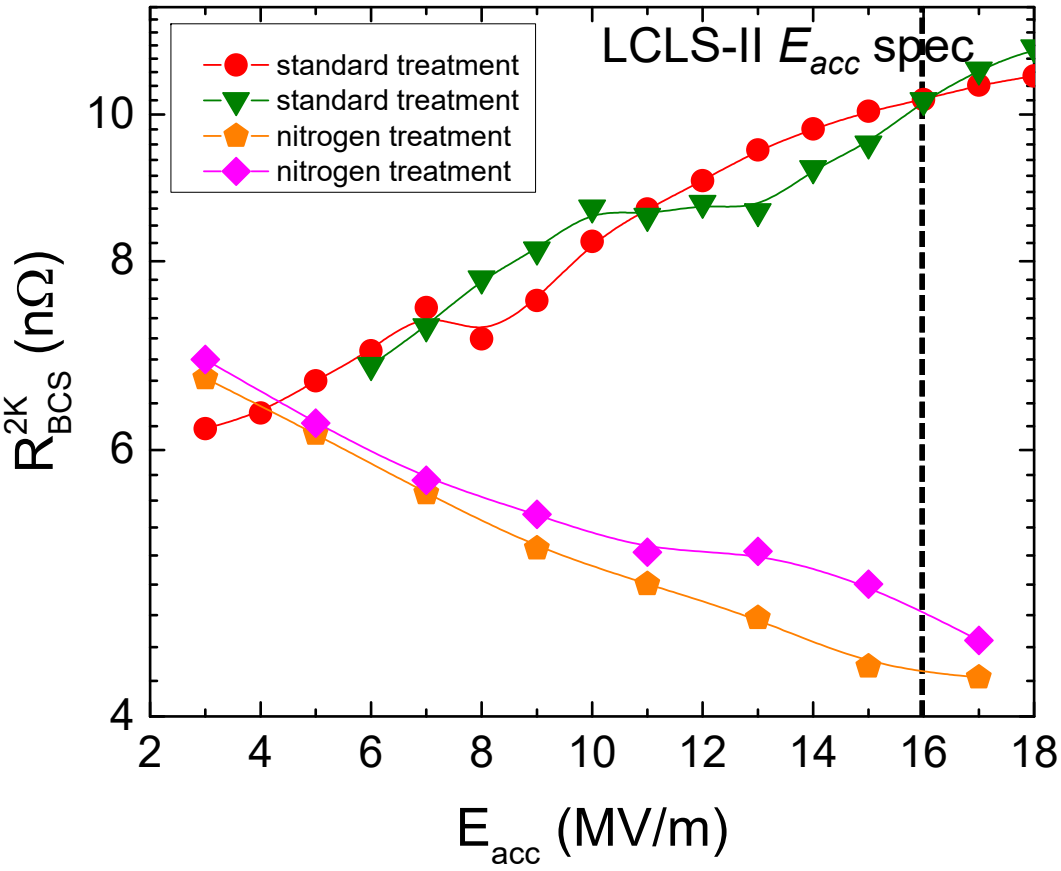


Anti-Q-slope emerges from the BCS surface resistance decreasing with field

→ **Unexpected, unprecedented**

- >2x $R_{BCS}$ improvement at 2 K, 16 MV/m
- 2-4 times higher quality factors achieved


A. Grassellino et al, 2013 Supercond. Sci. Technol. 26 102001 (Rapid Communication)
A. Romanenko and A. Grassellino, Appl. Phys. Lett. 102, 252603 (2013)

# Origin of Improved Surface Resistance due to N-Doping

LE-μSR measurements (Ba=25mT)

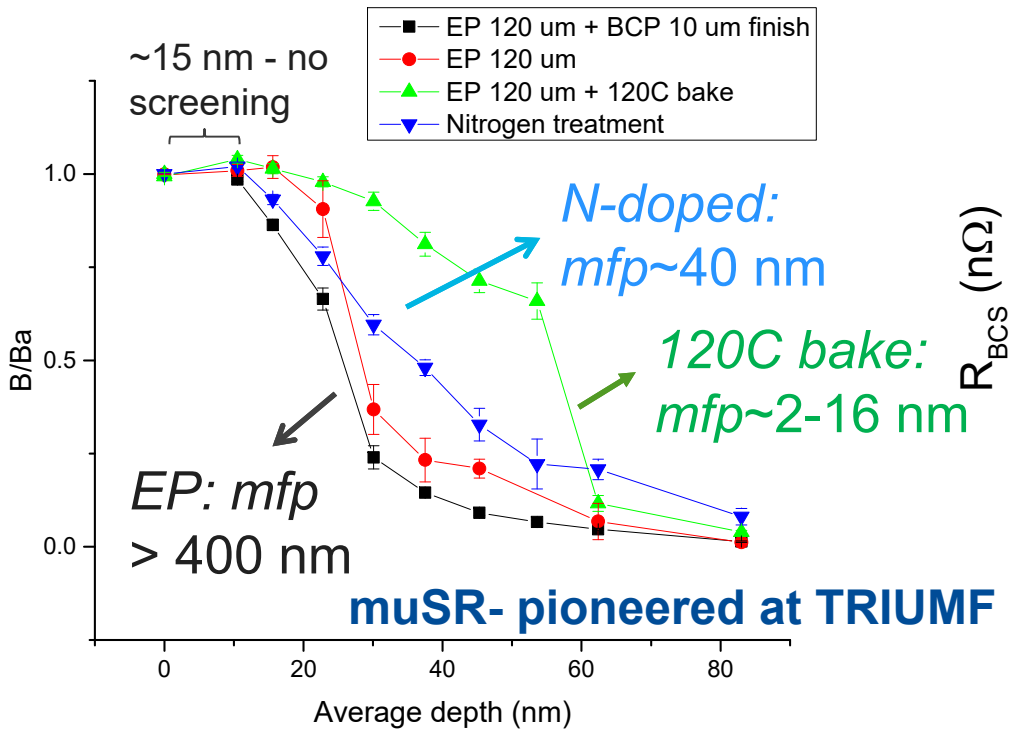


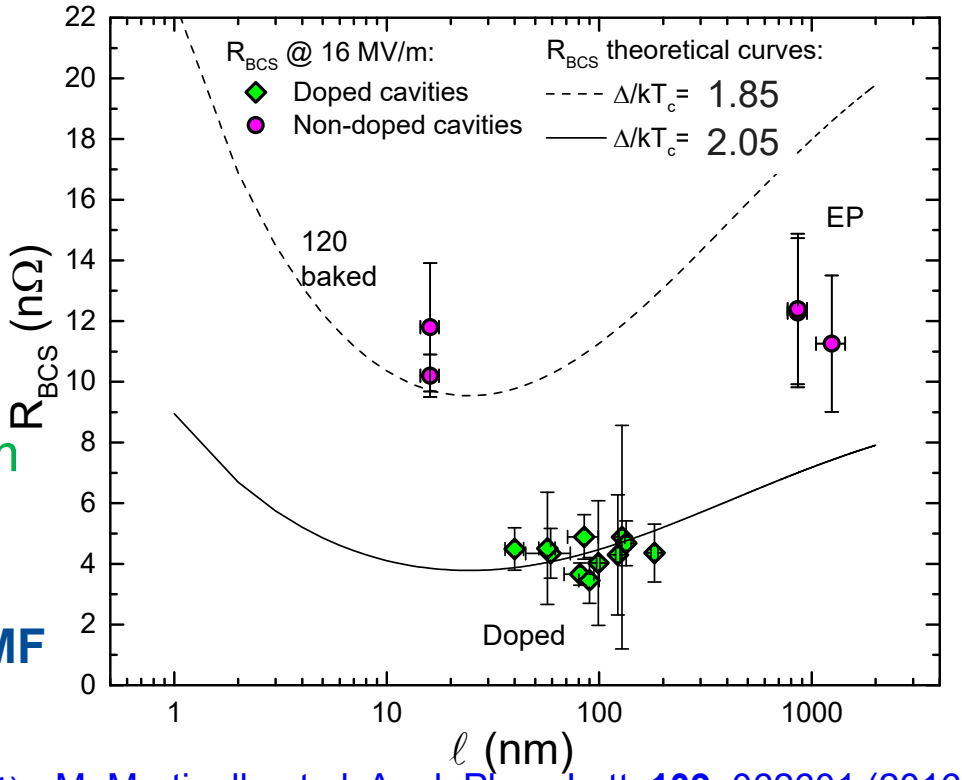


A. Romanenko et al, Appl. Phys. Lett. **104**, 072601 (2014)
A. Grassellino et al, Proc. of SRF2015

M. Martinello et al, Appl. Phys. Lett. **109**, 062601 (2016)

- ✓ N-doping modifies the mean free path
  →Mean free path close to theoretical minimum of $R_{BCS}$
- ✓ In addition, N-doping seems to increase the reduced energy gap $\Delta/k_B T_c$


*Slide adapted from M. Martinello*

# Can the Q increase be related to removal of nano-hydrides?

## Size and Distribution of NbH phases vary with cavity surface treatment condition

I. Hot Spot cut-out (EP'ed cavity, non-degaussed)

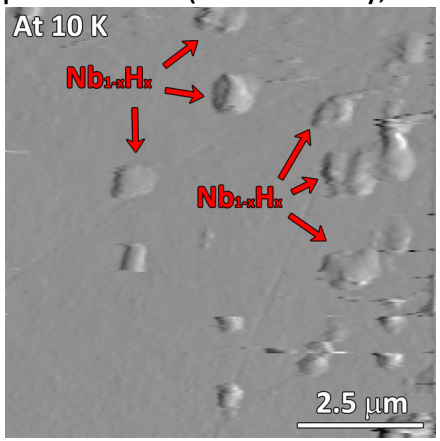


II. 800°C + BCP on hot spot cut-out

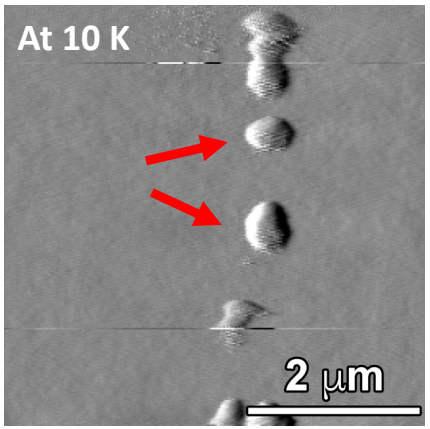


III. N-doped cavity cut-out (@800°C 25mT)

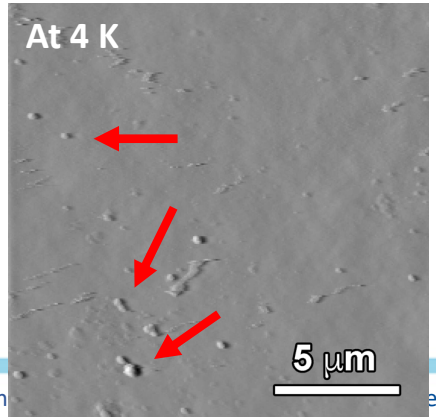


IV. 120°C baked cavity cut-out

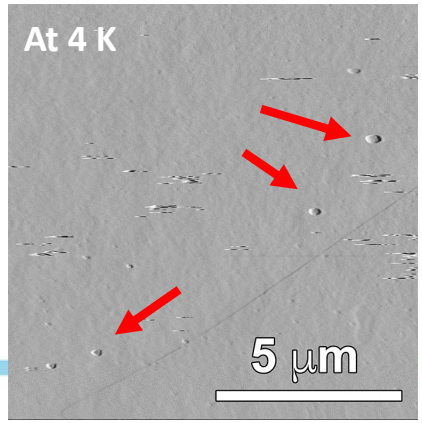

# Understanding the reversal of $R_{BCS}$ with the RF field

The non-equilibrium quasiparticle distribution driven by microwave fields is shown to stimulate the superconductivity[1,2,3]:

Δ increases with the RF field amplitude (absorbed power)

$R_{BCS}$ decreases with the RF field amplitude (absorbed power)

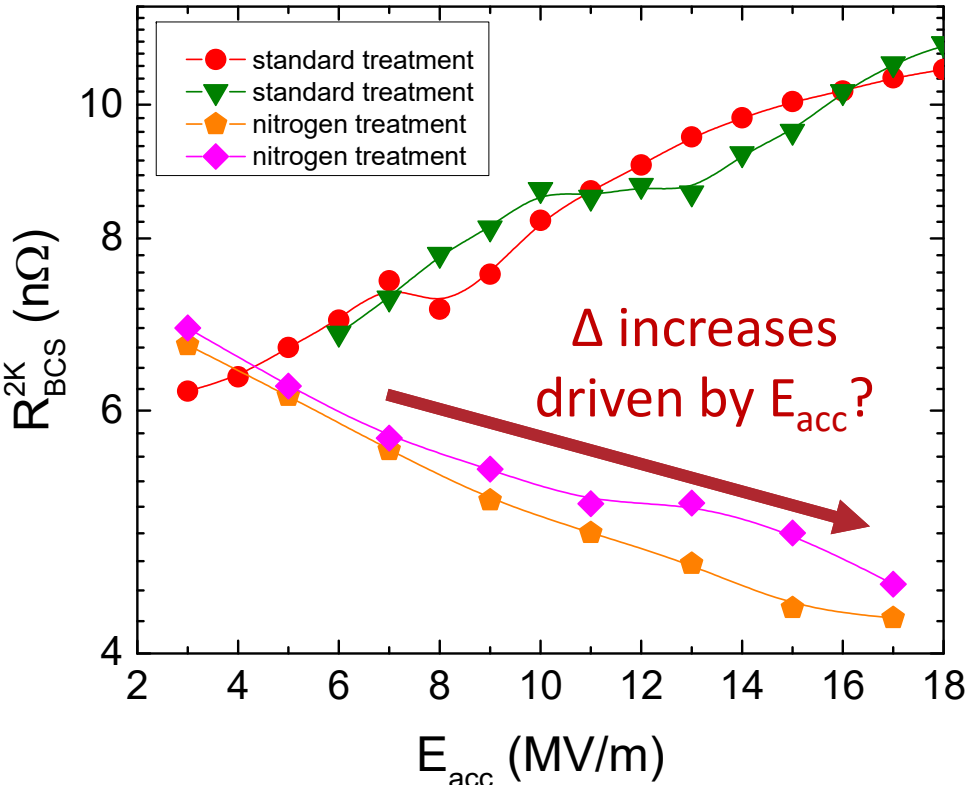


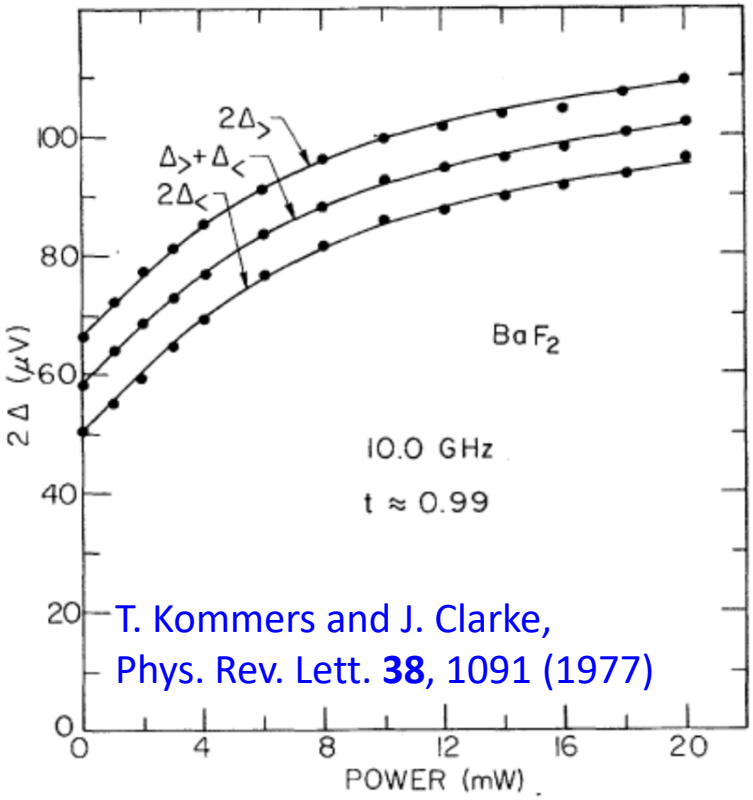


T. Kommers and J. Clarke, Phys. Rev. Lett. **38**, 1091 (1977)

[1] G.M. Eliashberg, ZhETF Pis. Red. **11**, 186 (1970)

[2] J.-J. Chang and D. J. Scalapino, Phys. Rev. B **15**, 2051 (1977)

[3] D. J. Goldie and S. Withington, Supercond. Sci. Technol. **26,** 015004 (2013)

# Thermal equilibrium distribution of quasiparticles

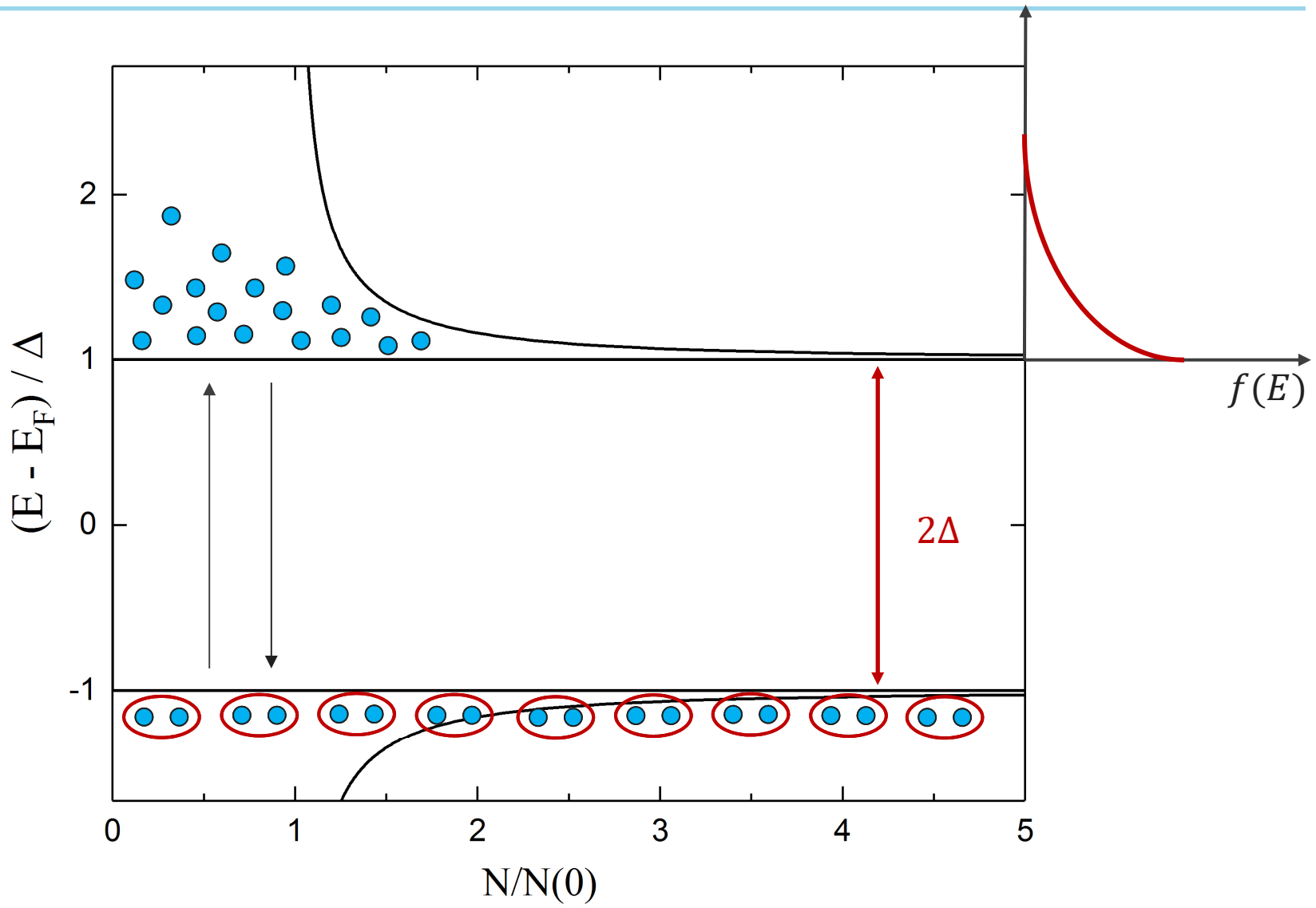

# Non-equilibrium distribution of quasiparticles

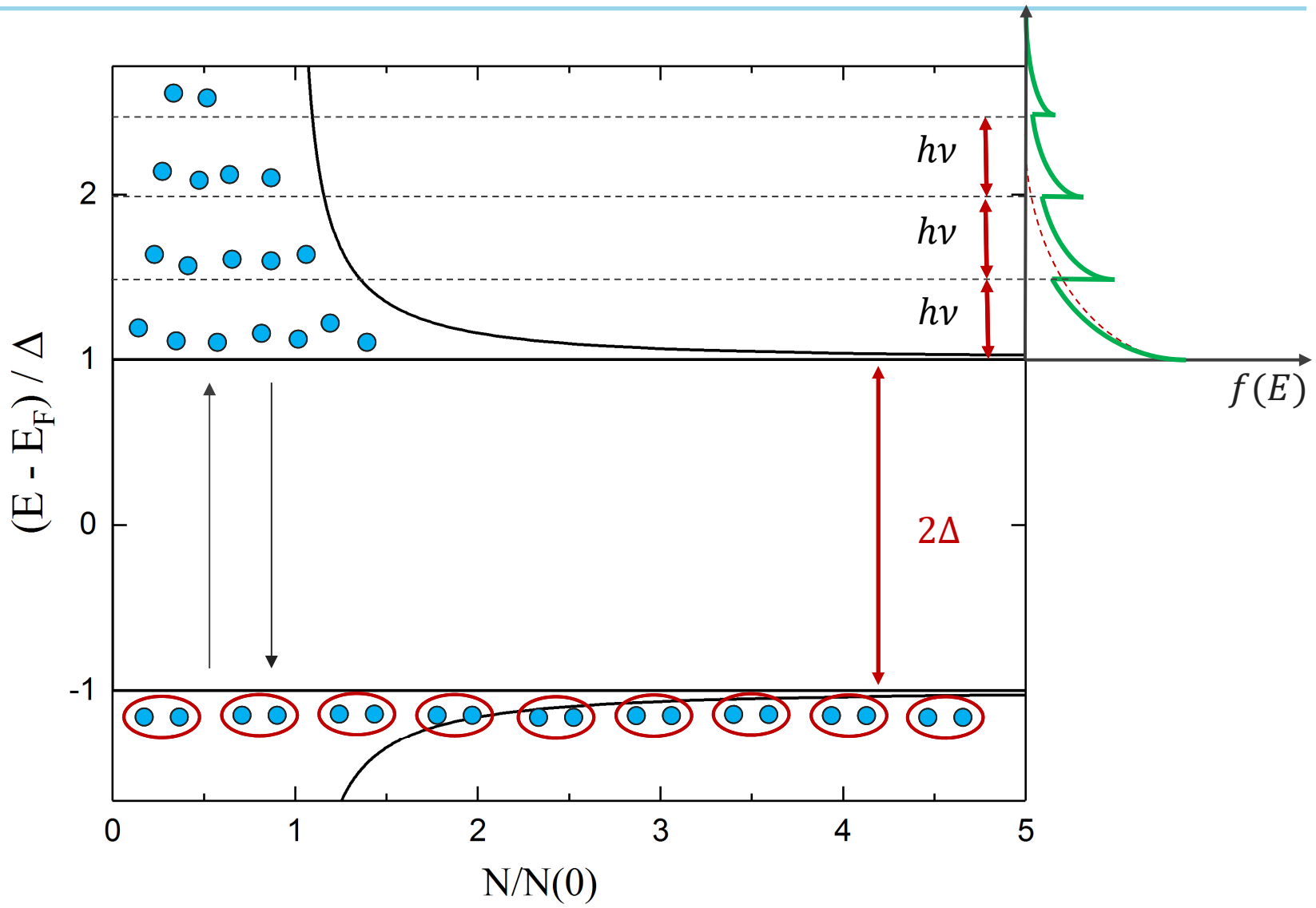

# Non-equilibrium distribution of quasiparticles

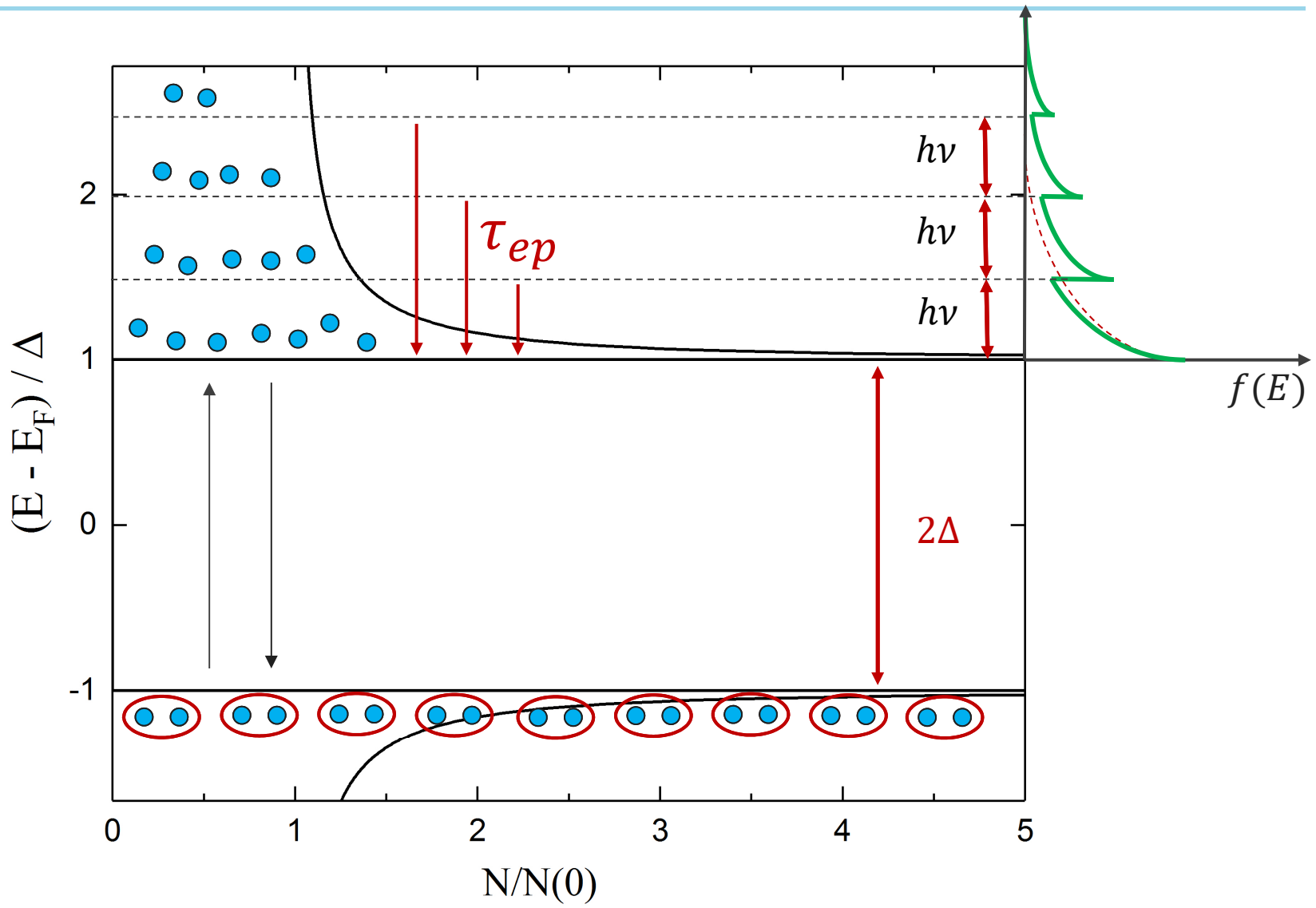


$\tau_{ep}$: electron-phonons inelastic scattering time

# Non-equilibrium distribution of quasiparticles

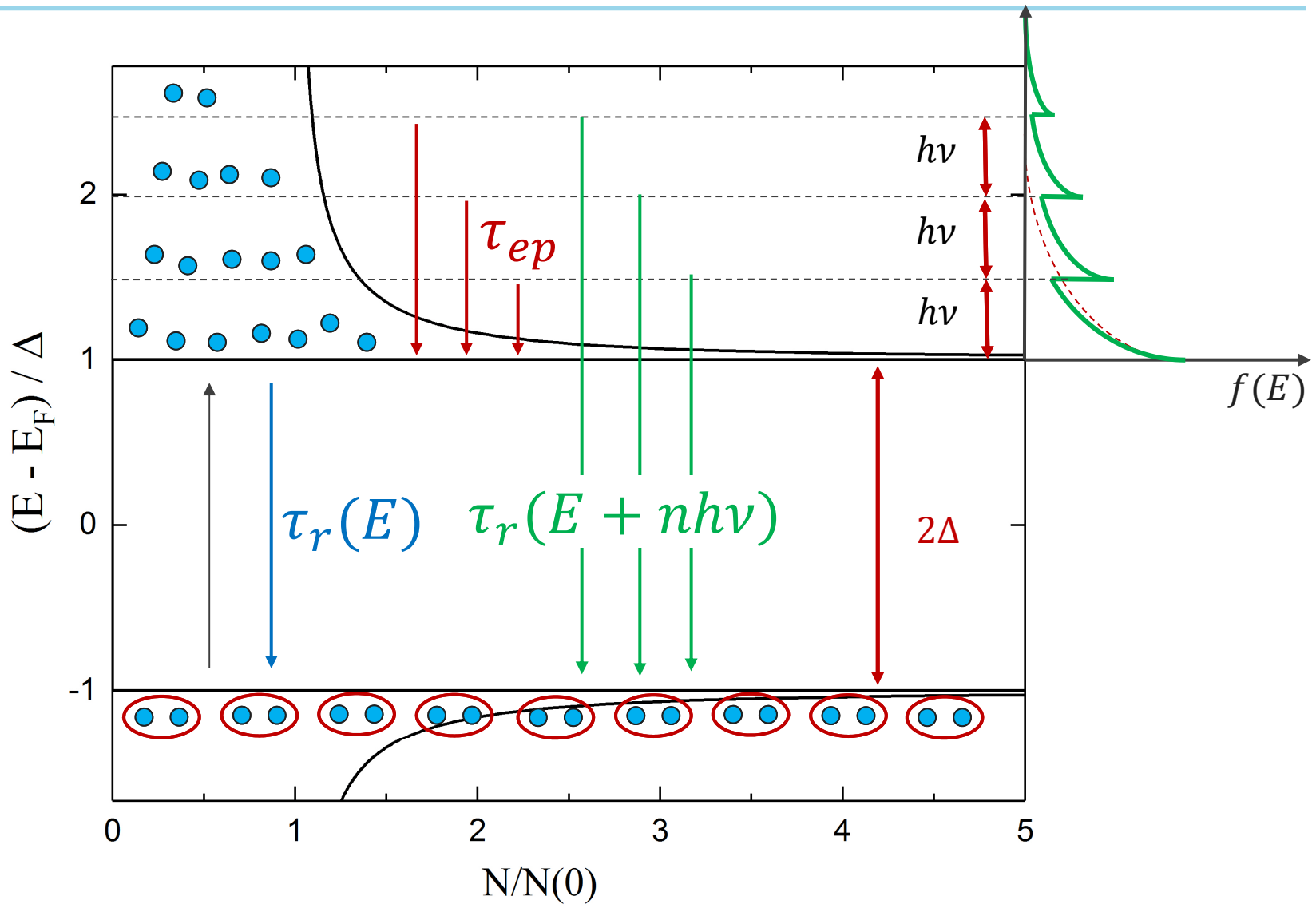


$\tau_{ep}$: electron-phonons inelastic scattering time

$\tau_r$: quasi-particles recombination time

# Non-equilibrium distribution of quasiparticles

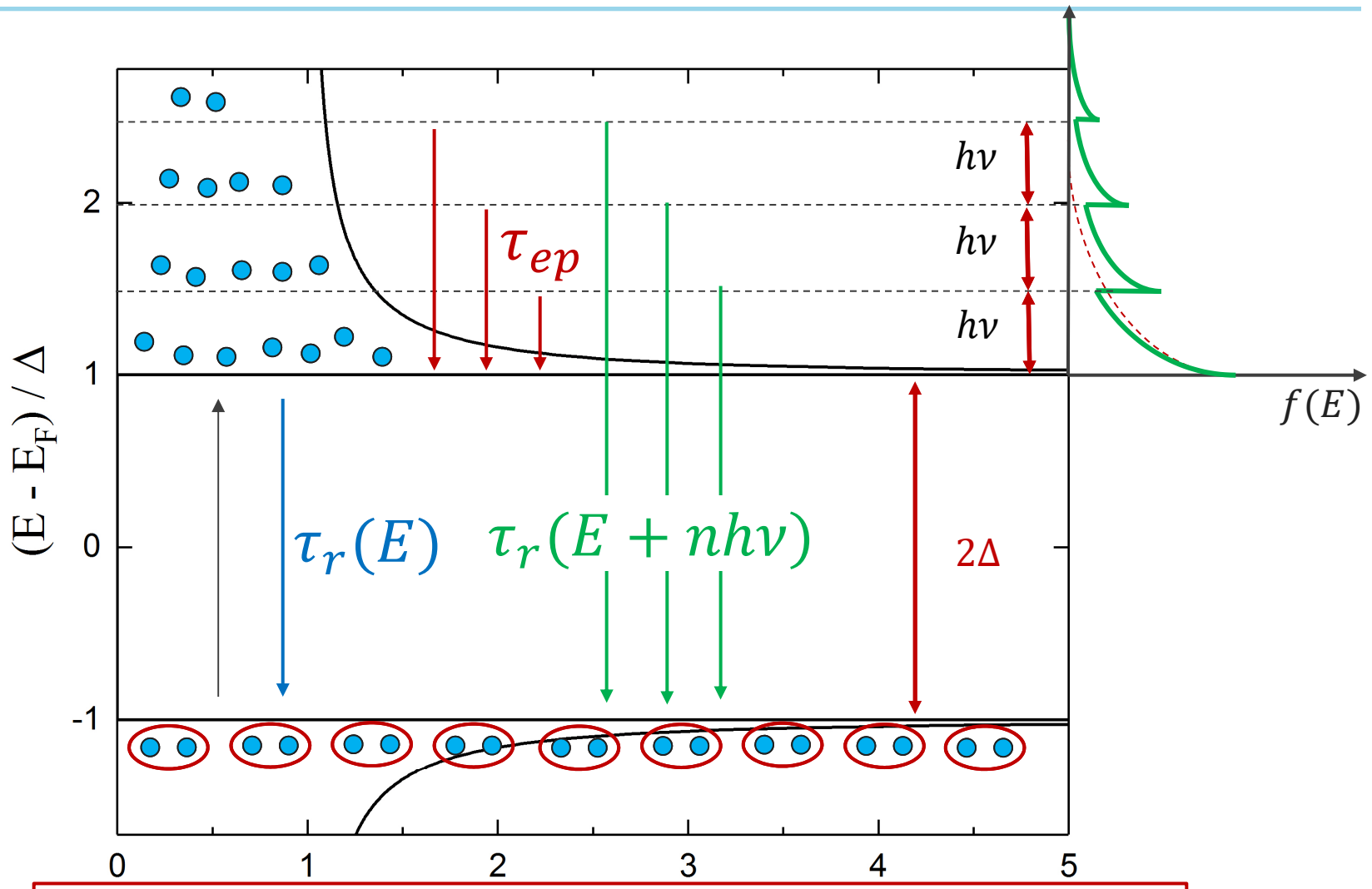


**N-doping may modify $\tau_{ep}$ and $\tau_r$ enhancing the non-equilibrium effects**

$\tau_{ep}$: electron

$\tau_r$: quasi-particles recombination time

# Varying the frequency:
# SRF Cavities from accelerator to quantum regime

# Frequency dependence of the “anti-Q-slope”

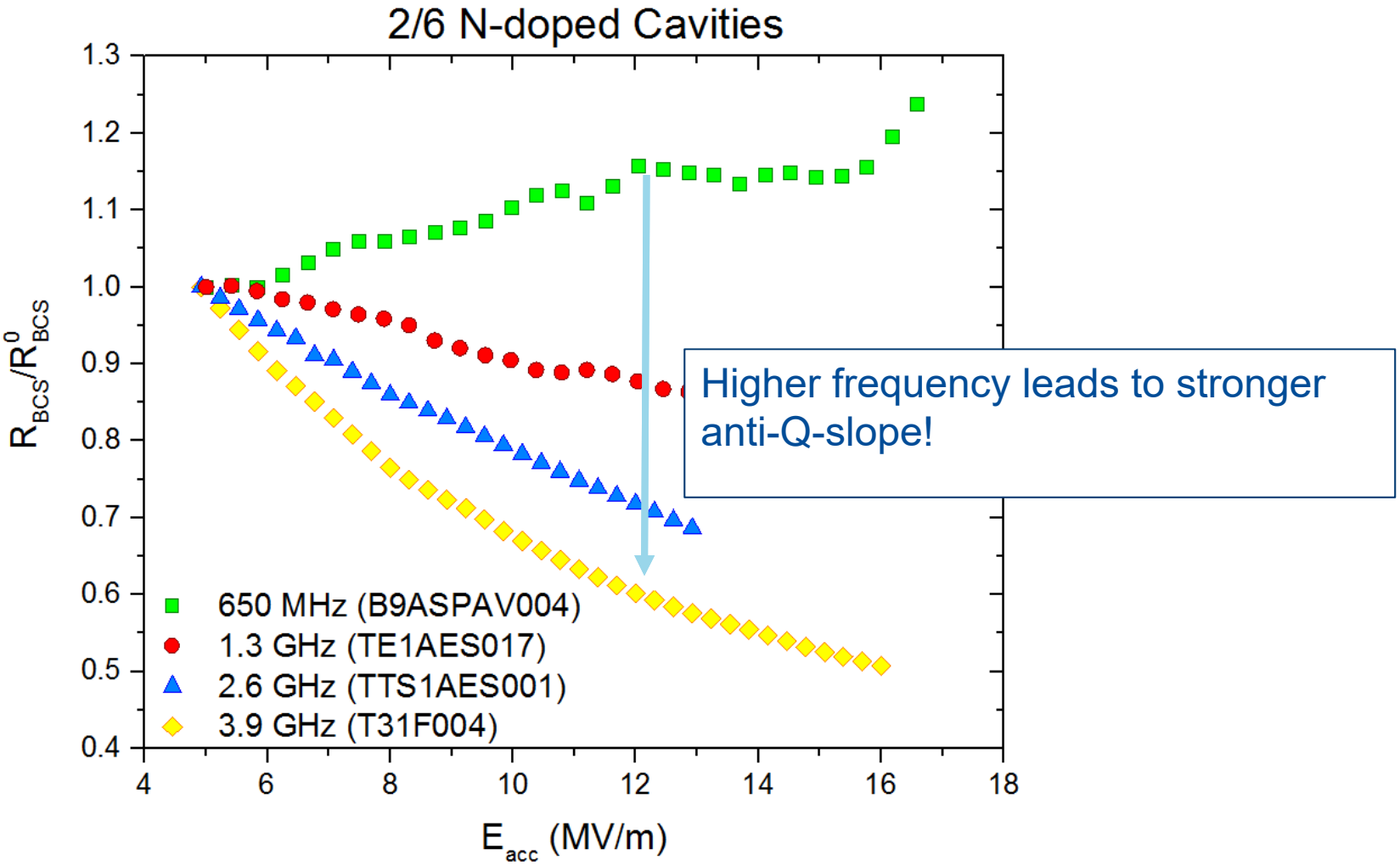


M. Martinello et al, https://arxiv.org/abs/1707.07582

# Higher frequency cavities favor higher fields

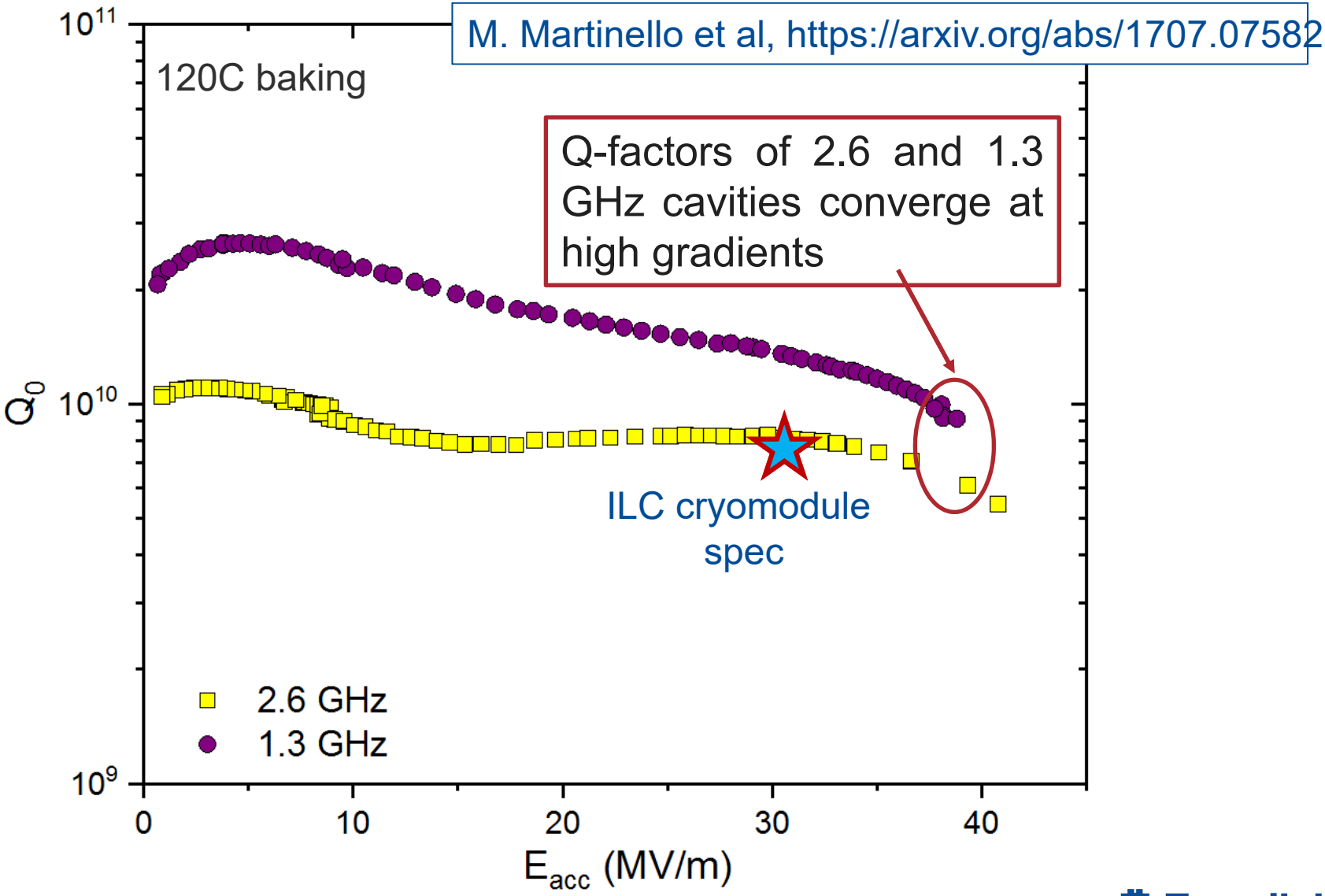

# High frequency cavities favorable at high field

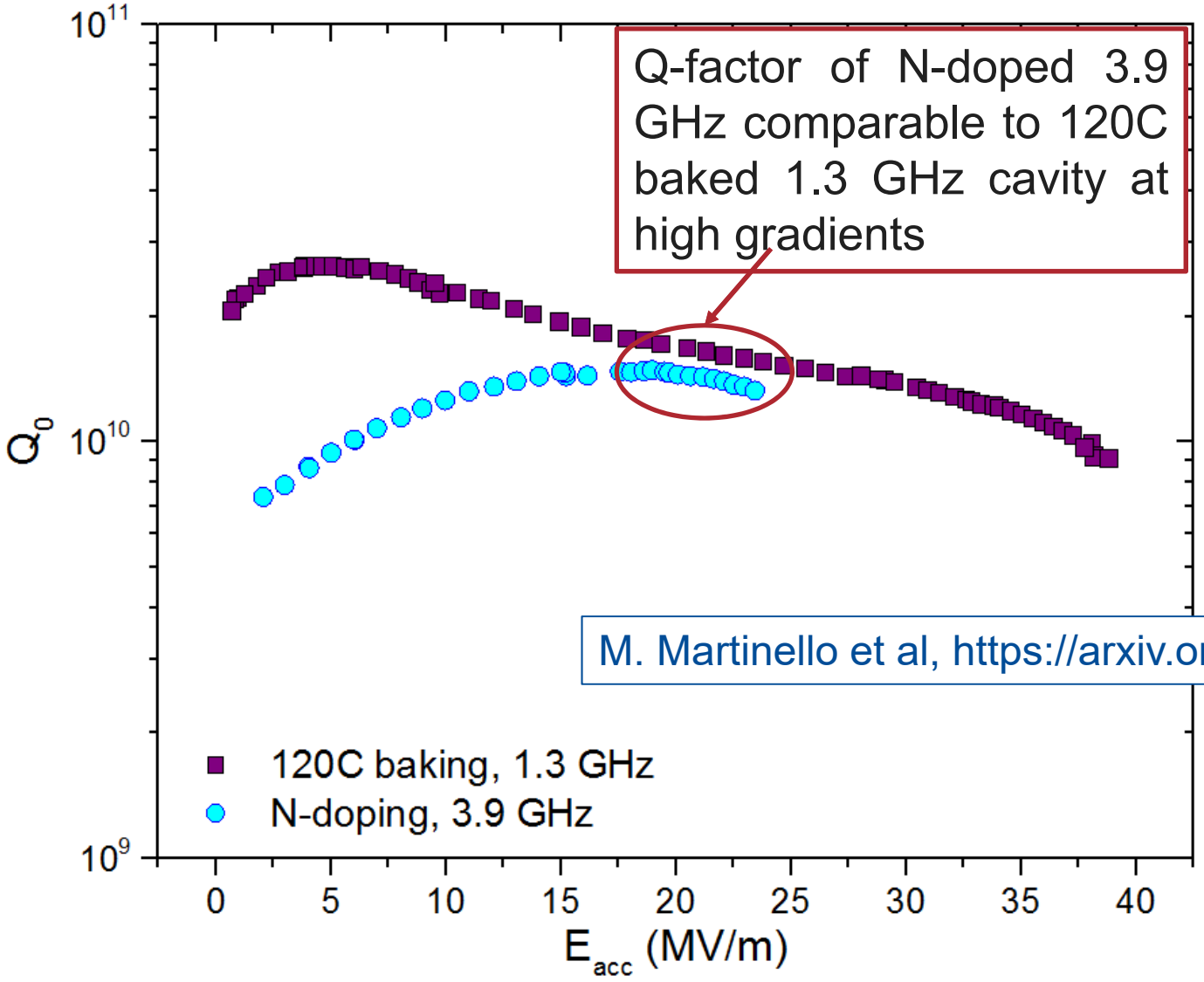

# Effect of the frequency on the slope of $R_{BCS}$(Eacc)

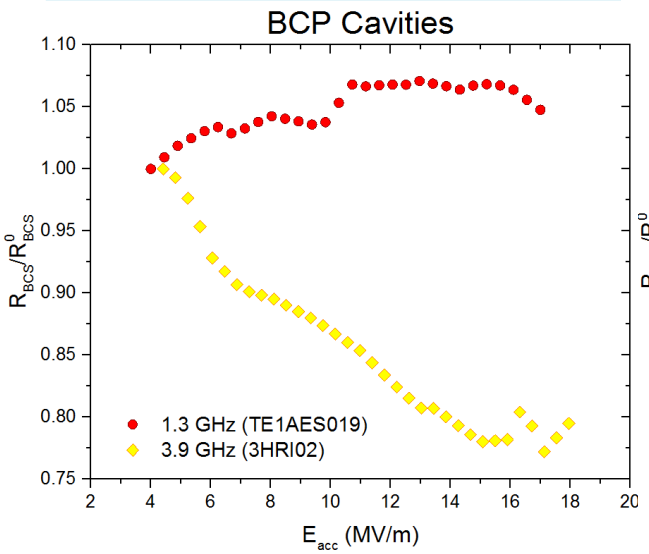


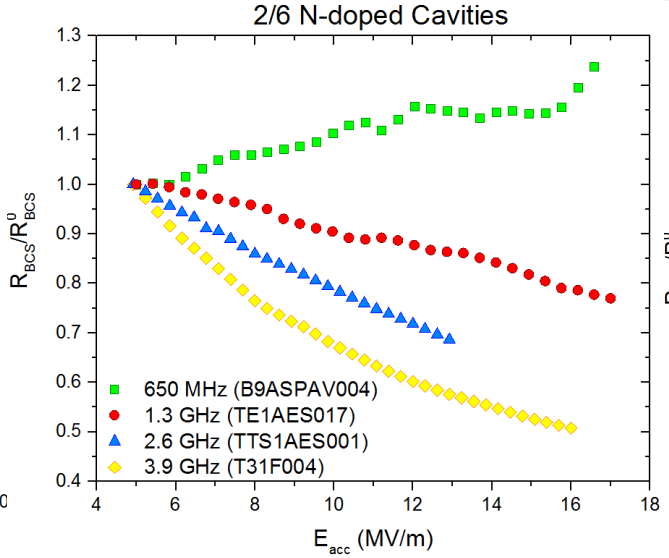


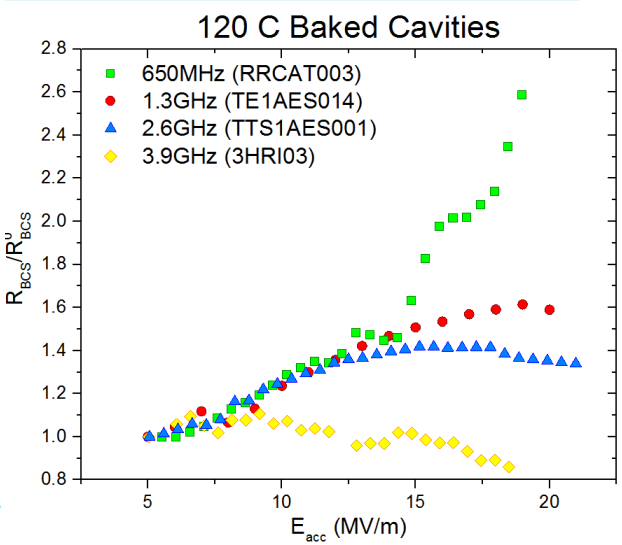


- The $R_{BCS}$ reversal, key of N-doping increase in Q, can also be observed in clean Nb but at high frequency

Higher frequency is favorable for Q, and can be also for higher gradients

M. Martinello et al, https://arxiv.org/abs/1707.07582

# Beyond BCS: Magnetic flux lines can be trapped and cause large RF losses

Trapped vortices imaged via Bitter Decoration

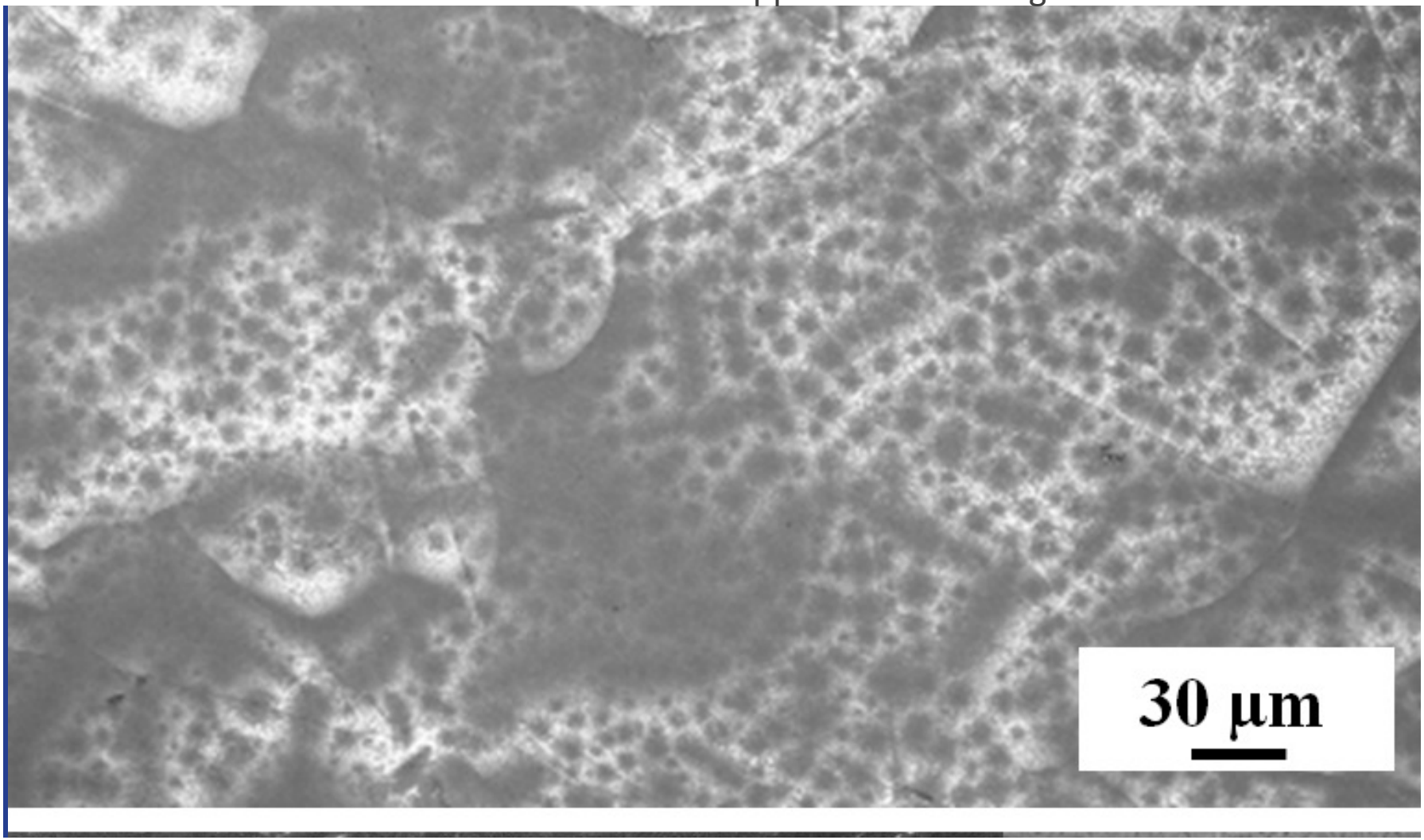

# Cooldown through Critical Temperature for maximum magnetic flux expulsion and preservation of Q

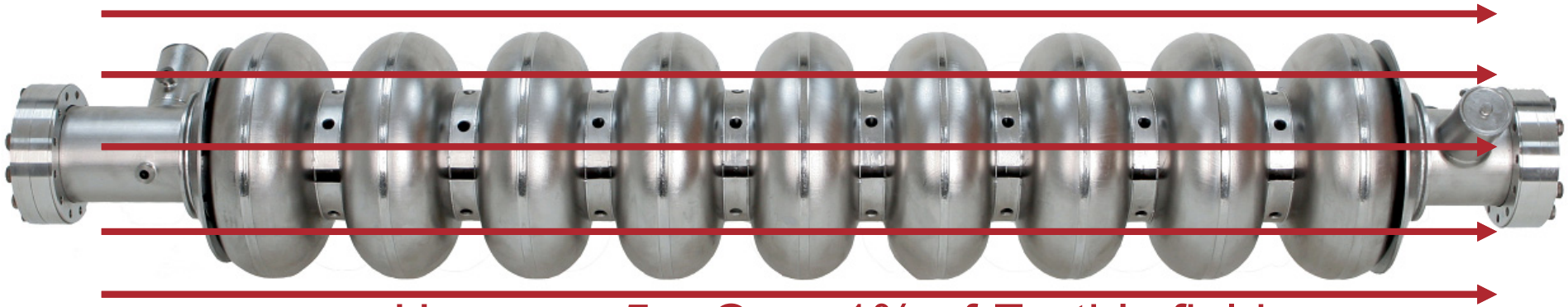

$H_{shielded}$ ~ 5 mOe ~ 1% of Earth's field



*Flux image from Rose-Innes and Roderick, Introduction to Superconductivity*

# Cooldown through Critical Temperature for maximum magnetic flux expulsion and preservation of Q

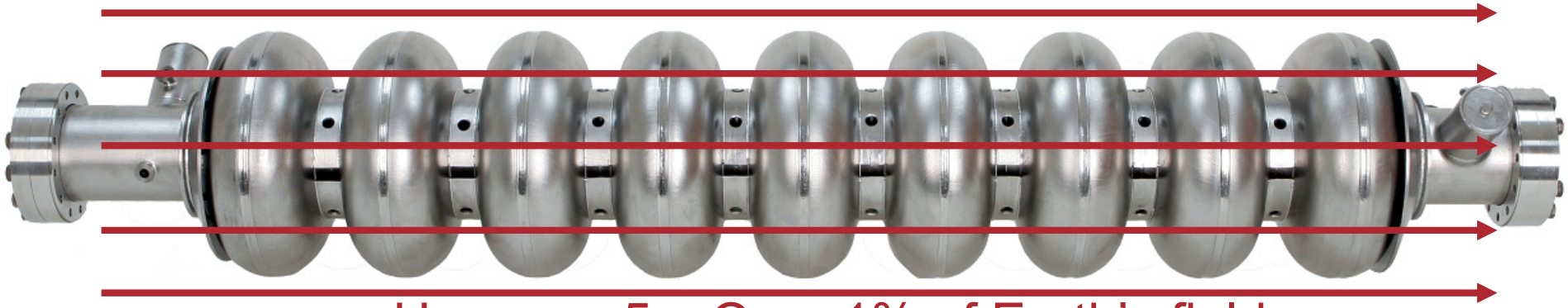

$H_{shielded}$ ~ 5 mOe ~ 1% of Earth's field

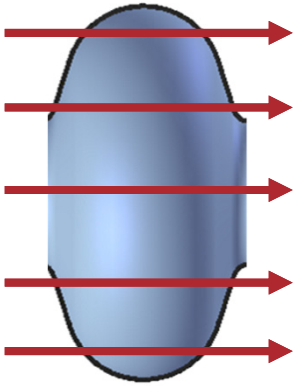

Magnetic Flux Trapping



Fermilab

*Flux image from Rose-Innes and Roderick, Introduction to Superconductivity*

# Cooldown through Critical Temperature for maximum magnetic flux expulsion and preservation of Q

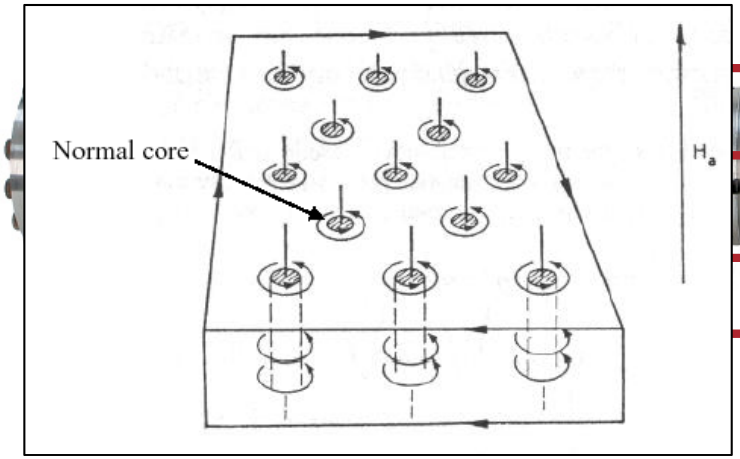


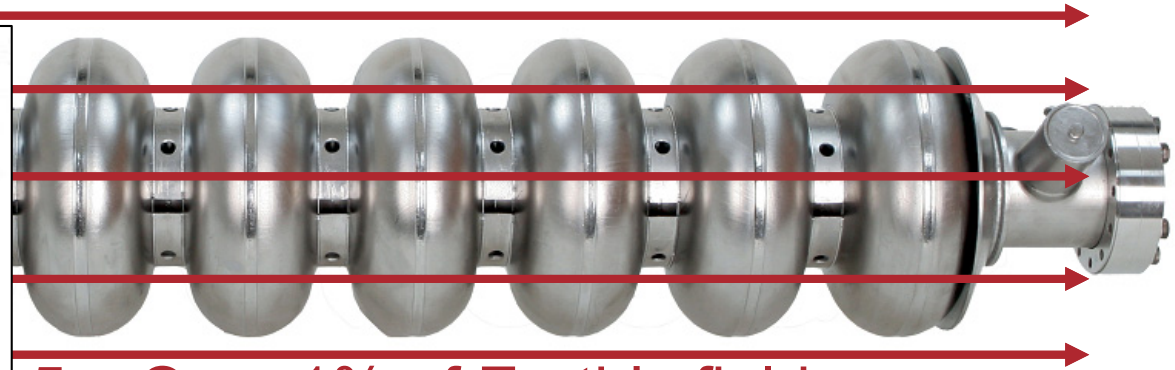

5 mOe ~ 1% of Earth's field

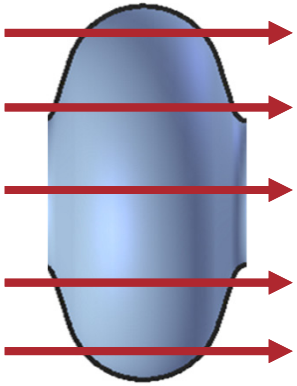

Magnetic Flux Trapping



*Flux image from Rose-Innes and Roderick, Introduction to Superconductivity*

# Cooldown through Critical Temperature for maximum magnetic flux expulsion and preservation of Q

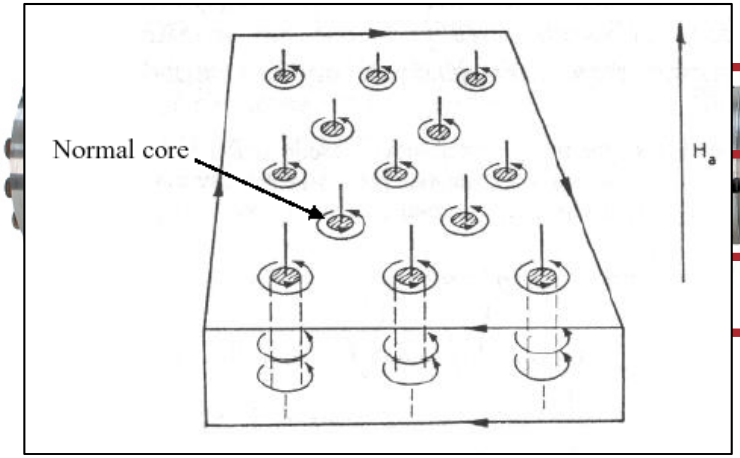




5 mOe ~ 1% of Earth's field

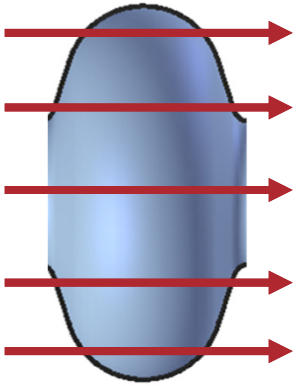

Magnetic Flux Trapping

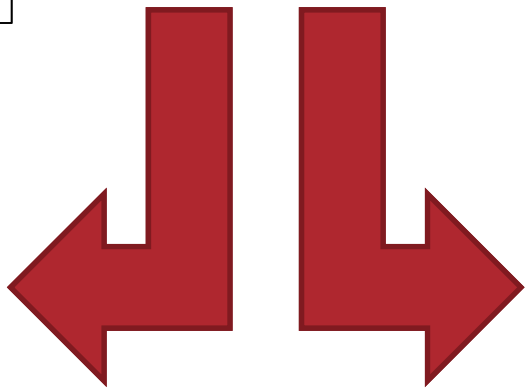

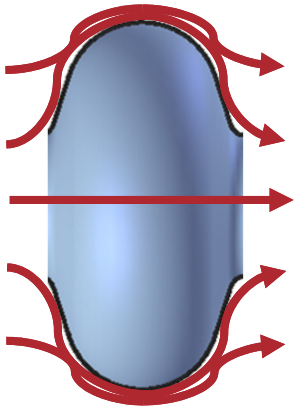

Magnetic Flux Expulsion



*Flux image from Rose-Innes and Roderick, Introduction to Superconductivity*

# Cooldown through Critical Temperature for maximum magnetic flux expulsion and preservation of Q

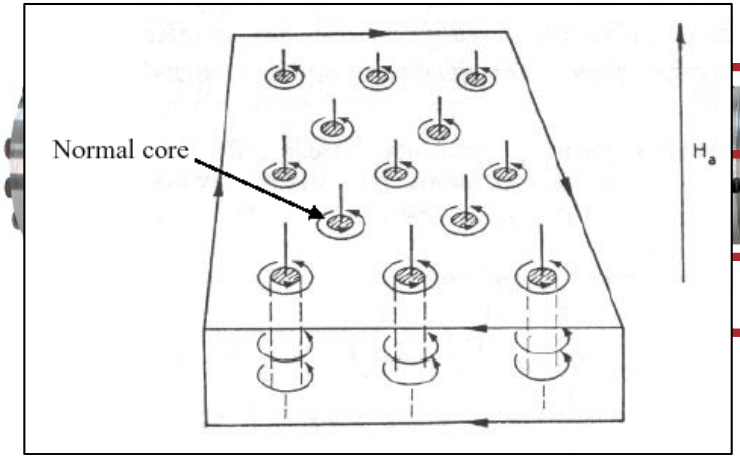


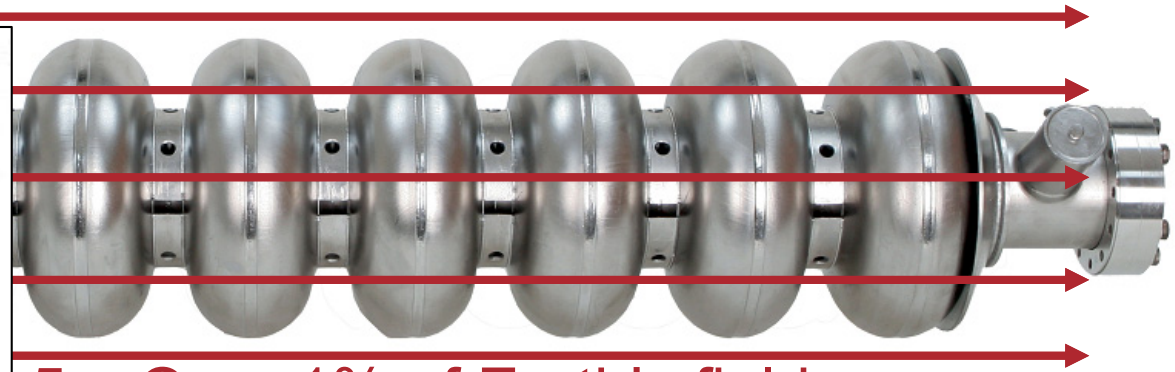

5 mOe ~ 1% of Earth's field

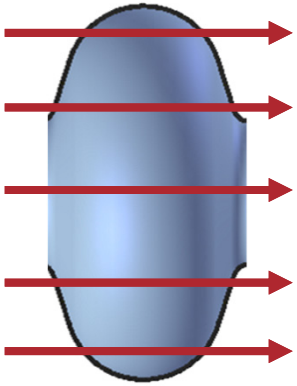

Magnetic Flux Trapping

Trapped flux increases $R_{res}$

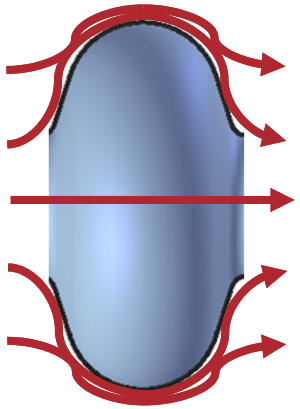

Magnetic Flux Expulsion



*Flux image from Rose-Innes and Roderick, Introduction to Superconductivity*

# Cooldown through Critical Temperature for maximum magnetic flux expulsion and preservation of Q

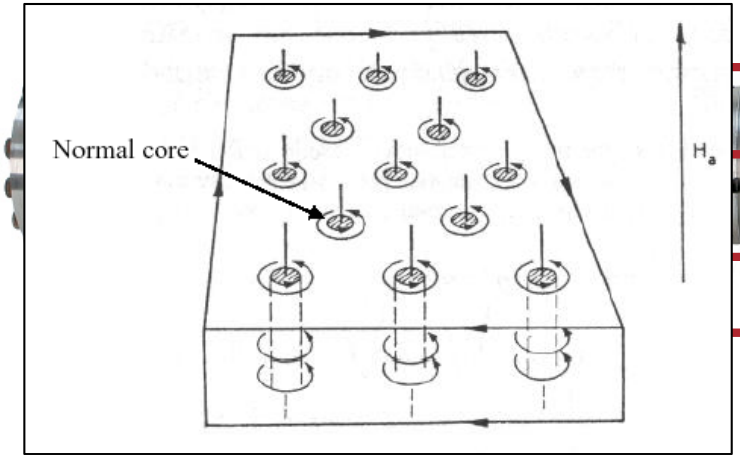


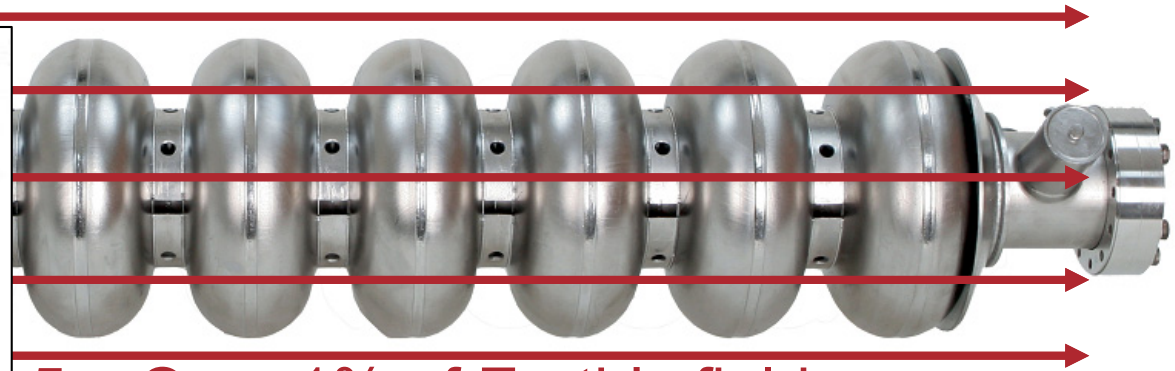

5 mOe ~ 1% of Earth's field

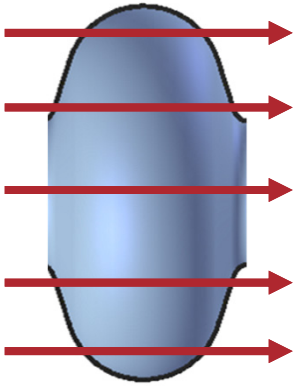

Magnetic Flux Trapping

Trapped flux increases $R_{res}$

Closer to intrinsic $R_{res}$

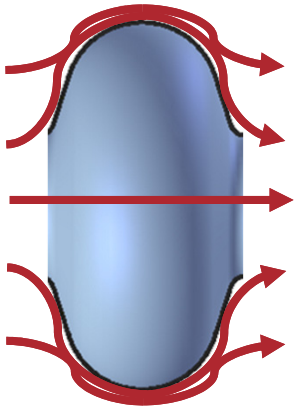

Magnetic Flux Expulsion



*Flux image from Rose-Innes and Roderick, Introduction to Superconductivity*

# At FNAL, found that slow cooldown can kill high Q

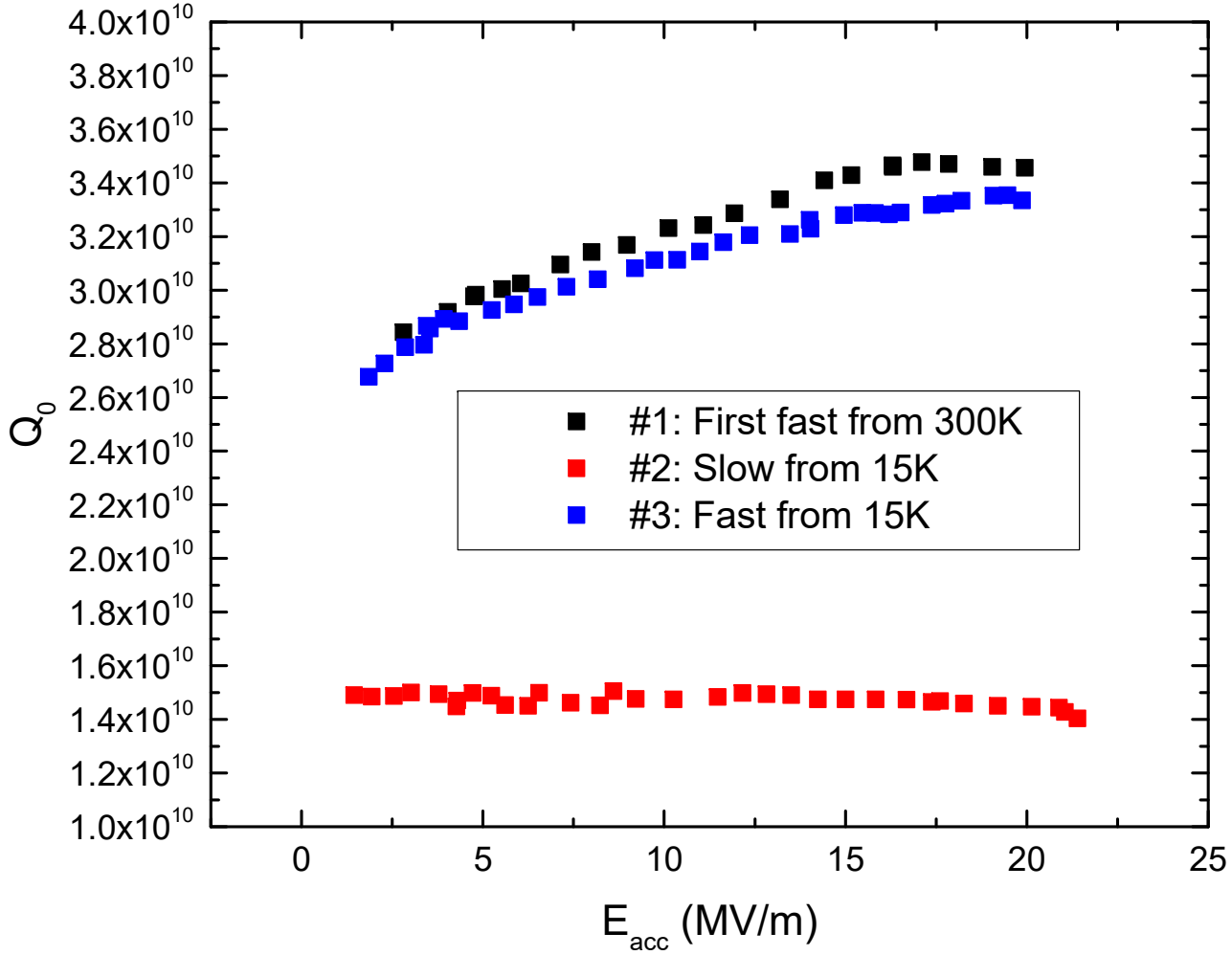


N doped nine cell in 5 mGauss!

A. Romanenko, A. Grassellino, O. Melnychuk, D. A. Sergatskov, J. Appl. Phys. **115**, 184903 (2014)

# Magnetic probes revealed the new physics – flux gets trapped or detrapped depending on cooling

Full expulsion of the magnetic field should increase the field at equator ~2 times when going superconducting

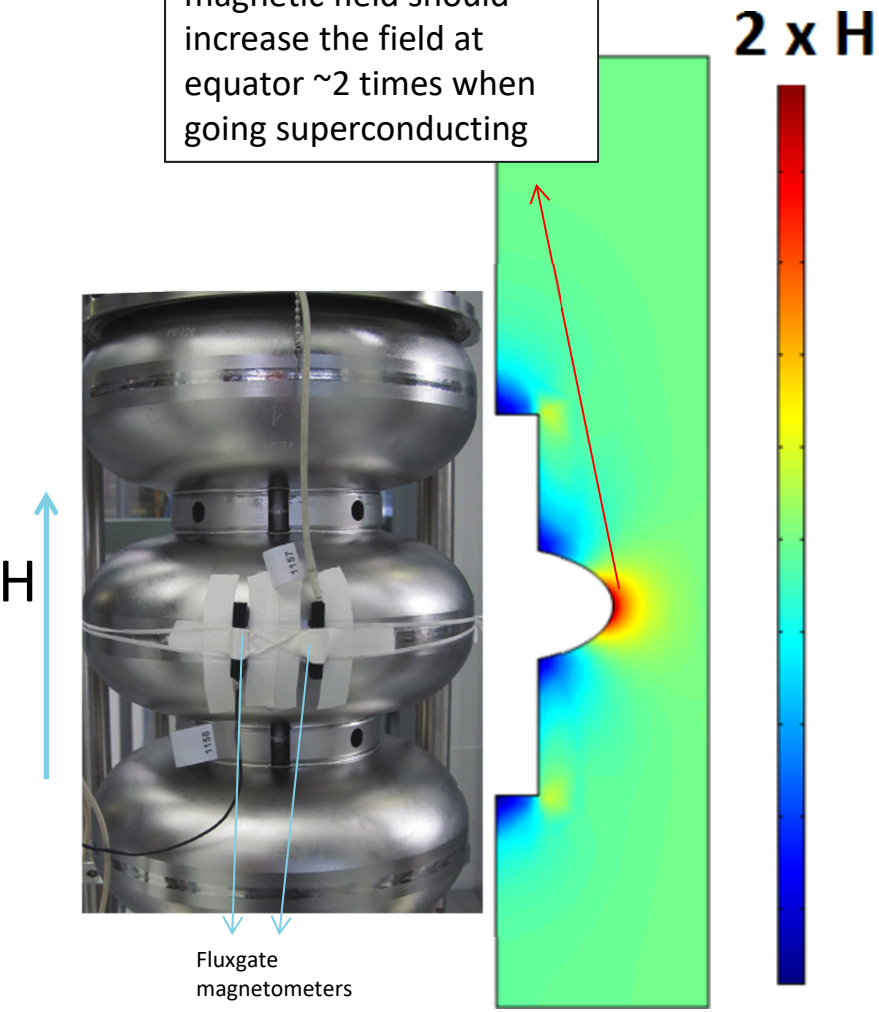

# Magnetic probes revealed the new physics – flux gets trapped or detrapped depending on cooling

Full expulsion of the magnetic field should increase the field at equator ~2 times when going superconducting

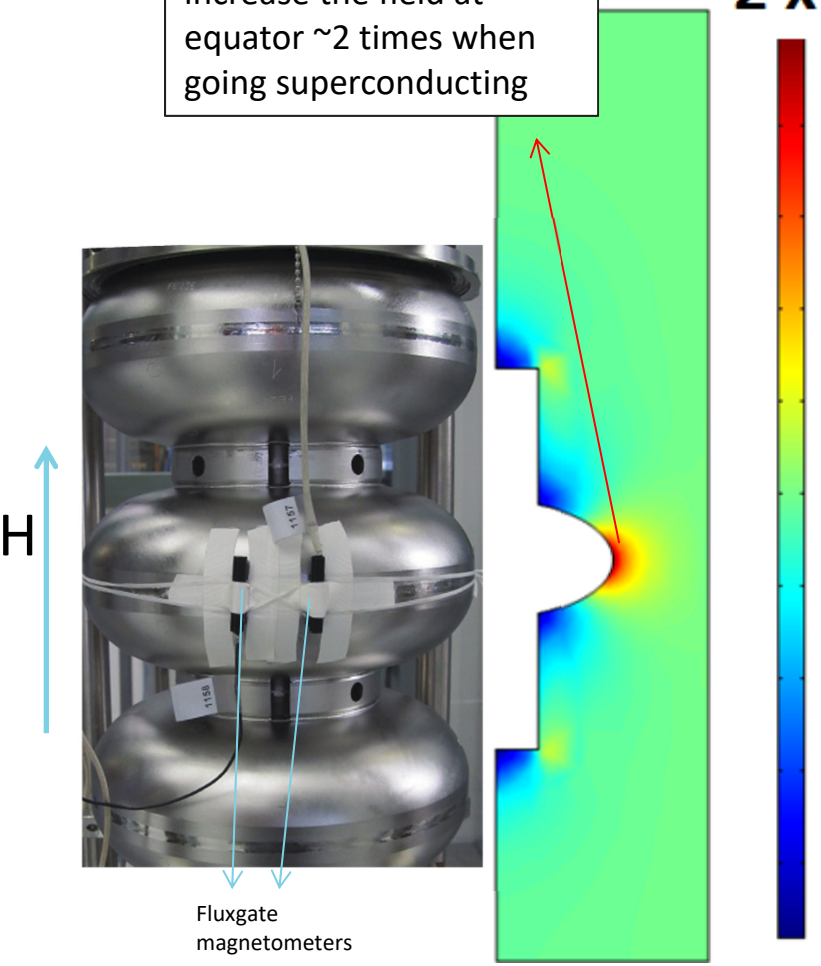


It turns out the expulsion efficiency can be controlled by the cooldown procedure through Tc=9.2K (fast/slow, uniform or not)

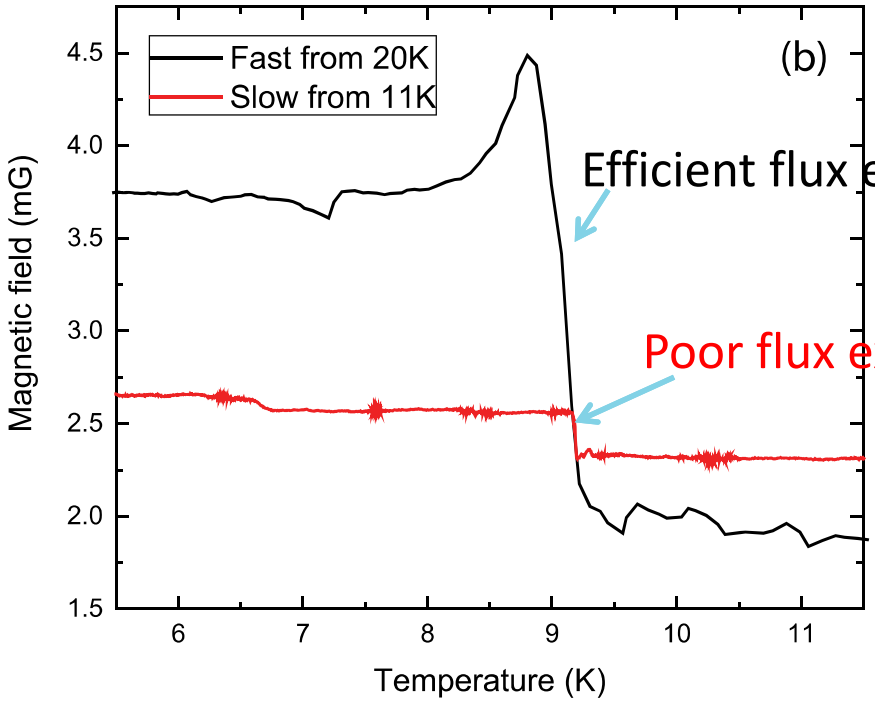


Same Meissner behavior for EP, EP+120C, N doping, fine/single grain, cooling is what matters

# Differences between fast/slow

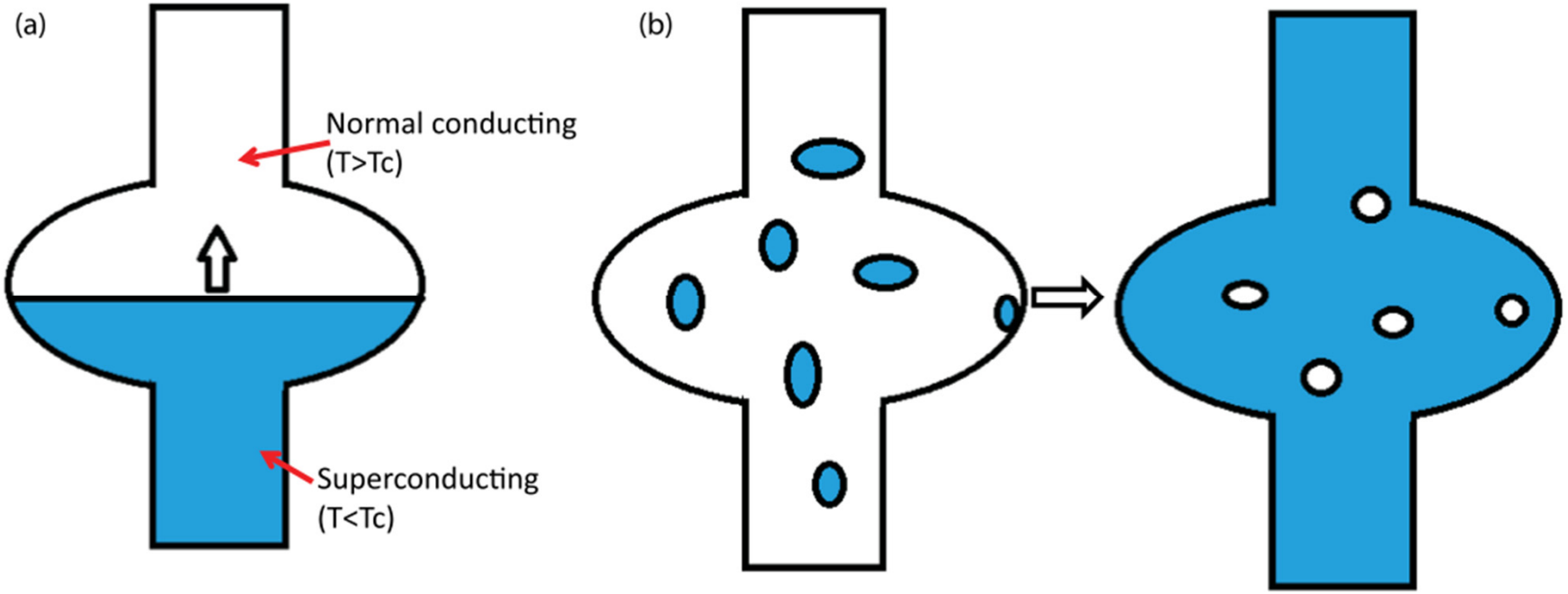


#1: Difference in geometry of transition

# Driving parameter of expulsion

A. Romanenko, A. Grassellino, A. C. Crawford, D. A. Sergatskov, and O. Melnychuk, Appl. Phys. Lett. **105**, 234103 (2014)

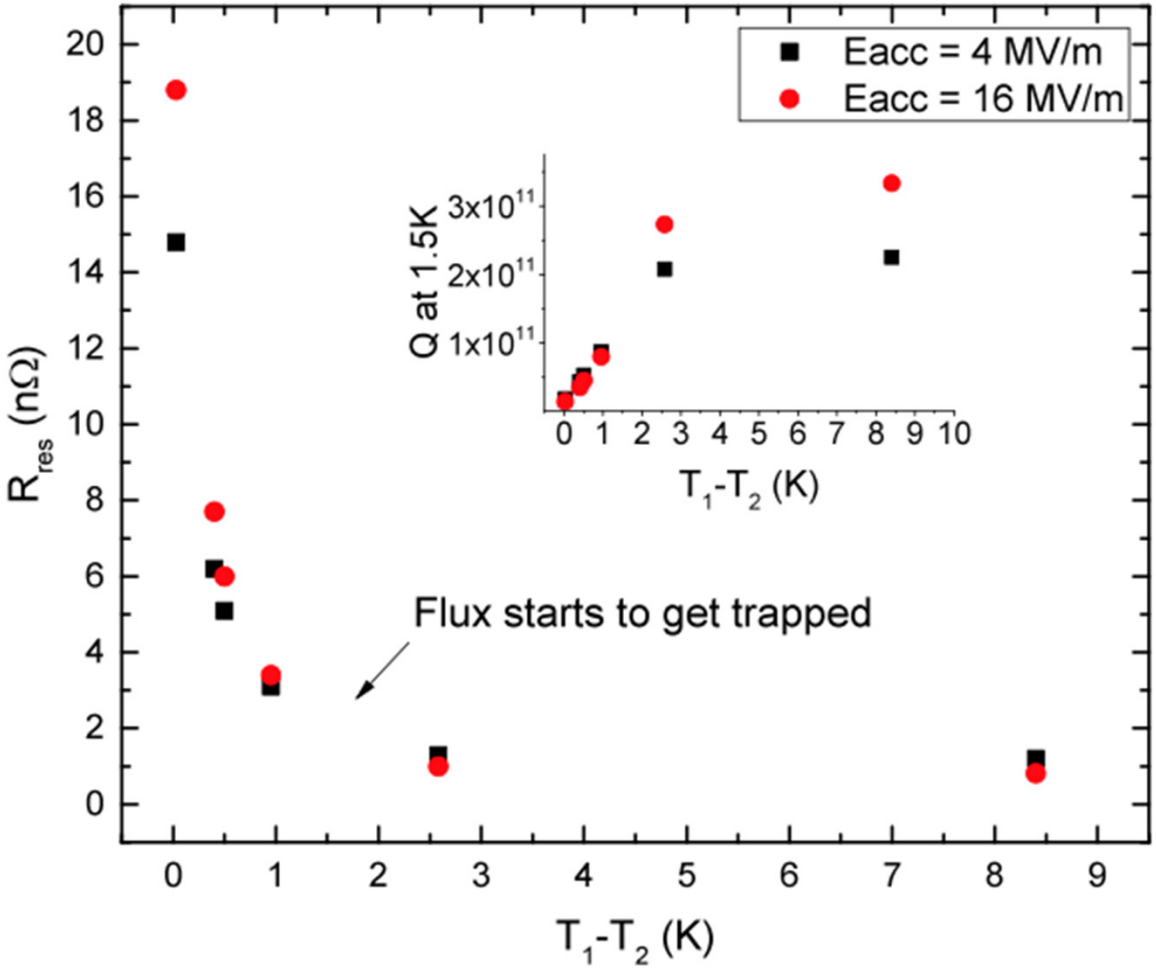


Temperature difference at the phase front (dT/dx)

# Observing fast and slow cooldown dynamics

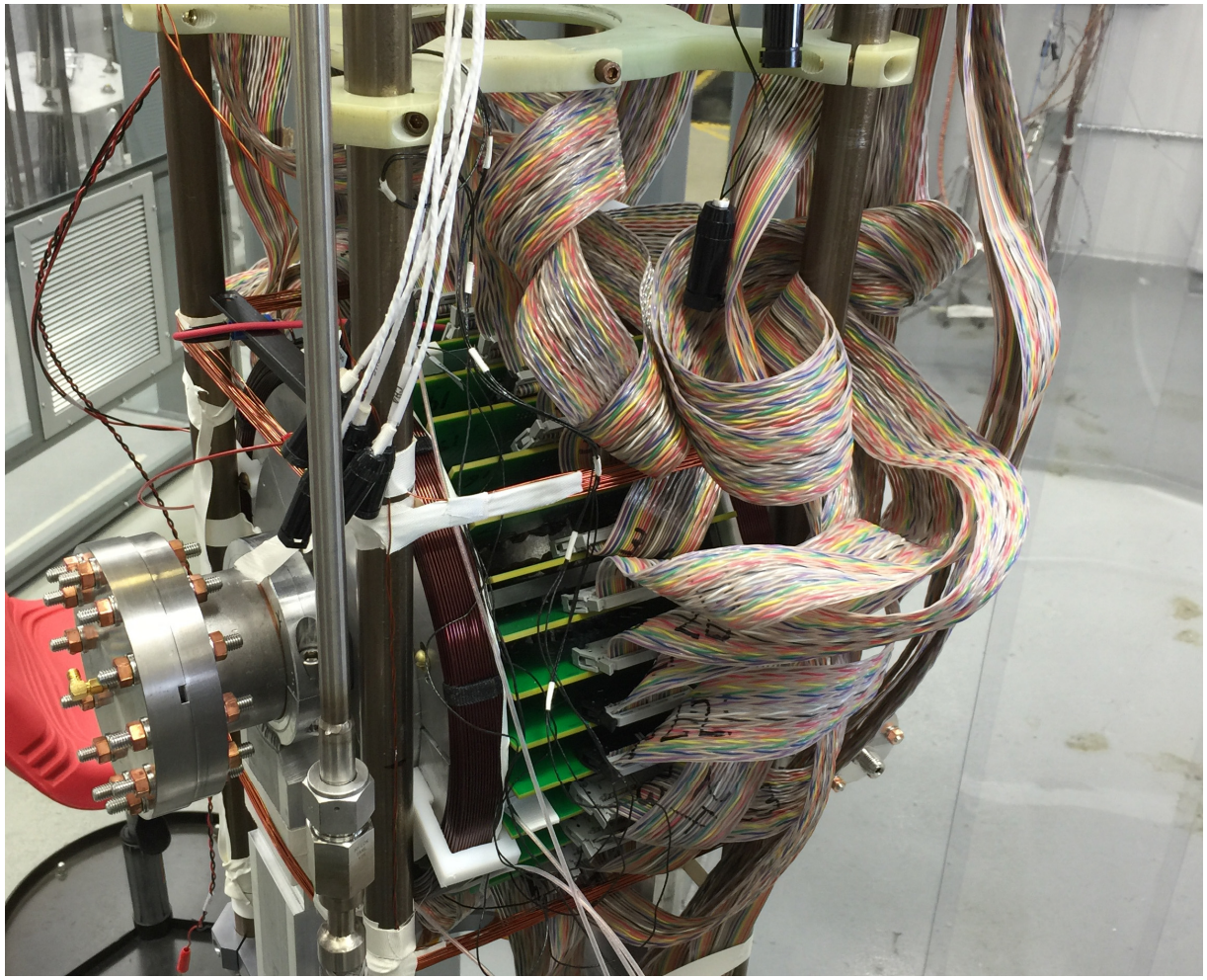

# Fast and slow cooldown dynamics captured

Fast from 300K

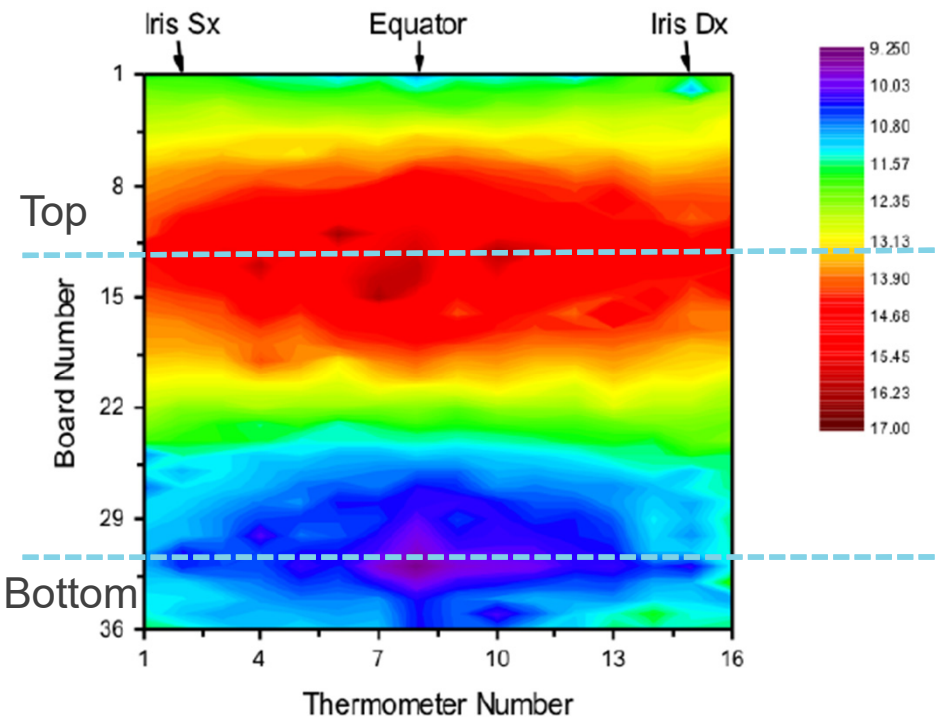


Slow from 12K

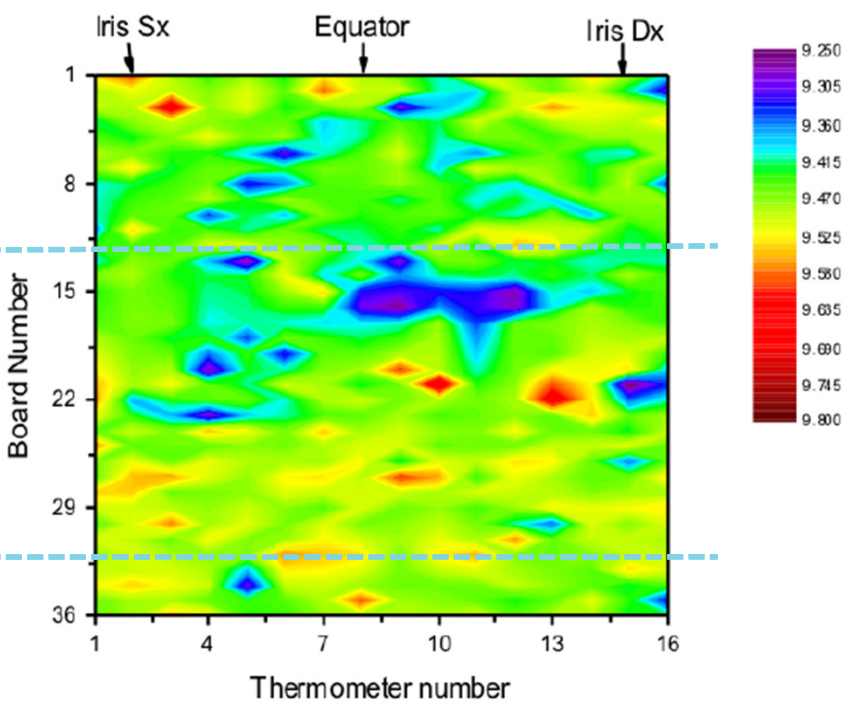


M. Martinello, M. Checchin - PhD work

- Fast cooldown

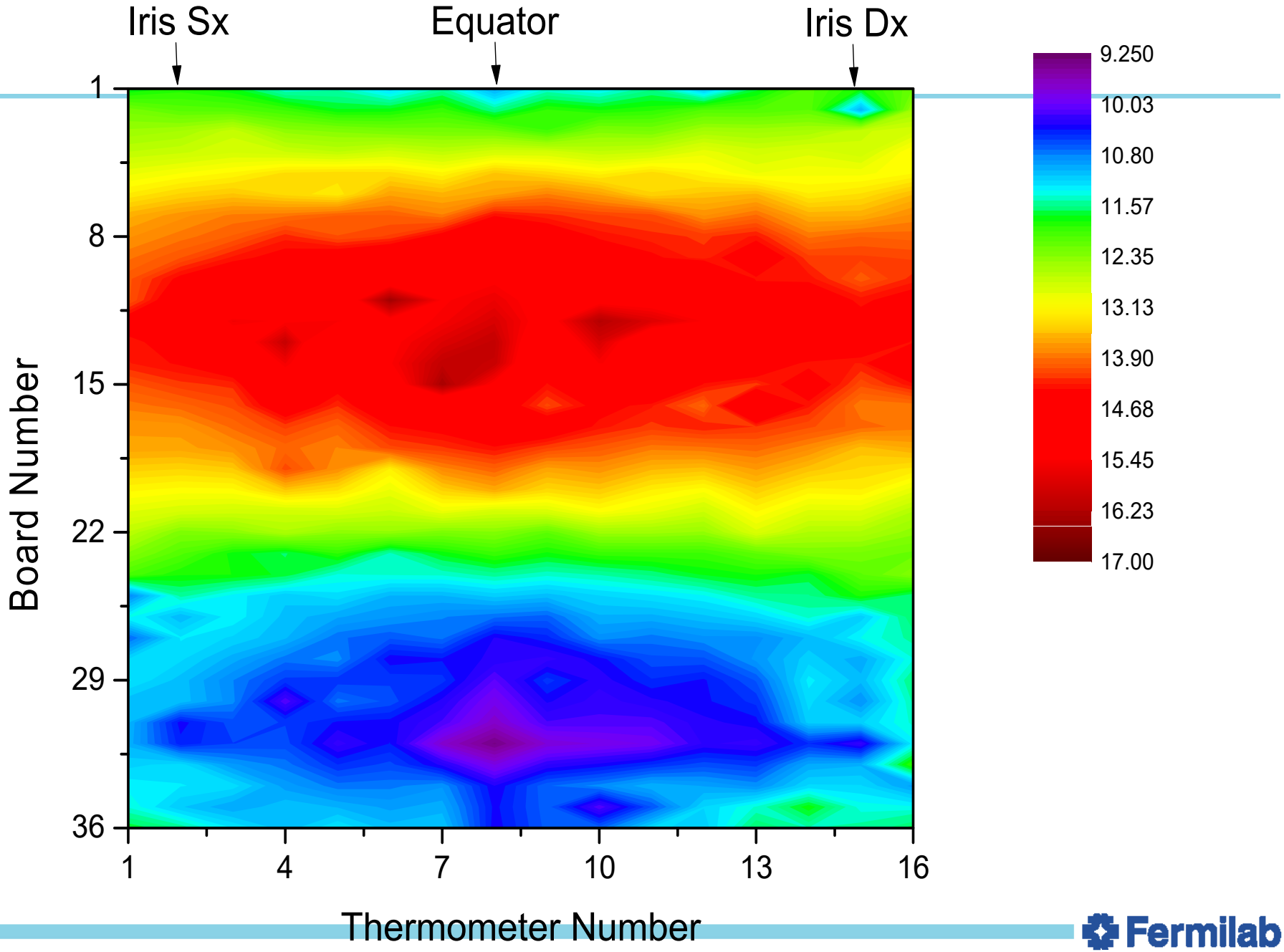
Iris Sx
Equator
Iris Dx
Board Number
1
8
15
22
29
36
1
4
7
10
13
16
Thermometer Number
9.250
10.03
10.80
11.57
12.35
13.13
13.90
14.68
15.45
16.23
17.00

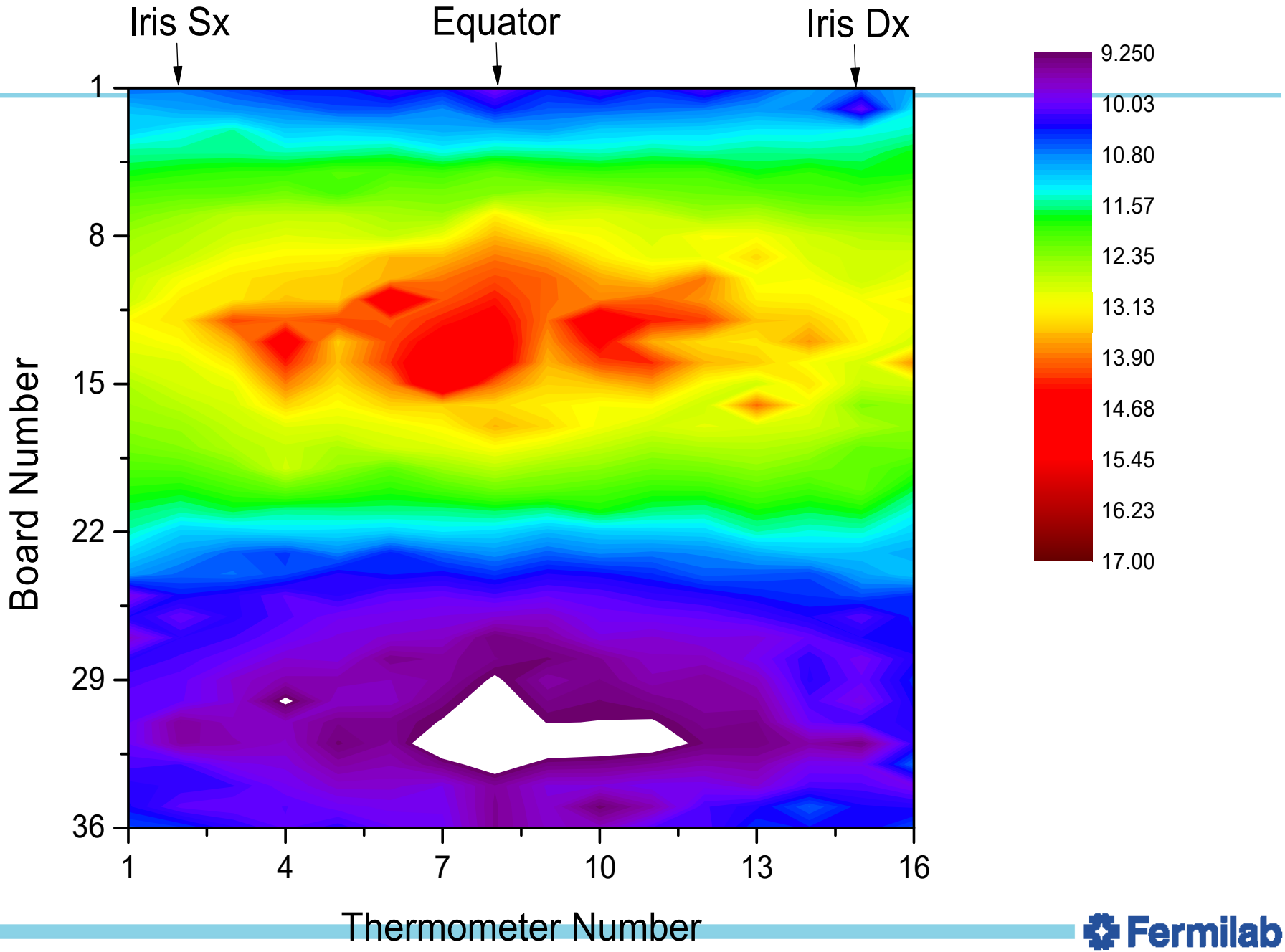
Iris Sx
Equator
Iris Dx
1
8
15
22
29
36
Board Number
1
4
7
10
13
16
Thermometer Number
9.250
10.03
10.80
11.57
12.35
13.13
13.90
14.68
15.45
16.23
17.00

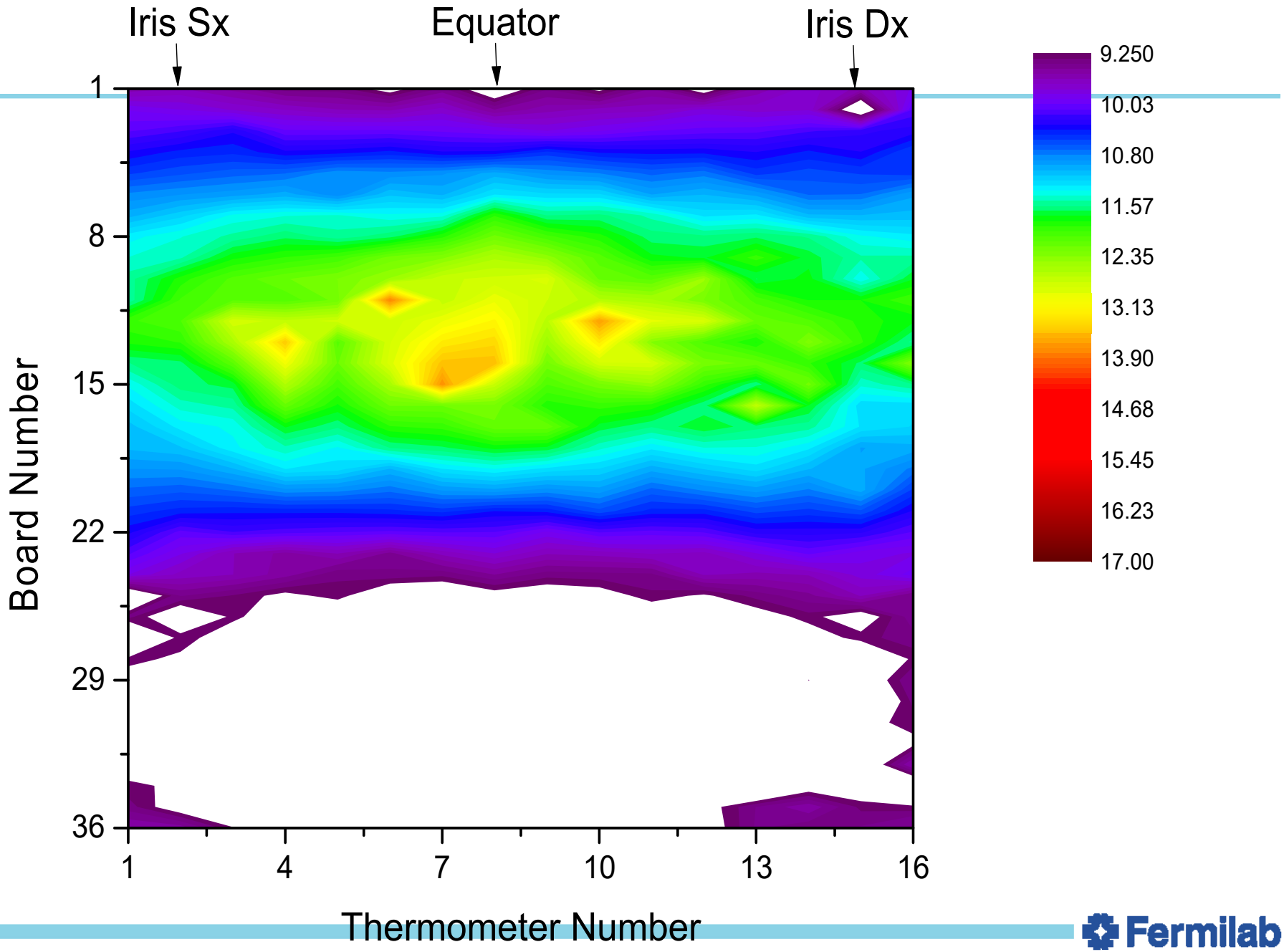
Iris Sx
Equator
Iris Dx
1
8
15
22
29
36
Board Number
1
4
7
10
13
16
Thermometer Number
9.250
10.03
10.80
11.57
12.35
13.13
13.90
14.68
15.45
16.23
17.00

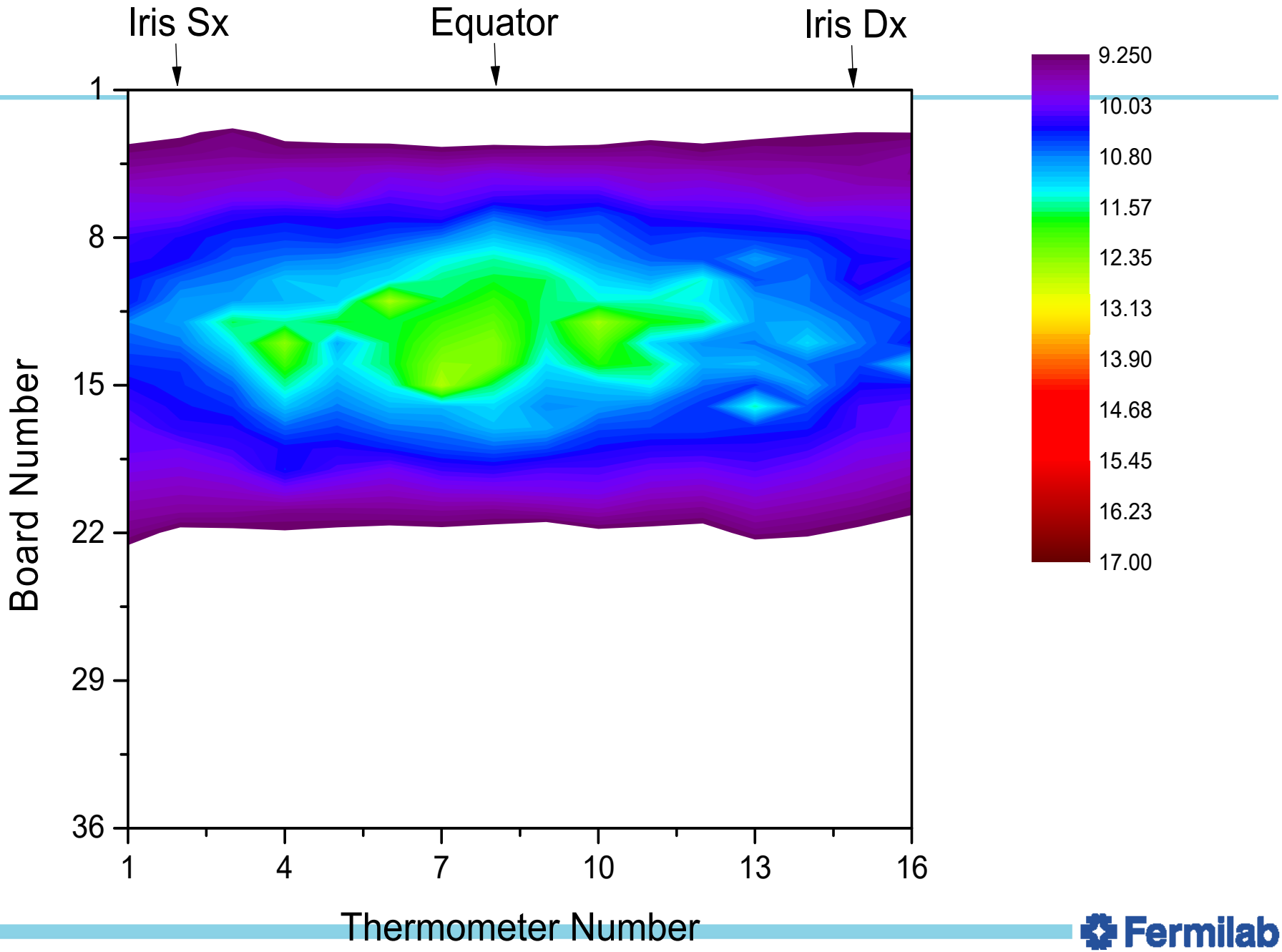
Iris Sx
Equator
Iris Dx
1
8
15
22
29
36
Board Number
1
4
7
10
13
16
Thermometer Number
9.250
10.03
10.80
11.57
12.35
13.13
13.90
14.68
15.45
16.23
17.00

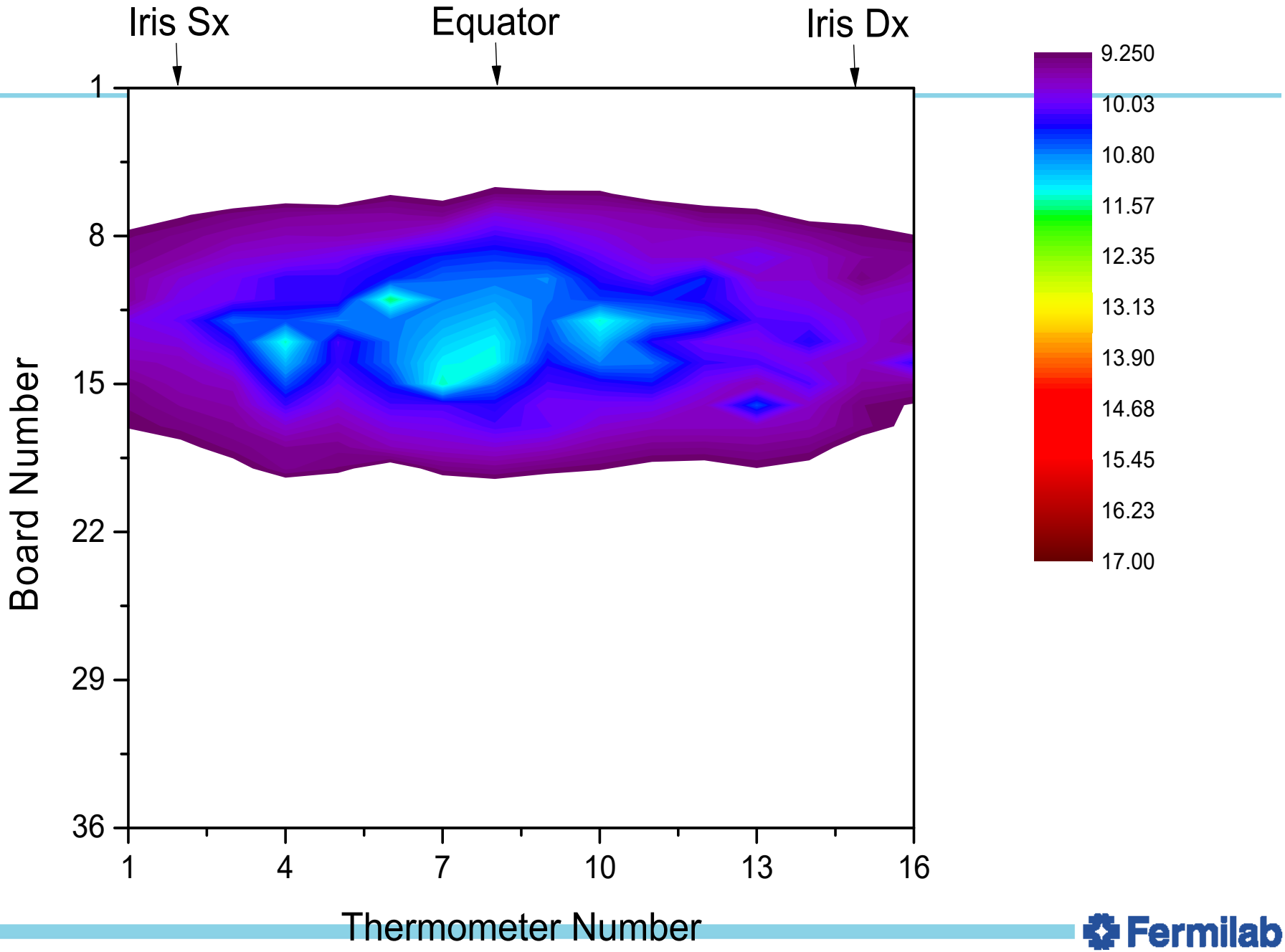
Iris Sx
Equator
Iris Dx
1
8
15
22
29
36
Board Number
1
4
7
10
13
16
Thermometer Number
9.250
10.03
10.80
11.57
12.35
13.13
13.90
14.68
15.45
16.23
17.00

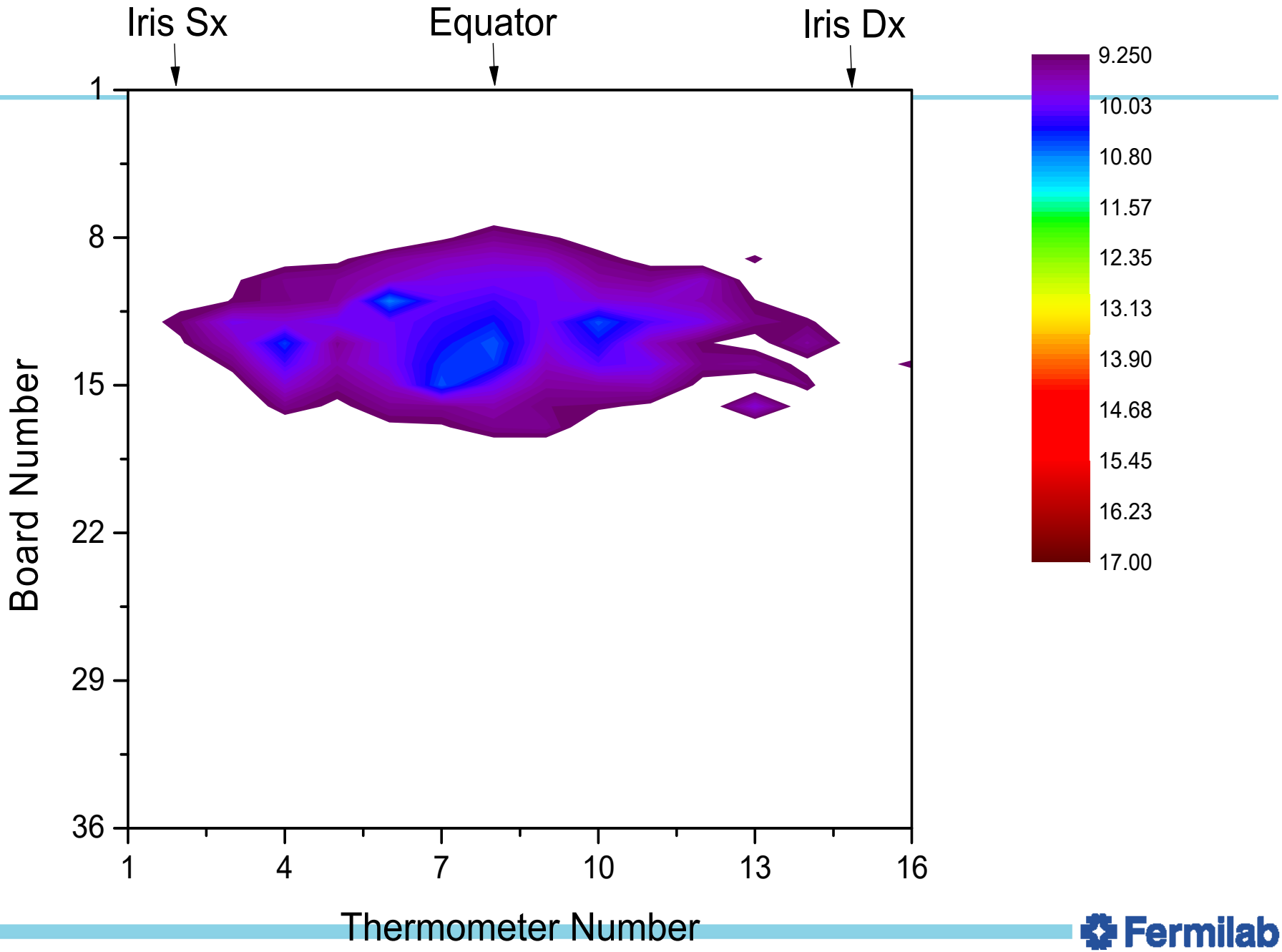
Iris Sx
Equator
Iris Dx
1
8
15
22
29
36
Board Number
1
4
7
10
13
16
Thermometer Number
9.250
10.03
10.80
11.57
12.35
13.13
13.90
14.68
15.45
16.23
17.00

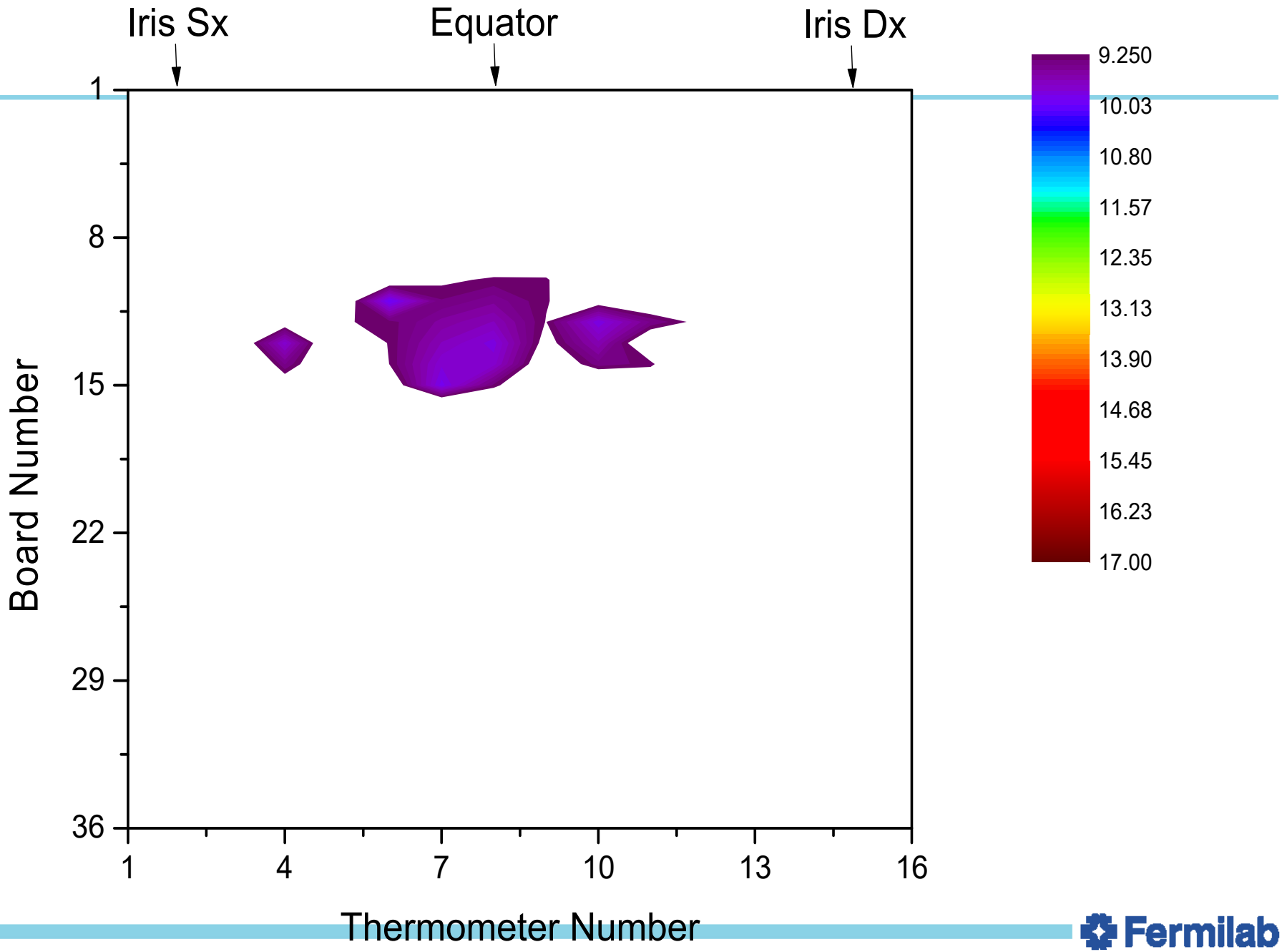
Iris Sx
Equator
Iris Dx
1
8
15
22
29
36
Board Number
1
4
7
10
13
16
Thermometer Number
9.250
10.03
10.80
11.57
12.35
13.13
13.90
14.68
15.45
16.23
17.00

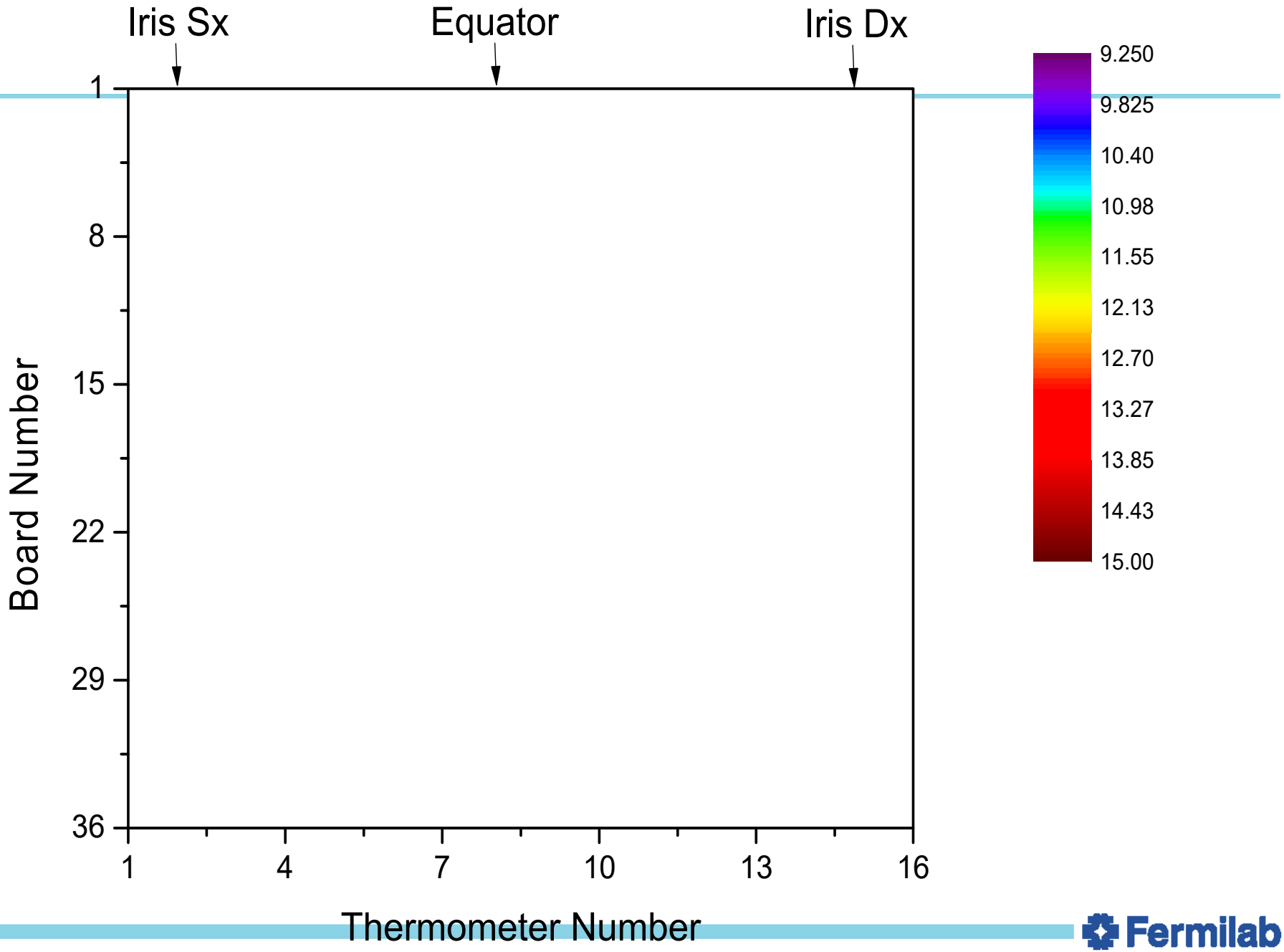
Iris Sx
Equator
Iris Dx
1
8
15
22
29
36
Board Number
1
4
7
10
13
16
Thermometer Number
9.250
9.825
10.40
10.98
11.55
12.13
12.70
13.27
13.85
14.43
15.00

- Slow cooldown – encircling normal areas

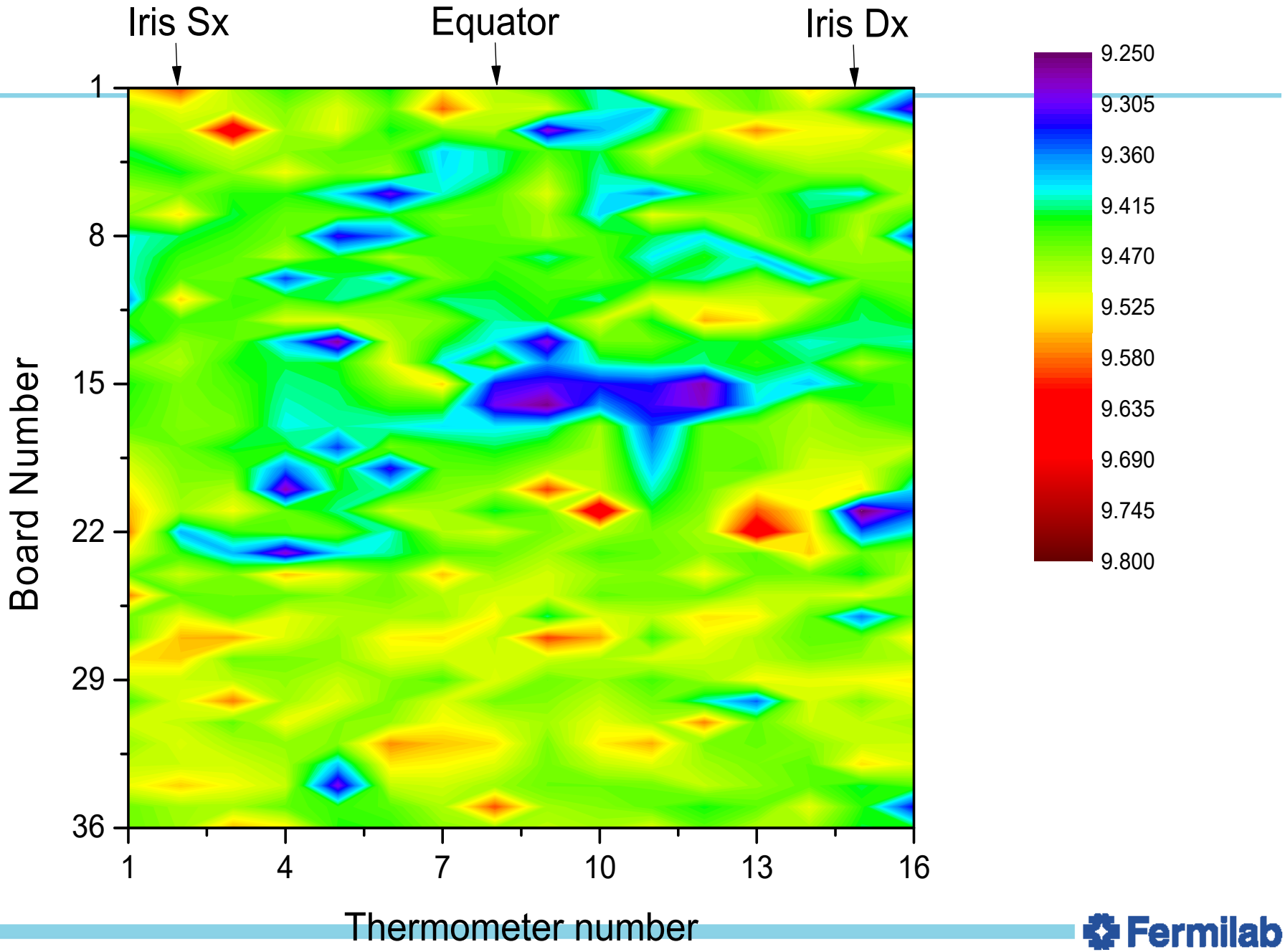
Iris Sx
Equator
Iris Dx
1
8
15
22
29
36
Board Number
1
4
7
10
13
16
Thermometer number
9.250
9.305
9.360
9.415
9.470
9.525
9.580
9.635
9.690
9.745
9.800

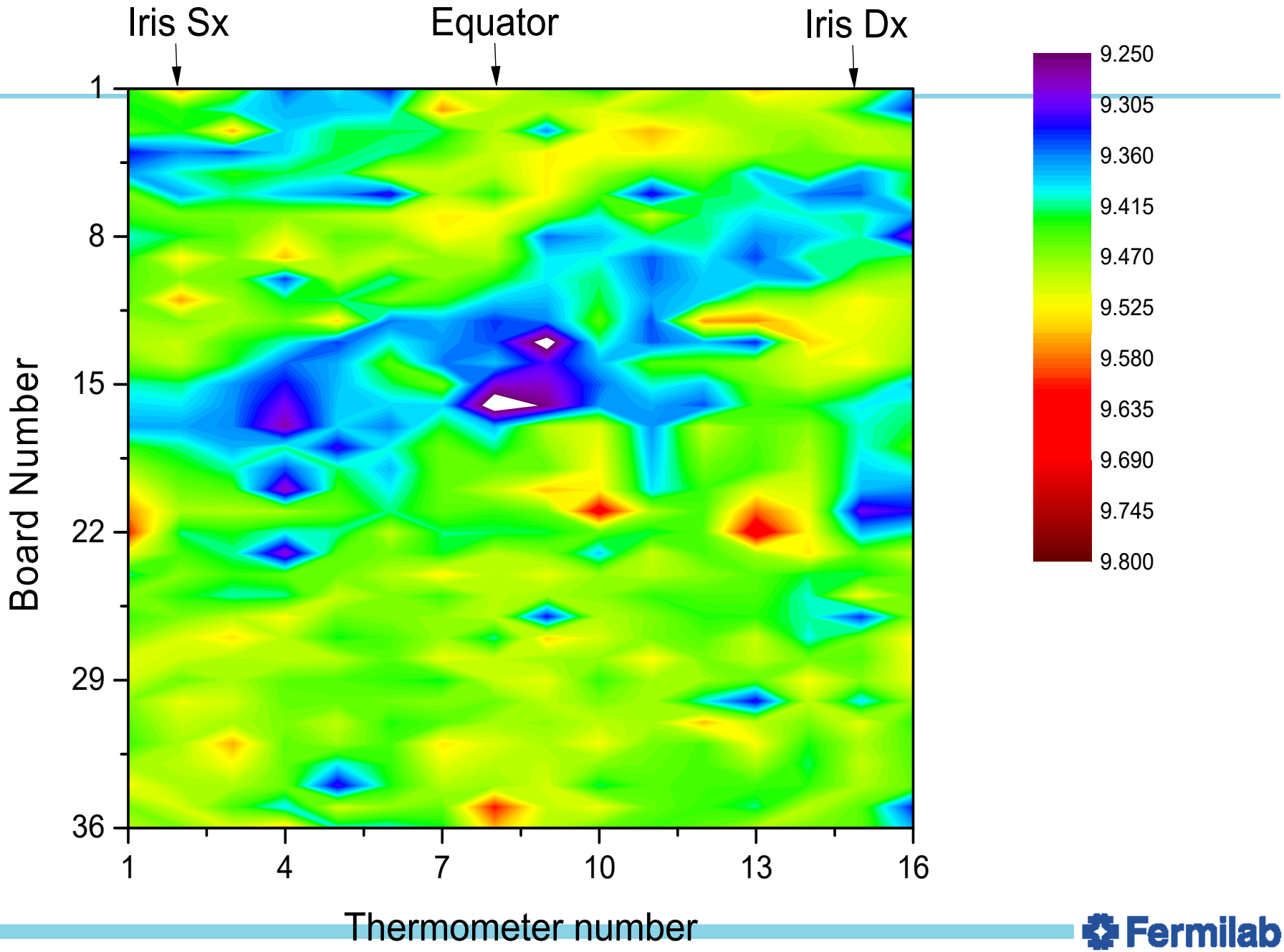
Iris Sx
Equator
Iris Dx
Board Number
1
8
15
22
29
36
1
4
7
10
13
16
Thermometer number
9.250
9.305
9.360
9.415
9.470
9.525
9.580
9.635
9.690
9.745
9.800

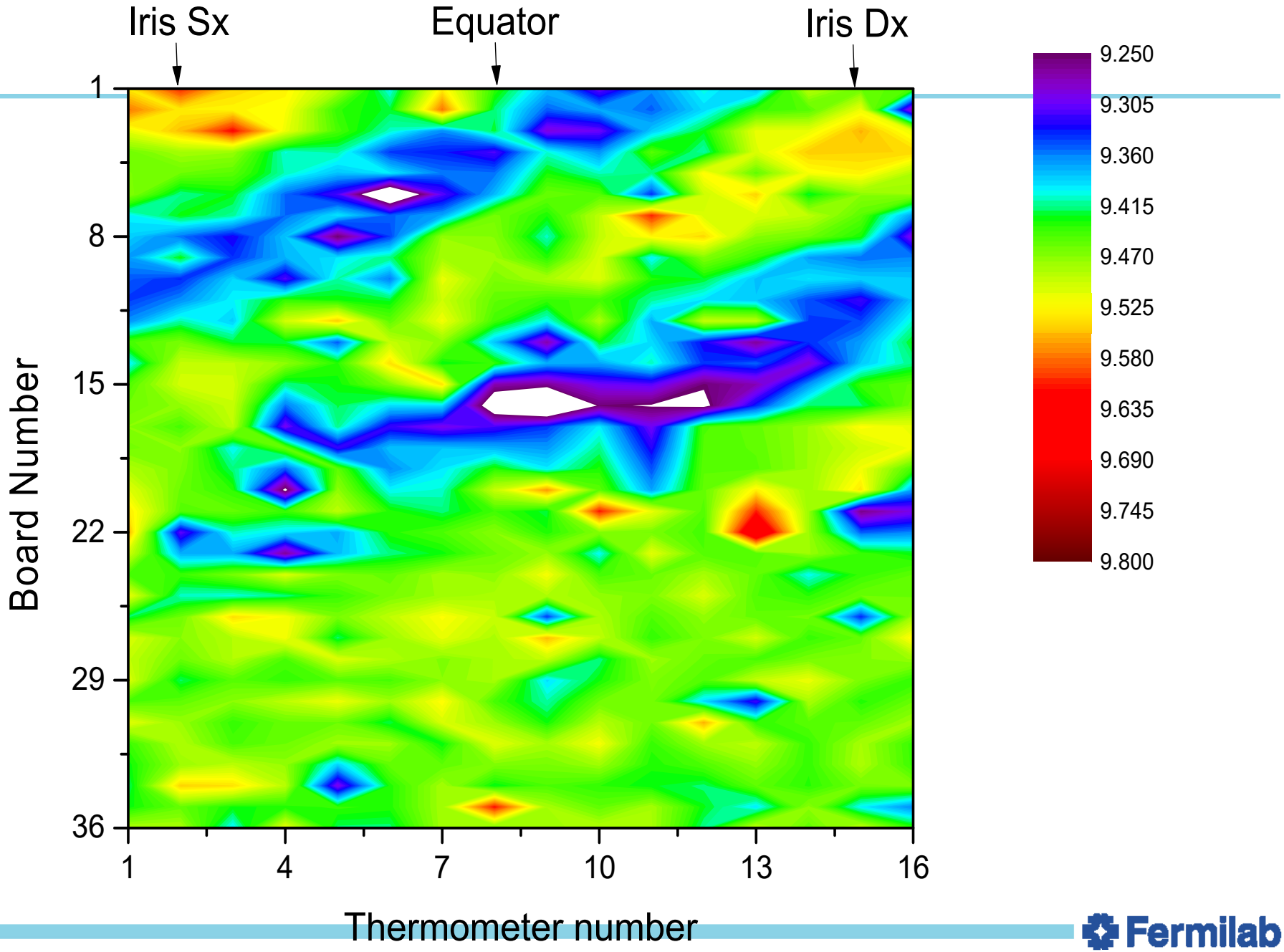
Iris Sx
Equator
Iris Dx
Board Number
1
8
15
22
29
36
1
4
7
10
13
16
Thermometer number
9.250
9.305
9.360
9.415
9.470
9.525
9.580
9.635
9.690
9.745
9.800

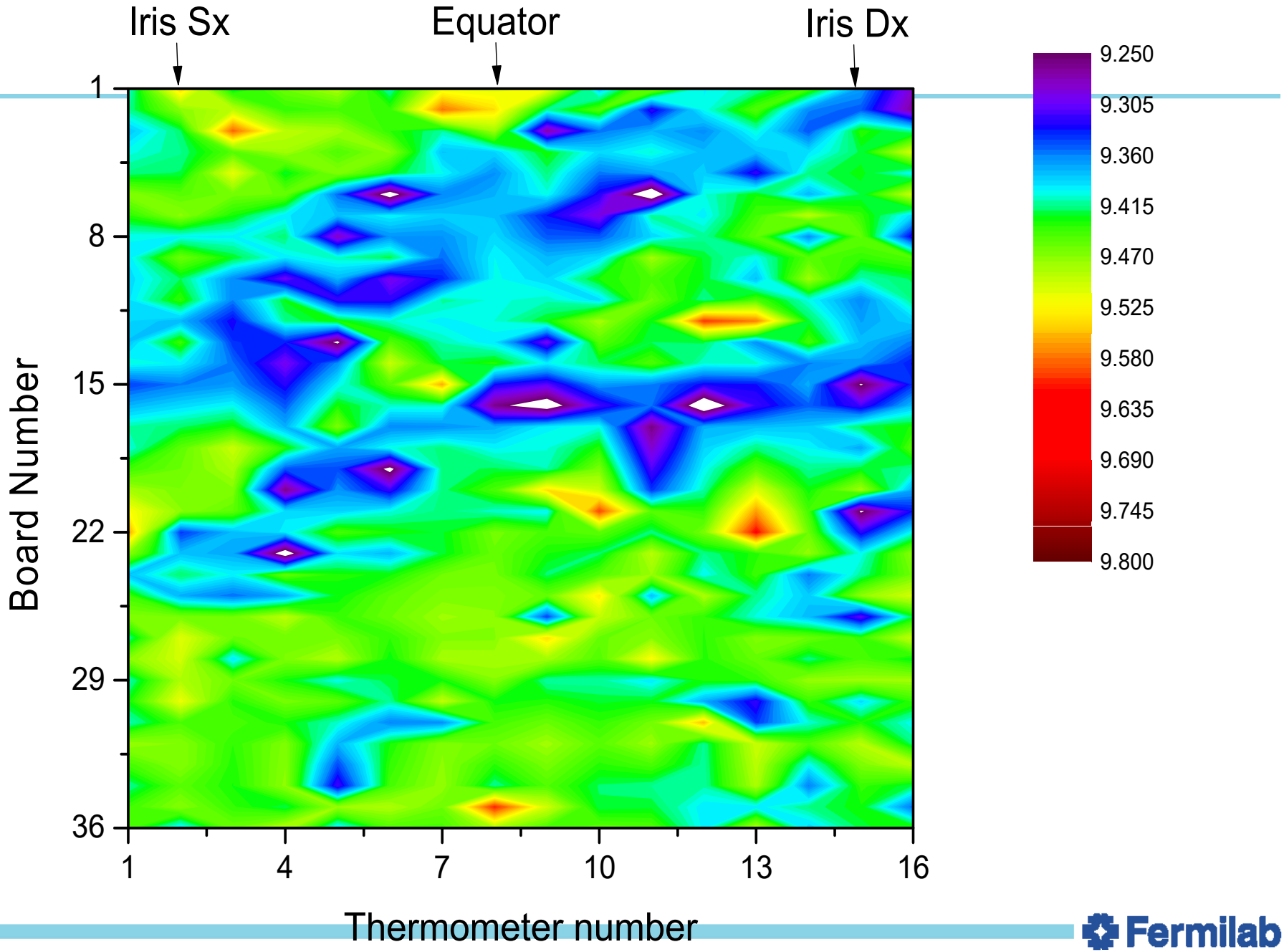
Iris Sx
Equator
Iris Dx
1
8
15
22
29
36
Board Number
1
4
7
10
13
16
Thermometer number
9.250
9.305
9.360
9.415
9.470
9.525
9.580
9.635
9.690
9.745
9.800

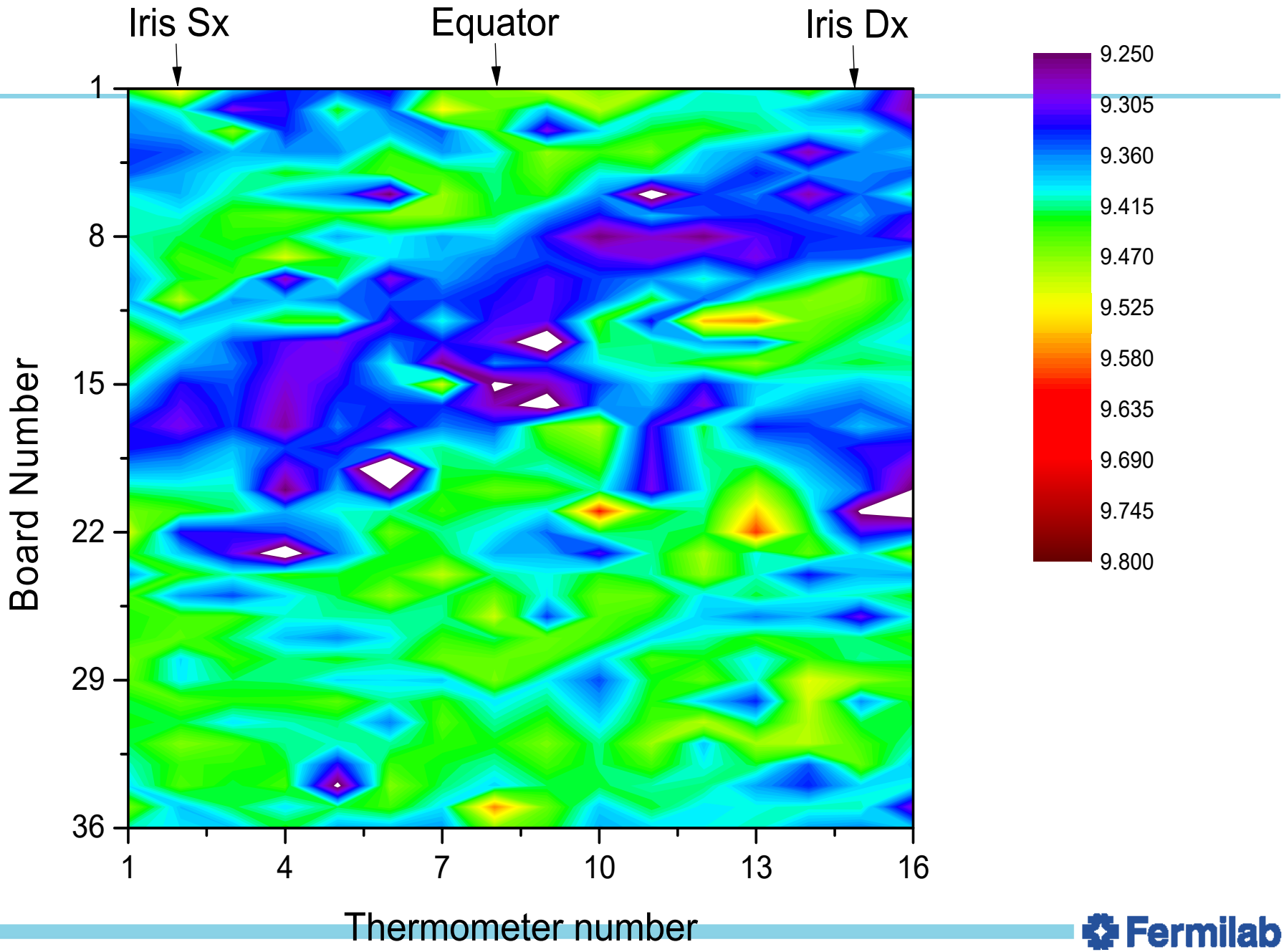
Iris Sx
Equator
Iris Dx
1
8
15
22
29
36
Board Number
1
4
7
10
13
16
Thermometer number
9.250
9.305
9.360
9.415
9.470
9.525
9.580
9.635
9.690
9.745
9.800

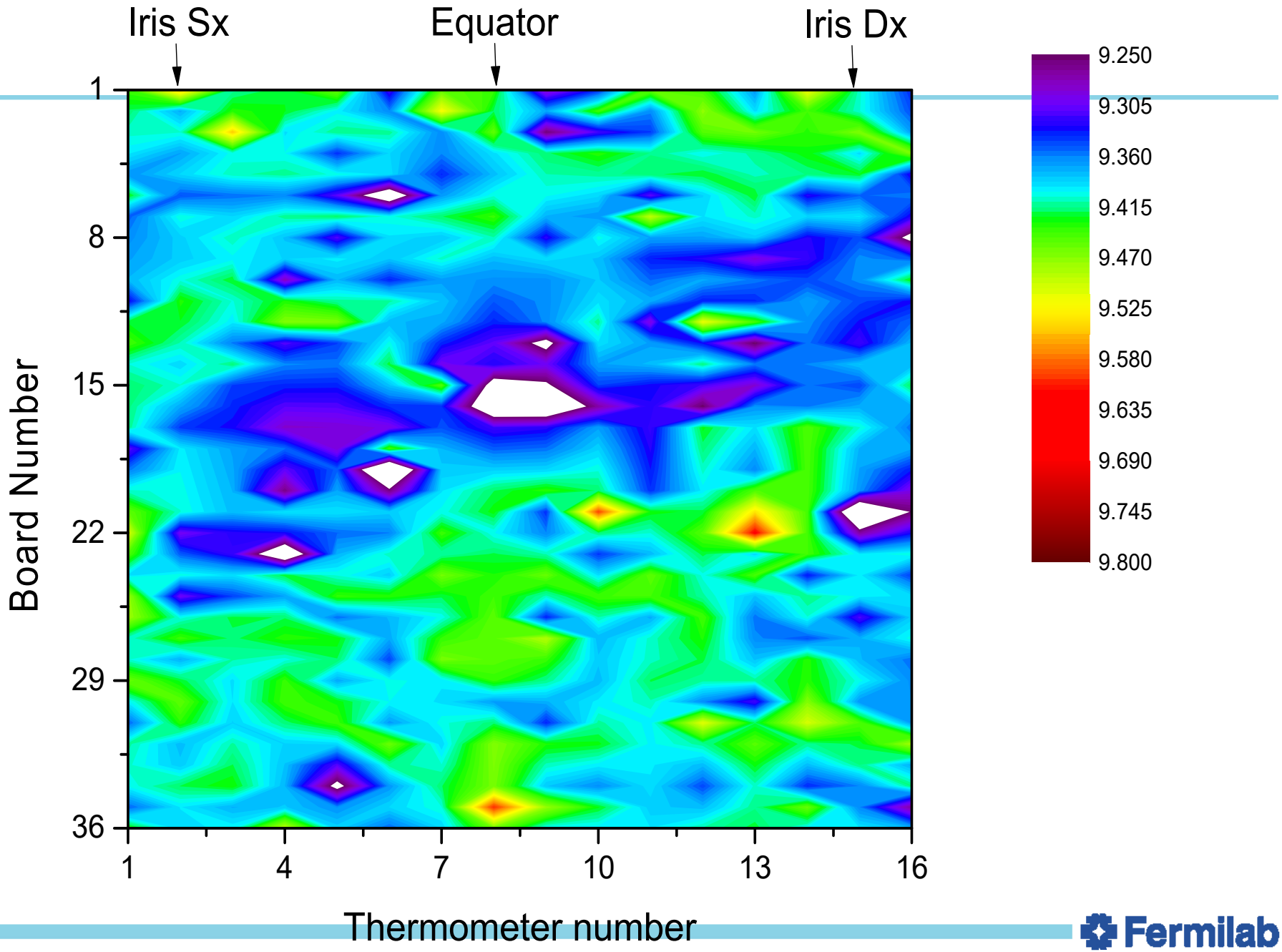
Iris Sx
Equator
Iris Dx
1
8
15
22
29
36
Board Number
1
4
7
10
13
16
Thermometer number
9.250
9.305
9.360
9.415
9.470
9.525
9.580
9.635
9.690
9.745
9.800

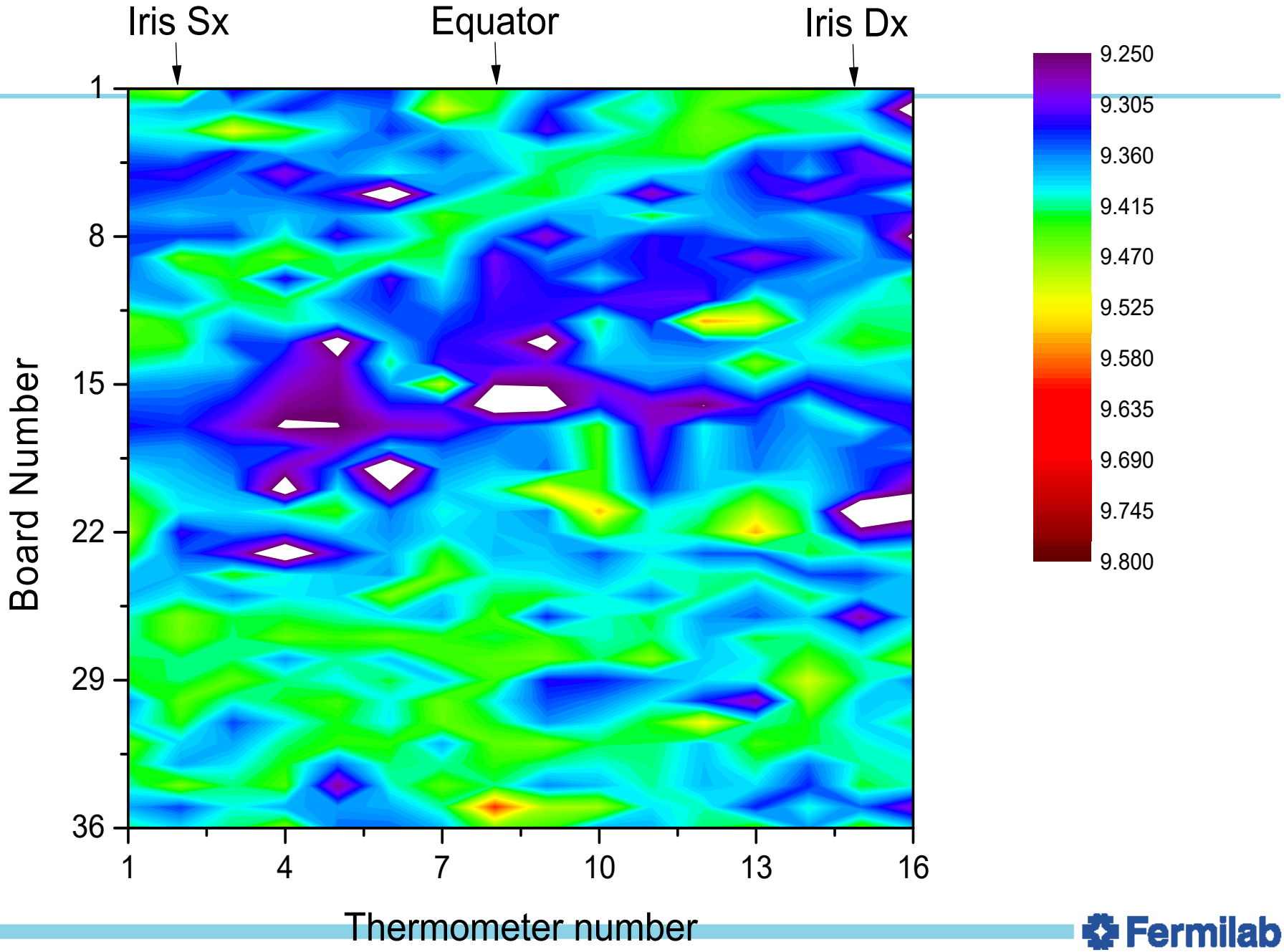
Iris Sx
Equator
Iris Dx
Board Number
1
8
15
22
29
36
1
4
7
10
13
16
Thermometer number
9.250
9.305
9.360
9.415
9.470
9.525
9.580
9.635
9.690
9.745
9.800

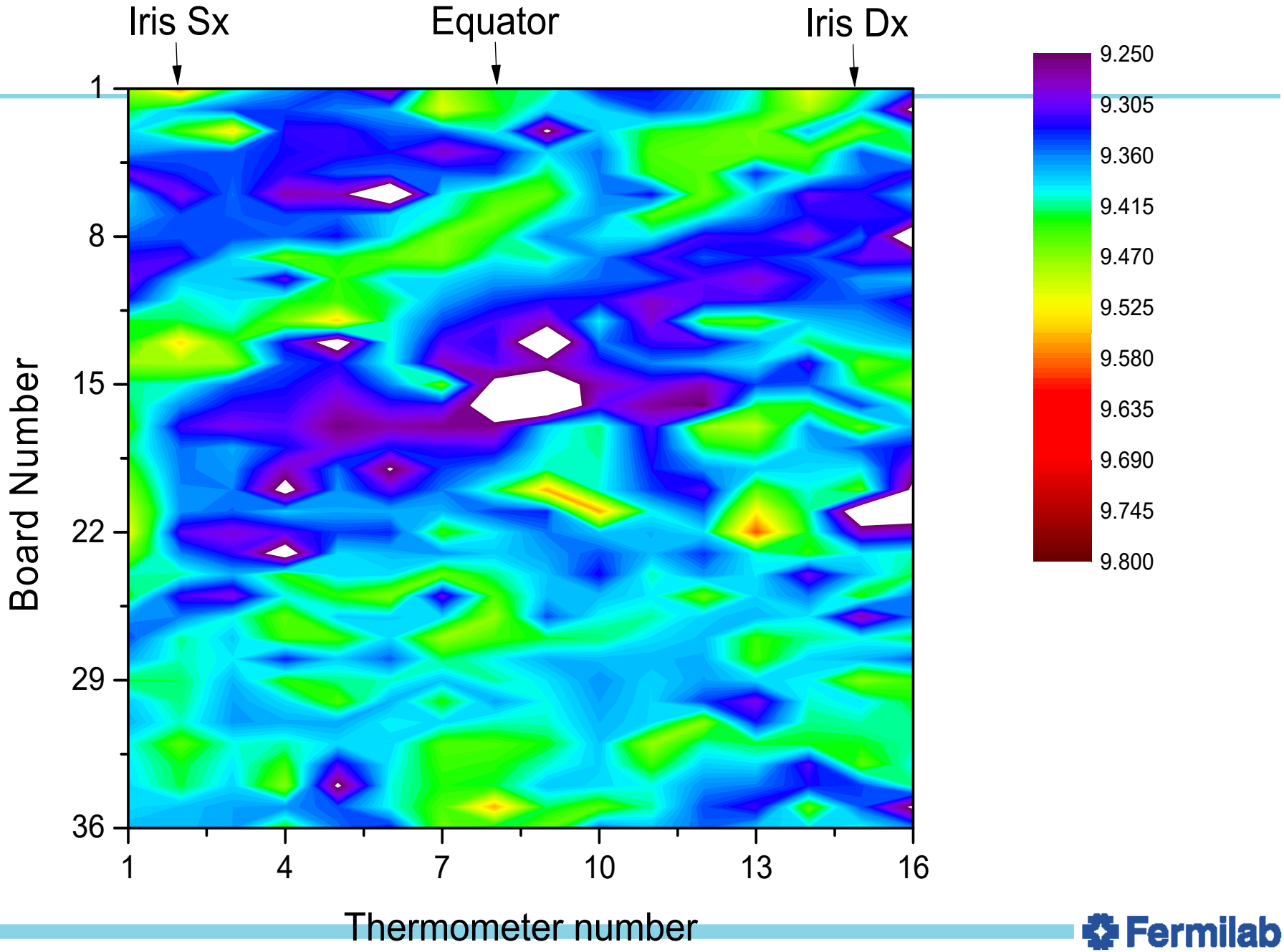
Iris Sx
Equator
Iris Dx
1
8
15
22
29
36
Board Number
1
4
7
10
13
16
Thermometer number
9.250
9.305
9.360
9.415
9.470
9.525
9.580
9.635
9.690
9.745
9.800

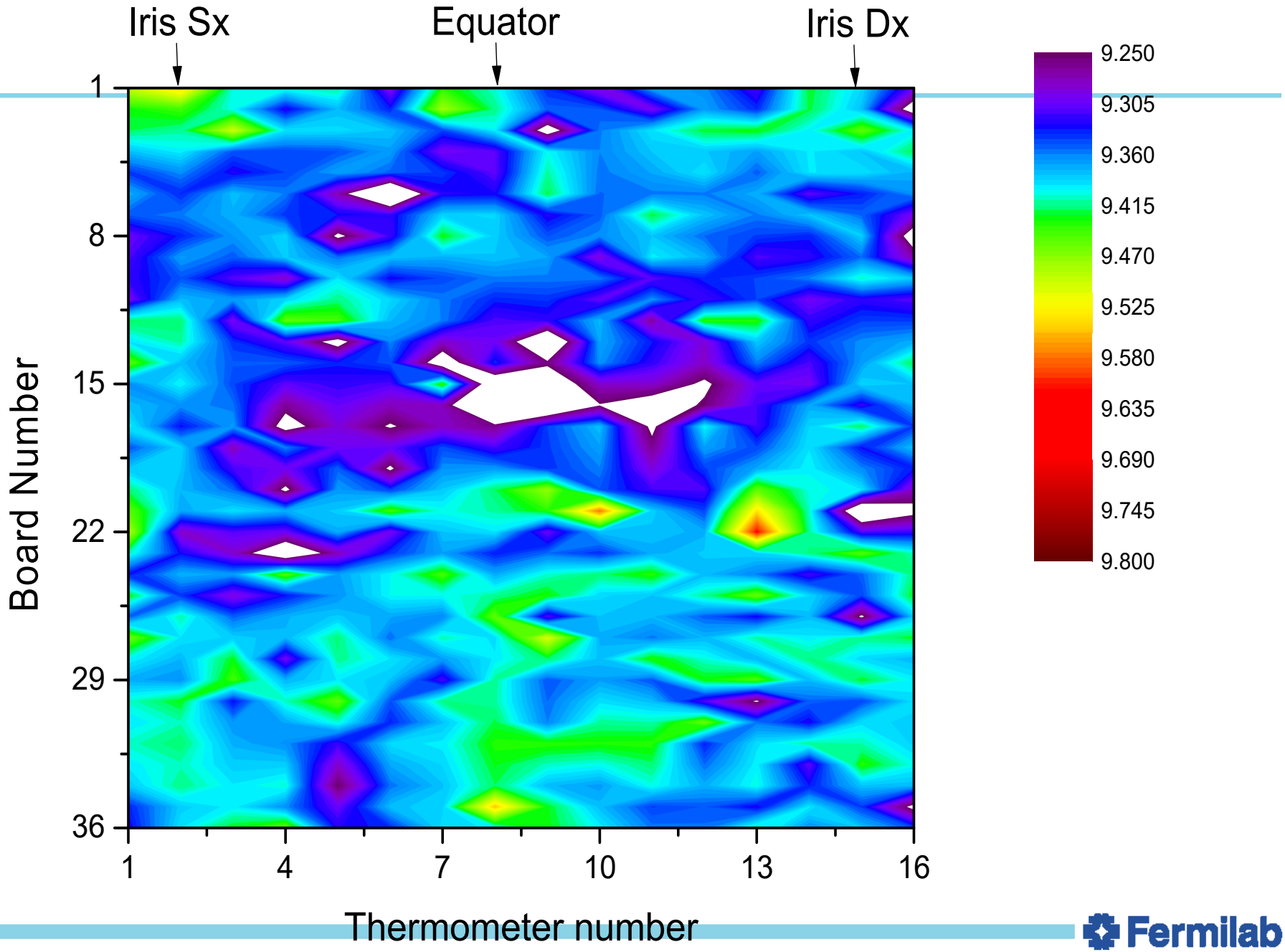
Iris Sx
Equator
Iris Dx
Board Number
1
8
15
22
29
36
1
4
7
10
13
16
Thermometer number
9.250
9.305
9.360
9.415
9.470
9.525
9.580
9.635
9.690
9.745
9.800

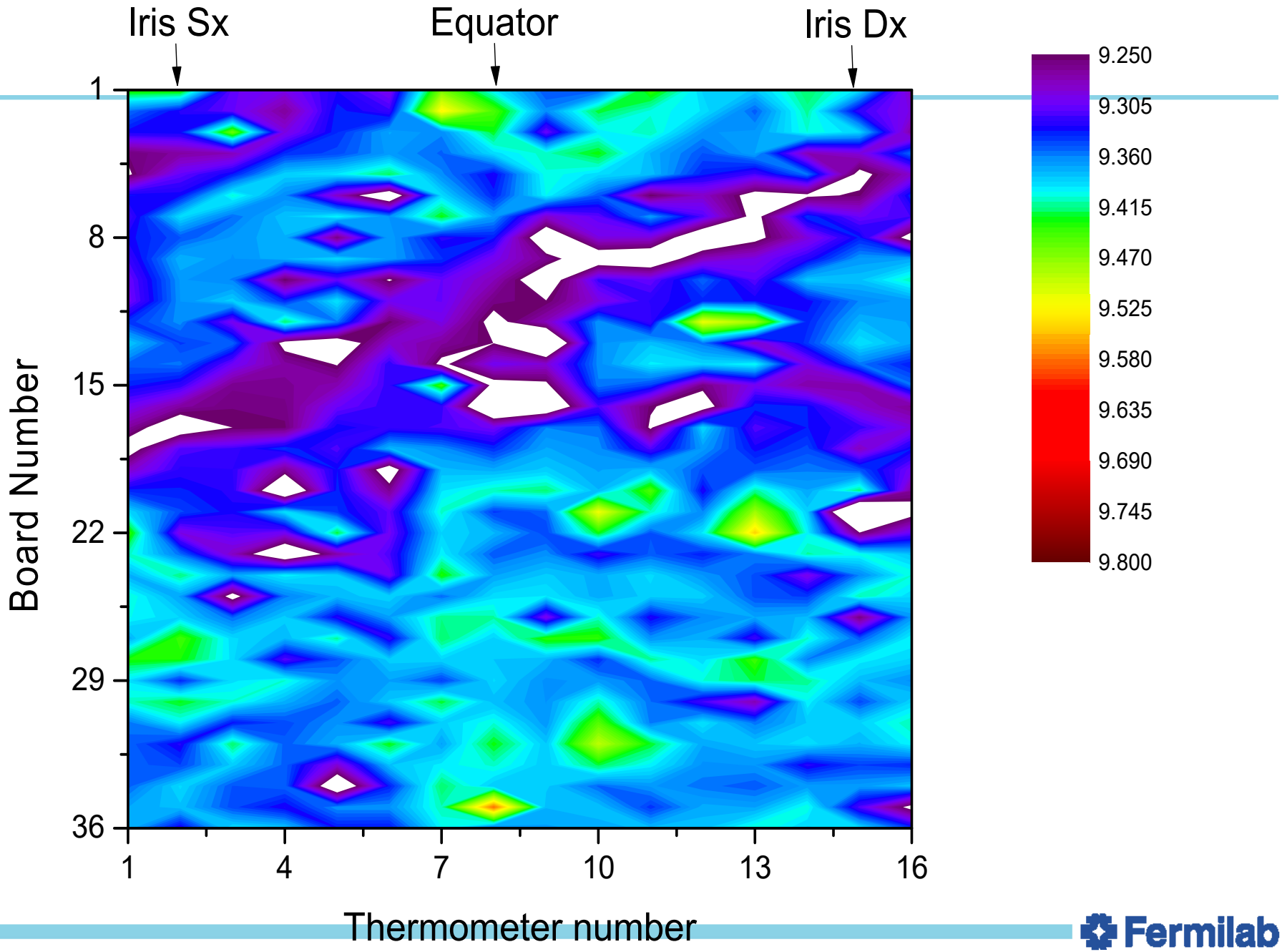
Iris Sx
Equator
Iris Dx
Board Number
1
8
15
22
29
36
1
4
7
10
13
16
Thermometer number
9.250
9.305
9.360
9.415
9.470
9.525
9.580
9.635
9.690
9.745
9.800

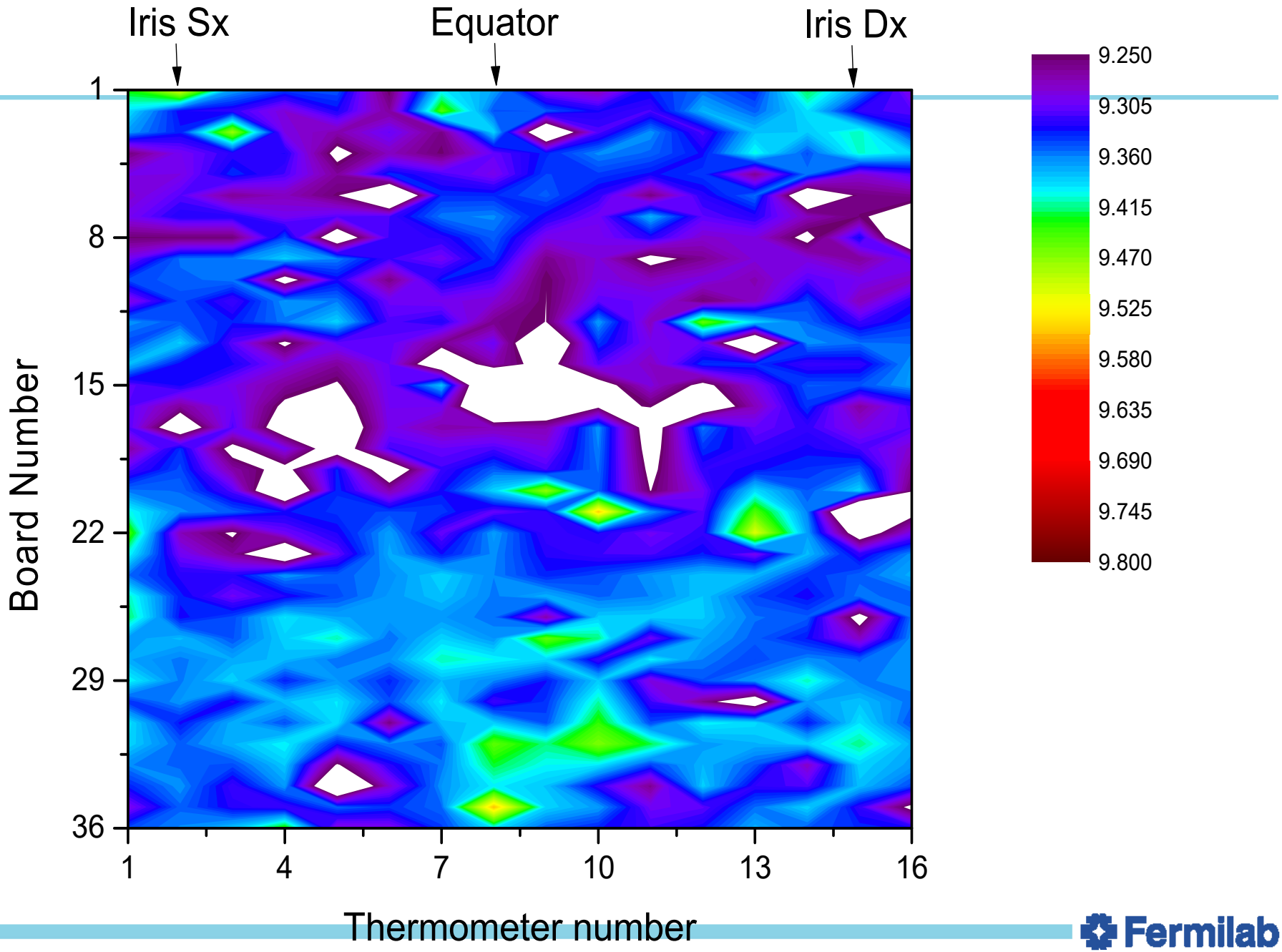
Iris Sx
Equator
Iris Dx
Board Number
1
8
15
22
29
36
1
4
7
10
13
16
Thermometer number
9.250
9.305
9.360
9.415
9.470
9.525
9.580
9.635
9.690
9.745
9.800

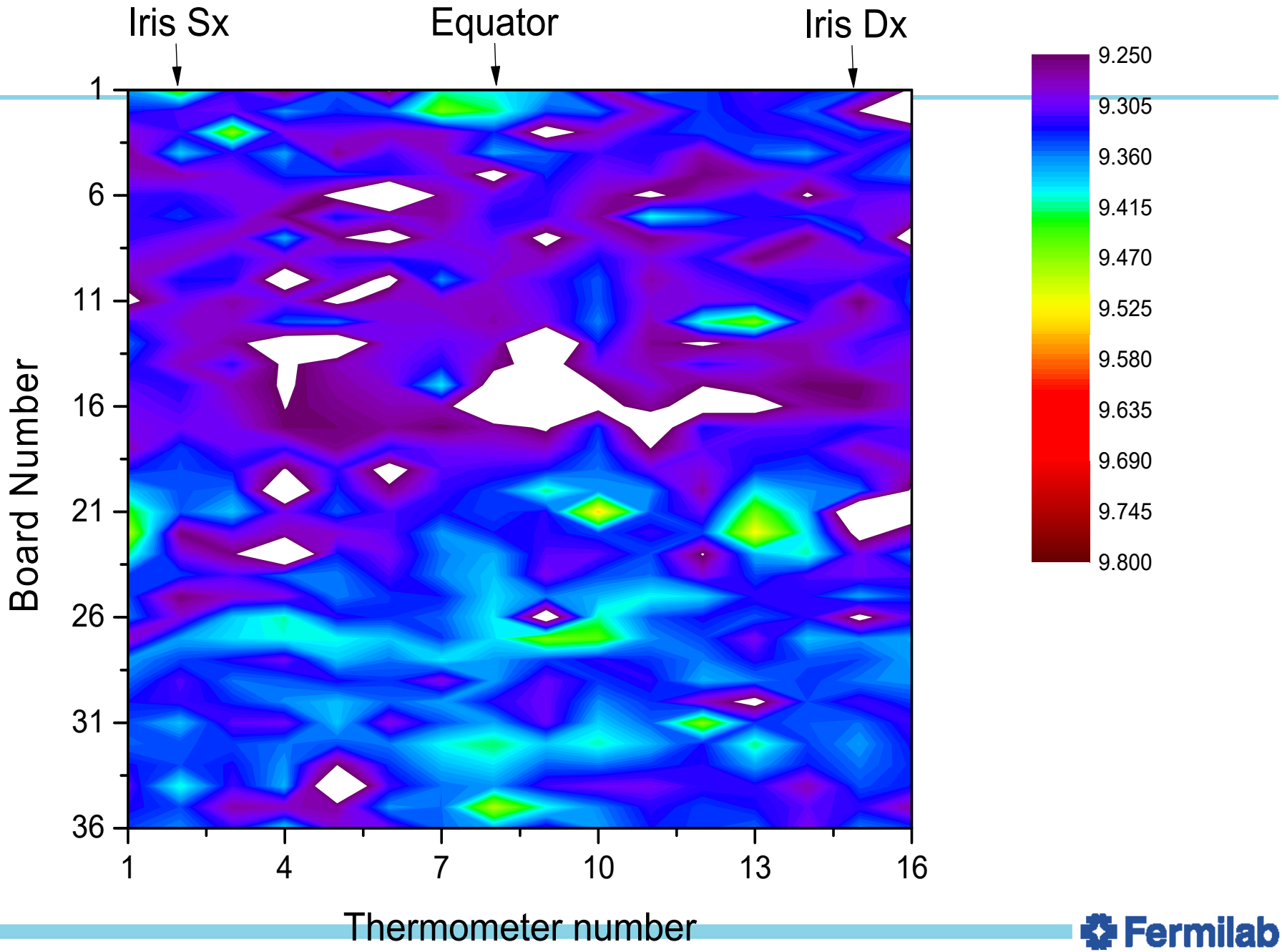
Iris Sx
Equator
Iris Dx
Board Number
1
6
11
16
21
26
31
36
1
4
7
10
13
16
Thermometer number
9.250
9.305
9.360
9.415
9.470
9.525
9.580
9.635
9.690
9.745
9.800

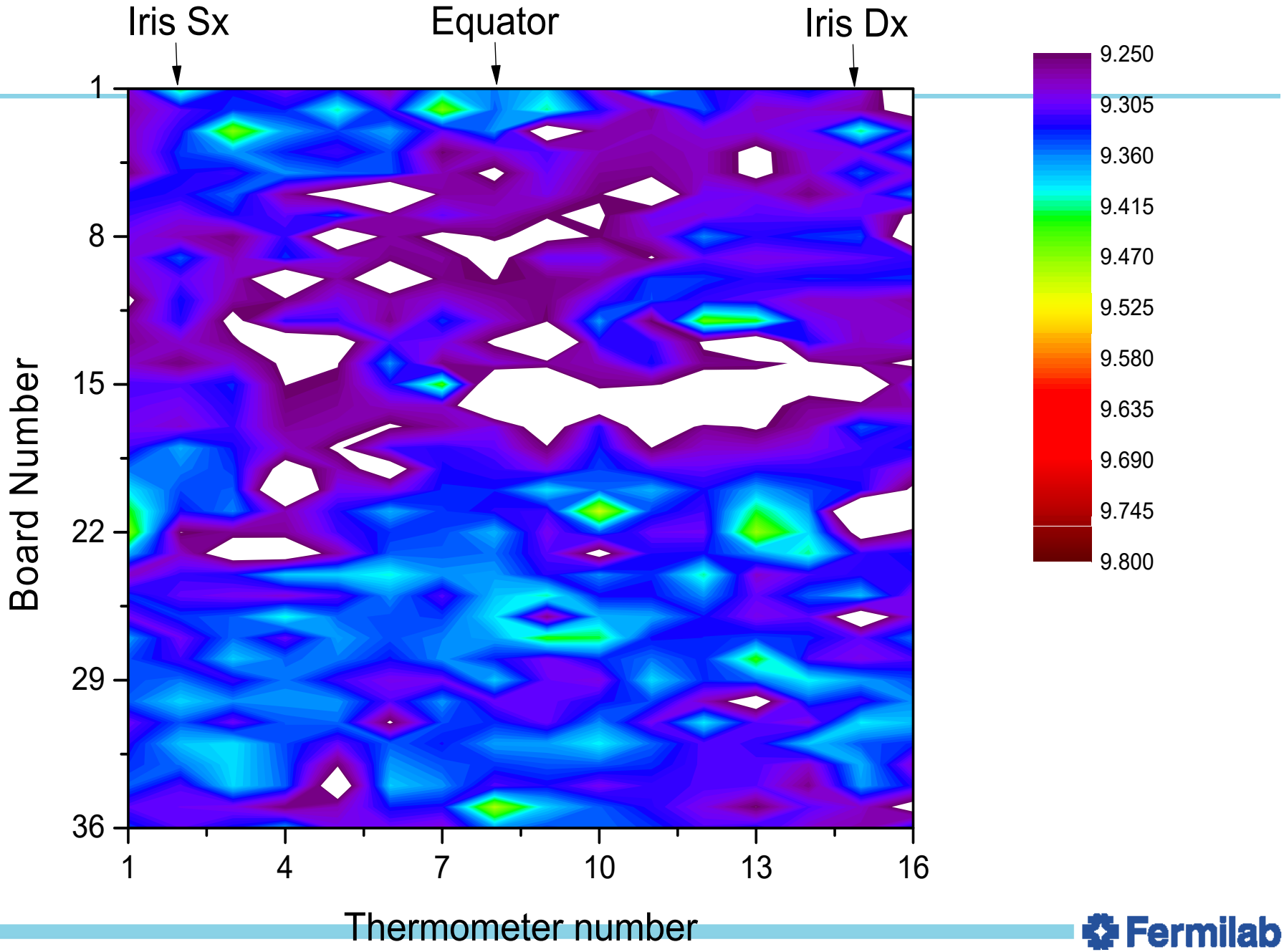
Iris Sx
Equator
Iris Dx
1
8
15
22
29
36
Board Number
1
4
7
10
13
16
Thermometer number
9.250
9.305
9.360
9.415
9.470
9.525
9.580
9.635
9.690
9.745
9.800

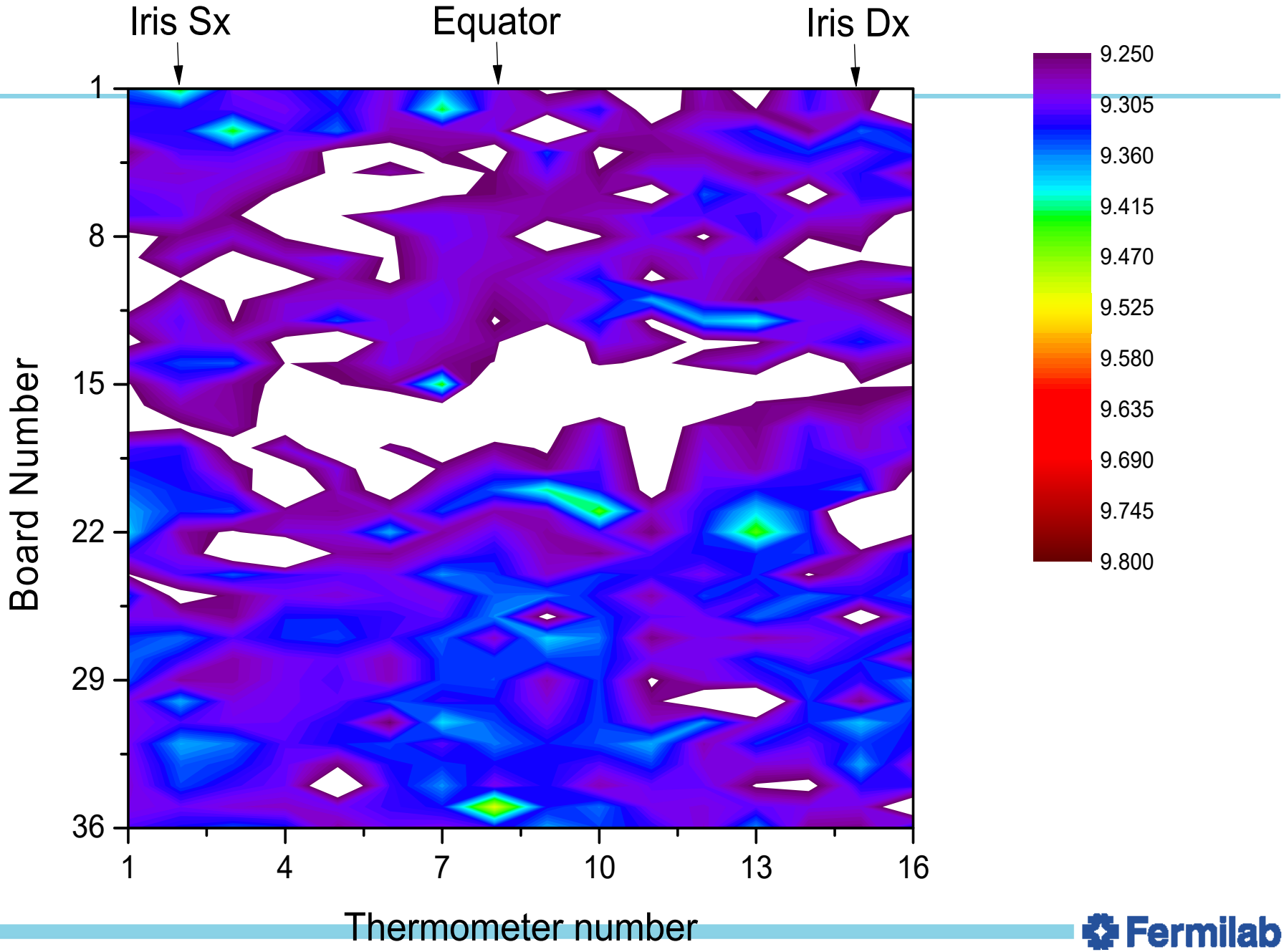
Iris Sx
Equator
Iris Dx
Board Number
1
8
15
22
29
36
1
4
7
10
13
16
Thermometer number
9.250
9.305
9.360
9.415
9.470
9.525
9.580
9.635
9.690
9.745
9.800

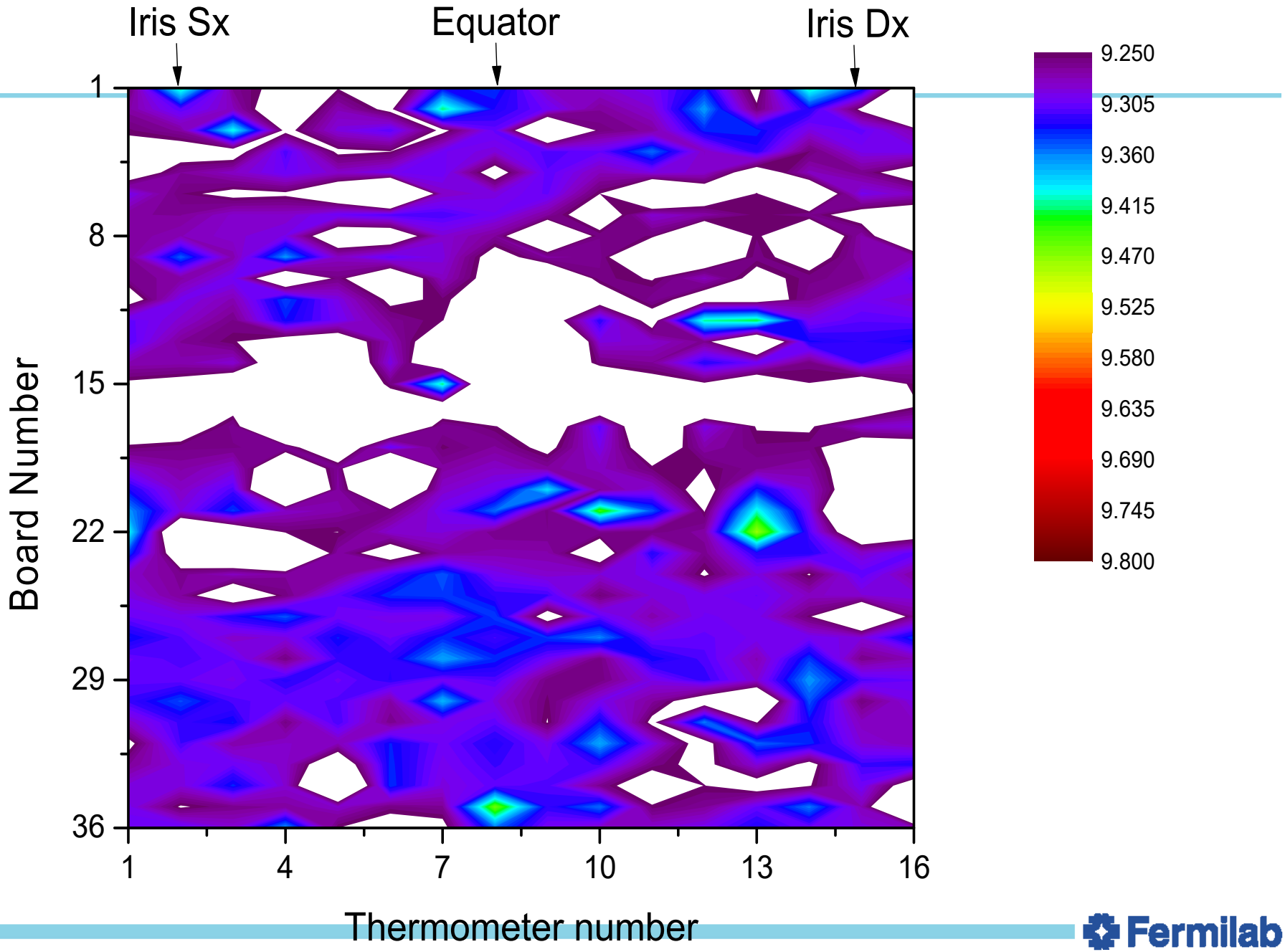
Iris Sx
Equator
Iris Dx
1
8
15
22
29
36
Board Number
1
4
7
10
13
16
Thermometer number
9.250
9.305
9.360
9.415
9.470
9.525
9.580
9.635
9.690
9.745
9.800

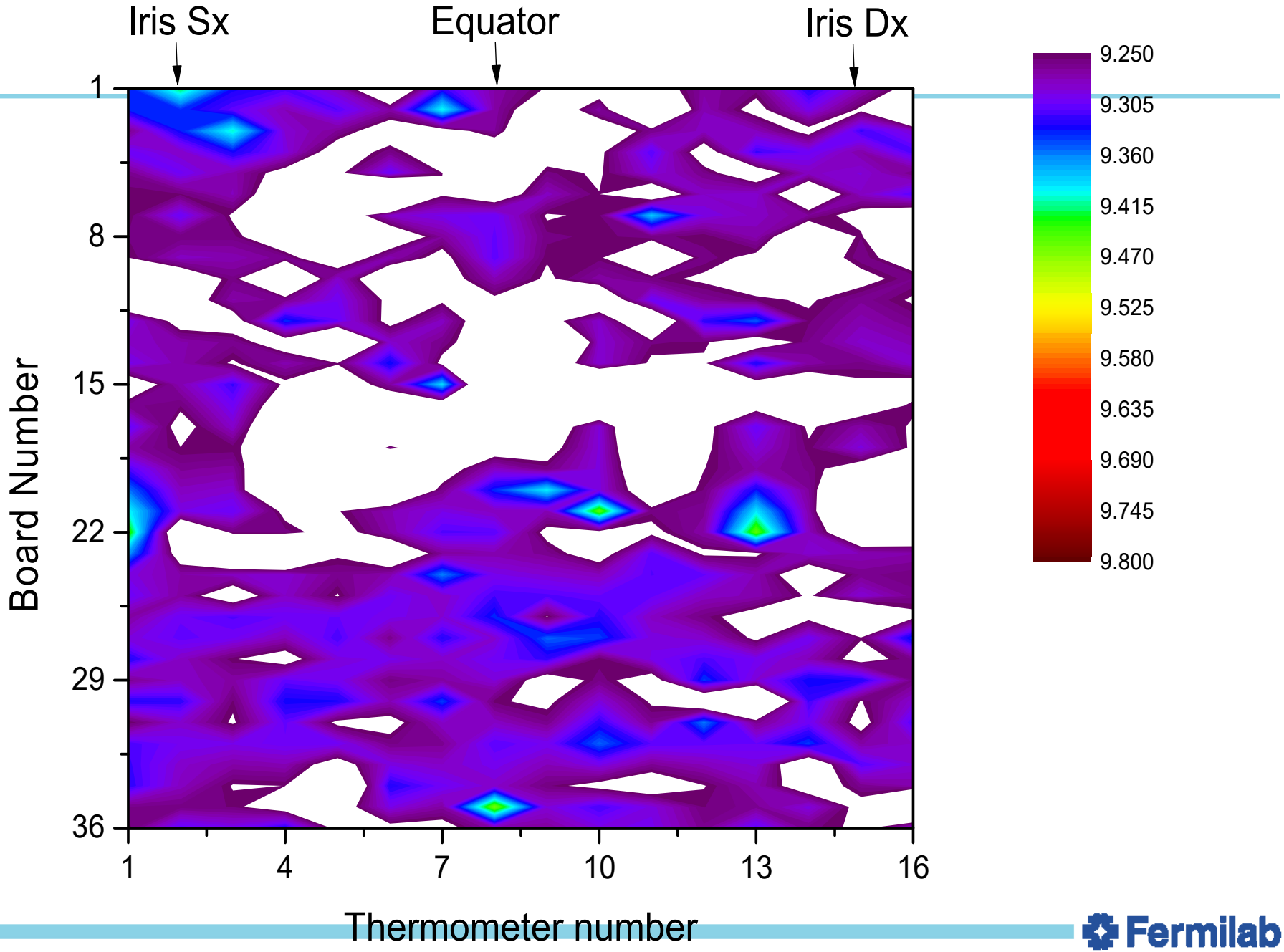
Iris Sx
Equator
Iris Dx
1
8
15
22
29
36
Board Number
1
4
7
10
13
16
Thermometer number
9.250
9.305
9.360
9.415
9.470
9.525
9.580
9.635
9.690
9.745
9.800

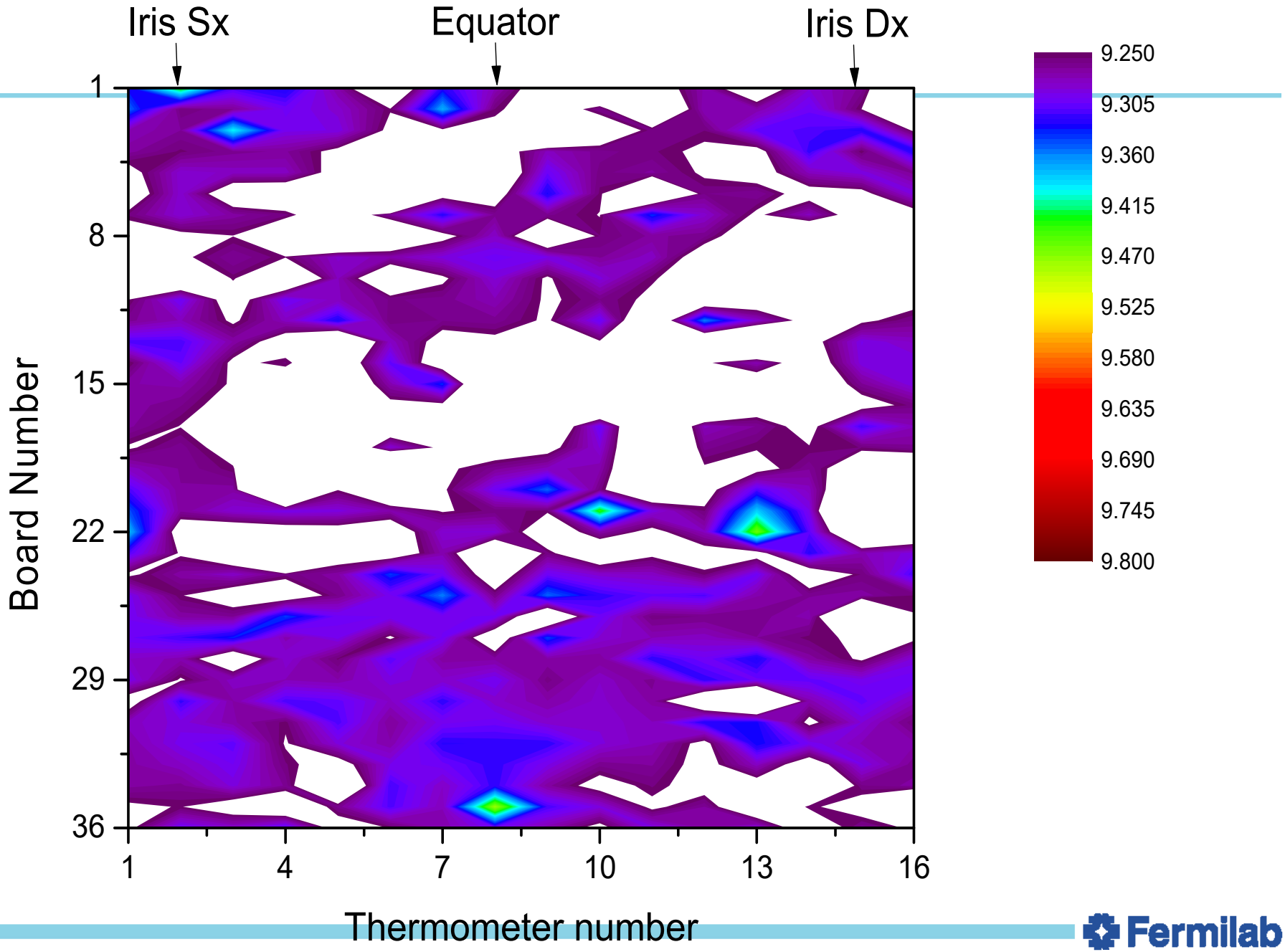
Iris Sx
Equator
Iris Dx
Board Number
1
8
15
22
29
36
1
4
7
10
13
16
Thermometer number
9.250
9.305
9.360
9.415
9.470
9.525
9.580
9.635
9.690
9.745
9.800

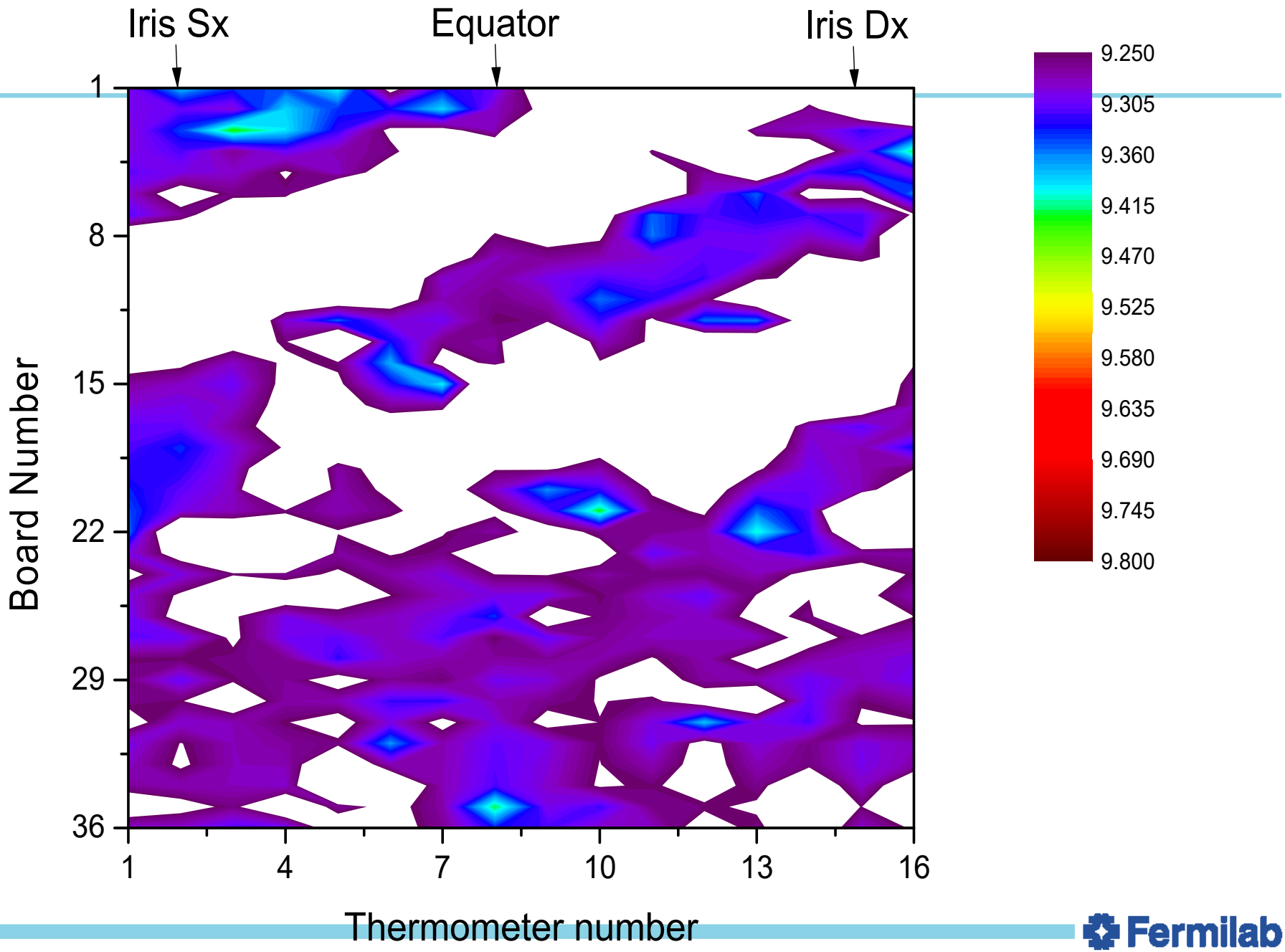
Iris Sx
Equator
Iris Dx
1
8
15
22
29
36
Board Number
1
4
7
10
13
16
Thermometer number
9.250
9.305
9.360
9.415
9.470
9.525
9.580
9.635
9.690
9.745
9.800

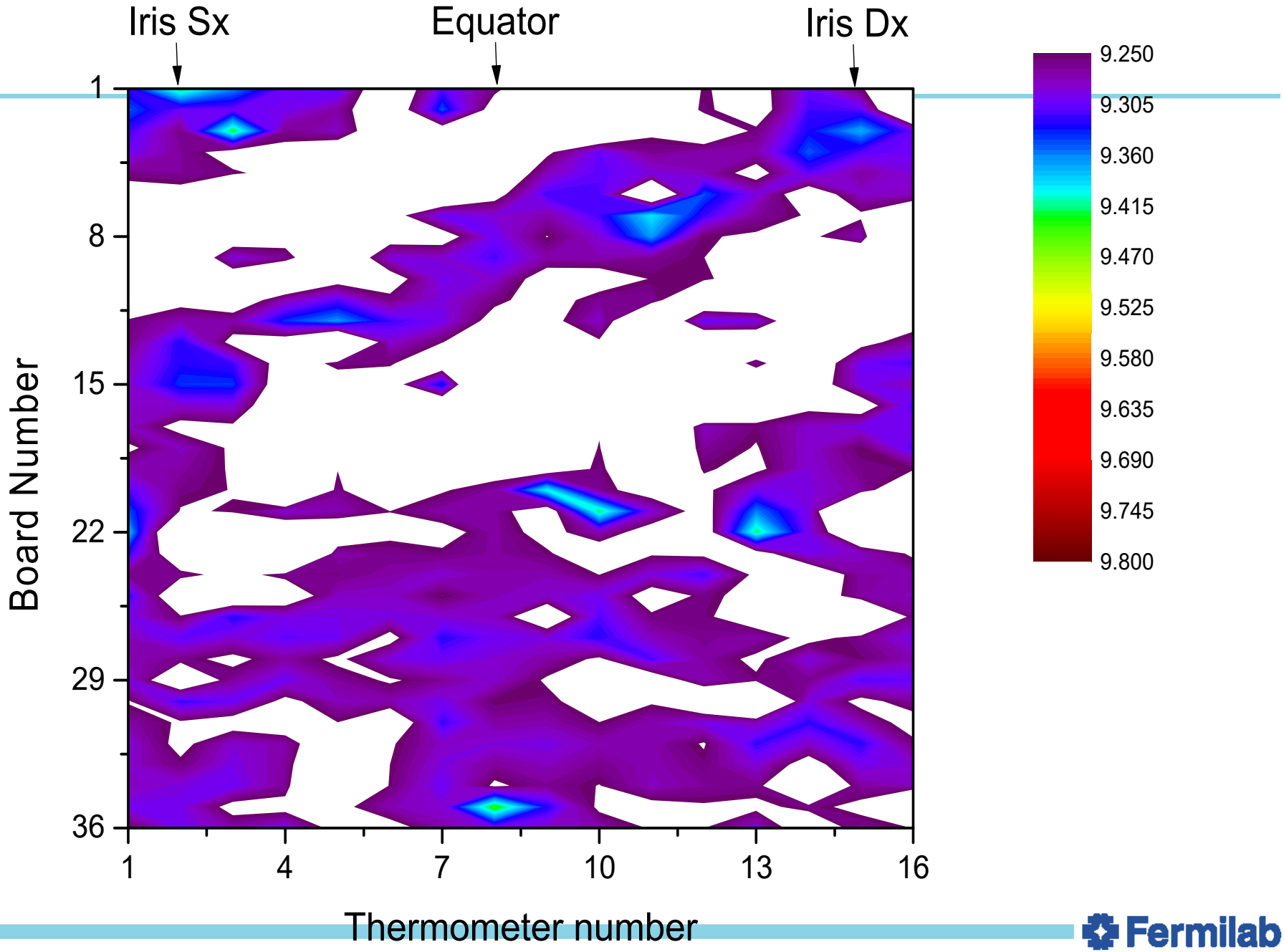
Iris Sx
Equator
Iris Dx
1
8
15
22
29
36
Board Number
1
4
7
10
13
16
Thermometer number
9.250
9.305
9.360
9.415
9.470
9.525
9.580
9.635
9.690
9.745
9.800

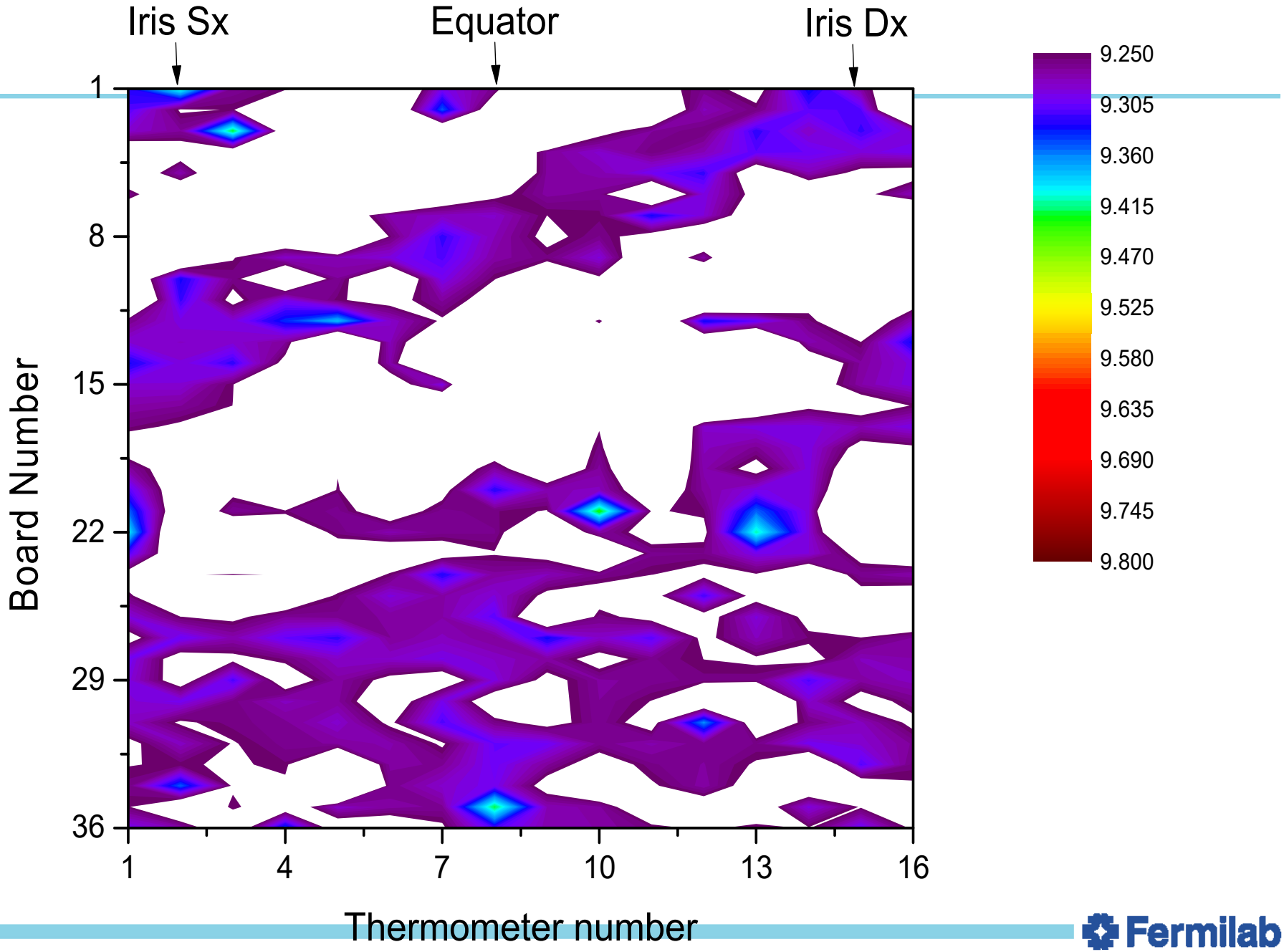
Iris Sx
Equator
Iris Dx
1
8
15
22
29
36
Board Number
1
4
7
10
13
16
Thermometer number
9.250
9.305
9.360
9.415
9.470
9.525
9.580
9.635
9.690
9.745
9.800

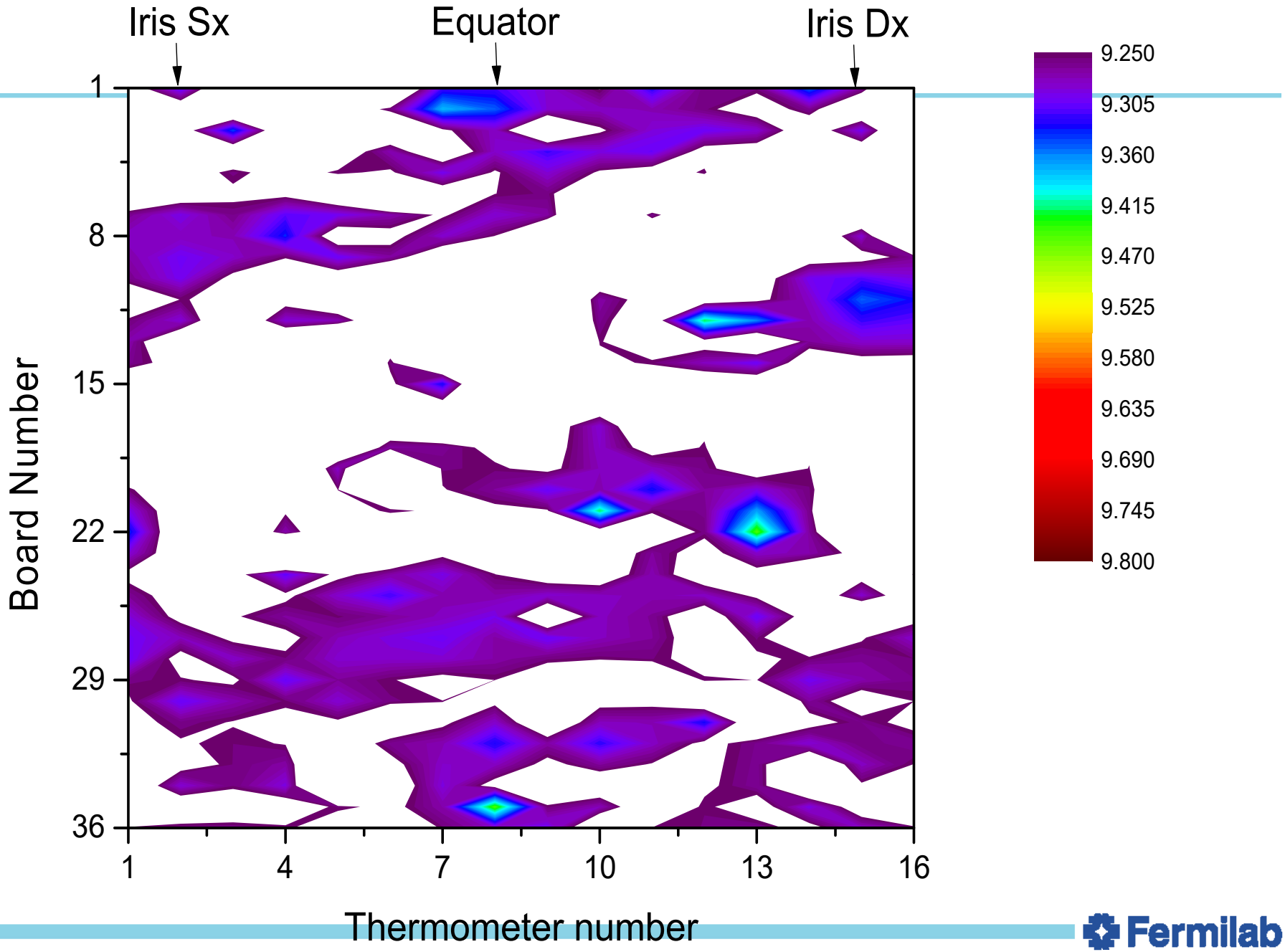
Iris Sx
Equator
Iris Dx
1
8
15
22
29
36
Board Number
1
4
7
10
13
16
Thermometer number
9.250
9.305
9.360
9.415
9.470
9.525
9.580
9.635
9.690
9.745
9.800

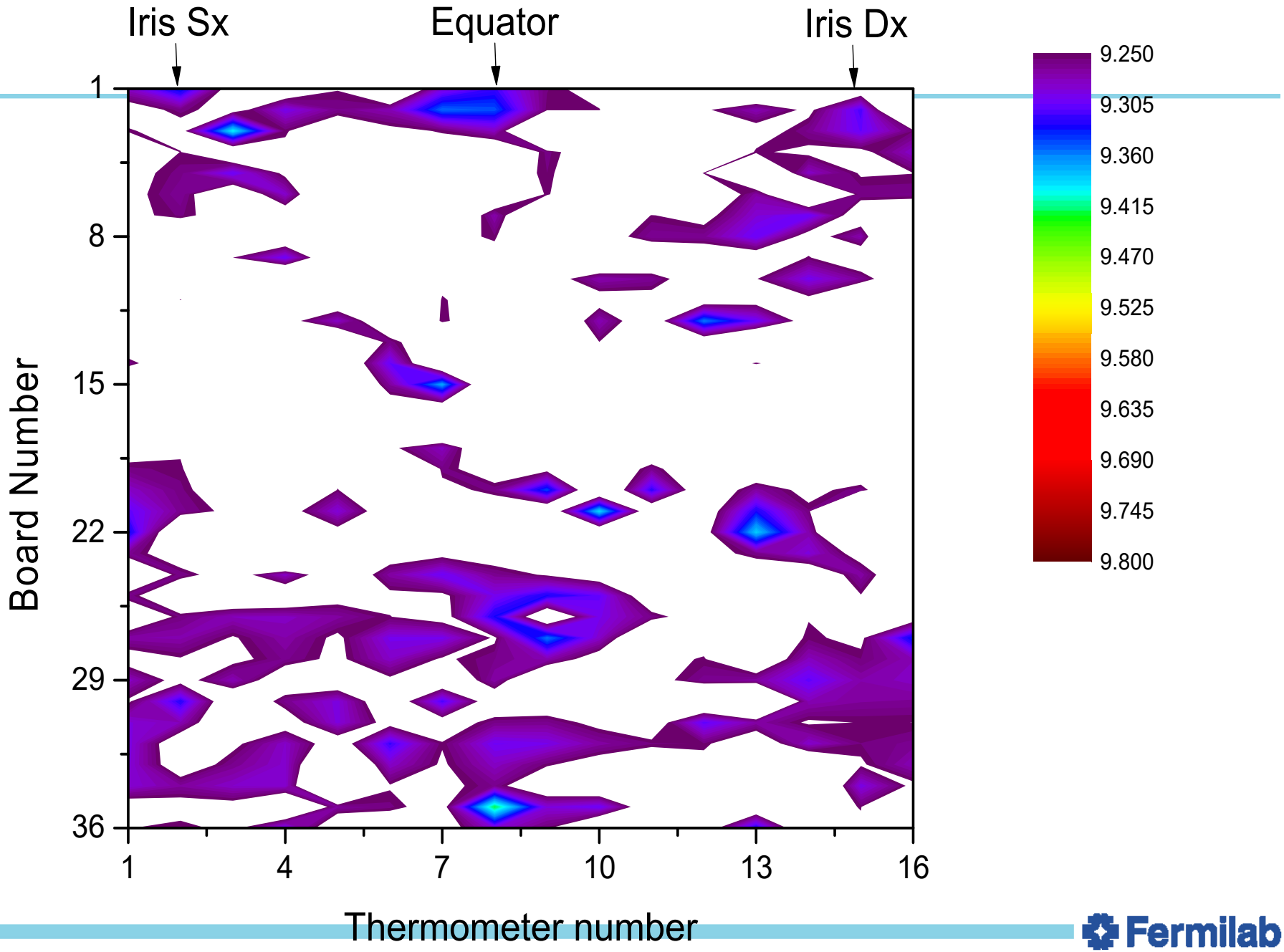
Iris Sx
Equator
Iris Dx
1
8
15
22
29
36
Board Number
1
4
7
10
13
16
Thermometer number
9.250
9.305
9.360
9.415
9.470
9.525
9.580
9.635
9.690
9.745
9.800

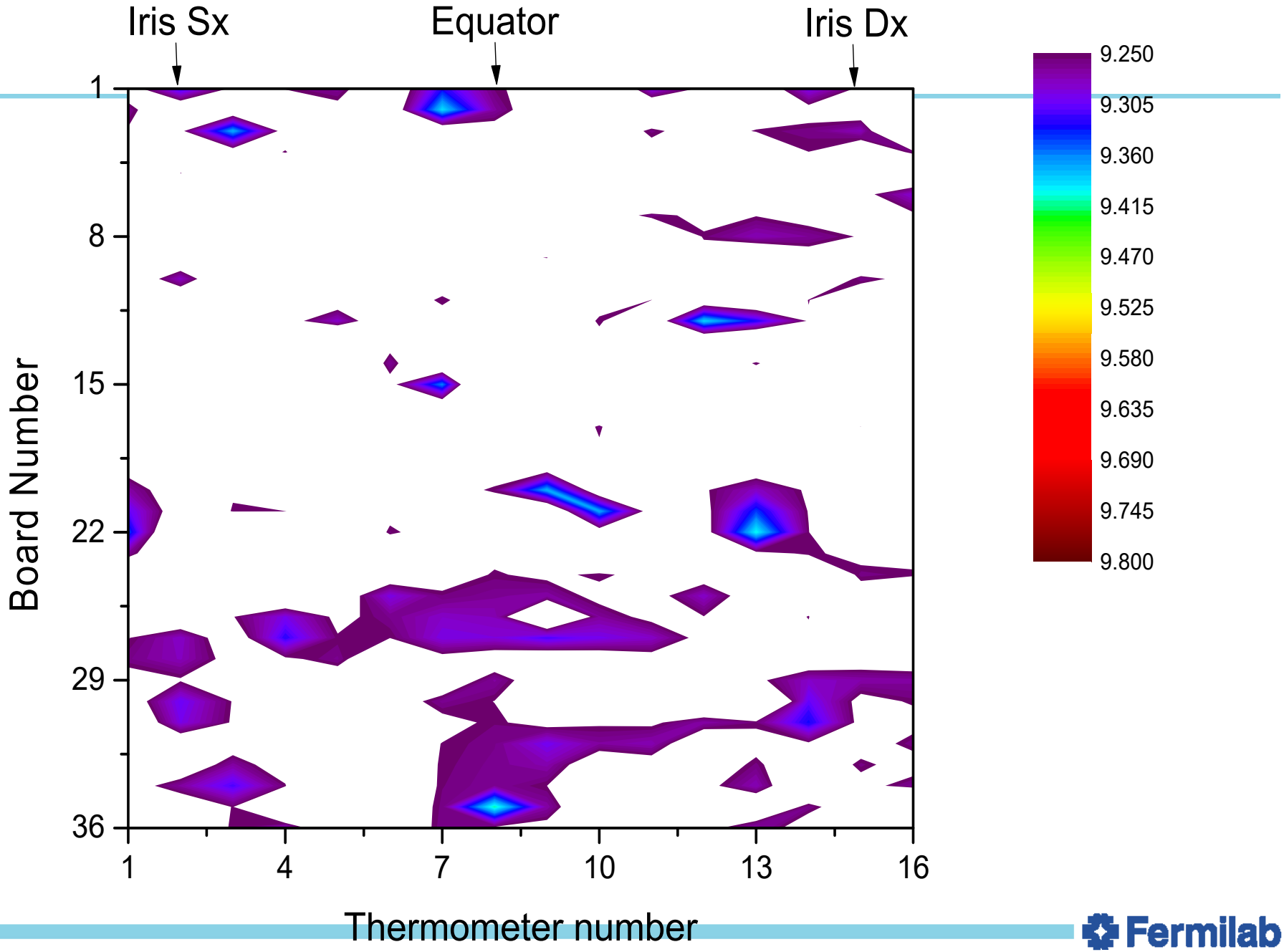
Iris Sx
Equator
Iris Dx
1
8
15
22
29
36
Board Number
1
4
7
10
13
16
Thermometer number
9.250
9.305
9.360
9.415
9.470
9.525
9.580
9.635
9.690
9.745
9.800

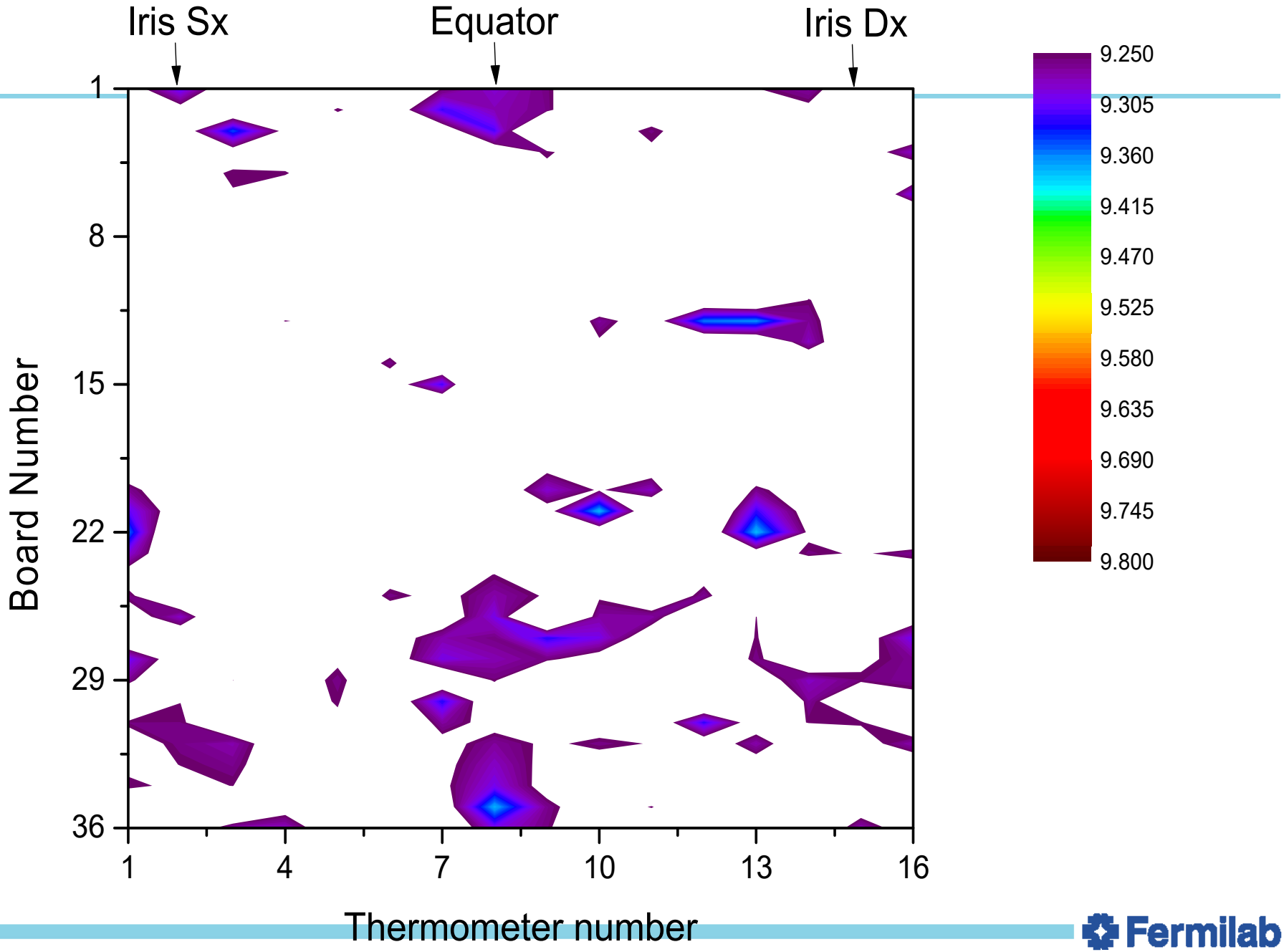
Iris Sx
Equator
Iris Dx
1
8
15
22
29
36
Board Number
1
4
7
10
13
16
Thermometer number
9.250
9.305
9.360
9.415
9.470
9.525
9.580
9.635
9.690
9.745
9.800

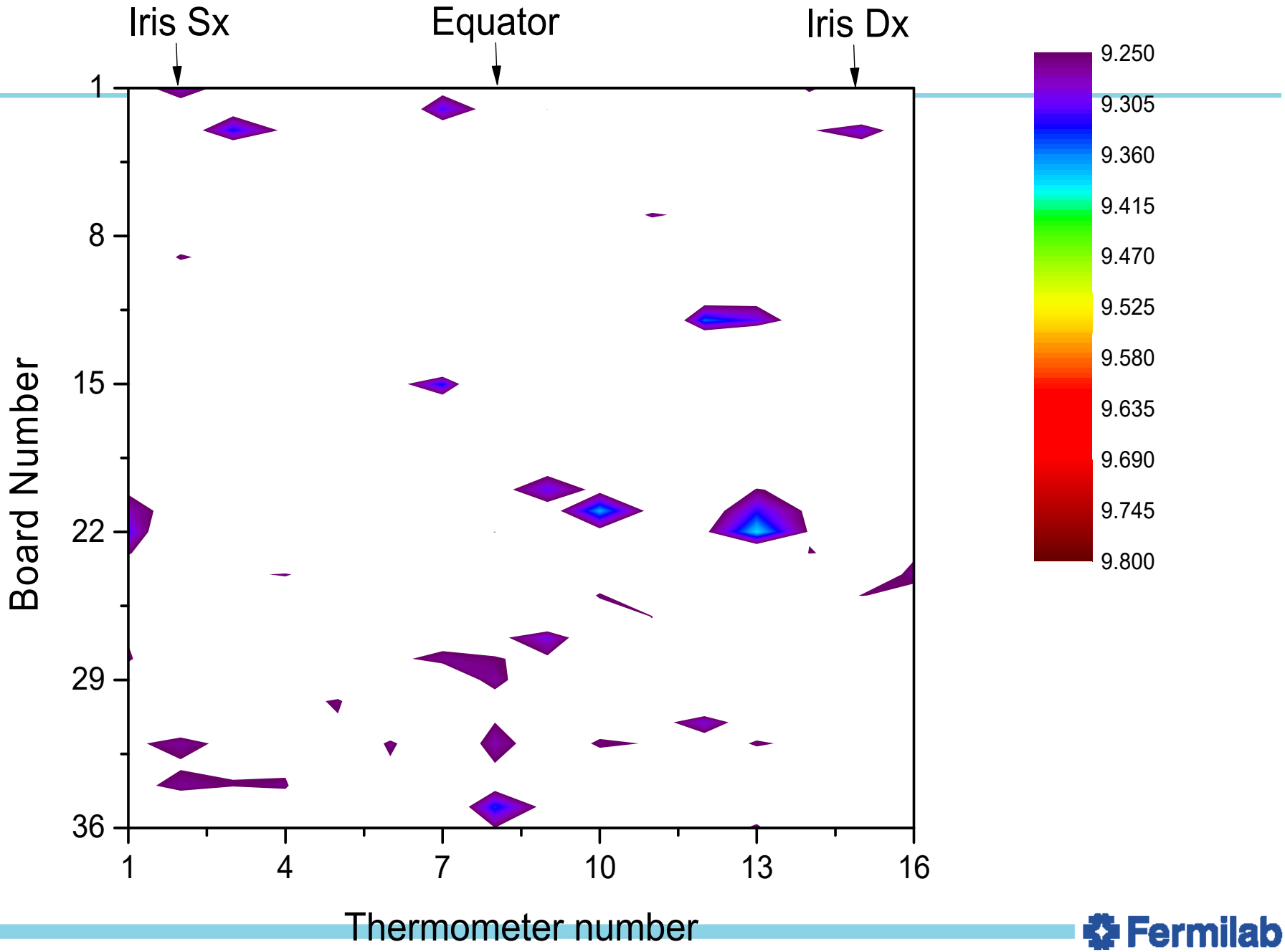
Iris Sx
Equator
Iris Dx
1
8
15
22
29
36
Board Number
1
4
7
10
13
16
Thermometer number
9.250
9.305
9.360
9.415
9.470
9.525
9.580
9.635
9.690
9.745
9.800

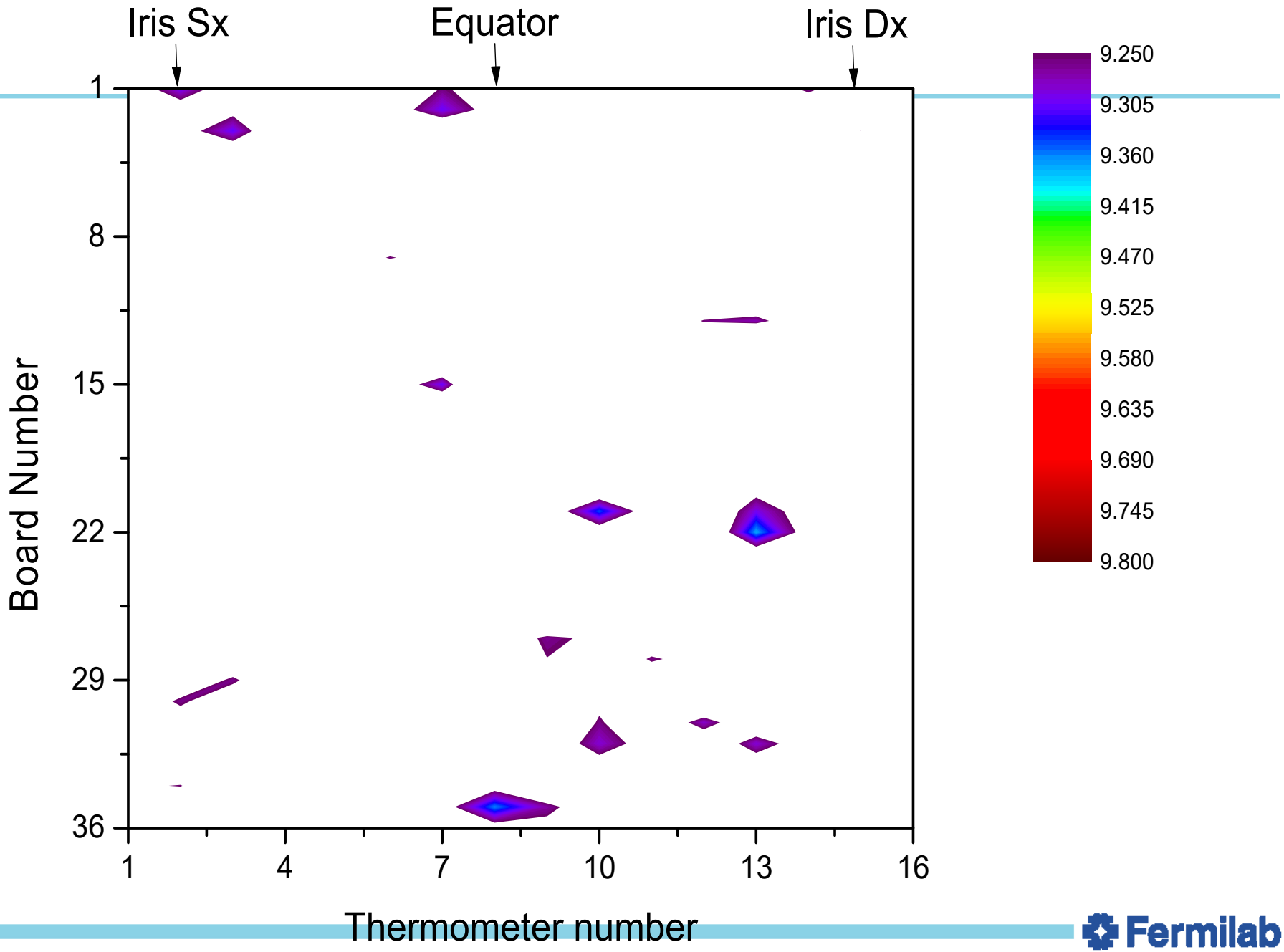
Iris Sx
Equator
Iris Dx
1
8
15
22
29
36
Board Number
1
4
7
10
13
16
Thermometer number
9.250
9.305
9.360
9.415
9.470
9.525
9.580
9.635
9.690
9.745
9.800

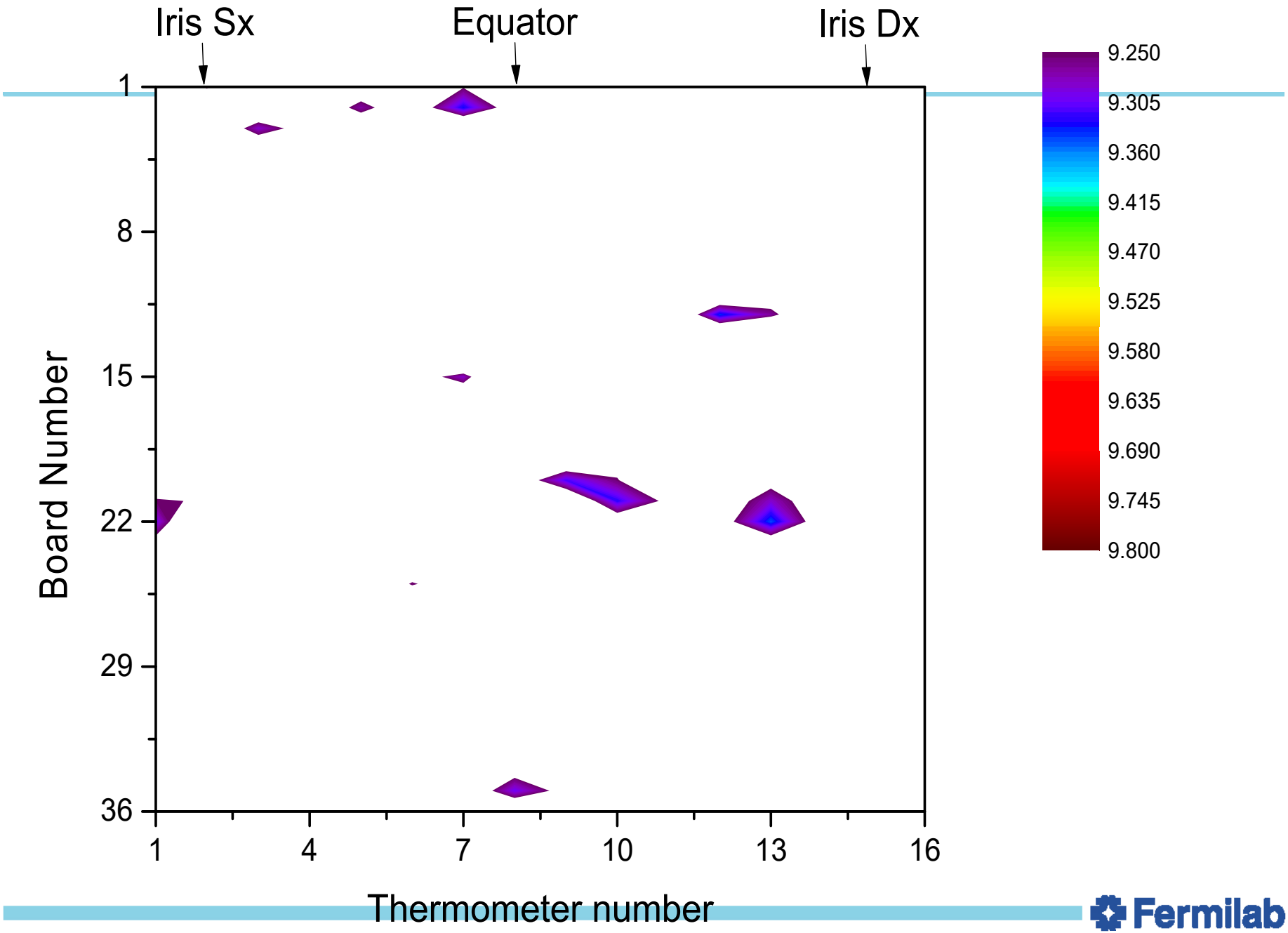
Iris Sx
Equator
Iris Dx
1
8
15
22
29
36
Board Number
1
4
7
10
13
16
Thermometer number
9.250
9.305
9.360
9.415
9.470
9.525
9.580
9.635
9.690
9.745
9.800

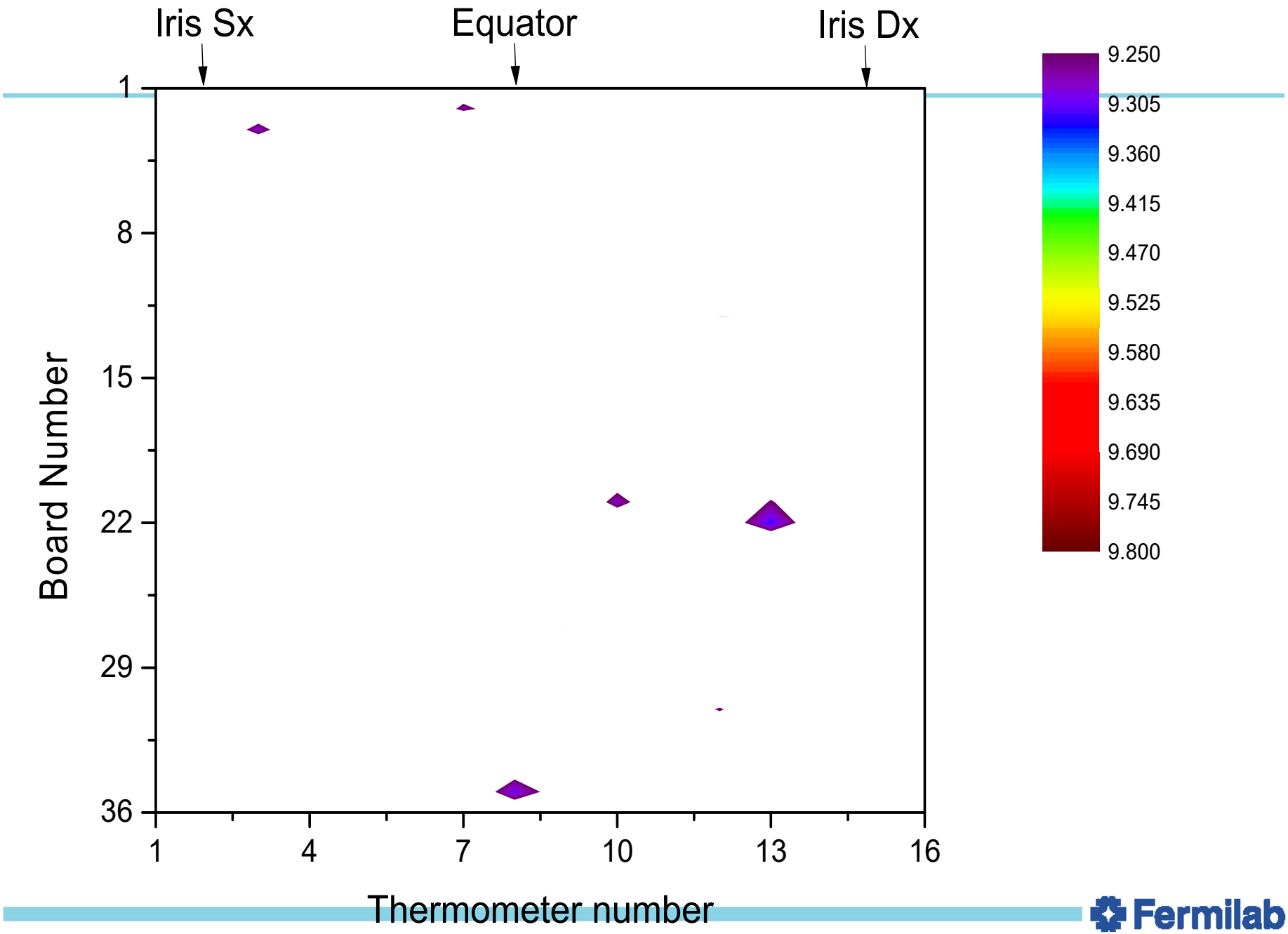
Iris Sx
Equator
Iris Dx
1
8
15
22
29
36
Board Number
1
4
7
10
13
16
Thermometer number
9.250
9.305
9.360
9.415
9.470
9.525
9.580
9.635
9.690
9.745
9.800

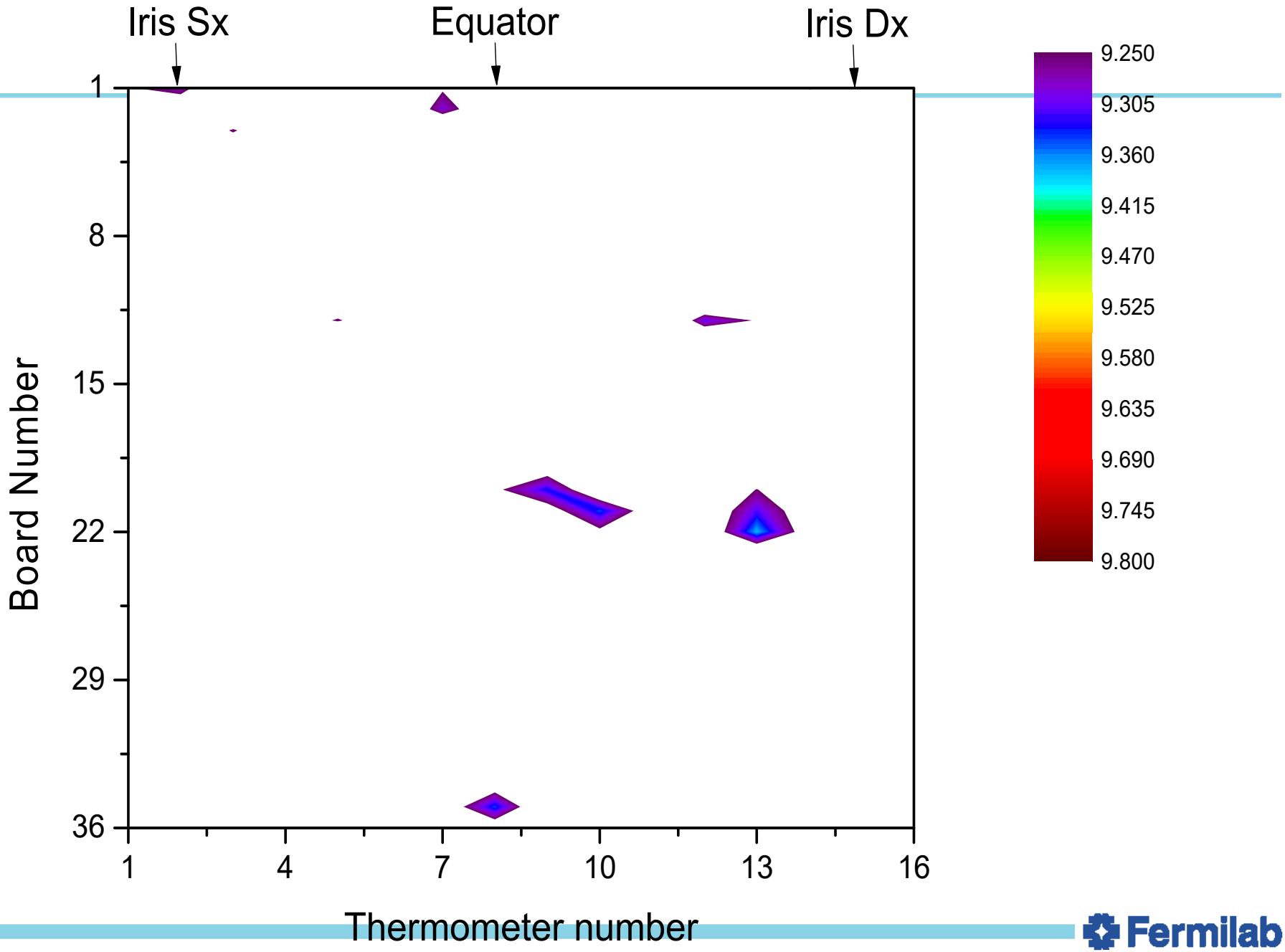
Iris Sx
Equator
Iris Dx
1
8
15
22
29
36
Board Number
1
4
7
10
13
16
Thermometer number
9.250
9.305
9.360
9.415
9.470
9.525
9.580
9.635
9.690
9.745
9.800

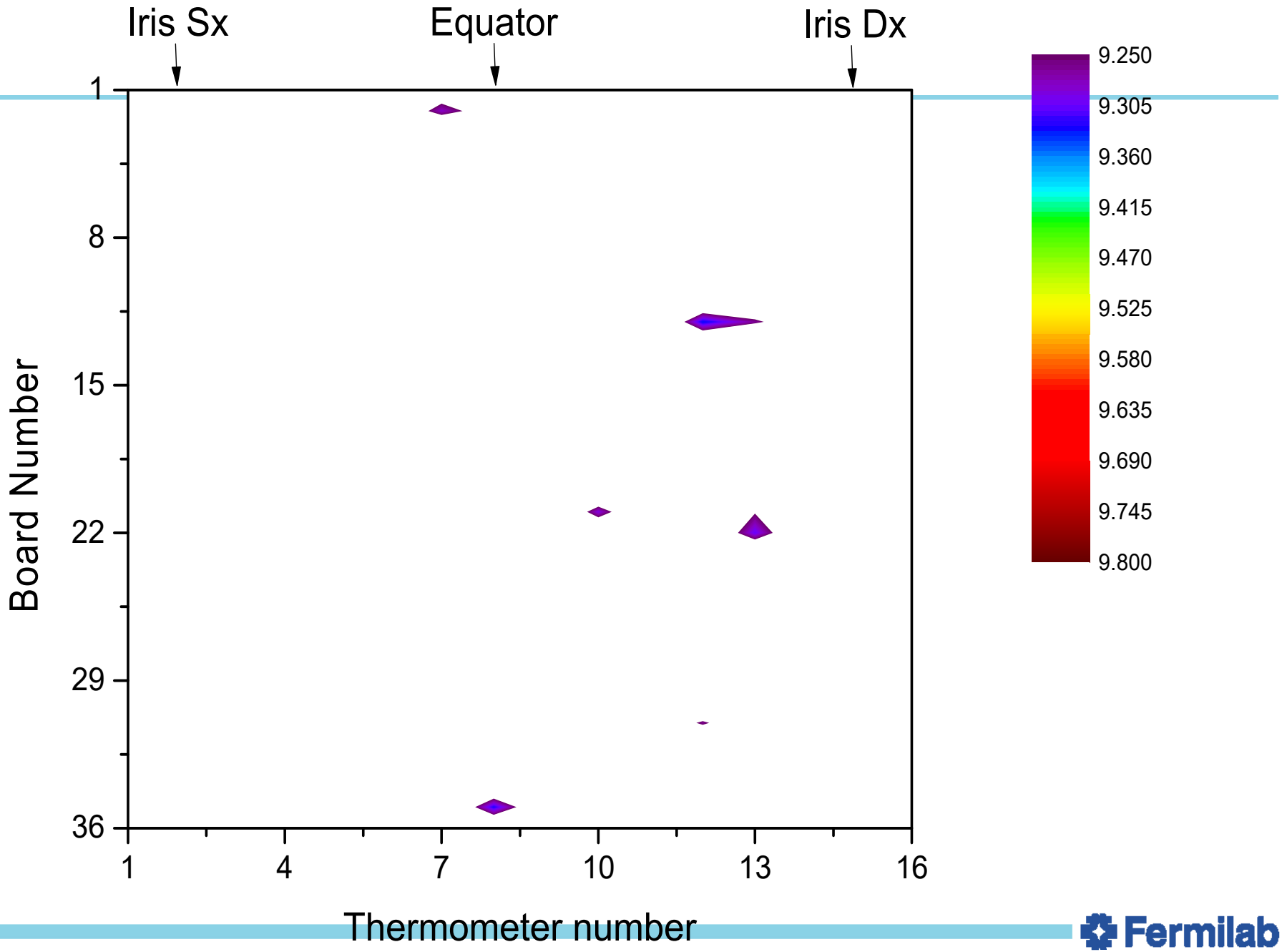
Iris Sx
Equator
Iris Dx
1
8
15
22
29
36
Board Number
1
4
7
10
13
16
Thermometer number
9.250
9.305
9.360
9.415
9.470
9.525
9.580
9.635
9.690
9.745
9.800

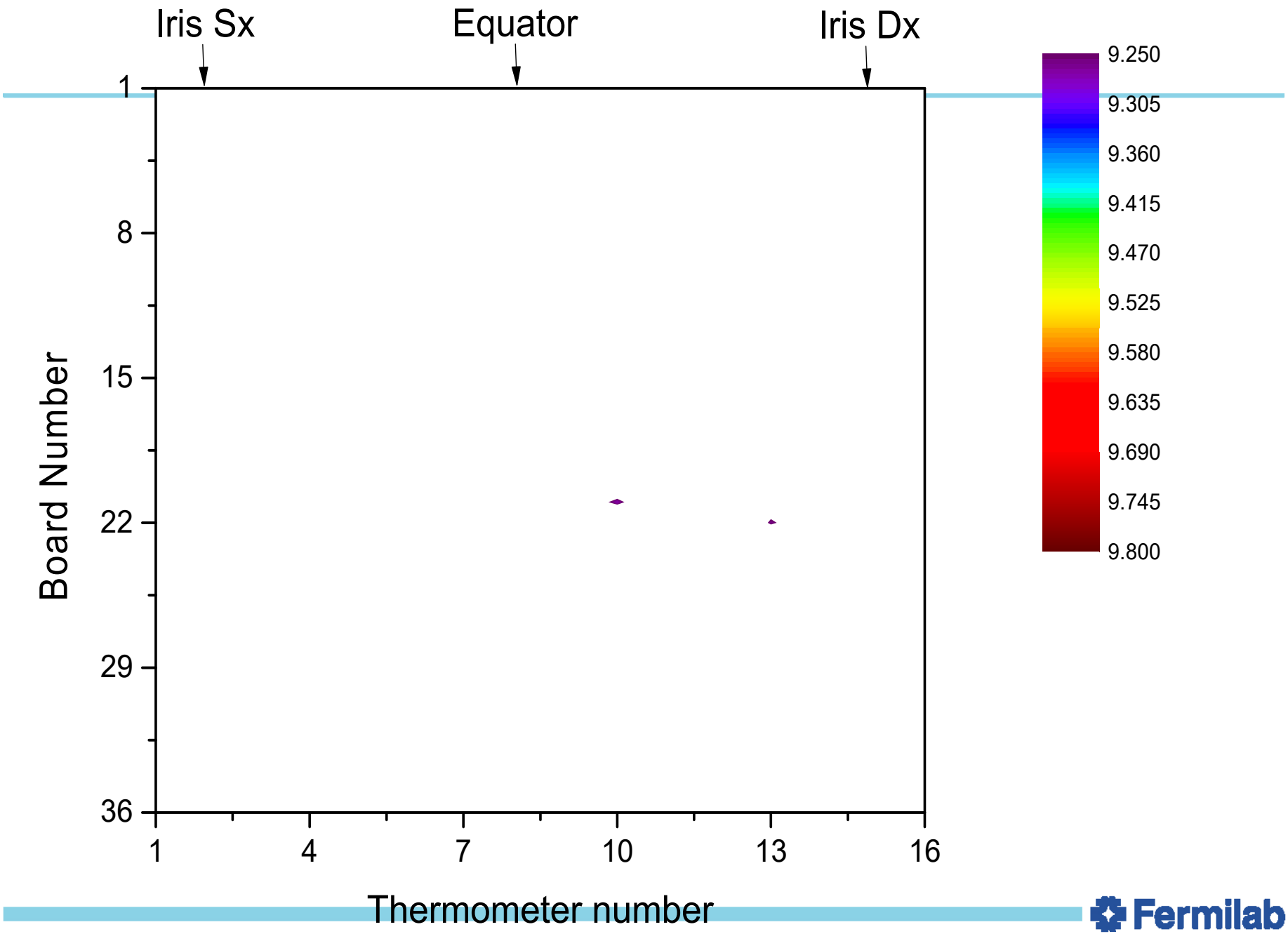
Iris Sx
Equator
Iris Dx
1
8
15
22
29
36
Board Number
1
4
7
10
13
16
Thermometer number
9.250
9.305
9.360
9.415
9.470
9.525
9.580
9.635
9.690
9.745
9.800

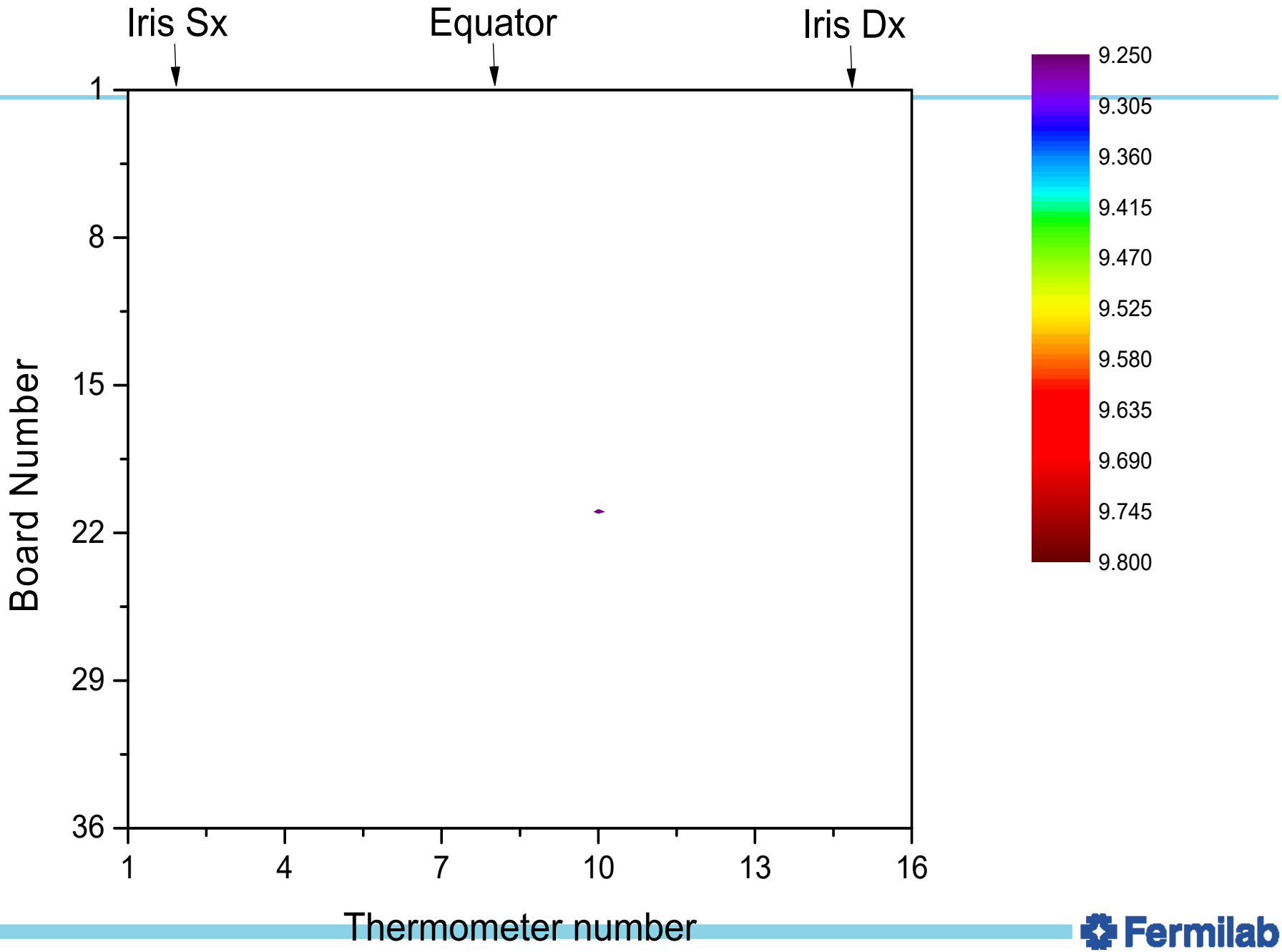
Iris Sx
Equator
Iris Dx
1
8
15
22
29
36
Board Number
1
4
7
10
13
16
Thermometer number
9.250
9.305
9.360
9.415
9.470
9.525
9.580
9.635
9.690
9.745
9.800

# Utilizing new physics for record high Qs

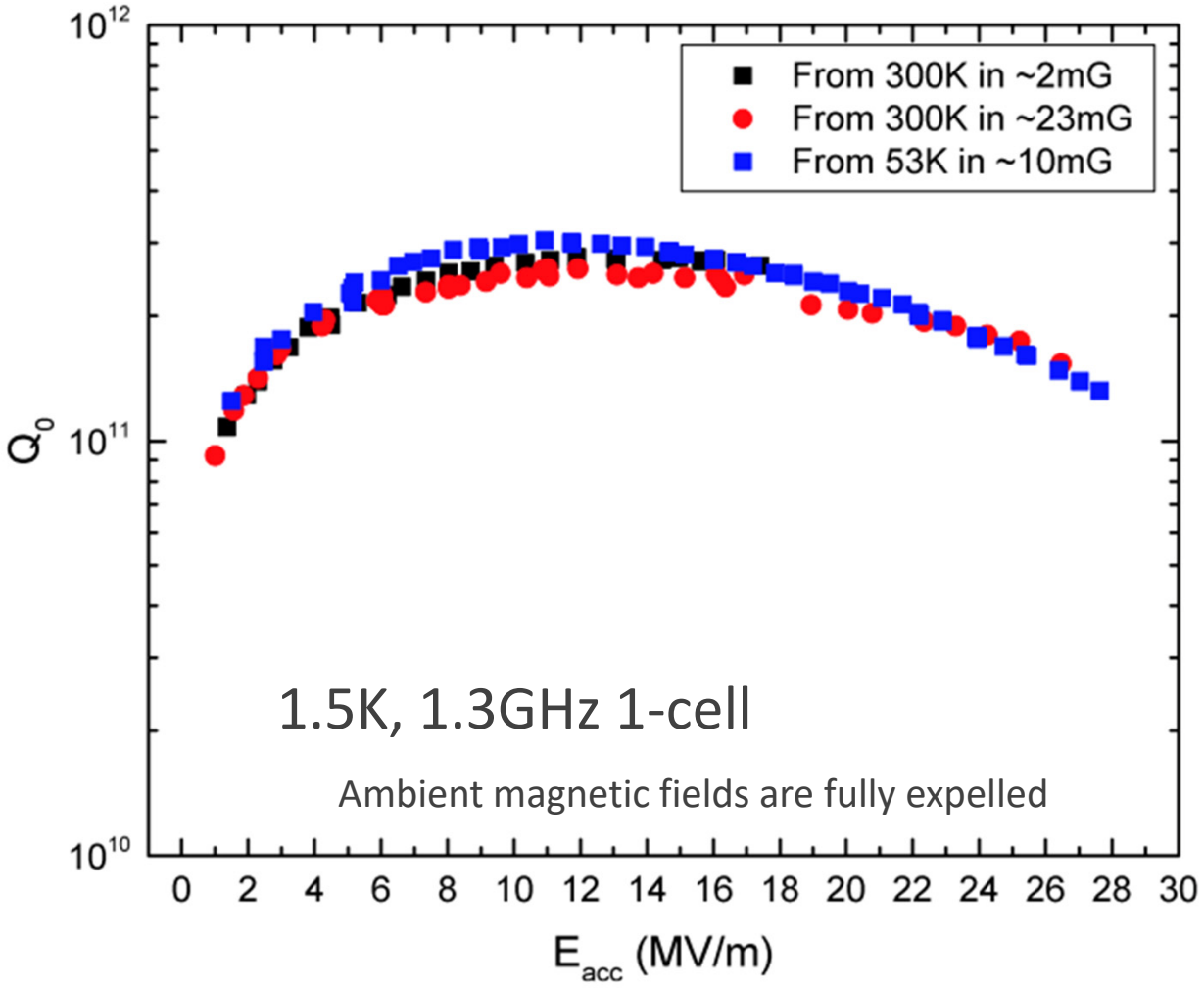


Combination of nitrogen doping and efficient flux expulsion => Record high Q >1e11 up to 28 MV/m in SRF cavities

A. Romanenko, A. Grassellino, A. C. Crawford, D. A. Sergatskov, and O. Melnychuk, Appl. Phys. Lett. **105**, 234103 (2014)

# Dependence on material, and flux sensitivity

- Substantial progress in doping refinement and magnetic field management:
  - Flux trapping/detrapping
  - sensitivity to mag field optimization
  - magnetic shielding improvement/new ideas
- Crucial to retain performance in accelerator

S. Posen et al, Journal of Applied Physics **119**, 213903 (2016)

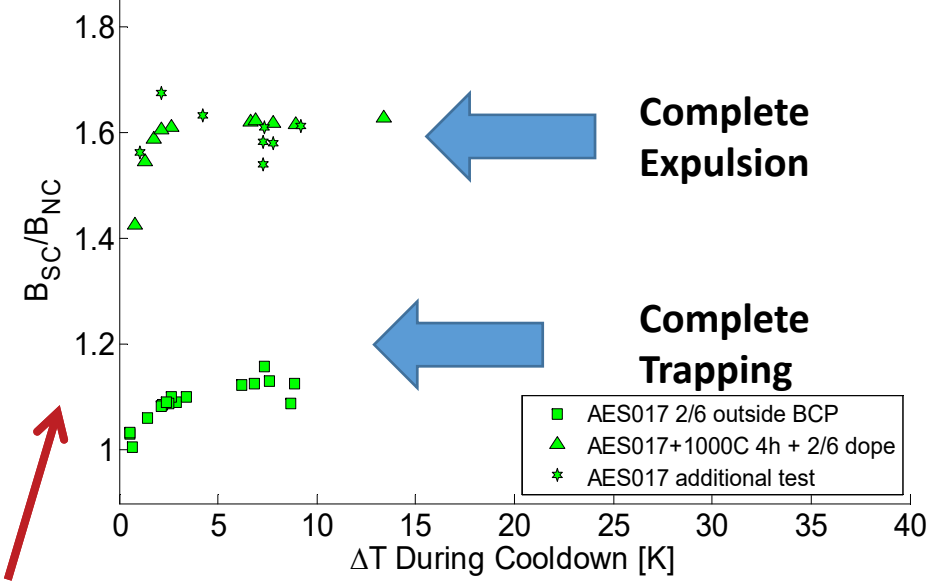


M. Martinello et al, Appl. Phys. Lett. **109**, 062601 (2016)

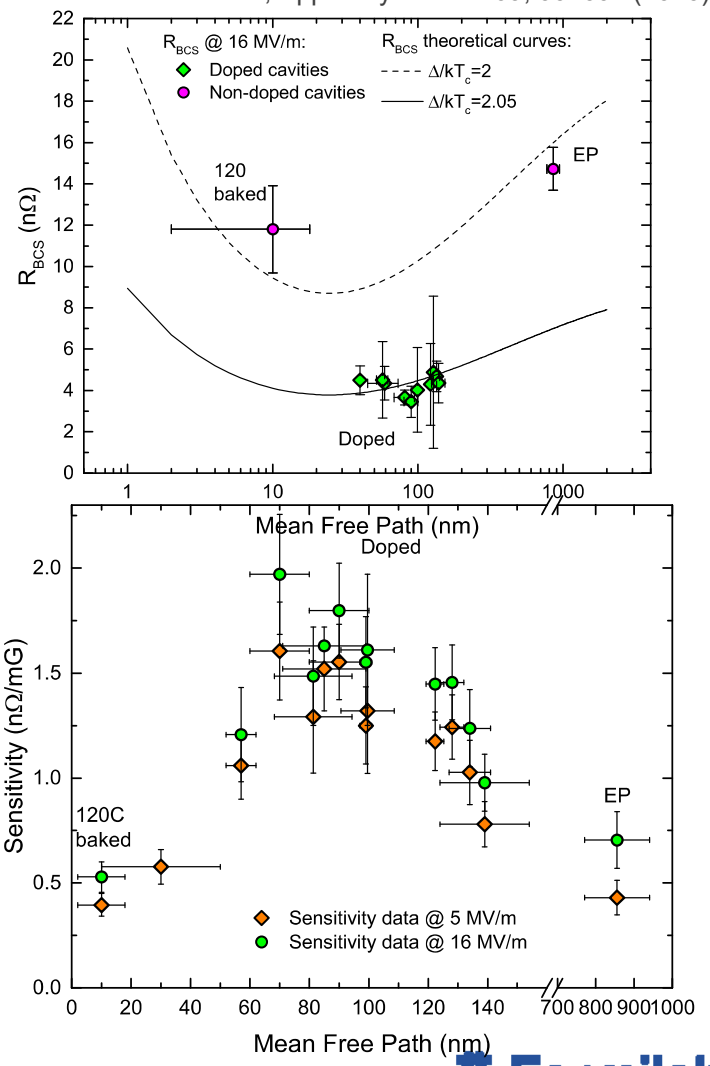


These new findings guided a crucial modification of the baseline processing for LCLS-2

# Understanding trapped flux losses

- In the *pinning regime* vortices are constrained by the pinning centers
- In the *flux-flow regime* the vortex oscillation is counteracted by the material viscosity

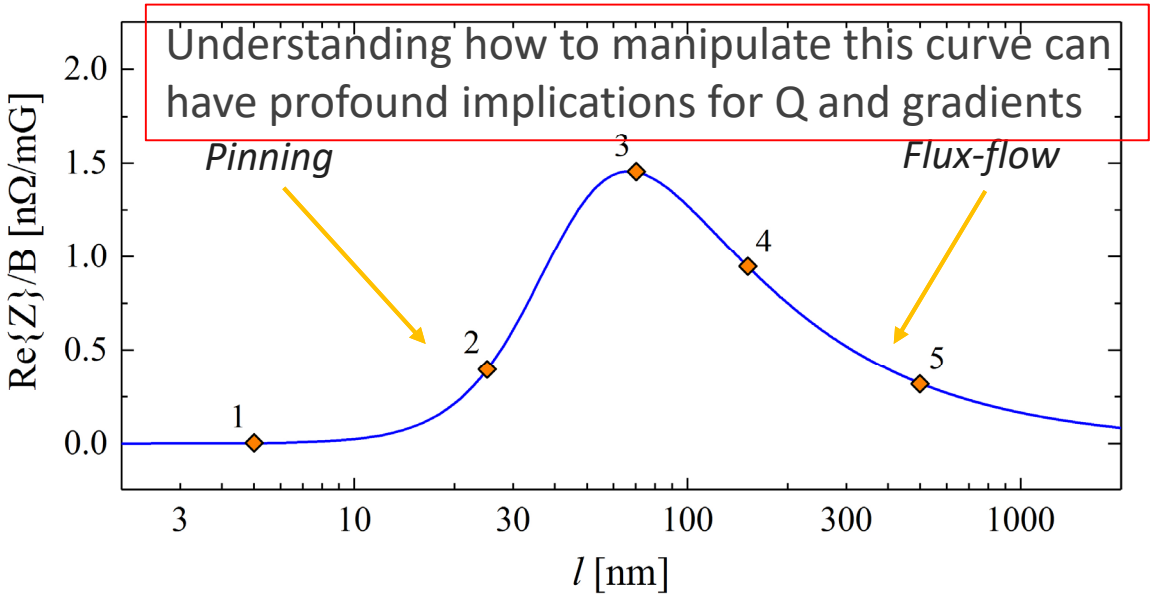


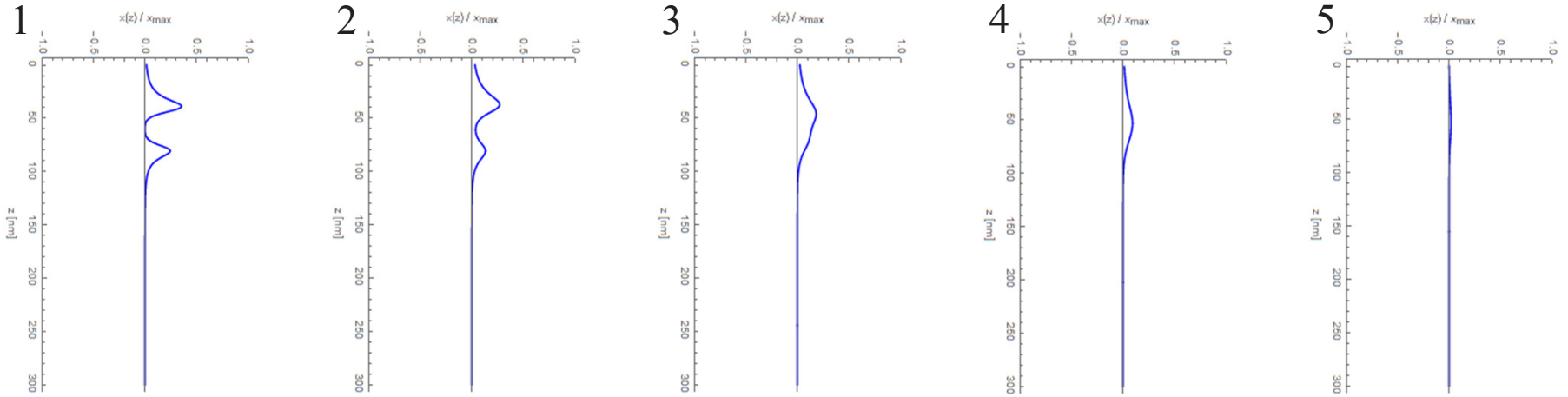


M. Checchin *et al.*, Supercond. Sci. Technol. **30**, 034003 (2017)

# Quickly Apparent Trend With Batches of AES Cavities

S. Posen et al, Journal of Applied Physics **119**, 213903 (2016)

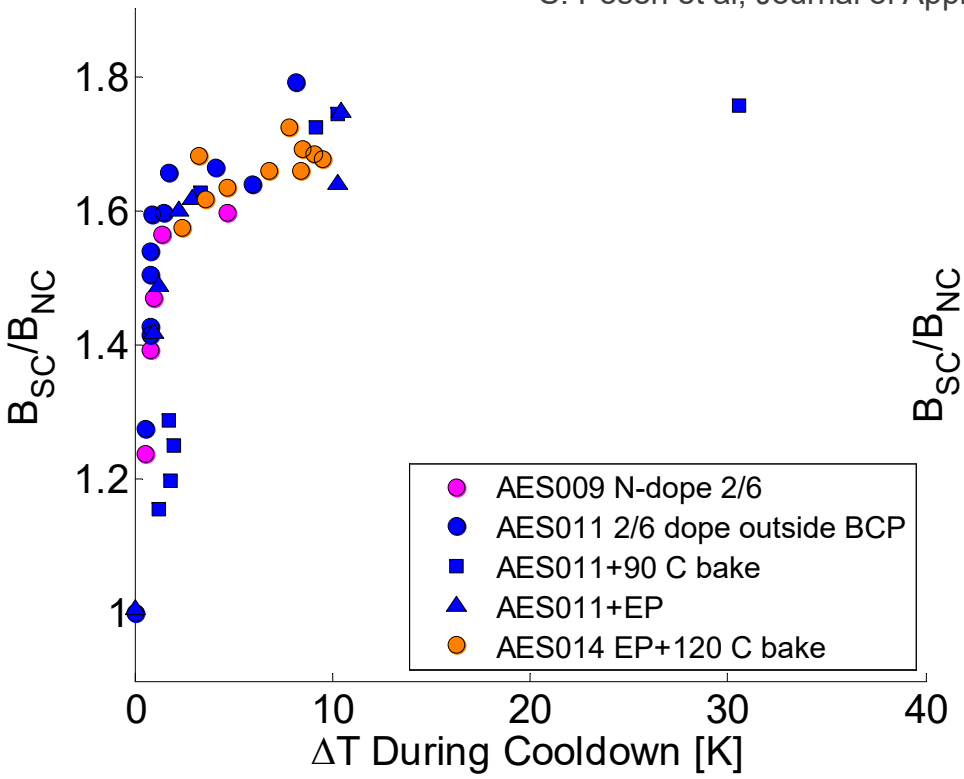


AES Single Cells Batch 1

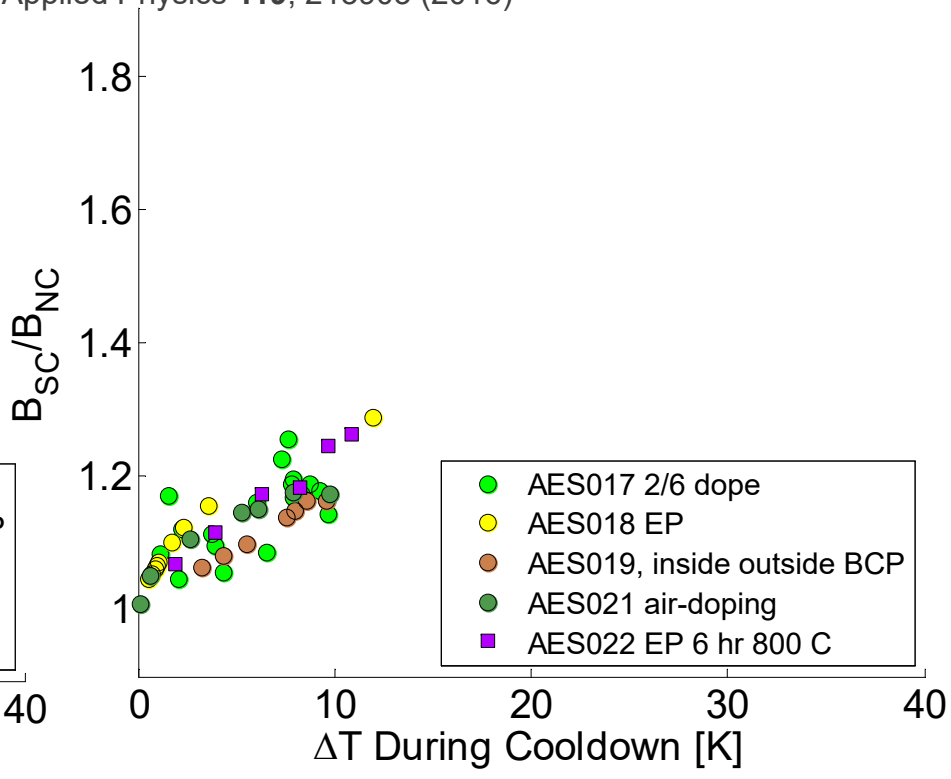


AES Single Cells Batch 2

# Conversion to From Poor to Strong Expulsion

arxiv.org/pdf/1509.03957

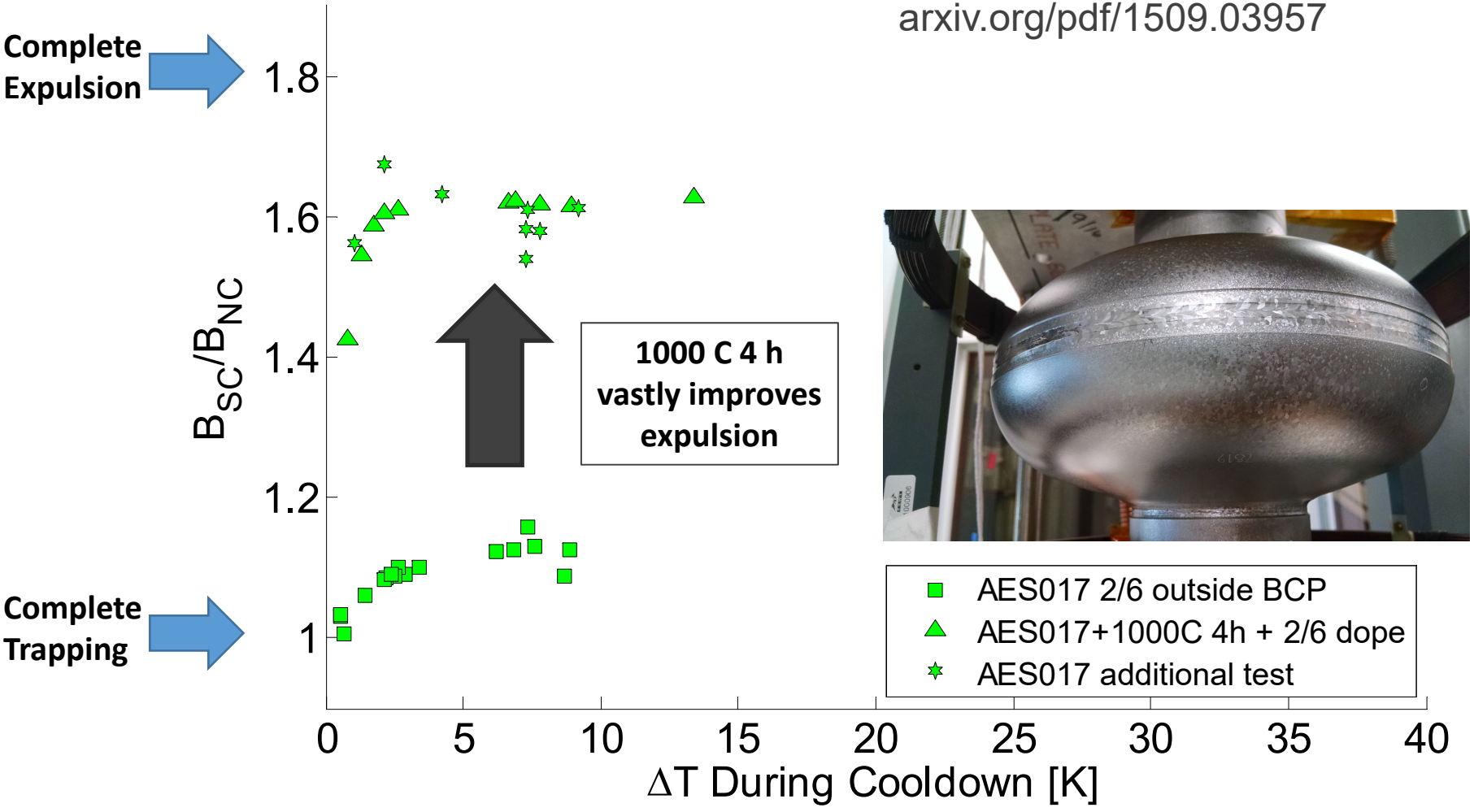

# Effect on Q vs E

AES017 cooled in 10 mG

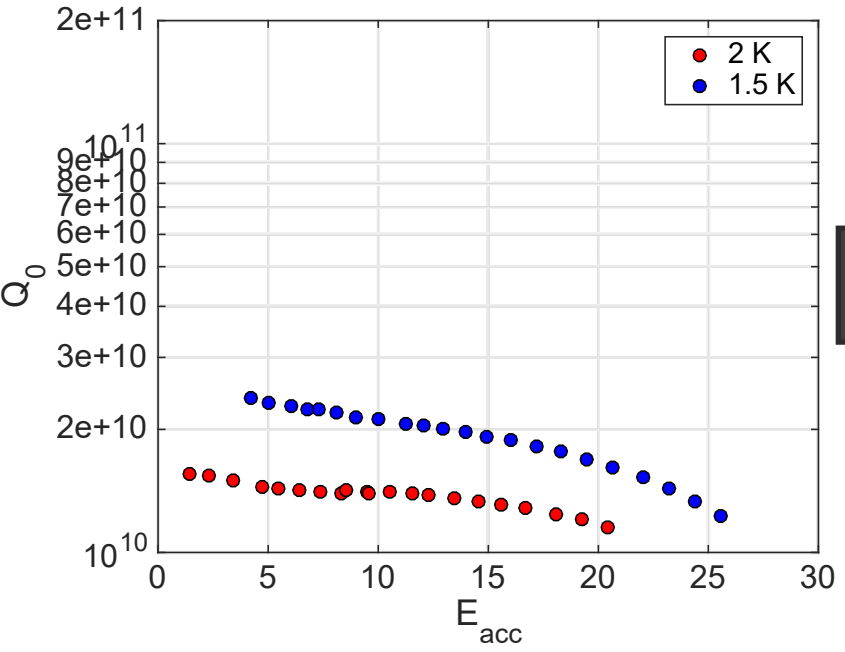


1000 C Bake

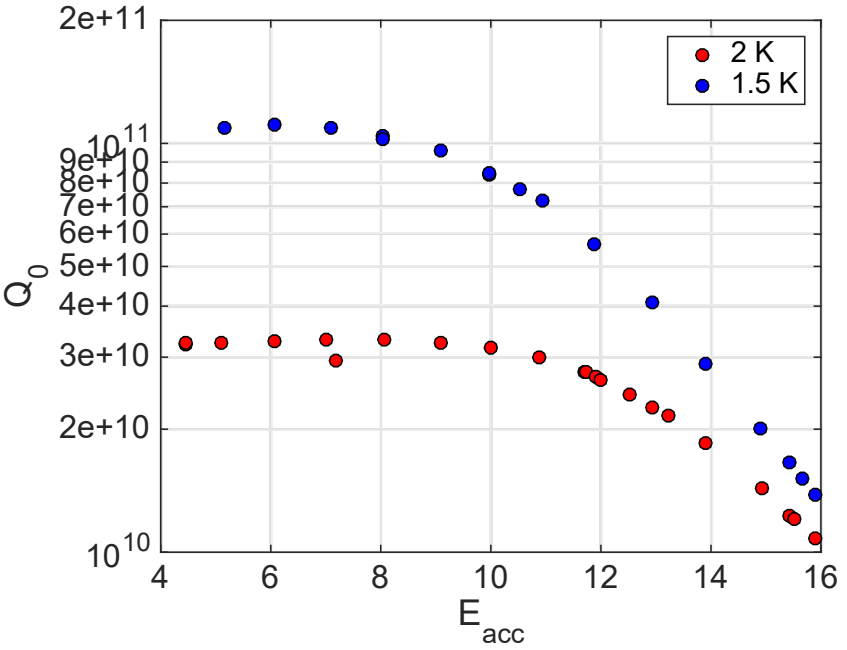


Poor expulsion: $B_{SC}/B_{NC}$ ~ 1.1

Good expulsion: $B_{SC}/B_{NC}$ ~ 1.6

# Surface Alteration With No Significant Effect on Expulsion

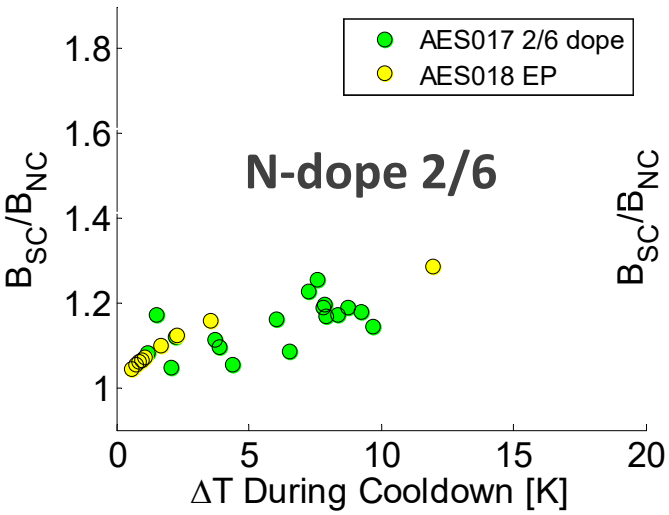


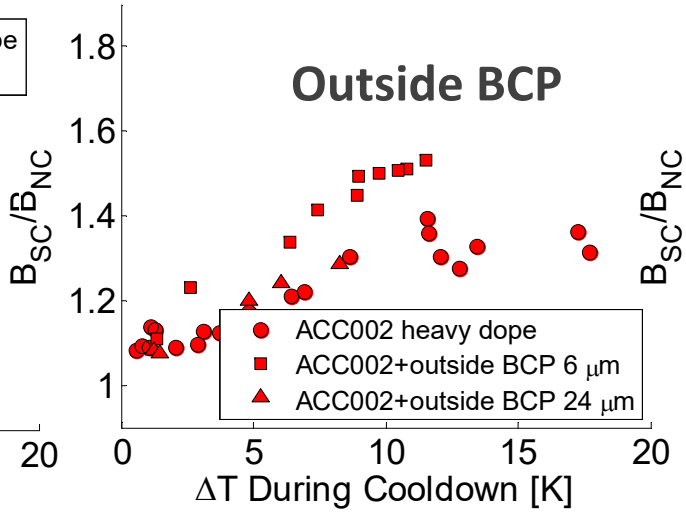


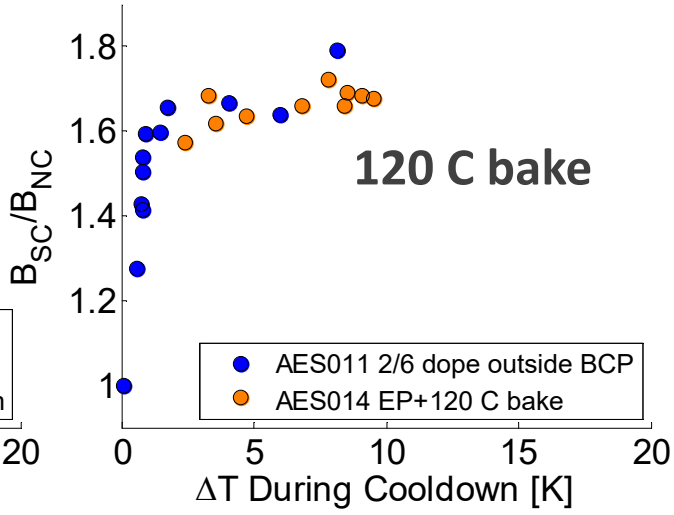


Different surface conditions in cavities with similar bulk history: similar expulsion

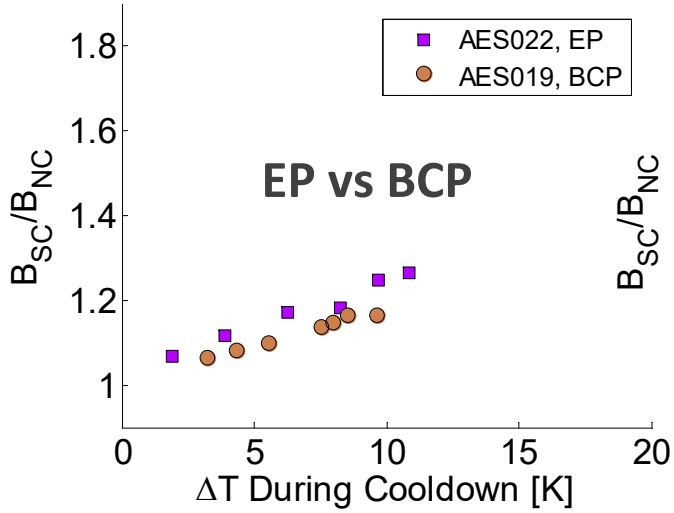


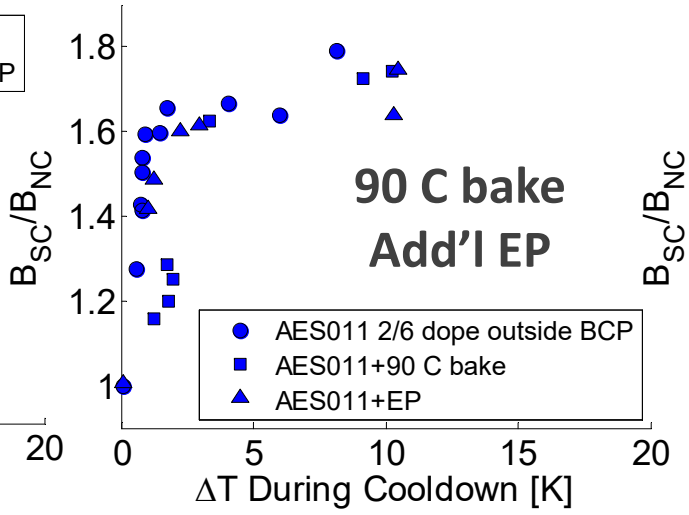


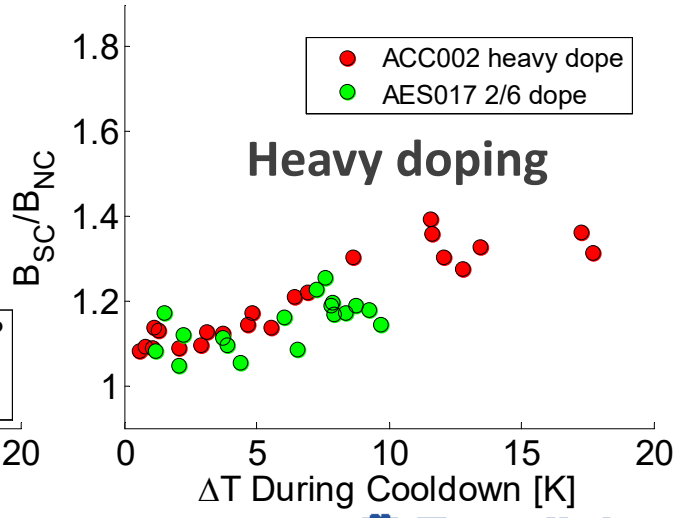

# Fermilab Prototype LCLS-II Cryomodule

| Cavity | Usable Gradient* [MV/m] | Q0 @16MV/m* 2K Fast Cool Down |
|---|---|---|
| TB9AES021 | 18.2 | 2.6E+10 |
| TB9AES019 | 18.8 | 3.1E+10 |
| TB9AES026 | 19.8 | 3.6E+10 |
| TB9AES024 | 20.5 | 3.1E+10 |
| TB9AES028 | 14.2 | 2.6E+10 |
| TB9AES016 | 16.9 | 3.3E+10 |
| TB9AES022 | 19.4 | 3.3E+10 |
| TB9AES027 | 17.5 | 2.3E+10 |
| **Average** | **18.2** | **3.0E+10** |
| **Total Voltage** | **148.1 MV** | |

Spec: 133 MV

Spec: $2.7 \times 10^{10}$

World record cryomodule with twice efficiency than state of the art

# The Gradient Frontier

# Extending High Q to high gradients: motivation behind experiments

- Composition and mean free path in first nanometers of cavity surface have been shown to be crucial for both Q and gradient performance
- **N Doping** at T> 800C proven to manipulate mean free path, but constantly throughout several microns, **giving high Q**
- **120C bake** known to manipulate mean free path at very near surface on clean bulk, and **produce the highest gradients**

A. Romanenko et al, Appl. Phys. Lett. **102**, 232601 (2013)

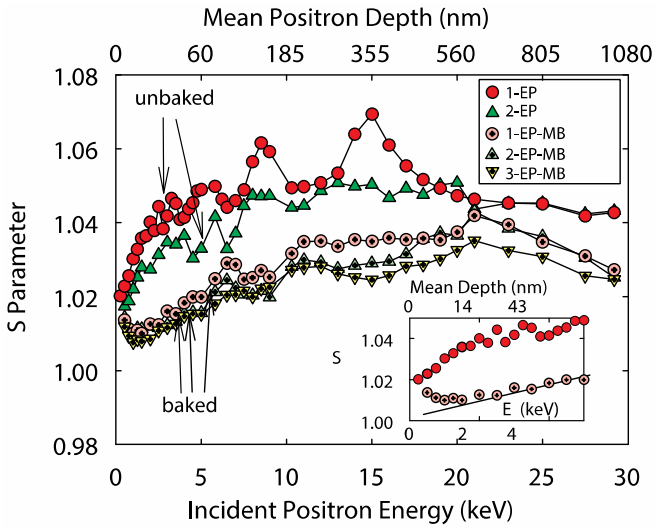


A. Grassellino et al, Proceedings of SRF 2015

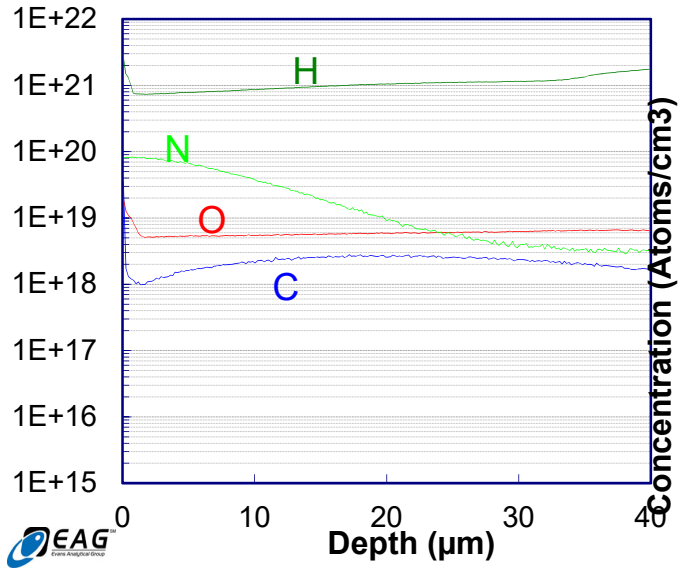


**120C bake, vacancies in first ~ 60 nanometers N doping, nitrogen throughout several micro**

# Motivation behind experiments

- Therefore, we decided to study how to better **“engineer”** a dirty layer on top a clean bulk, using low T nitrogen treatments → aim to **create few to several nanometers of nitrogen enriched layer** on top of clean EP bulk, to attempt to bring together the benefit of the Q and gradient

- Nitrogen enriched nanometric layer to be created in the furnace post 800C treatment – when no oxide is present at the moment of injection of nitrogen at low T

# New breakthrough at FNAL: N infusion (dirty SC on clean SC) produces very high Q at very high gradient

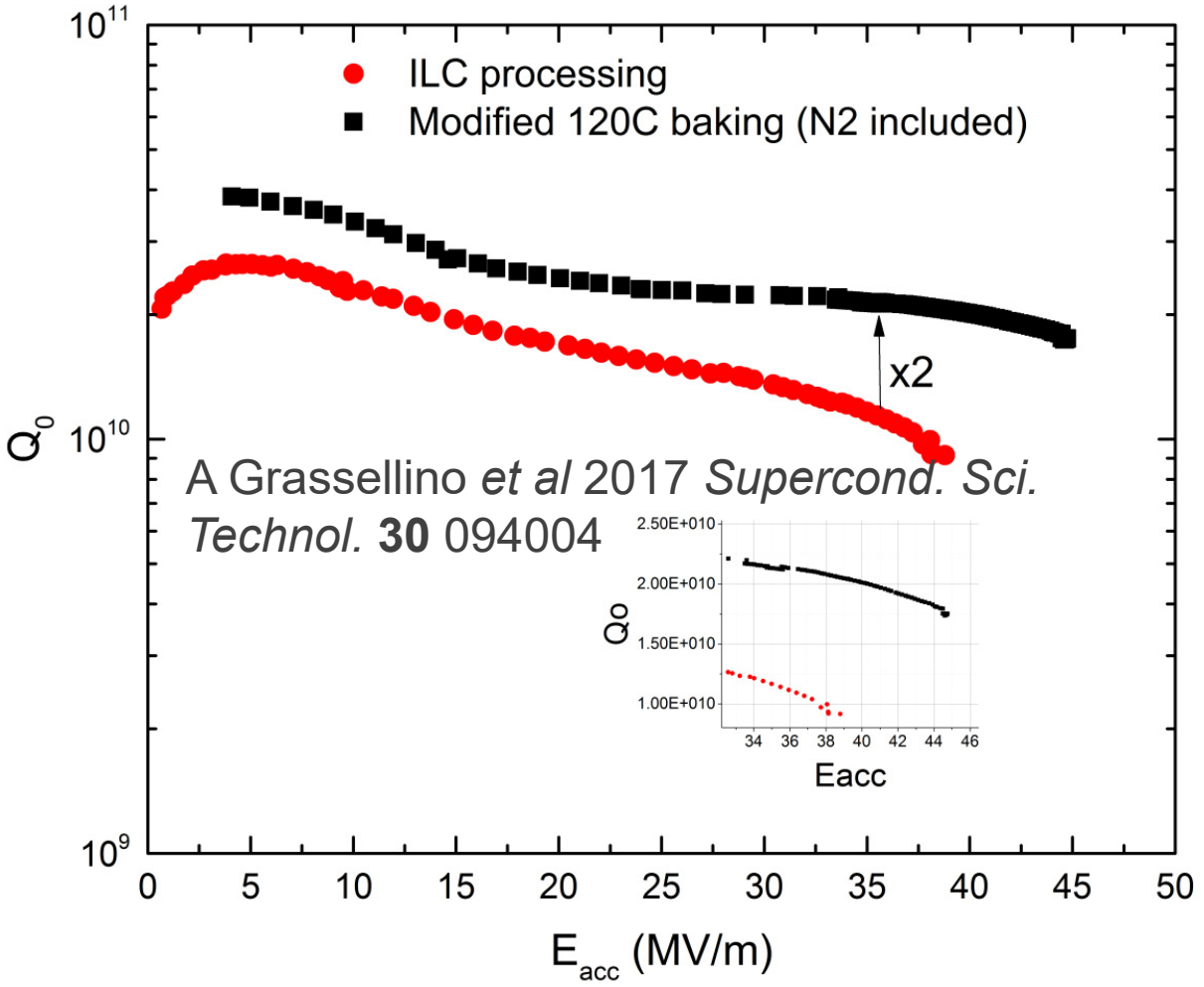


- Same cavity, sequentially processed, no EP in between
- Achieved: 45.6 MV/m → 194 mT With Q ~ 2e10!
- Q at ~ 35 MV/m ~ 2.3e10
- First nine cell results confirm the findings
- Working on applying to higher frequencies

**Increase in Q factor of two, increase in gradient ~20%**



*Slide from A. Grassellino*

# ILC cost reduction global effort: FNAL, Jlab, Cornell, KEK, DESY

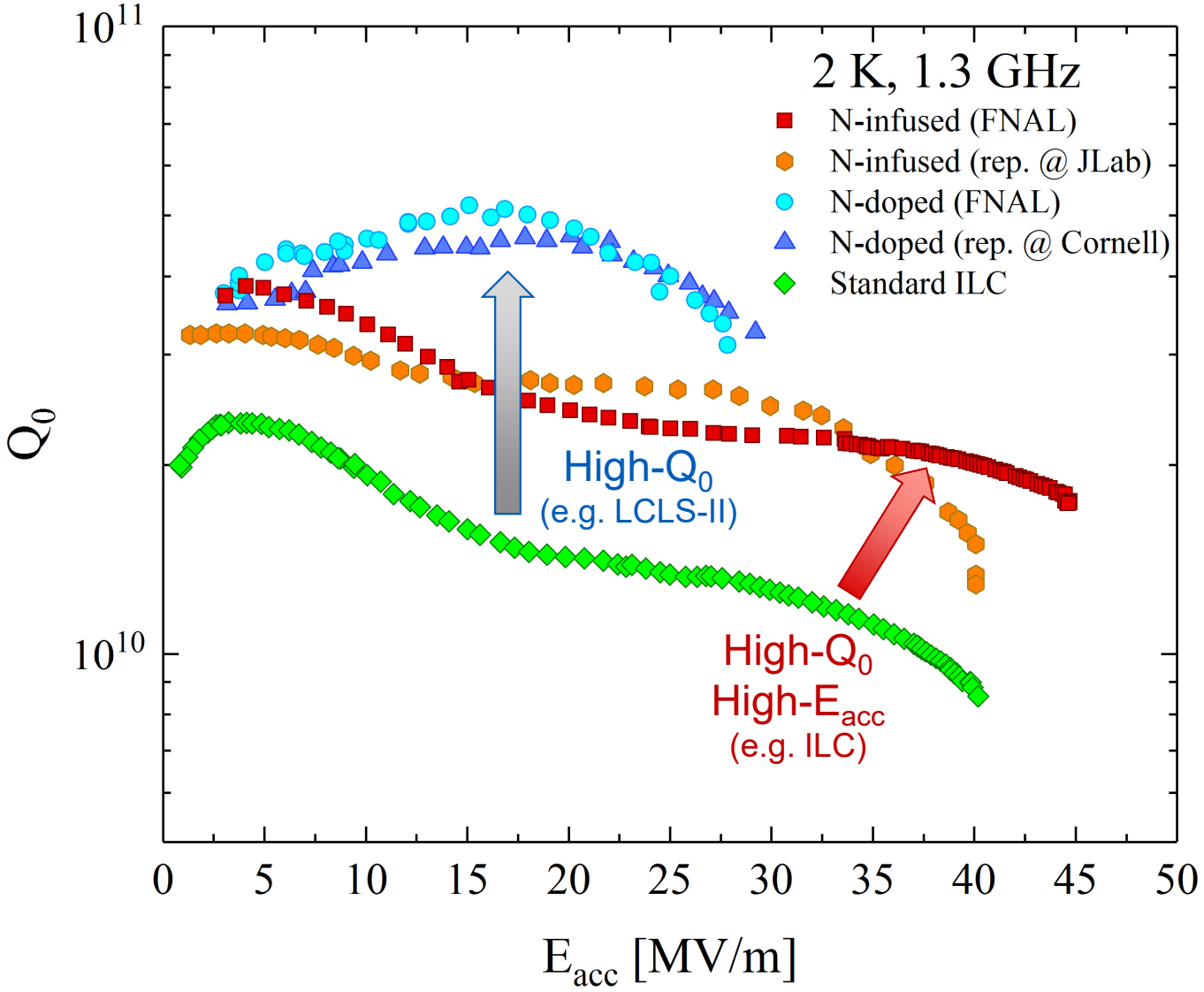


ILC Cost Reduction R&D global effort will explore doping parameter space to extend high Q at the highest gradients

# Intuitive picture of trick to delay flux penetration - layering



The vortex is pushed by the S-S boundary to the direction of the material with a larger λ.

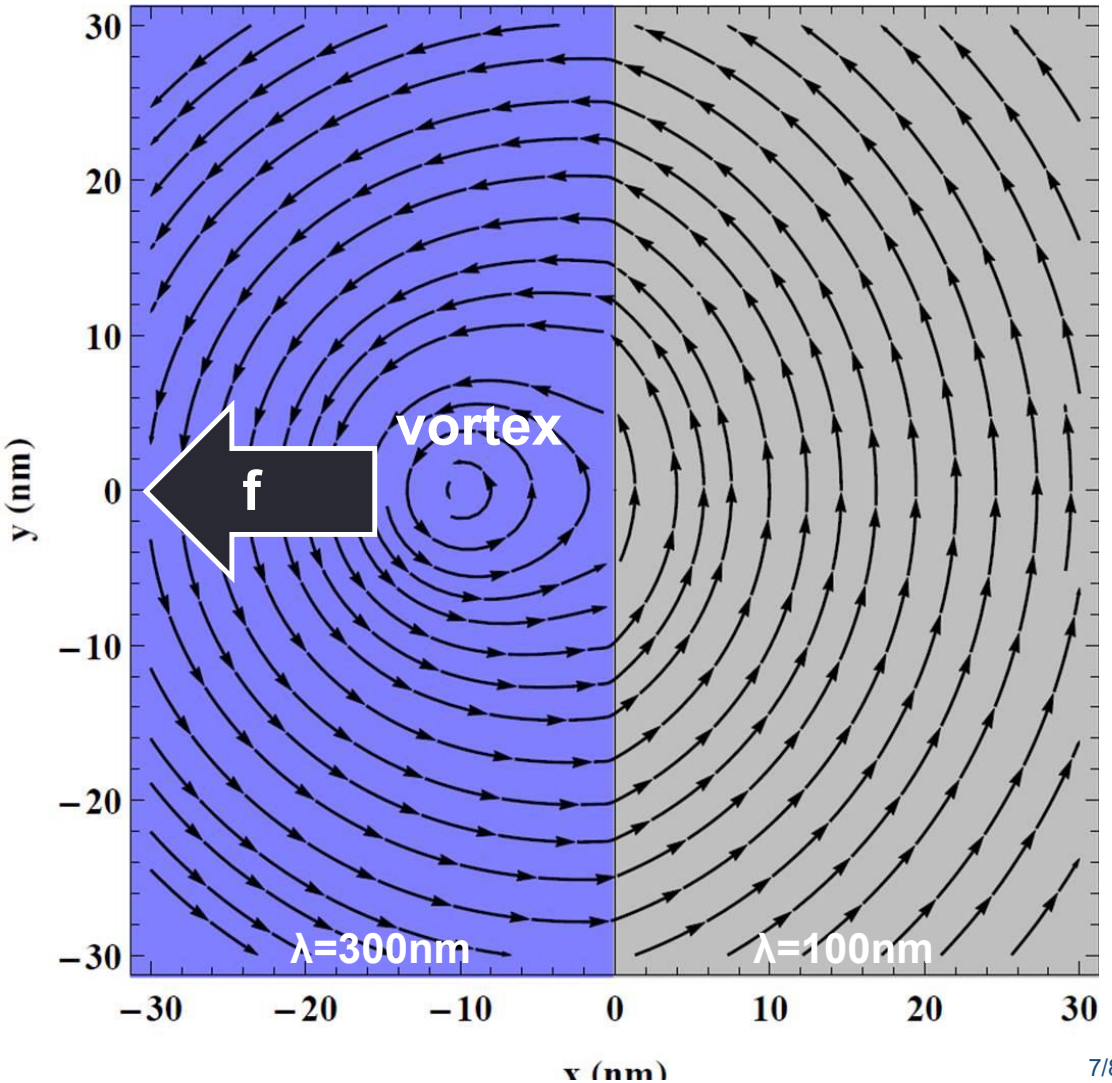


T.Kubo, in proceedings of LINAC14, Geneva, Switzerland (2014), p. 1026, THPP074

G. S. Mkrtchyan, F. R. Shakirzyanova, E. A. Shapoval, and V. V. Shmidt, Zh. Eksp. Theor. Fiz. **63**, 667 (1972).

# Intuitive picture of trick to delay flux penetration - layering



In addition to the BL barrier, we have the second barrier due to the S-S boundary. The second barrier is also imperfect: easily weakened by defects. However, we have a second chance to stop the vortex penetration.

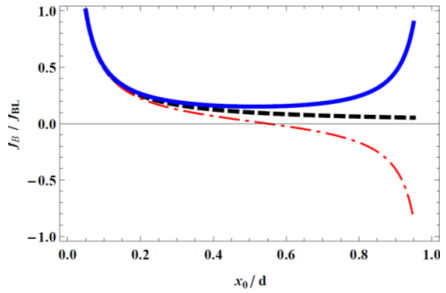


**The S-S bilayer structure**

# Superconductor-Superconductor (Dirty Layer) Potential

- High $\kappa$ film: analytical from London eqs.
  T. Kubo, *Supercond. Sci. Technol.* **30,** 023001 (2017)

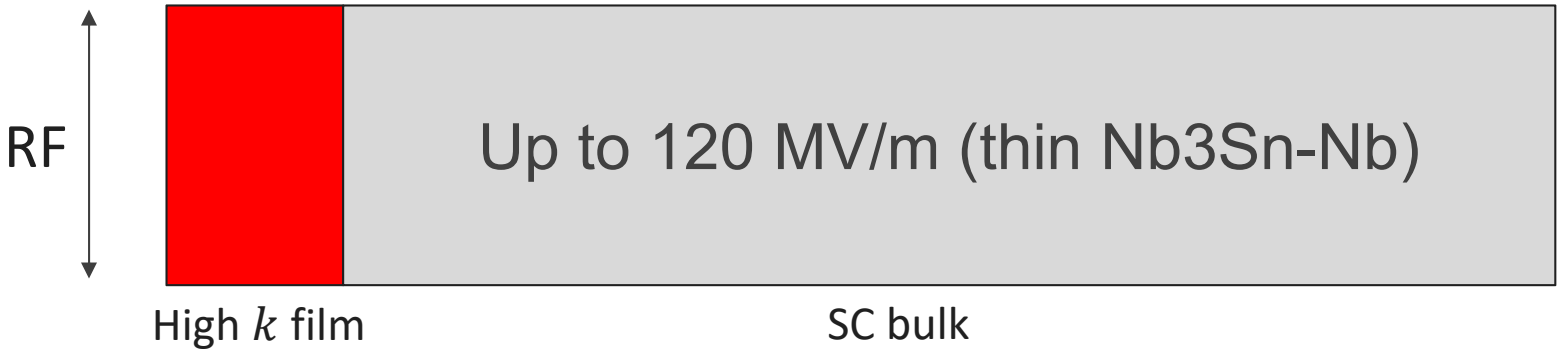


- Diffused $\kappa$ profile: numerical from Ginzburg-Landau eqs.
  M. Checchin *et al.*, IPAC 2016 & LINAC 2016

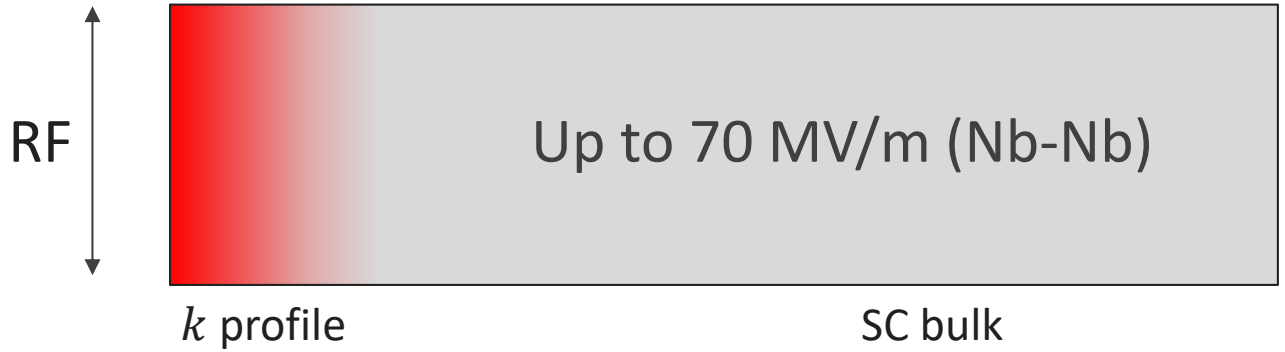


Can be produced by thermal diffusion!

# Vortex Nucleation Time – can we beat DC superheating field?

*DC regime*: magnetic flux vortices can nucleate when the magnetic field amplitude is larger than $B_{sh}$

*RF regime*: we should consider that $B(t)$ oscillates. The vortex nucleation may depend on the field frequency $f$:

- The vortex nucleation happens in a certain characteristic time $\tau_n$
- If the frequency is high enough so that $1/f \gg \tau_n$ then the vortex should not have enough time to nucleate

*Can the field be sustained above the superheating field in such a regime?*
***Can we modify the nucleation time via surface treatments?***

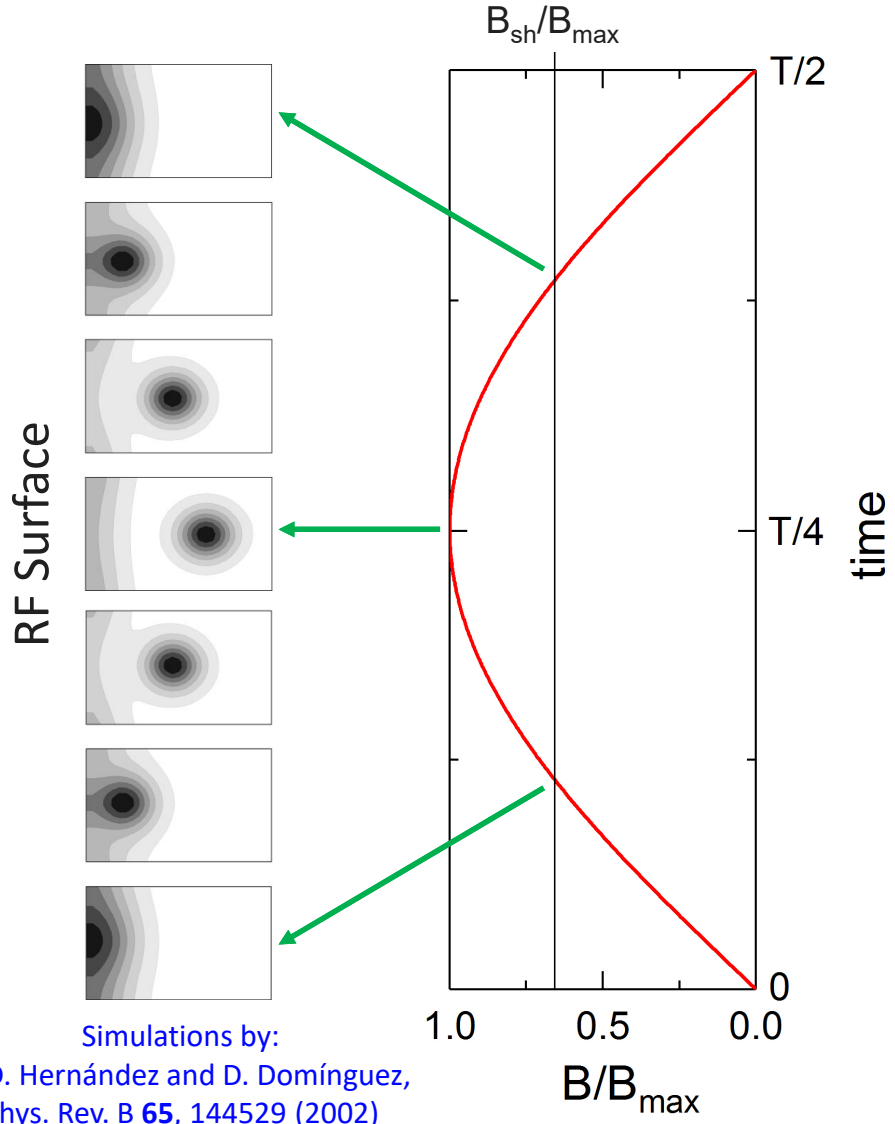


Simulations by:
A. D. Hernández and D. Domínguez,
Phys. Rev. B **65**, 144529 (2002)

# Up to what fields does superconductivity exist in the walls?

A. Romanenko, FNAL

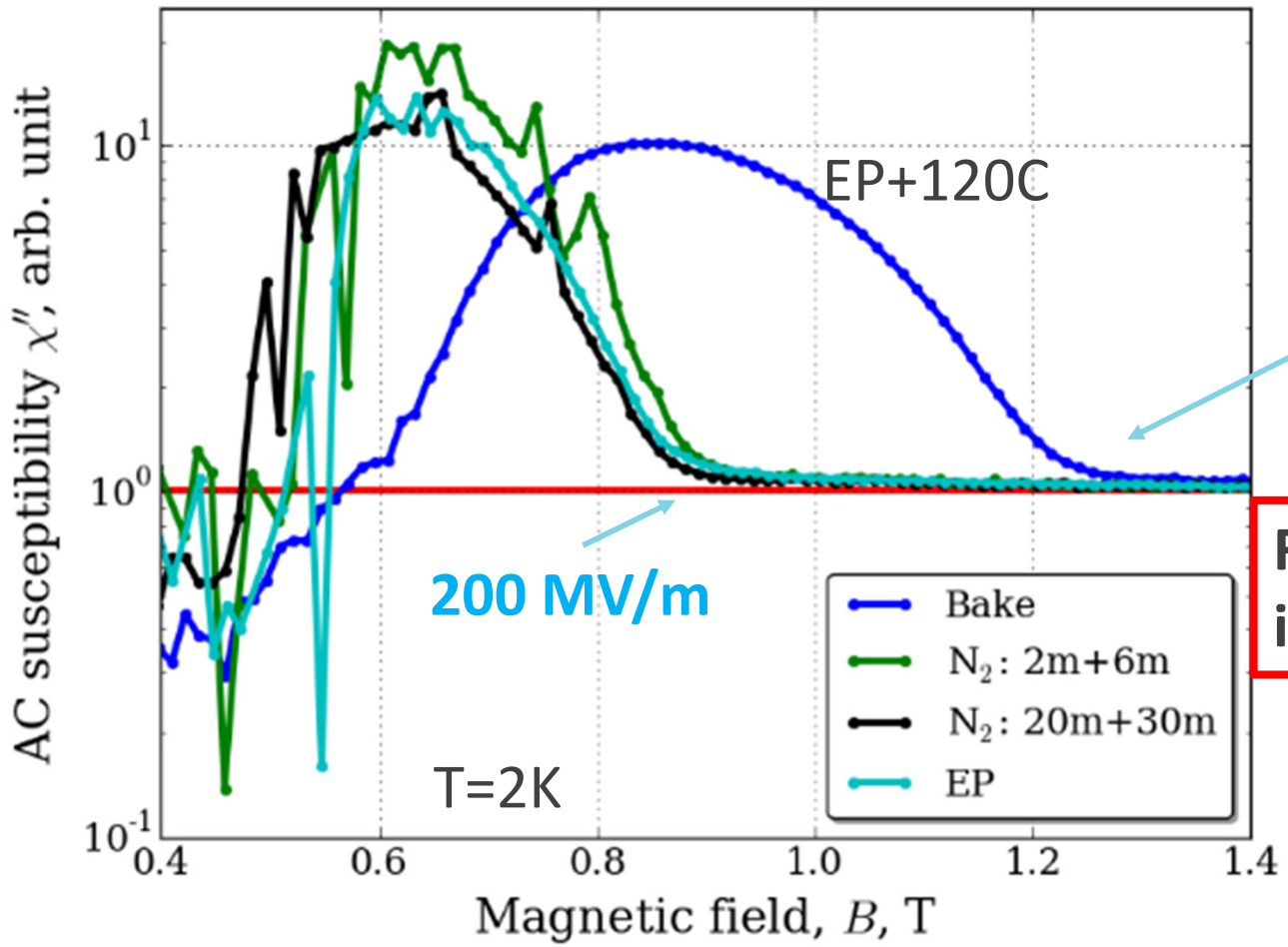


**For Nb3Sn Hc2 is 7 GV/m!**

# Experimental progress with N infusion at FNAL

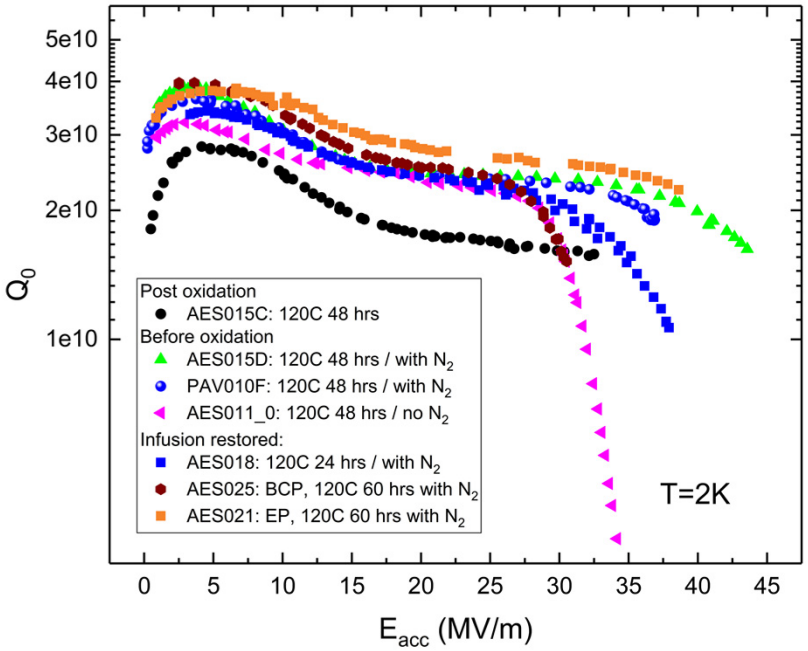


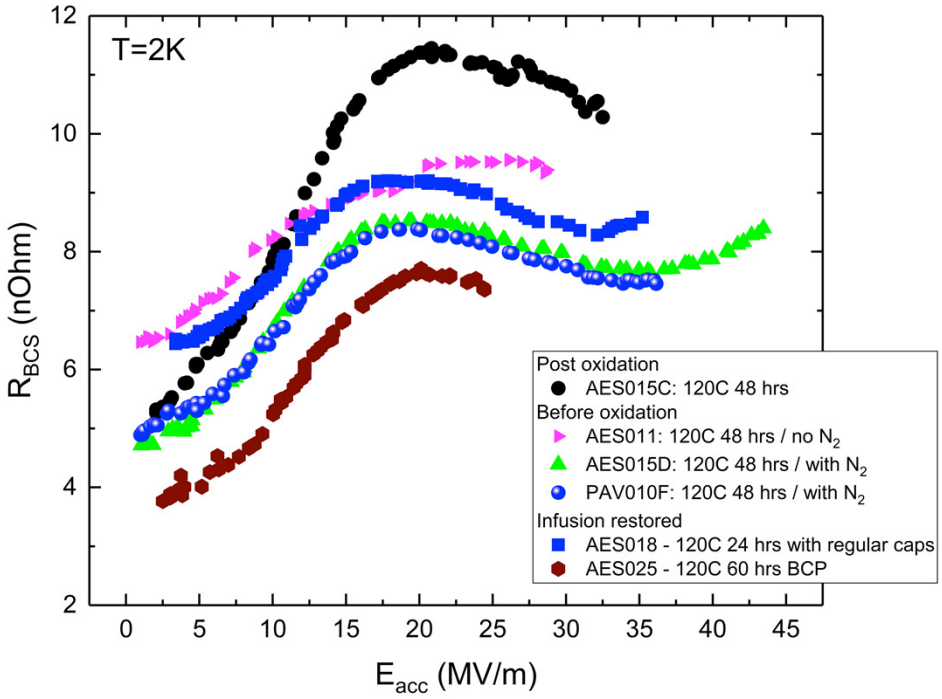


Exploring T, duration and pressure parameter space

A. Grassellino et al



Fermilab

# N infusion on BCP surface – record Q/grad values for BCP

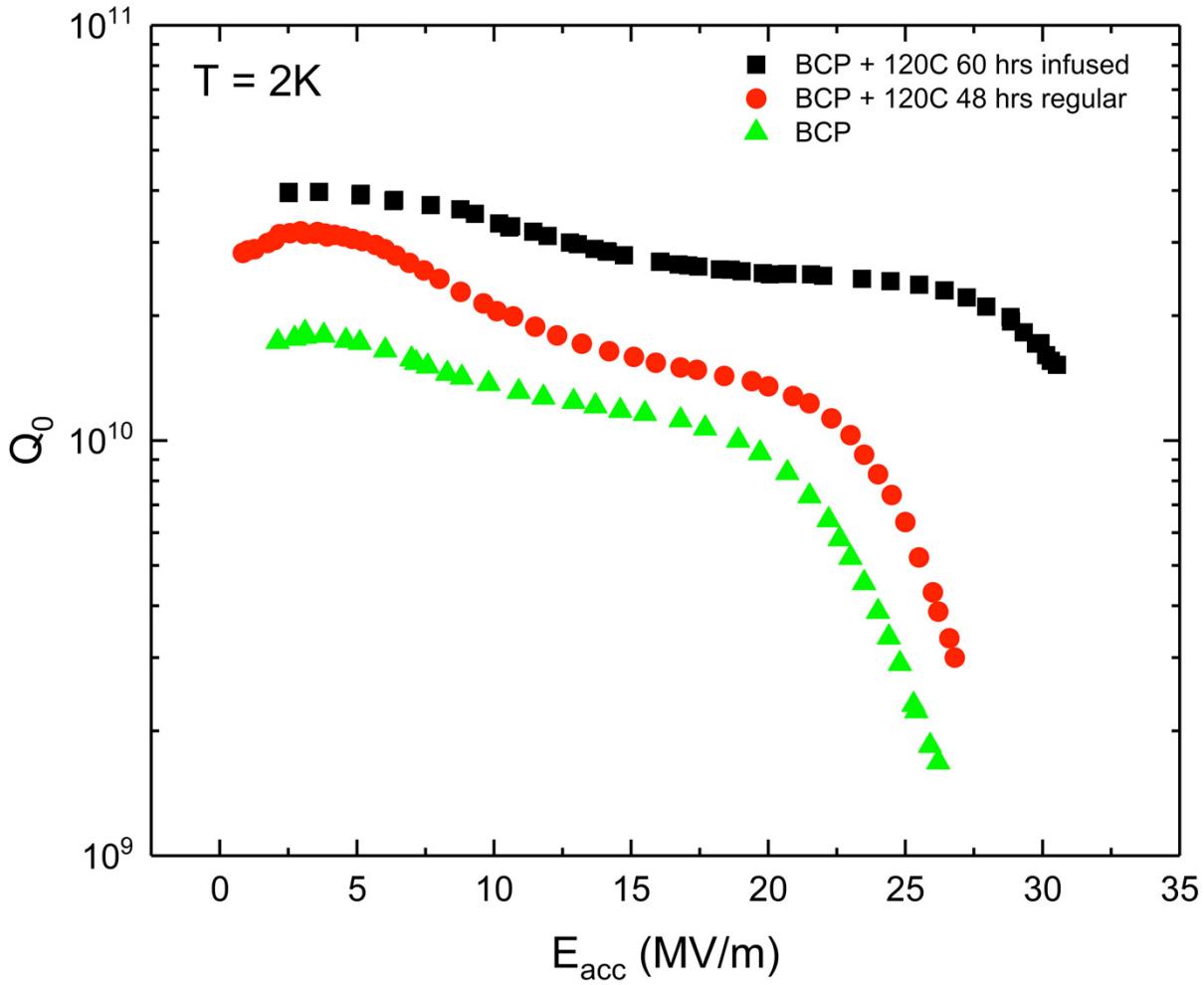


A. Grassellino et al, tbp

# New Furnace procured for clean/robust N infusion, and CVD/ALD capability for bi-layer structures

- CLEAN - Induction furnace with Doping capabilities:
  - N, Cl, C, Sn, Al, Ge, Ga, B, Si, …
- Deposition capabilities:
  - Large variety of superconducting compounds:
    - A15 ($Nb_3Sn$, $Nb_3Ge$, $Nb_3Al$, …)
    - Nitrides ($MoN$, $NbN$, $NbTiN$, …)
  - Superconducting elements:
    - Nb, Al, Pb, V, …
  - Insulators:
    - Oxides ($Al_2O_3$, $Ce_2O_3$, $SiO_2$, …)
    - Nitrides ($AlN$, $SiN$, …)

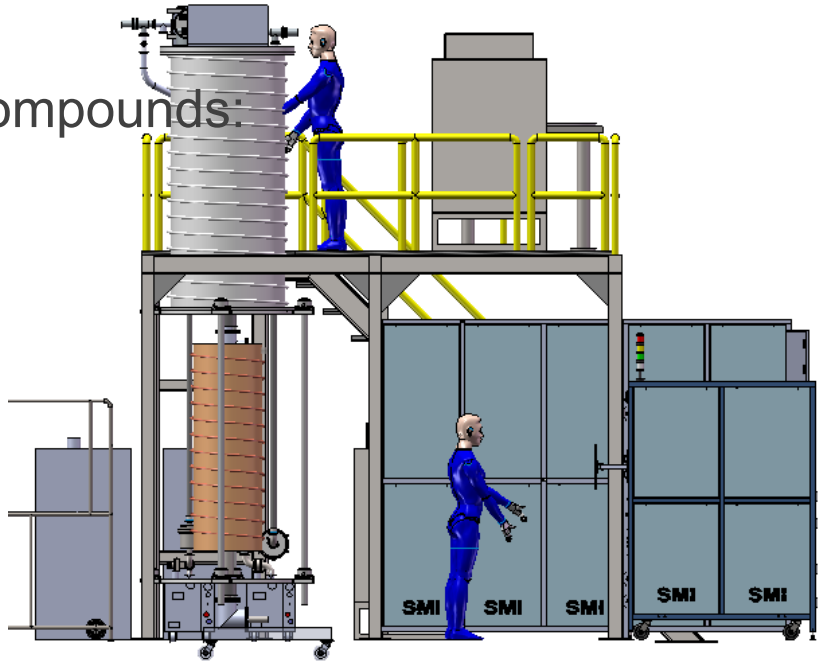


Jul 2017 — Jan 2018 — Jan 2019 — Dec 2019

System purchased

Design optimization

Final design

Commissioning at FNAL

Fermilab

# The Quantum Frontier

# SRF first measurements towards quantum regime - FNAL

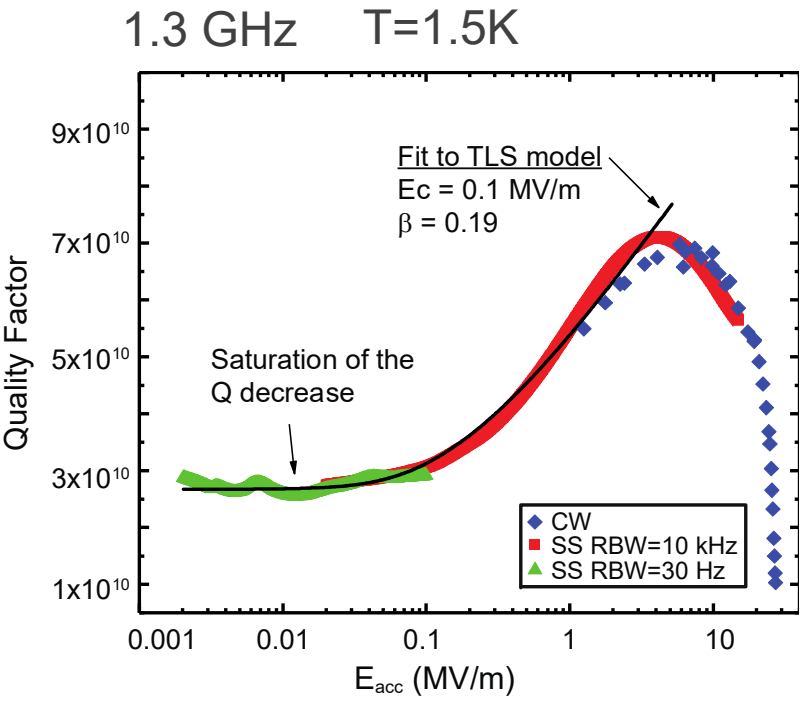


Now measured down to <N> ~ $10^3$ photons

Good news: low field Q saturates at Q~**5 x $10^{10}$**

**Understanding Quality Factor Degradation in Superconducting Niobium Cavities at Low Microwave Field Amplitudes***

A. Romanenko†
*Fermi National Accelerator Laboratory, Batavia, IL 60510, USA*

D. I. Schuster‡
*The James Franck Institute and Department of Physics, University of Chicago, Chicago, Illinois 60637, USA*

(Dated: October 27, 2017)

In niobium superconducting radio frequency (SRF) cavities for particle acceleration a decrease of the quality factor at lower fields - a so called *low field Q slope or LFQS* - has been a long-standing unexplained effect. By extending the high $Q$ measurement techniques to ultralow fields we discover two previously unknown features of the effect: i) saturation at rf fields lower than $E_{acc} \sim 0.1$ MV/m; ii) strong degradation enhancement by growing thicker niobium pentoxide. Our findings suggest that the LFQS may be caused by the two level systems in the natural niobium oxide on the inner cavity surface, thereby identifying a new source of residual resistance and providing guidance for potential non-accelerator low field applications of SRF cavities.

Modern and planned state-of-the-art particle accelerators employ hundreds or thousands of three-dimensional superconducting radio frequency (SRF) niobium cavities [1, 2] for particle acceleration. In operation, a beam of charged particles (e.g. electrons, positrons, protons, heavy ions) is accelerated by the electric field along the axis of the cavity. The phase of the field is such that particles always see an accelerating field along their trajectories. Maintaining the large electromagnetic fields inside cavities leads to dissipation, and - compared to normal conducting technology - SRF cavities provide an extremely low power consumption thereby permitting continuous wav… beam qualit…

ual resistance currently sets the limit to the maximum possible SRF cavity quality factors [11], and plays the dominant role for sub-gigahertz range SRF-based accelerators. Understanding the physics of all the mechanisms behind residual resistance is among the major remaining challenges for further SRF progress.

In addition to the physics of residual resistance, understanding of the LFQS has recently acquired strong practical cross-discipline interest as a range of potential non-accelerating applications of high $Q$ SRF cavities emerged in particle physics [12], quantum computing [13–15], astrophysics [16], superconducting parametric …e detection [18, 19], for …v low rf fields (down to

To appear in Phys Rev Lett

A. Romanenko and D. I. Schuster, https://arxiv.org/abs/1705.05982



Fermilab

# Towards quantum regime at FNAL SRF

- Goal: Demonstration of T = 10 mK and <N> ~ 1 photon high Q


Large dilution refrigerator capable of fitting up to 9-cell 1.3 GHz cavities or many (>50) 3D-SRF qubits

Extensive wiring for multi-SRF-3D qubit implementation

- Advanced magnetic shielding

Can be explored for dark sector searches

# Non-accelerator applications: dark sector searches

S. R. Parker *et al*, Phys. Rev. D 88, 112004 (2013)
J. Hartnett *et al*, Phys. Lett. B 698 (2011) 346
J. Jaeckel and A. Ringwald, Phys. Lett. B 659, 509 (2008)

$Q_{DET}$, $Q_{EM}$ < $10^5$ so far used

## Looking for hidden paraphotons

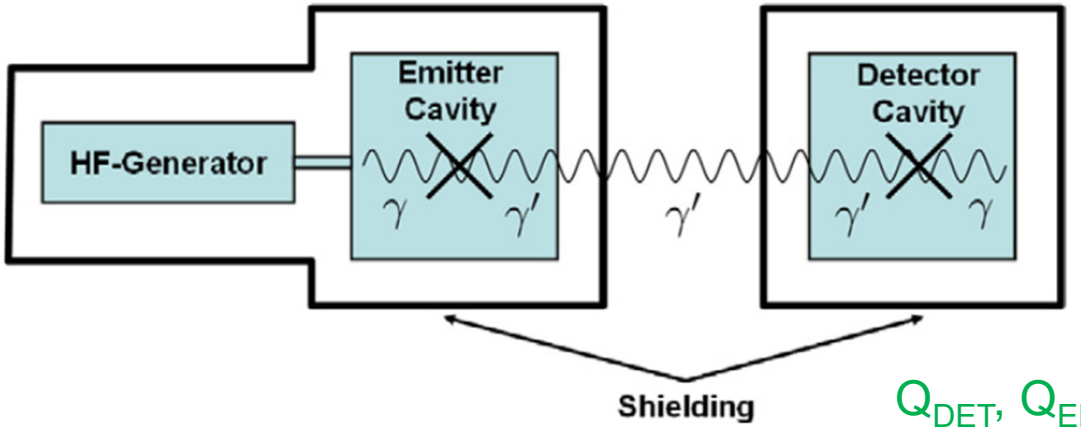


$$\frac{P_{DET}}{P_{EM}} = \chi^4 Q_{DET} Q_{EM} \left(\frac{m_{\gamma\prime} c^2}{\hbar \omega_\gamma}\right)^8 |G|^2$$

$Q_{DET}$, $Q_{EM}$ > $10^{10}$ SRF can offer 10 orders of magnitude improvement in sensitivity to $\chi$

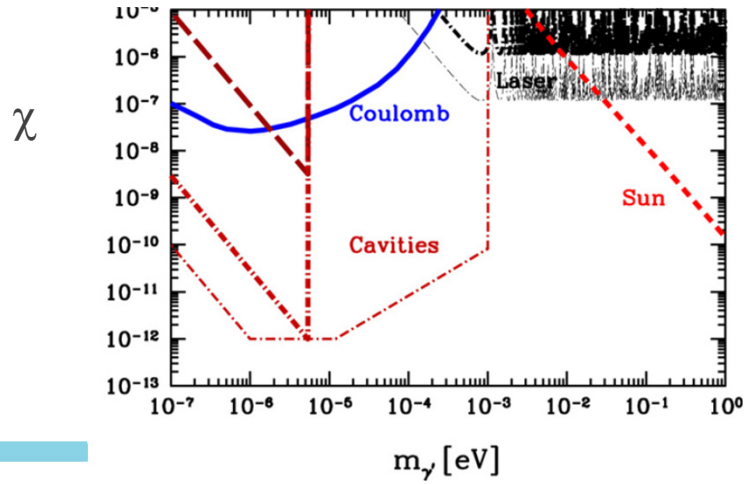

# Conclusions

- Superconducting RF technology for particle accelerators have come a long way but still have huge and unexplored potential
- SRF technology state of the art cavities have gradients up to 50 MV/m and quality factors exceeding 5e10 at 2K, 1.3 GHz, 2e11 at 1.5K, 2e10 at 4.2K (Nb3Sn)
- SRF is now at the beginning of a new phase. The next factor of 2-3 will require a strong focus on:
  - Physics of SRF surface (material science tools)
  - As much involvement as possible of superconductivity theory experts with strong ties to technology centers/labs
- Long term to focus on: what is the ultimate limit for achievable gradients and Q? Can we go to 100 MV/m or more? We need to understand the ultimate limitations and explore pathways forward
- Pathway forward will be challenging, but rewarding

# Thanks to Fermilab SRF Team Effort

- > 100 people with world leading SRF expertise, techs, engineers, scientists
- World class SRF facilities
- International collaborations with several institutions

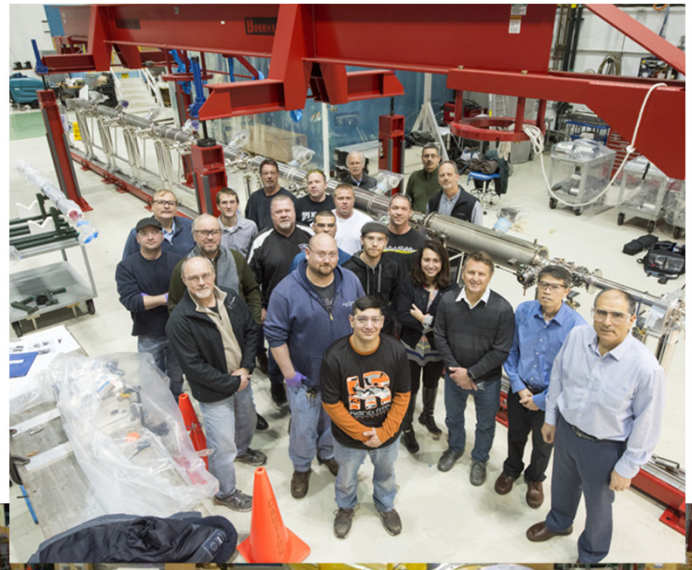

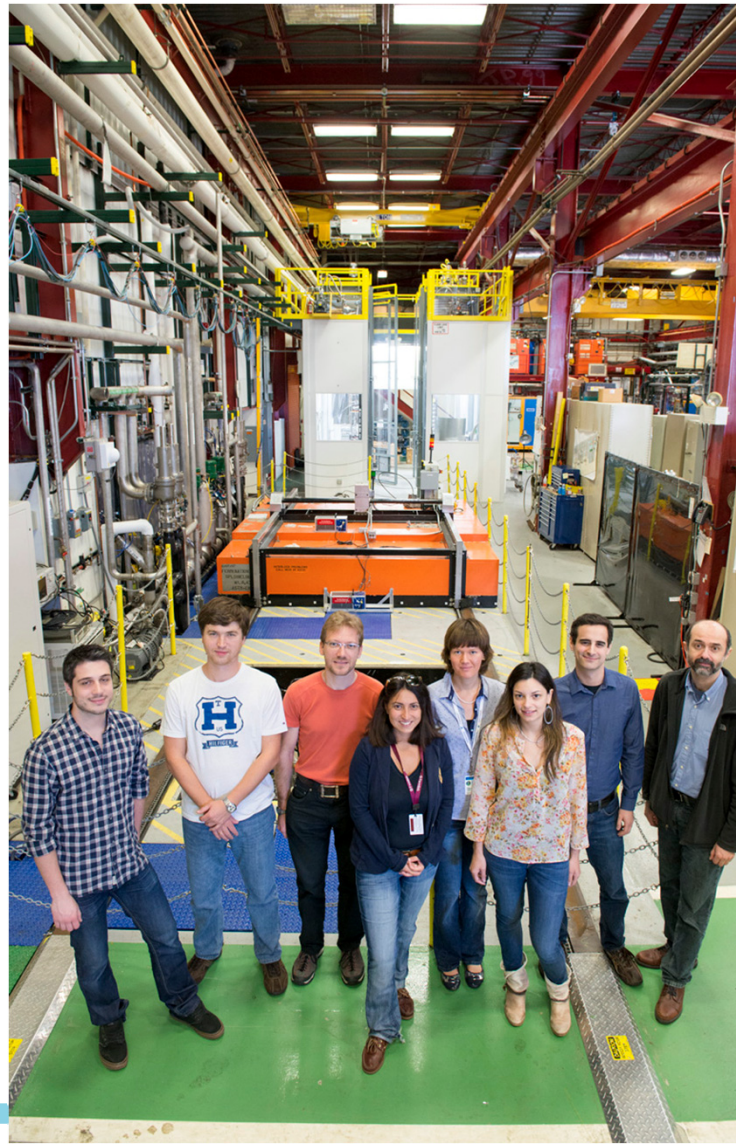

# Back up slides

# SRF Research milestone – Successful nitrogen doping technology transfer to industry for LCLS-II production

– Four times higher Q (cavity efficiency) at LCLS-II operating gradient

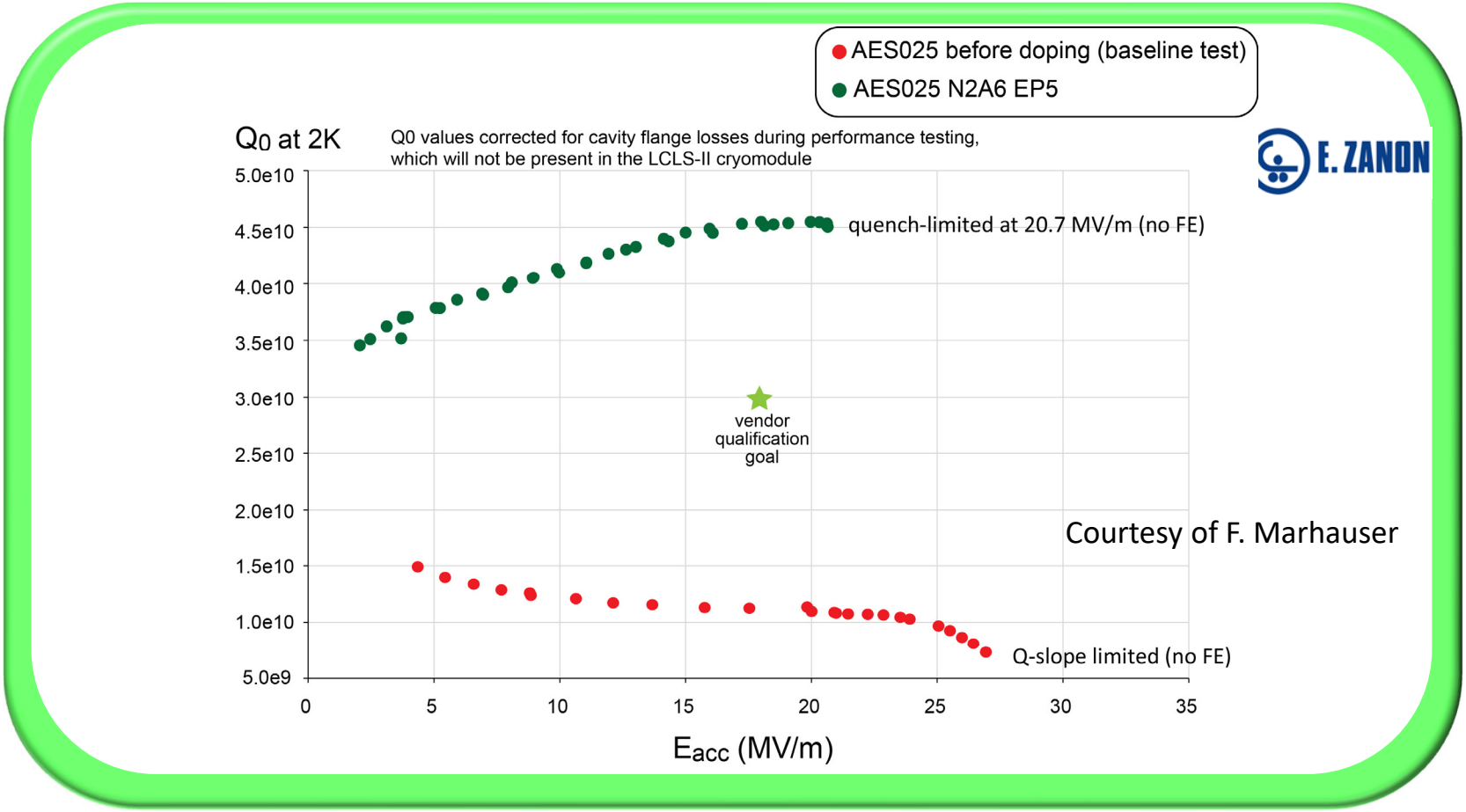

# Vertical Test Bare Nine Cell 2.0K Results, doping recipe 2/6

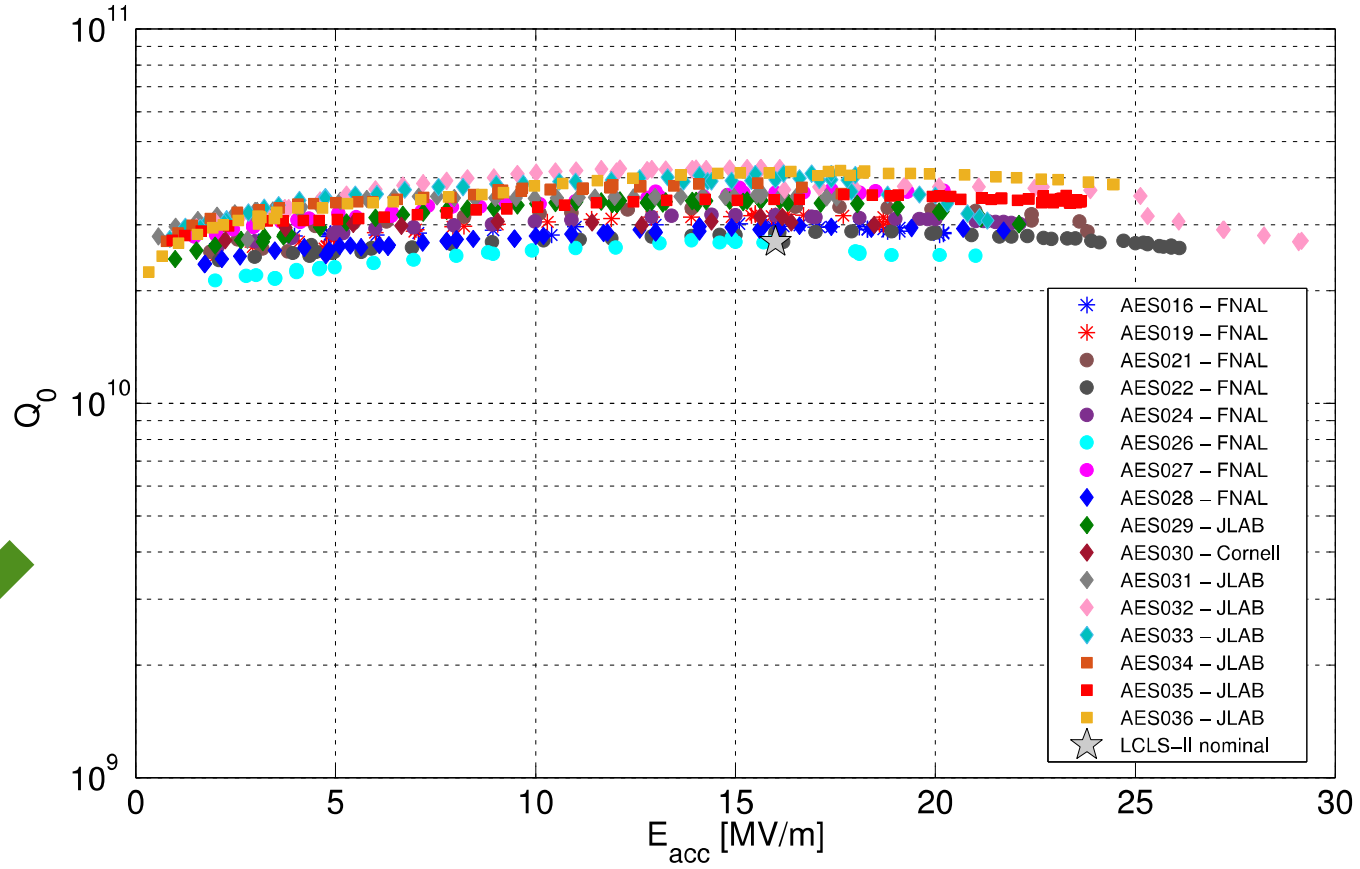


World record values: Avg Q (16 MV/m, 2K)= 3.5e10, Avg Quench field ~ 22 MV/m

# Fully Integrated Test at FNAL – TB9AES021

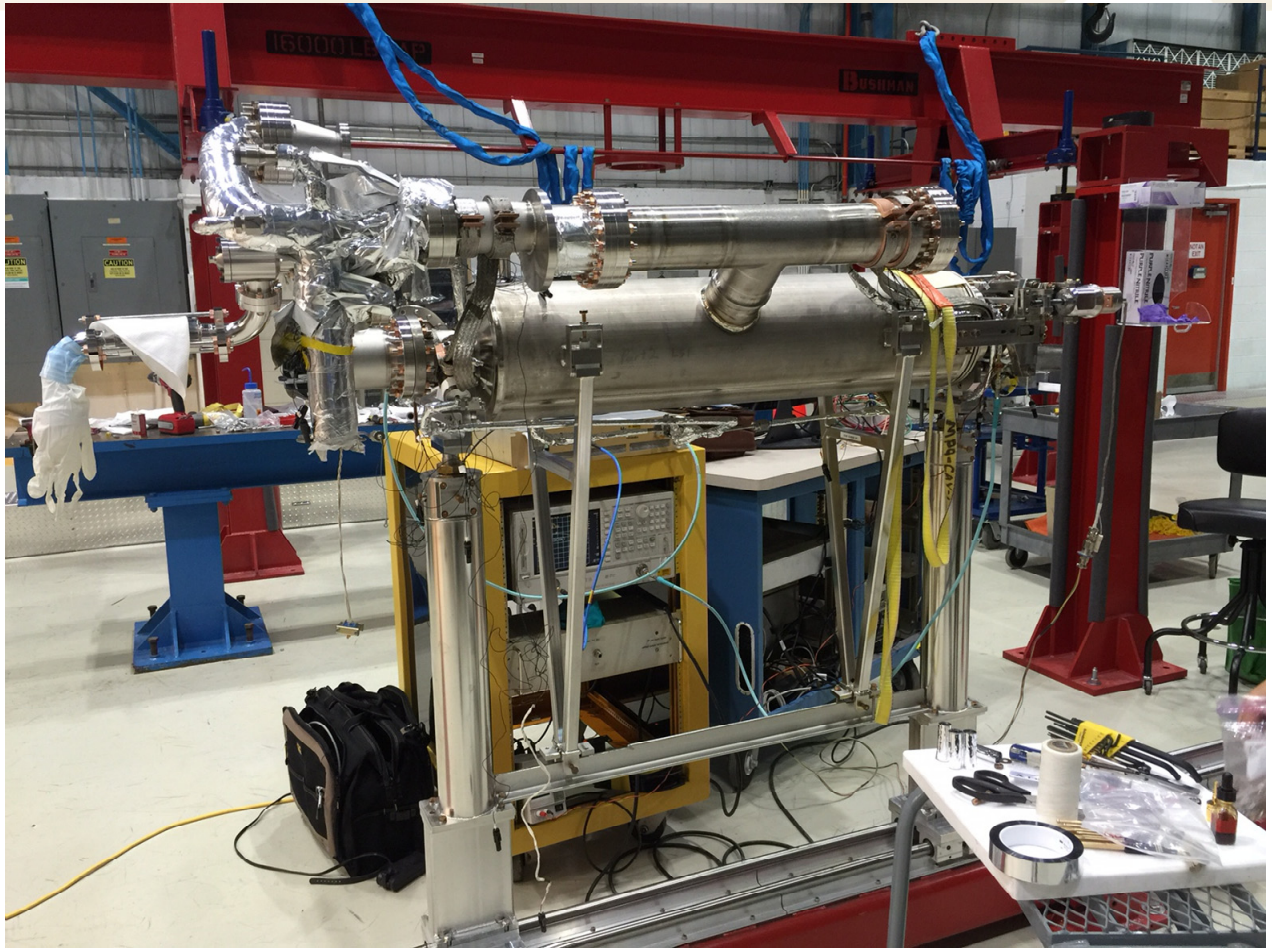

High power coupler, HOMs, tuner, double layer magnetic shielding…

# Record Q > 3e10 at 2K, 16 MV/m in cryomodule environment for LCLS-II cavity

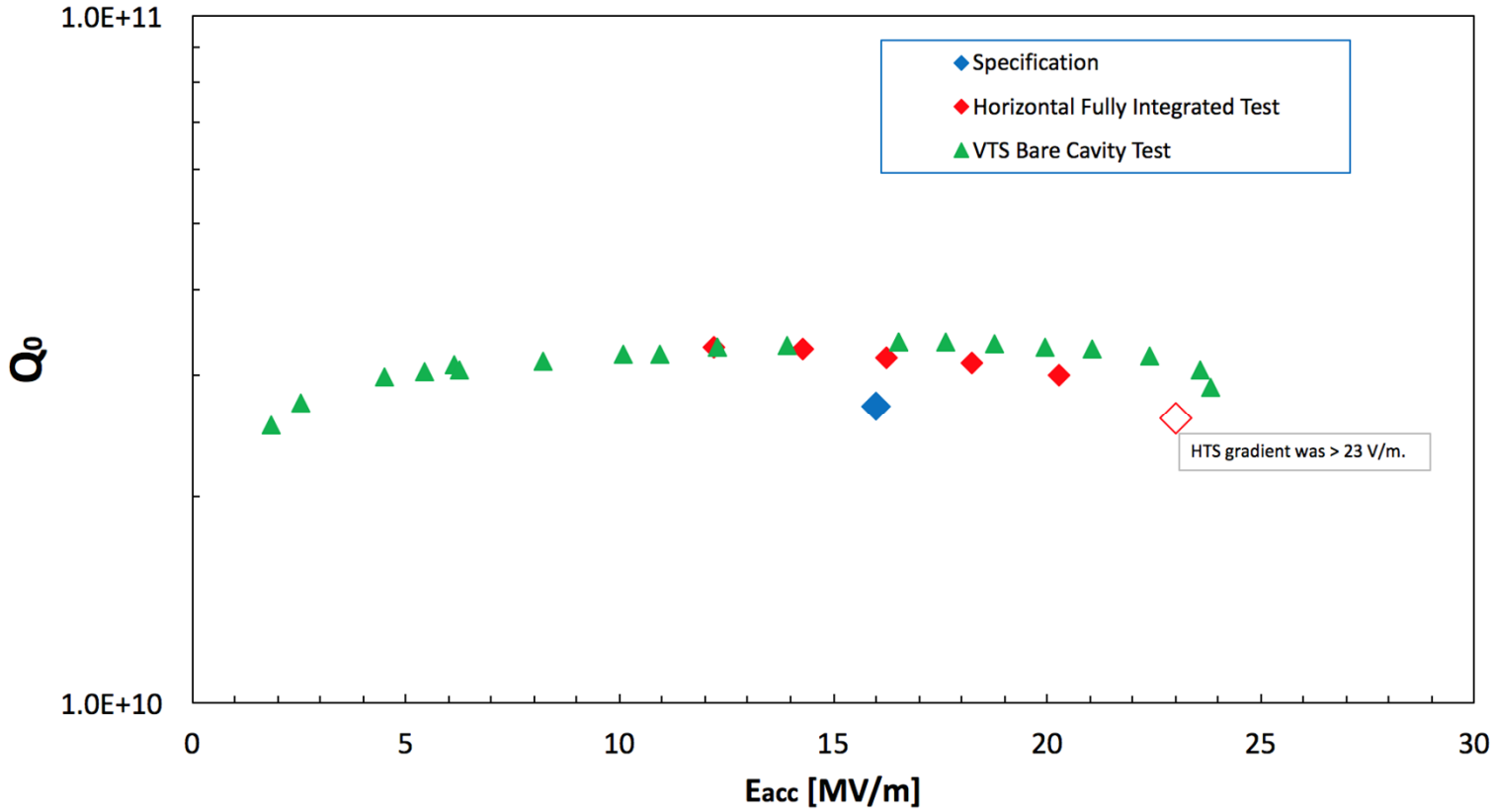


No Q degradation from vertical test to “accelerator conditions” with unique techniques discovered and developed at FNAL for: cooldown procedure through critical temperature, HOMs/high power coupler thermal strapping, and magnetic shielding

# N doping applied to 650 MHz cavities at FNAL
# Q~ 7e10 at 2K, 17 MV/m – record values also at this frequency!

Applying N doping to 650 MHz (beta=0.9) leads to double Q compared to 120C bake (standard surface treatment ILC/XFEL)

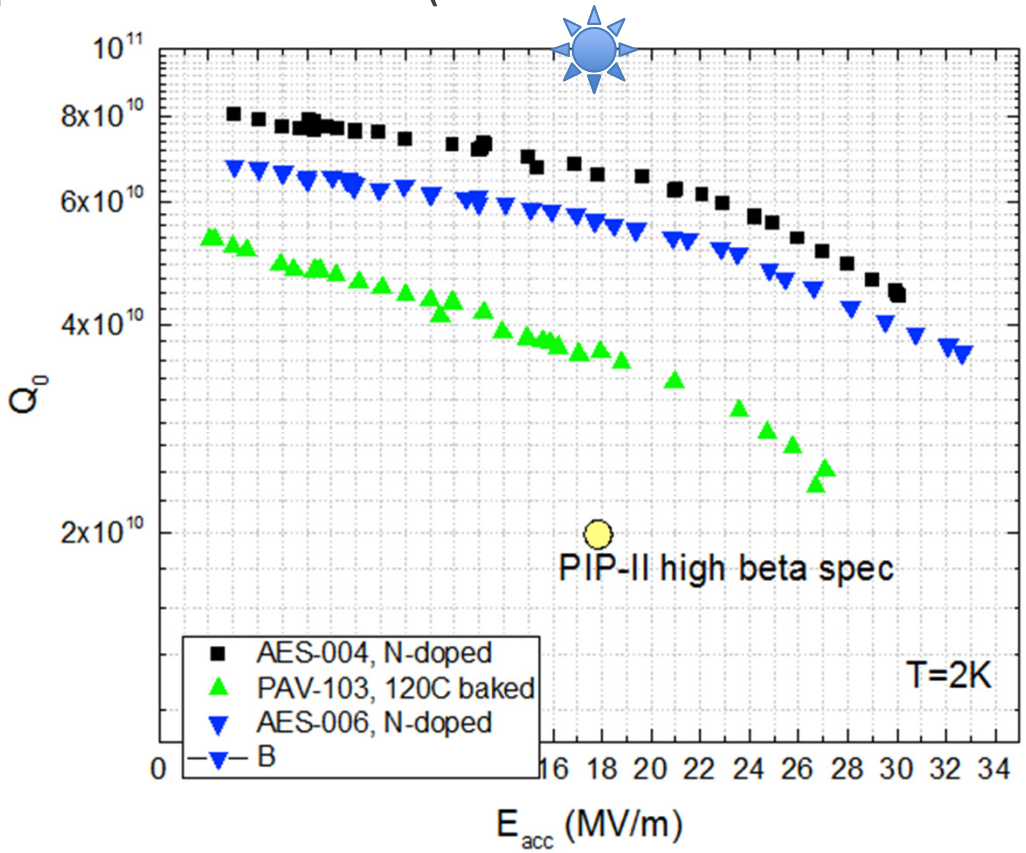


But from frequency scaling from 1.3GHz, with ideal recipe the projected Q value is ~1e11 at 17 MV/m, 2K! Need to optimize doping recipe at lower freq; Multicell doping ongoing

# *Progress in N doping understanding: what is the root of performance improvement?*

# Recipe optimization: $R_{BCS}$ vs flux sensitivity

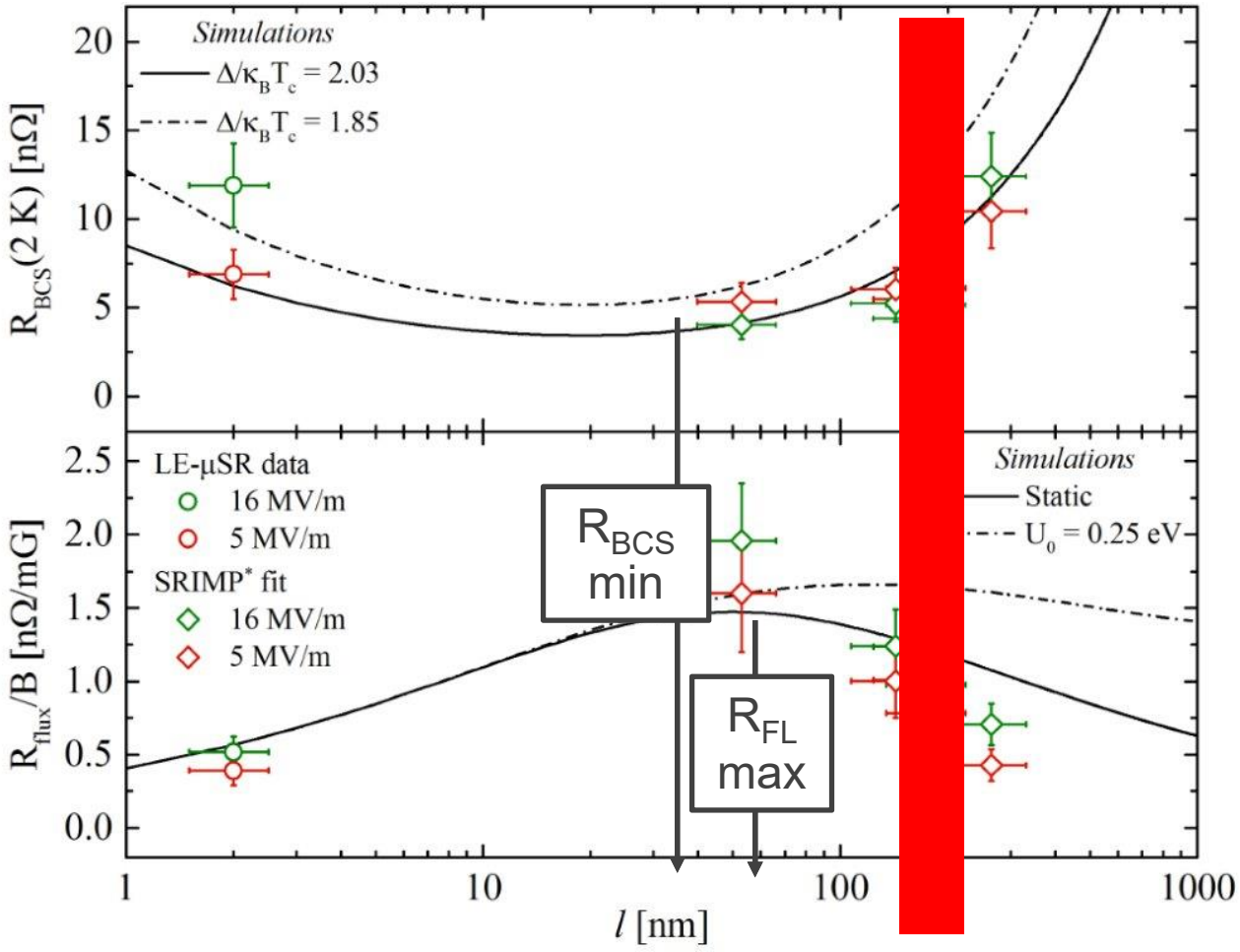


Larger mean free paths produce best performance…
But it is also interesting to notice the large windows of “unexplored”…

# Sensitivity vs Mean Free Path

STRONG DEPENDENCE

**The sensitivity of the trapped flux as a function of mean free path has a maximum around $l = 60nm$**

M. Martinello, M. Checchin, A. Grassellino, A. Romanenko et Al. In Proceeding of SRF 2015

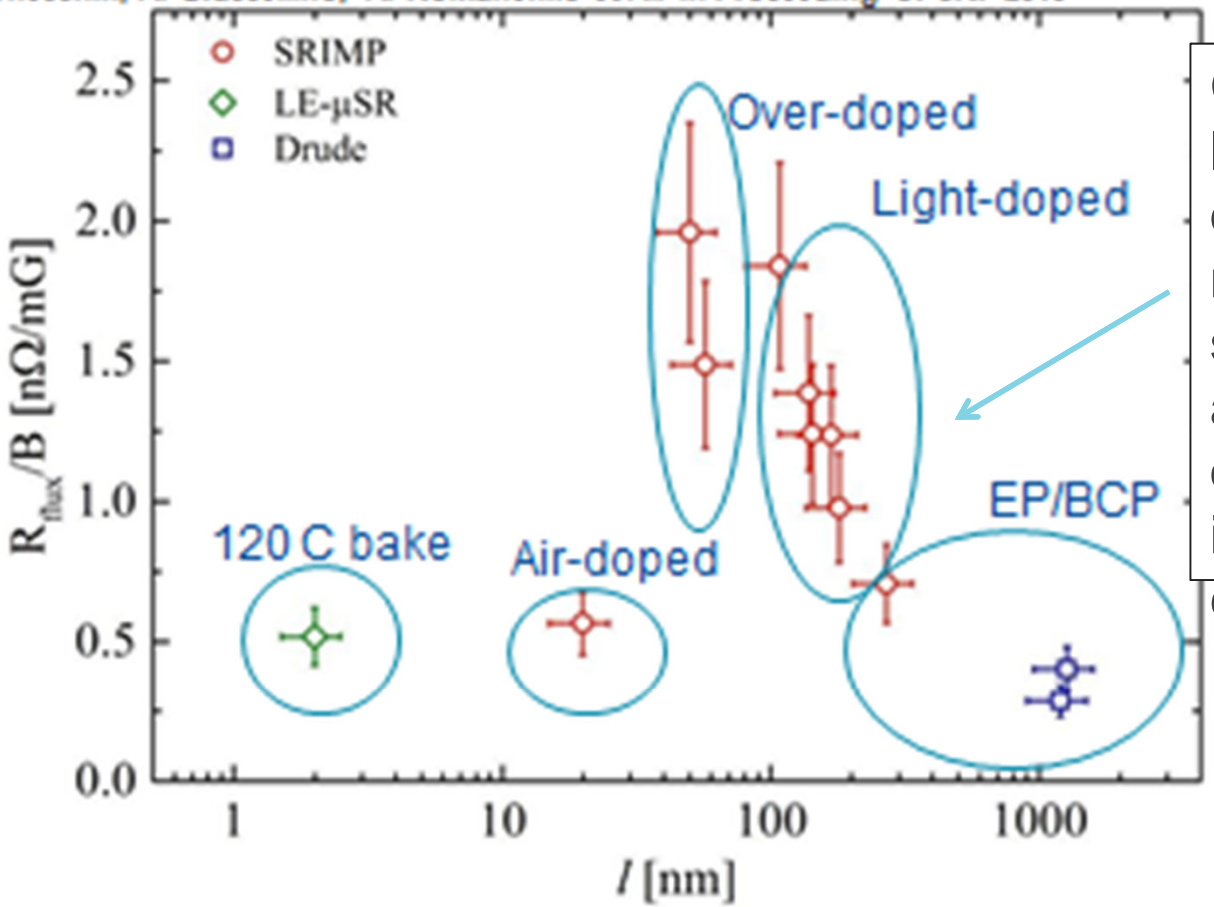


Cavities with light N doped are not far from standard and optimization is not completed

# Sensitivity vs Surface Treatments

| Cavity Name | Surface Treatment | m.f.p. (nm) | $R_{fl}/B_{tr}$ (nΩ/mG) |
|---|---|---|---|
| AES011 | 2/6 min $N_2$ + 7 $\mu m$ EP | 143 | 1.45 |
| AES017 | 2/6 min $N_2$ + 5$\mu m$ EP | 180 | 0.98 |
| AES018 | EP + 30 min He | 400* | 0.71 |
| AES019 | 10 min $N_2$ + 5$\mu m$ EP | 168 | 1.24 |
| ACC002 | 20 min $N_2$ + 5$\mu m$ EP | 50 | 1.96 |
| AES014 | 120C bake | 2* | 0.52 |
| AES009 | 2/6 min $N_2$ + 5$\mu m$ EP @Jlab | 57 | 1.49 |
| AES0017_2 | Additional 2/6 min $N_2$ + 8$\mu m$ EP | 138.6 | 1.39 |
| AES021 | Air 30 min + 2$\mu m$ EP | 19.9 | 0.56 |

*μ-SR measurement

# Sensitivity vs Surface Treatments

| Cavity Name | Surface Treatment | m.f.p. (nm) | $R_{fl}/B_{tr}$ (nΩ/mG) |
|---|---|---|---|
| AES011 | 2/6 min $N_2$ + 7 $\mu m$ EP | 143 | 1.45 |
| AES017 | 2/6 min $N_2$ + 5$\mu m$ EP | 180 | 0.98 |
| AES018 | EP + 30 min He | 400* | 0.71 |
| AES019 | 10 min $N_2$ + 5$\mu m$ EP | 168 | 1.24 |
| ACC002 | 20 min $N_2$ + 5$\mu m$ EP | 50 | 1.96 |
| AES014 | 120C bake | 2* | 0.52 |
| AES009 | 2/6 min $N_2$ + 5$\mu m$ EP @Jlab | 57 | 1.49 |
| AES0017_2 | Additional 2/6 min $N_2$ + 8$\mu m$ EP | 138.6 | 1.39 |
| AES021 | Air 30 min + 2$\mu m$ EP | 19.9 | 0.56 |

*μ-SR measurement

# Sensitivity vs Surface Treatments

| Cavity Name | Surface Treatment | m.f.p. (nm) | $R_{fl}/B_{tr}$ (nΩ/mG) |
|---|---|---|---|
| AES011 | 2/6 min $N_2$ + 7 $\mu m$ EP | 143 | 1.45 |
| AES017 | 2/6 min $N_2$ + 5$\mu m$ EP | 180 | 0.98 |
| AES018 | EP + 30 min He | 400* | 0.71 |
| AES019 | 10 min $N_2$ + 5$\mu m$ EP | 168 | 1.24 |
| ACC002 | 20 min $N_2$ + 5$\mu m$ EP | 50 | 1.96 |
| AES014 | 120C bake | 2* | 0.52 |
| AES009 | 2/6 min $N_2$ + 5$\mu m$ EP @Jlab | 57 | 1.49 |
| AES0017_2 | Additional 2/6 min $N_2$ + 8$\mu m$ EP | 138.6 | 1.39 |
| AES021 | Air 30 min + 2$\mu m$ EP | 19.9 | 0.56 |

*μ-SR measurement

# Sensitivity vs Surface Treatments

| Cavity Name | Surface Treatment | m.f.p. (nm) | $R_{fl}/B_{tr}$ (nΩ/mG) |
|---|---|---|---|
| AES011 | 2/6 min $N_2$ + 7 $\mu m$ EP | 143 | 1.45 |
| AES017 | 2/6 min $N_2$ + 5$\mu m$ EP | 180 | 0.98 |
| AES018 | EP + 30 min He | 400* | 0.71 |
| AES019 | 10 min $N_2$ + 5$\mu m$ EP | 168 | 1.24 |
| ACC002 | 20 min $N_2$ + 5$\mu m$ EP | 50 | 1.96 |
| AES014 | 120C bake | 2* | 0.52 |
| AES009 | 2/6 min $N_2$ + 5$\mu m$ EP @Jlab | 57 | 1.49 |
| AES0017_2 | Additional 2/6 min $N_2$ + 8$\mu m$ EP | 138.6 | 1.39 |
| AES021 | Air 30 min + 2$\mu m$ EP | 19.9 | 0.56 |

*μ-SR measurement

# Sensitivity vs Mean Free Path Explanation

The losses seems governed by the **static dissipation** of the vortexes which appears to be different in clean and dirty limits

## DIRTY LIMIT

The smaller the mean free path the smaller the NC core diameter

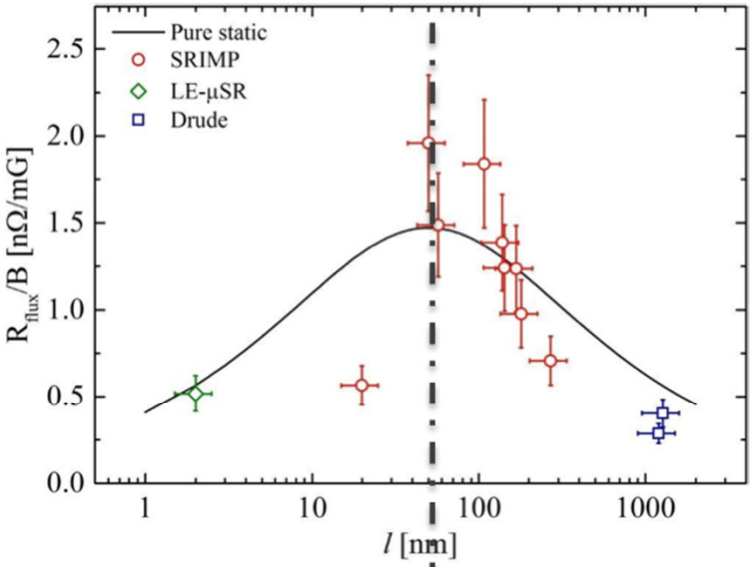


## CLEAN LIMIT

The NC core diameter does not depend anymore from mfp. The larger the mean free the lower the resistivity

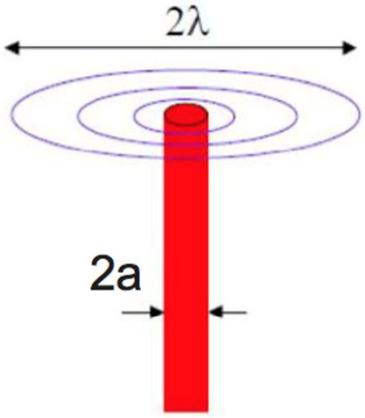


$$R_{static} = \sqrt{\frac{\rho\omega\mu}{2}} \cdot \frac{\pi a^2}{\Sigma}$$

$$a_{dirty} = \sqrt{\frac{\pi}{3}\xi_0 l} \qquad \rho = \frac{m v_F}{l n e^2}$$

$$\boldsymbol{R_{static} \propto \sqrt{l}}$$

$$R_{static} = \sqrt{\frac{\rho\omega\mu}{2}} \cdot \frac{\pi a^2}{\Sigma}$$

$$a_{clean} = 1.16\xi_0 \qquad \rho = \frac{m v_F}{l n e^2}$$

$$\boldsymbol{R_{static} \propto \frac{1}{\sqrt{l}}}$$



Fermilab
ILLINOIS INSTITUTE OF TECHNOLOGY

# Recipe optimization: quench fields

- Light doping yields to higher quench field than heavy doping
- For same length of the doping step, quench field decreases with subsequent ‘anneal’ time (why?)
- For same recipe, quench fields are worse in nine cell than single cell cavities
- Quench fields are not sparse, they always ‘cluster’ around a value – different N doping levels produce different quench barriers
- More severe quench limitation > ~200 ppm concentration
- There is a trend – similar to the BCS minimum – for quench fields vs mean free path

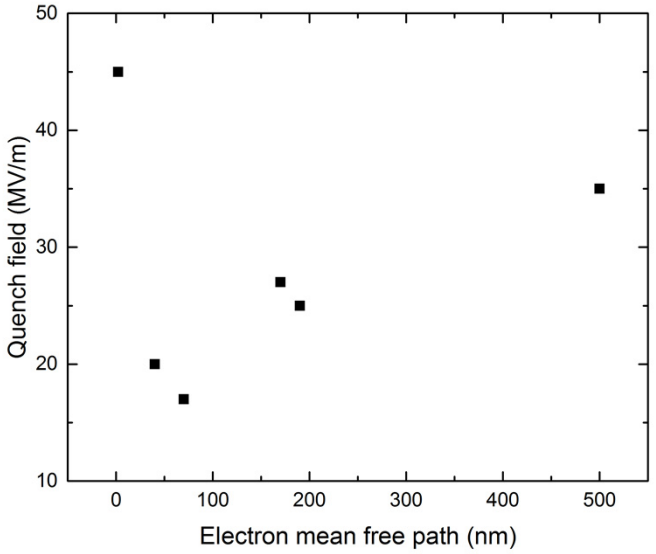


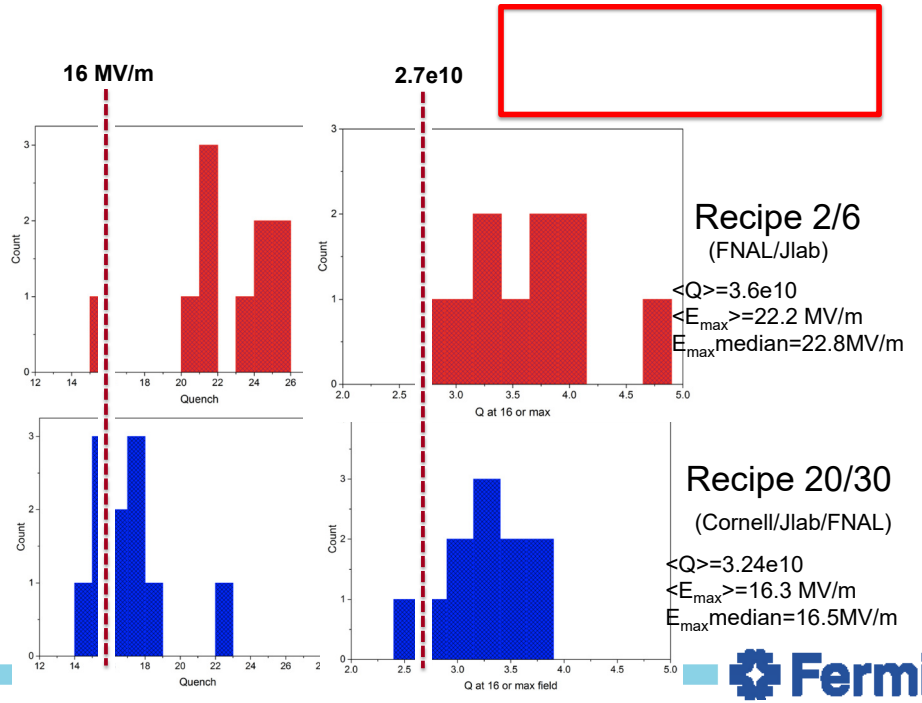

# New insights on quench in N doped cavities – magnetic peak field driven

Nitride teeth…residual nanonitrides post EP?
Or premature flux entry?

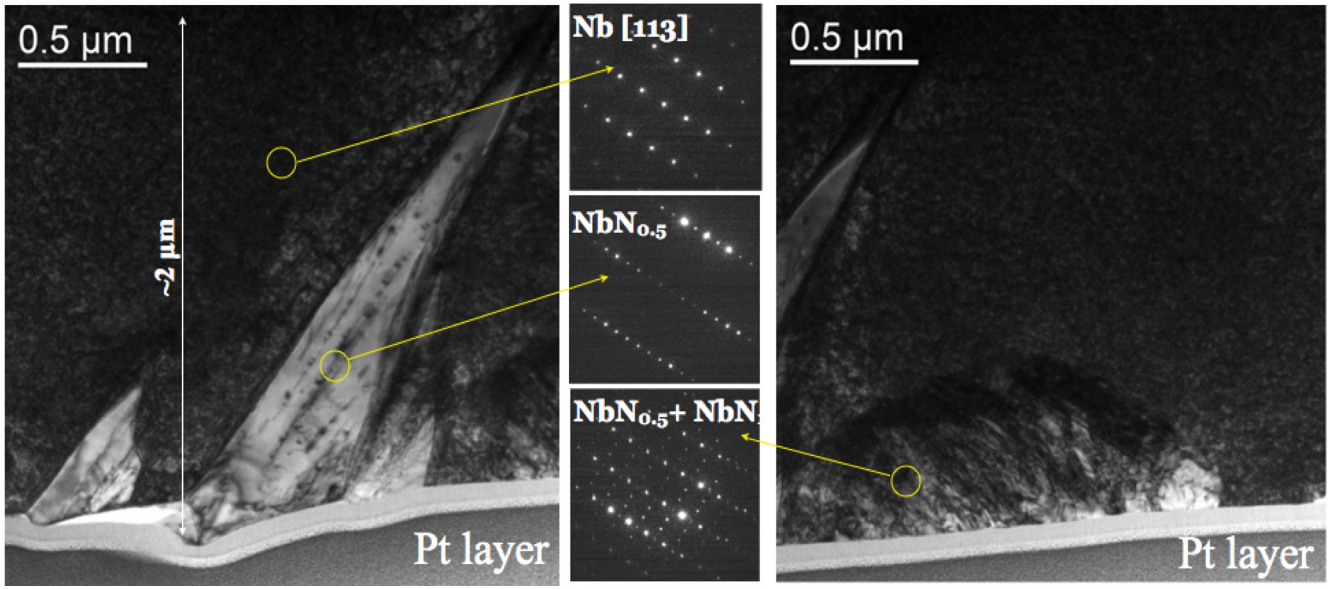


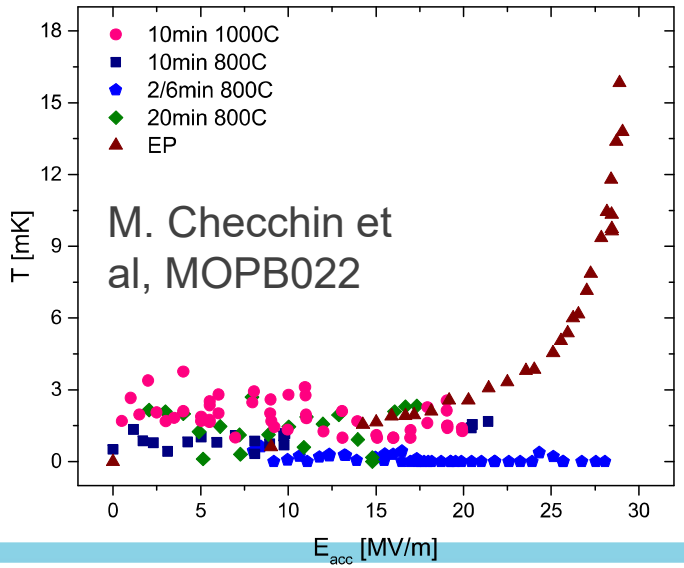


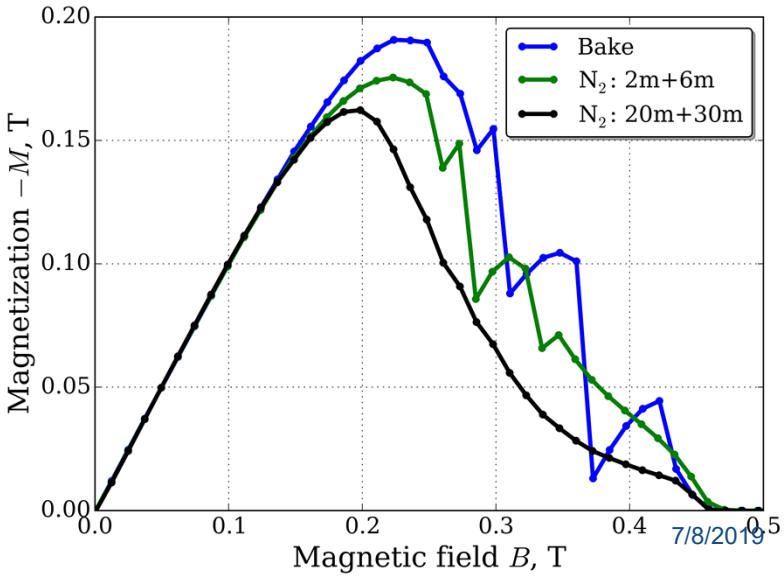


A. Vostrikov et al, MOPB027

# T-map apparatus

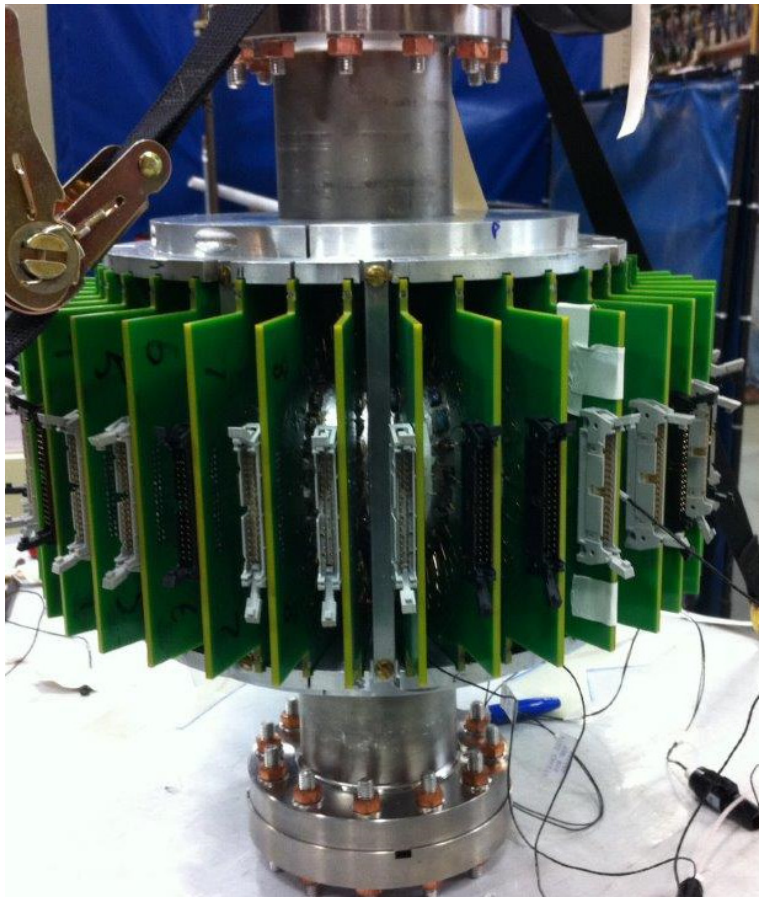

- FNAL T-map system
- 36 boards with 16 thermometers each

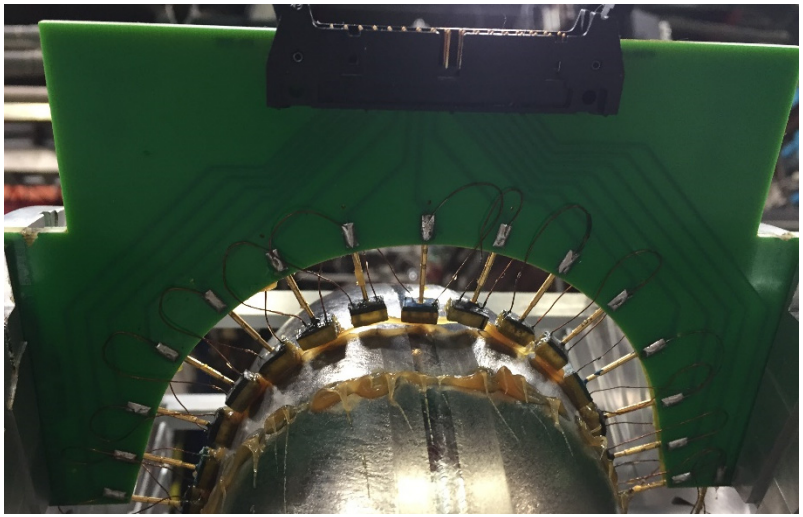

**576** thermometers
all around the cavity

# NEW – going further: study large sample of cavities of different material (vendors and treatment history)

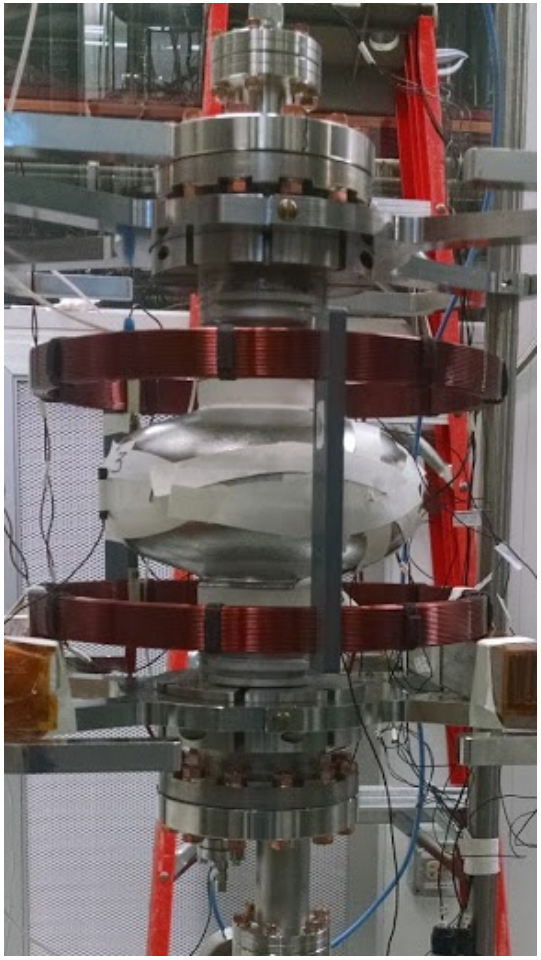

- Goal: measure flux trapping as a function of **thermal gradient** and **material treatment**
- Connection to $R_{res}$ – Performing study on cavities directly determines required conditions to avoid severely degraded RF performance

S. Posen et al, arxiv.org/pdf/1509.03957 (submitted to APL)

**Recommendations**

1. **The Project is ready to proceed to CD-2/3**
2. **Finalize cavity and cryomodule minimum acceptance criteria based on the current project baseline – by 3/2016**
3. **Conduct a supply chain risk assessment of critical cryomodule assembly components to identify items needing second sources or other mitigations – by 3/2016**
4. **Develop a cure to improve the flux expulsion of the procured niobium material and implement before cavity production.**
5. **Conduct an independent peer review of the detailed assembly methods for connecting cryomodules – prior to first connection in 2017**

# *3) Magnetic Shielding*

# Magnetic scope, specifications & sources

- First large CW project where magnetic shielding being analyzed stringently, especially longitudinal component of magnetic field
  - $B_{avg} \downarrow \rightarrow R_s \downarrow \rightarrow Q_0 \uparrow \rightarrow P_{diss} \downarrow \rightarrow \$_{oper} \downarrow$
- LCLS-II specification [1]:
  - $B_{avg}$<5 mG to reach $Q$ >2.7E10 at 2 K, 16 MV/m
- Major magnetic field sources: vacuum vessel, components, earth
  - $B_{vessel}$< 3 G [2]
  - $B_{components}$~ 1 G
  - $B_{earth} \approx$ 483 mG at SLAC [3]
  - $B_{//,beamline} \approx$ 150 mG
- Most analyses done assuming SLAC tunnel magnetic fields

[1] “1.3 GHz Superconducting RF Cryomodule,” Functional Requirements Document, LCLSII-4.5-FR-0053.
[2] A. Crawford, arXiv:1507.06582v1.
[3] National Oceanic and Atmospheric Administration, 2014--2019 World Magnetic Model.

# Benefits of degaussing vessel [4,5]

- Vessel must be degaussed after final handling
  - Fields in steel could be ~200 G when exposed to ~500 mG
- Edge ~factor of 3 reduction
- Central ~factor of 2 reduction

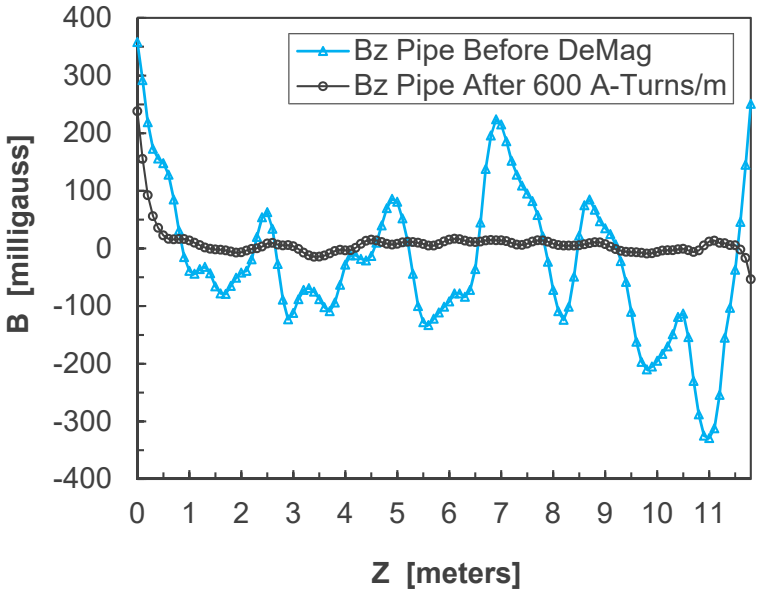


Expt. With $B_{//} \approx 50$ mG

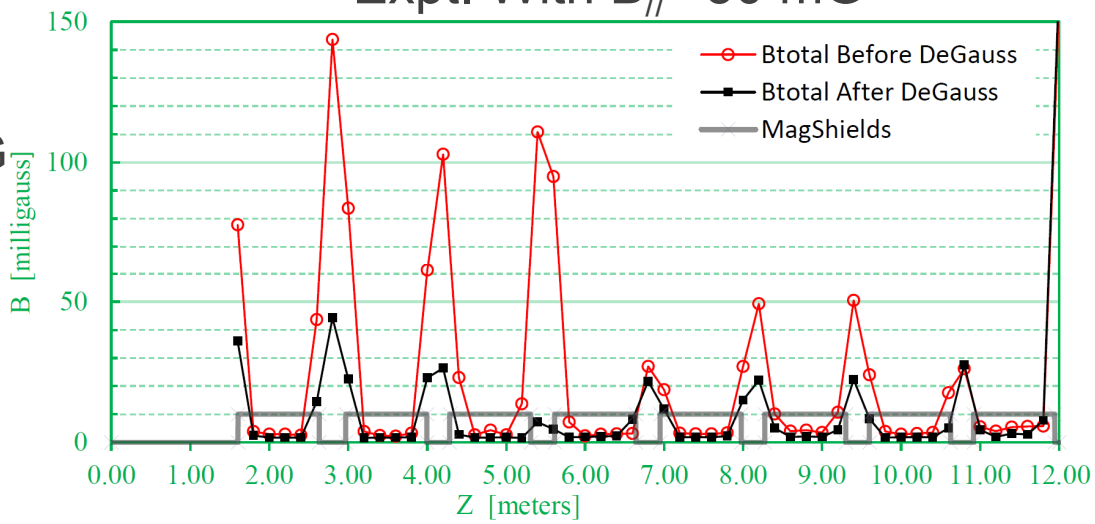


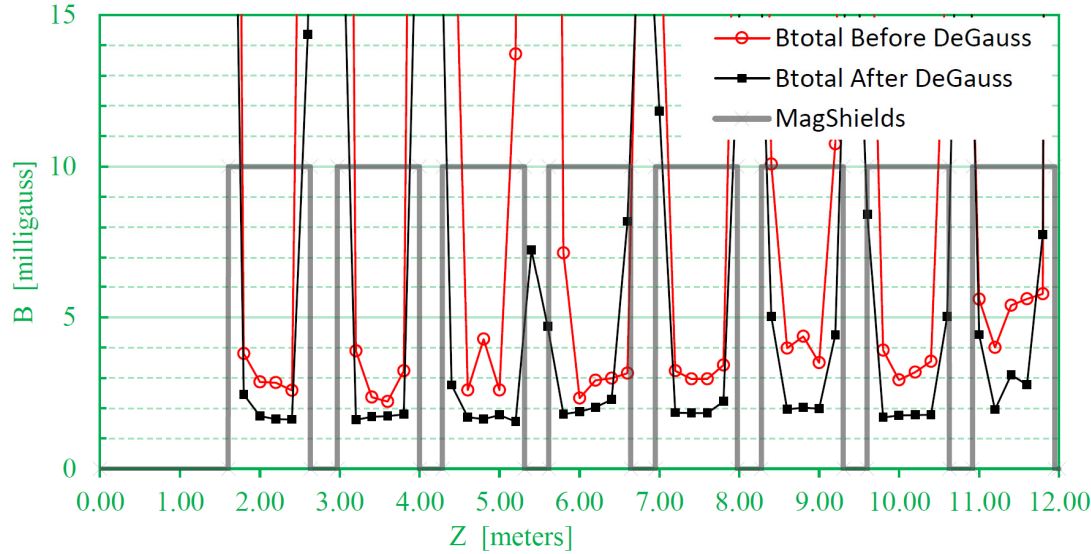



[4] A. Crawford, arXiv:1409.0828v1.
[5] A. Crawford, arXiv:1503.04736v1.

# Demagnetization coils

- Helmholtz coils on the outside of CM vessel
  - Main coil (5 turns x 21) + 2 end coils (100 turns each)
- End coils required to compensate end effects of vessel
- 650 Amp-turns/meter main coil
- 1% drop per cycle, 100 cycles

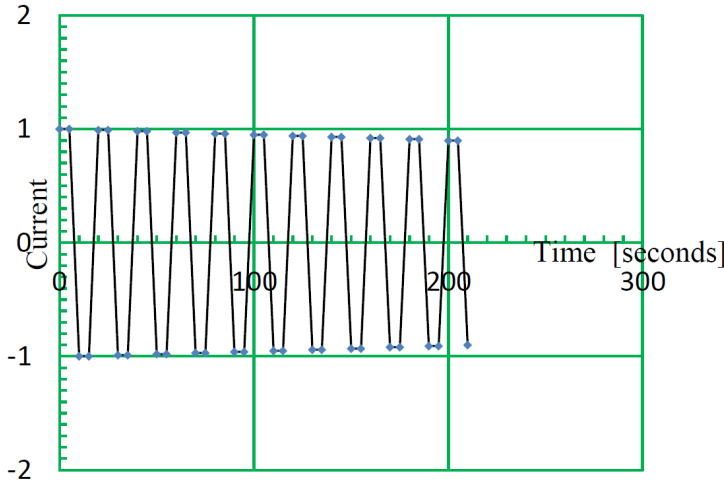


# Magnetic shielding: transverse component

- Dependent on
  - *t*/*d* ratio; *t*=thickness, *d*=diameter of shield
  - Magnetic permeability $\mu$
- For infinitely long cylinder [6]
  - $Atten. = \frac{\mu}{4}\left(1 - \frac{d}{d+t}\right) + 1$
- Maintaining high $\mu$ difficult
  - Handling biggest concern
- Multilayer shielding a solution
- LCLS-II: two layers

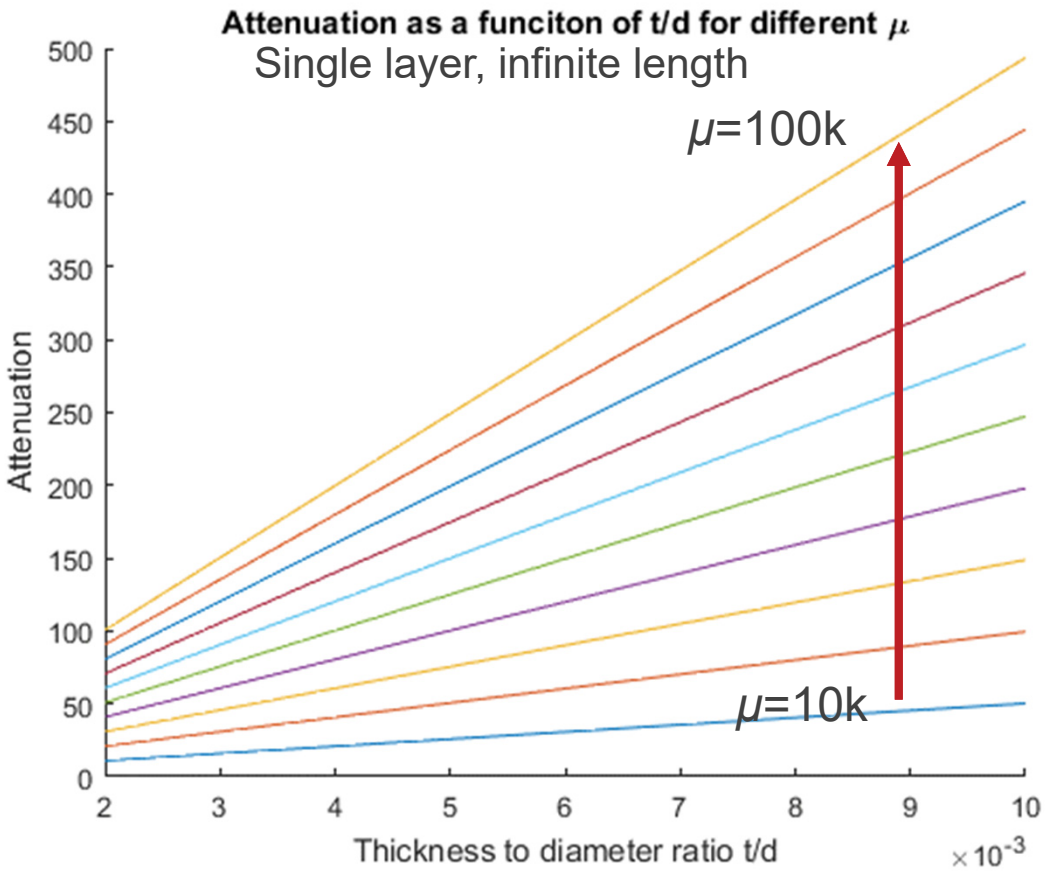


[6] A.J. Mager, IEEE T Magn, 1970.

# Longitudinal shielding: 2D analyses “perfect” shields

- $\mu_r$=10k, ~150 mG longitudinal field applied, beamline at center of vacuum vessel
- Line containing **equators**, parallel to beamline:

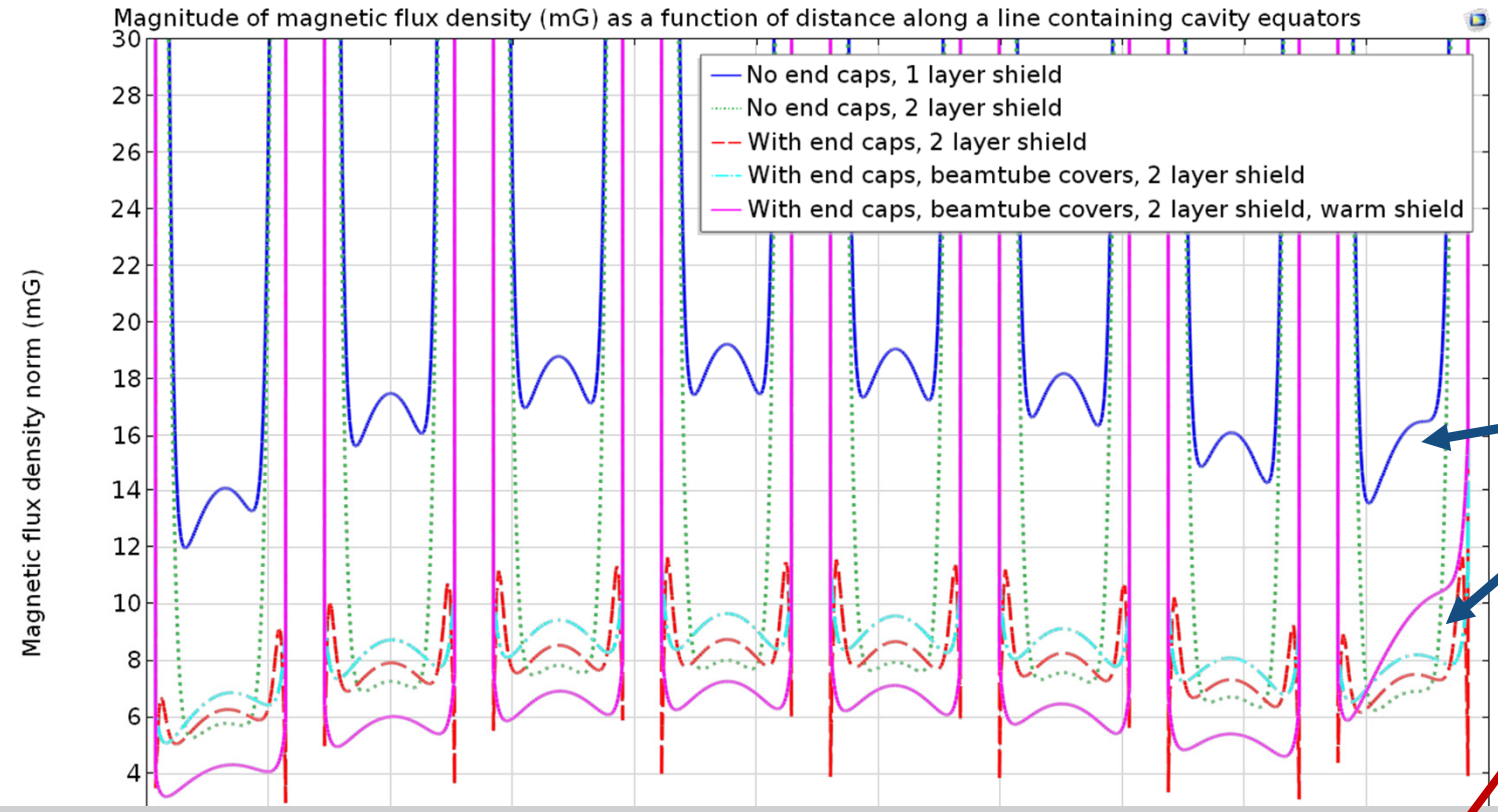


Enhancement due to end effects of vacuum vessel & warm shield (when present)

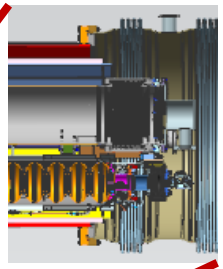



Fermilab

# Longitudinal shielding: effect of adjacent shields

- Adjacent magnetic shields can magnetically couple
- Adjacent CMs can magnetically couple too

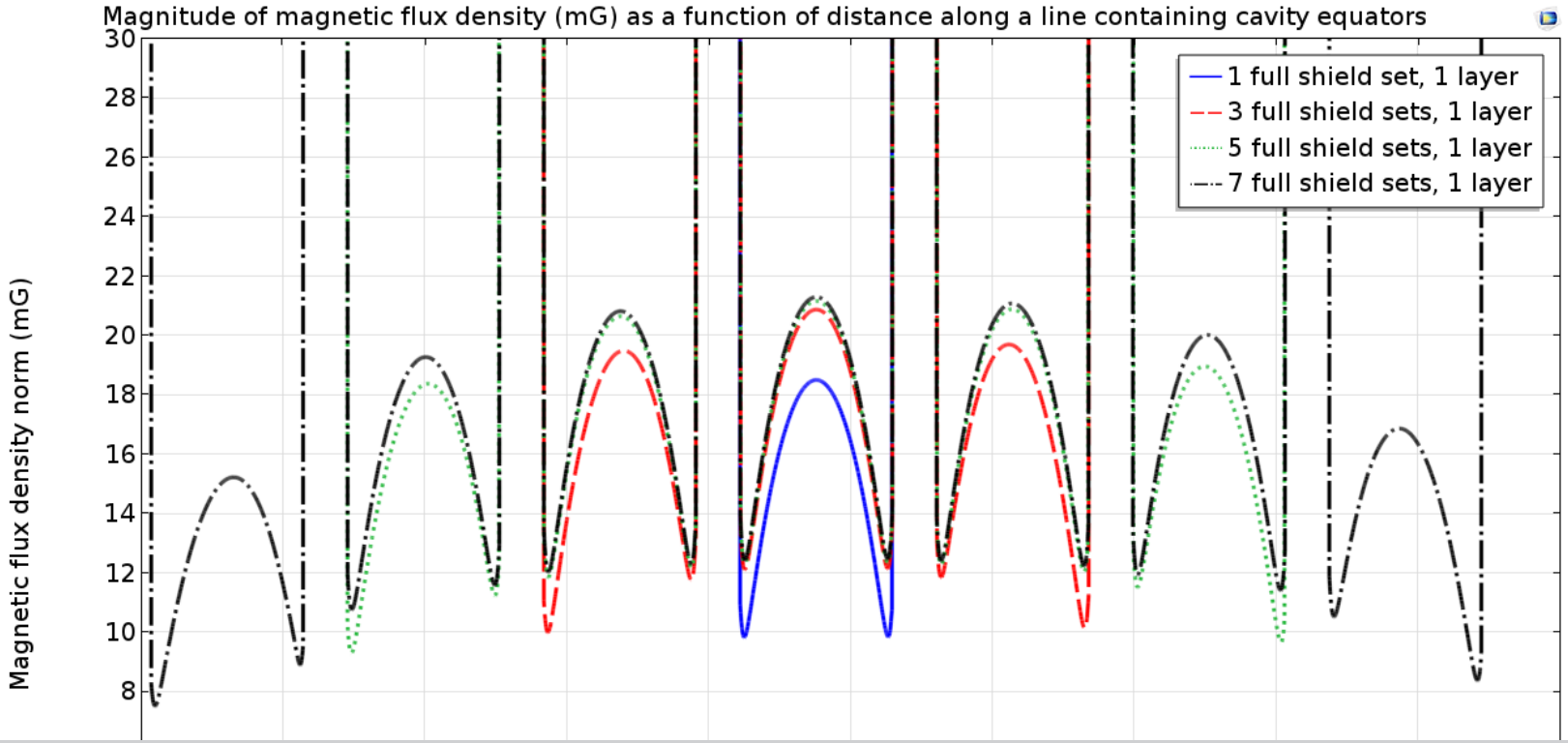


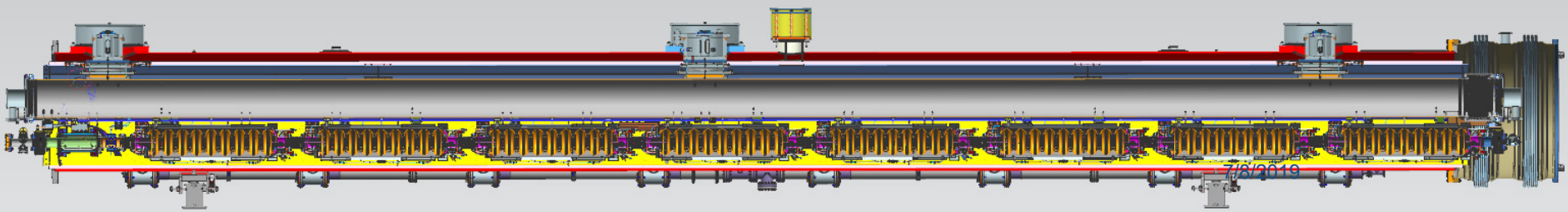

# Active longitudinal field compensation

- Same coils as those installed for demagnetization
- Helmholtz coils on the outside of CM vessel
  - Main coil + 2 end coils
- End coils required to compensate end effects of vessel

# Active longitudinal field compensation

- Need to shield longitudinal component of *B*
  - Active cancellation proven to be effective method [7,8,9]

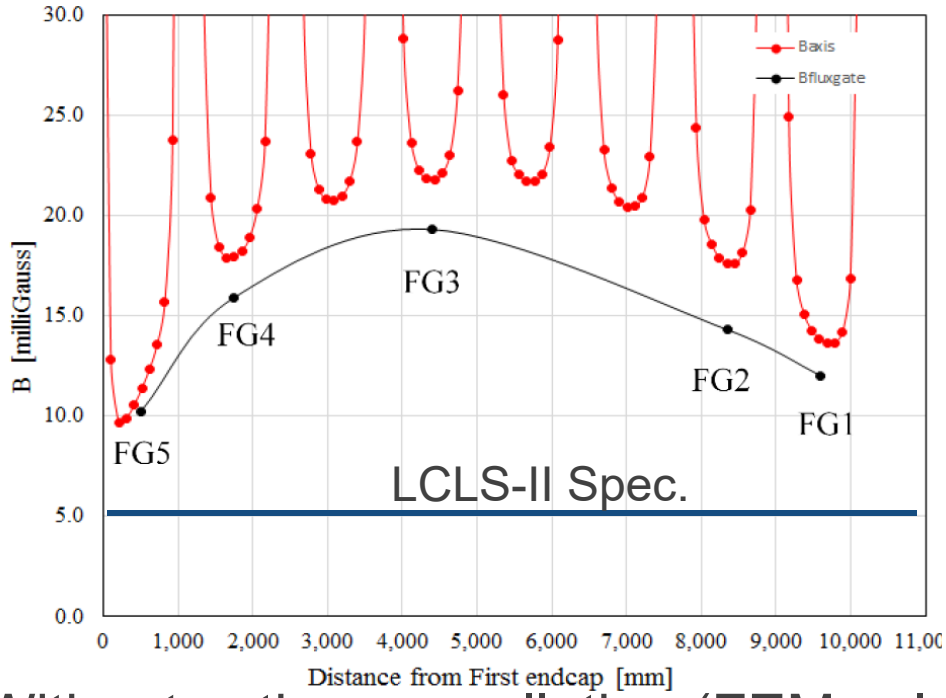


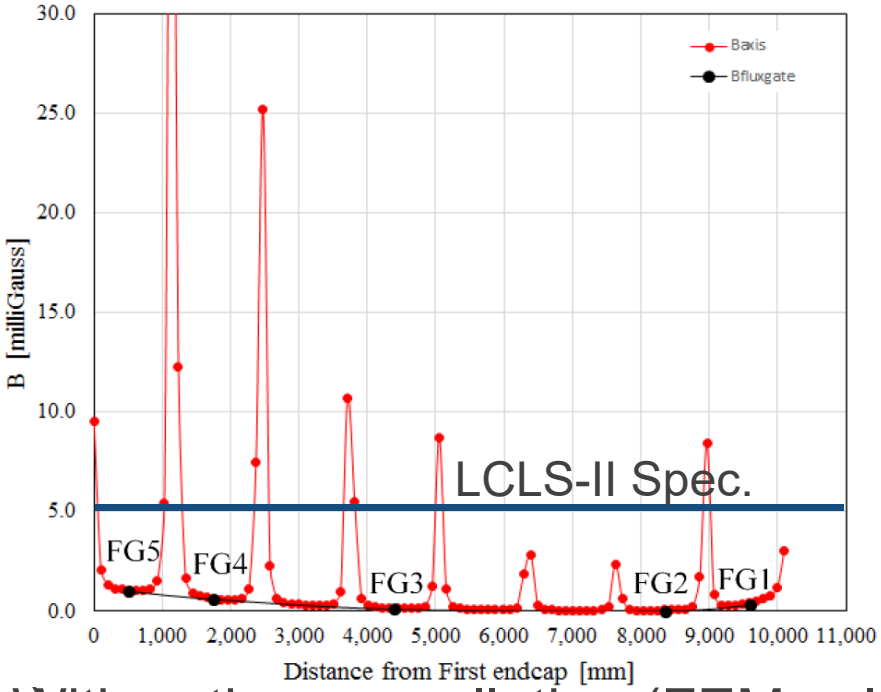


Without active cancellation (FEM calc.) we expect $B_{avg}$ ~ 15-20 mG

With active cancellation (FEM calc.) we expect $B_{avg}$ < 3 mG


[7] A. Crawford, arxiv.org/ftp/arxiv/papers/1507/1507.06582.pdf.
[8] The Conceptual Design Report for the TeSLA Test Facility Linac, Version 1, 1995.
[9] T. Bitter et al., Nucl. Instrum. Methods A, 309, 1991.